

Cover Page



Universiteit Leiden



The handle <http://hdl.handle.net/1887/28971> holds various files of this Leiden University dissertation

Author: Rosalia, Rodney Alexander

Title: Particulate based vaccines for cancer immunotherapy

Issue Date: 2014-10-02

Particulate based vaccines for cancer immunotherapy

Rodney Alexander Rosalia

The research presented in this thesis was performed at the Department of Immunohematology and Bloodtransfusion, Clinical Pharmacy and Toxicology of the Leiden University Medical Center and at the Leiden Academic Centre for Drug Research, Leiden, The Netherlands.

Financial support for the publication of this thesis was provided by AZL Onderzoeks- en Ontwikkelingskrediet Apotheek, and ISA Pharmaceuticals, Leiden, The Netherlands.

Cover design Andrew Ng, Rodney Rosalia
Layout Renate Siebes, Proefschrift.nu
Printed by Ipskamp Drukkers B.V.
ISBN 978-94-9202-6026

© 2014 R.A. Rosalia

All rights reserved. No part of this publication may be reproduced or transmitted in any form or by any means, electronic or mechanical, including photocopy, recording, or any information storage or retrieval system, without permission in writing from the author. The copyright of the articles that have been accepted for publication or that already have been published, has been transferred to the respective journals.

Particulate based vaccines for cancer immunotherapy

Proefschrift

ter verkrijging van
de graad van Doctor aan de Universiteit Leiden,
op gezag van Rector Magnificus prof. mr. C.J.J.M. Stolker,
volgens besluit van het College voor Promoties
te verdedigen op dinsdag 2 oktober 2014
klokke 13.45 uur

door

Rodney Alexander Rosalia

geboren te Willemstad, Curaçao
in 1981

Promotiecommissie

Promotor

Prof.dr. H-J. Guchelaar

Prof.dr. F. Ossendorp

Copromotor

Dr. J. Oostendorp

Overige leden

Prof.dr. T. de Gruijl

VUmc Amsterdam

Prof.dr. W. Hennink

UMC Utrecht

Dr. T. van Hall

Contents

Chapter 1	Introduction	7
Chapter 2	Dendritic cells process synthetic long peptides better than whole protein, improving antigen presentation and T-cell activation	37
Chapter 3	Optimization of encapsulation of a synthetic long peptide in PLGA nanoparticles: low burst release is crucial for efficient CD8 ⁺ T cell activation	71
Chapter 4	Co-encapsulation of synthetic long peptide antigen and Toll like receptor 2 ligand in poly-(lactic-co-glycolic-acid) particles results in sustained MHC class I cross-presentation by dendritic cells	95
Chapter 5	Efficient <i>ex vivo</i> induction of T cells with potent anti-tumor activity by protein antigen encapsulated in nanoparticles	123
Chapter 6	Poly-(lactic-co-glycolic-acid)-based particulate vaccines: nano-size is a key parameter for dendritic cell uptake and immune activation	153
Chapter 7	CD40-targeted dendritic cell delivery of PLGA-nanoparticle vaccine induce potent anti-tumor responses	183
Chapter 8	Targeting nanoparticles to CD40, DEC-205 or CD11c molecules on DC for efficient CD8 ⁺ T cell responses; a comparative study	213
Chapter 9	Discussion	243
Chapter 10	English summary – Nederlandse samenvatting	261
Chapter 11	Dankwoord, Acknowledgements & Palabranan di Danki vitae	273
Chapter 12	Curriculum vitae	281
Chapter 13	Publication list	283



Chapter 1

Introduction



1. The immune system; basic mechanisms and function

The immune system constitutes a network of specialized bone marrow derived cells which detect, isolate and eradicate potential harmful microorganisms or malignant cells. It consists of two arms; the innate and the adaptive immune system which collectively protect the human body from pathogens ^{1,2}. Communication between cells of the immune system and other non-immune cells proceeds via cell-surface and secreted signaling molecules ³⁻⁵ produced in response to the detection of danger signals ^{5,6}.

The innate immune system is activated after the detection of danger signals, for example an invading pathogen. The innate immune system comprises immune cells that can rapidly engage and elicit their effector functions forming the first line of defense. Innate immune cells are characterized by their antigen (Ag) non-specific effector functions, and lack of immunological memory. Innate immune cells recognize genetically conserved patterns expressed on non-self- and altered self-tissues ⁷⁻⁹.

Failure of the innate immune system to eliminate an invading pathogen leads to the activation of a more “tailor-made” immune defense mechanism; the adaptive immune system. Initial encounter of the adaptive immune system with a potentially harmful pathogen is characterized by a reaction time of 3 – 7 days. During this period, pathogen-specific lymphoid cells; B cells, CD4⁺ and CD8⁺ T cells are primed (activated). Upon priming, B and T cells vigorously multiply (proliferate) and exert their Ag-specific effector functions. The adaptive immune system can form immunological memory resulting in a rapid, within hours, secondary response which efficiently clears the pathogen upon reinfection with the same pathogen. For instance, the long lived protection against measles is based on the formation of immunological memory against the virus after original infection and clearance.

Some aspects of the immune system and vaccination will be briefly introduced in the following paragraphs which will facilitate the reader to interpret the research data described in this thesis.

2. First line of defense; the innate immune system and the detection of “danger”

Micro-organisms encode and express various molecular motifs, pathogen-associated molecular pattern (PAMP), crucial for their pathogenicity ^{2,10,11}, such as DNA/RNA and/

or glycosylated proteins and lipids. The innate immune system has evolved to recognize these molecular motifs as danger signals and thus alarming for the presence of an invading pathogen.

Recognition of PAMP proceeds via several intra- and extracellular genetically conserved pathogen recognition receptors (PRRs). An important group of PRRs are the Toll-like receptors (TLRs). Ligation of TLRs results in intracellular signaling cascades and ultimately, cell activation and expression of cell-surface co-stimulatory molecules, chemokines and cytokines that signal to other cells in their environment, initiating inflammation^{4,12,13}.

Phagocytic myeloid cells form a major subset of the innate immune system, they are distributed throughout the body and participate in the surveillance of (non-)lymphoid tissues for the presence of invading microbiological threats. Phagocytic cells continuously engulf, process and “analyze” the content for possible PAMPs. The majority of phagocytic cells are formed by monocytes and macrophages (MΦ). The latter are also referred to as “scavenger cells and have an important role in the clearance of cellular debris, apoptotic bodies and pathogens from the body¹⁴. MΦ are specially equipped for this purpose as they efficiently translocate engulfed Ag into intracellular degradation compartments.

Monocytes are subdivided into two subsets based on their functional properties, the first subset, the “patrolling monocytes” have a special role in tissue repair and wound healing. The second subset are the so called “inflammatory monocytes” which produce tumor-necrosis factor and inducible nitric oxide synthase during infections¹⁵. Monocytes are also thought to contribute to an immune response by differentiating into macrophage- or dendritic cell (DC) like effector cells^{15,16}. The final differentiation of monocytes is largely dependent on the type of danger signal detected.

Dendritic cells form a small percentage of the phagocytic cell population, 5–15%, but DCs are arguably the most important cell type of the innate immune arm as they link the innate and adaptive immune response. DCs and their functions will be described in more detail in paragraph 2.1.

2.1 Dendritic cells; linking innate and adaptive immunity

DCs function as the gate-keepers of the immune system¹⁷⁻¹⁹. DCs are strategically located throughout the body at sites where contact with “non-self” material is the most frequent, such as the skin and mucosal lining of the lungs and the gut. DCs use their extensive

arsenal of PRRs to detect invading pathogens and have a pivotal role during the onset and control of immune responses (Figure 1.1).

TLRs contain transmembrane signaling motifs and their ligands triggers intracellular signaling cascades which regulates among others NF- κ B gene-transcription, important for cell activation. Ultimately, these signaling cascades result in the transformation of DCs into fully competent Ag presentation cells (APC), a process termed "DC maturation" (Figure 1.1). DC maturation is characterized by efficient processing of internalized exogenous Ag

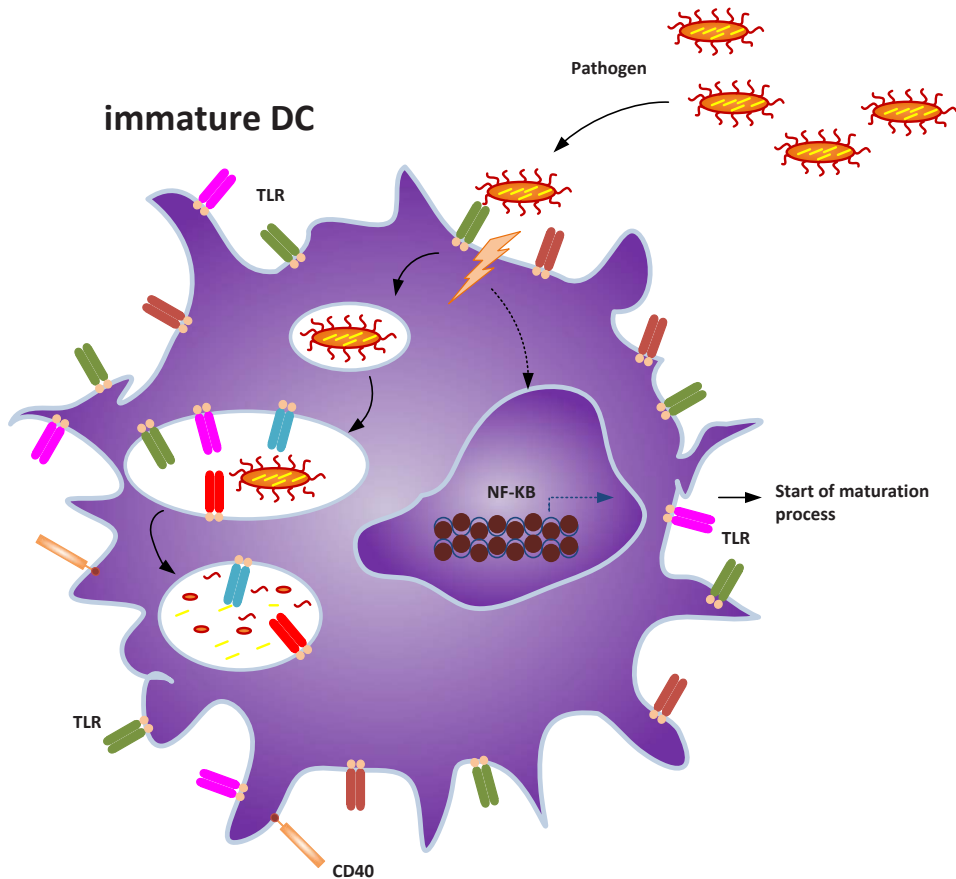


Figure 1.1 Immature DC encounters a pathogen and becomes activated.

Invading pathogens express molecular patterns which are recognized by DC via their TLRs expressed on the cell surface or inside intracellular compartments. TLR triggering activates intracellular signaling pathways which culminate in the NF- κ B transcription and the initiation of DC maturation. The engulfed pathogens are translocated inside intracellular compartments, phagosomes, where they are killed and degraded.

and presentation in the context of major histocompatibility class (MHC) class I and class II molecules, increased expression of T co-stimulatory molecules and secretion of pro-inflammatory cytokines. These changes endow DC with the superior capacity to prime naïve and T cells (Figure 1.2).

At the site of inflammation, DCs internalize pathogen-derived material present in the extracellular environment. In parallel, PAMPs are recognized as danger signals and initiate DC maturation. Mature DCs express the lymph node homing chemokine receptor, CCR7, permitting migration from the infection site towards the lymph nodes (LNs). In the LN the mature DC encounter T cells²⁰.

Stimulation of T cells by DCs is the first step in the activation of the adaptive immune system. In summary, DCs dictate the breadth and potency of an immune response via their capacity to activate the adaptive immune arm when the innate immune arm is incapable of clearing the disease causing entity. DCs play a critical role in balancing an ensuing response; a weak immune-response leaves the body vulnerable to the pathogen but an excessive immunological response can result in epitope spreading²¹⁻²⁵ which might cause damage to healthy tissues of the host^{26,27}. Systemic Lupus Erythematosus (SLE) is a well-known disease resulting from excessive stimulation of auto-reactive T cells by DC presenting self-Ag derived from apoptotic cells²⁸.

3. The adaptive immunity; “acquired, antigen specific” effector functions

Adaptive immune responses can be sub-divided into a humoral response, carried out by B cells and type 2 CD4⁺ T cells, and cellular response, carried out by type 1 CD4⁺ and CD8⁺ T cells. In contrast to immune cells of the innate immune system, B and T cells are characterized by their Ag-specific effector functions.

The nearly unlimited different Ag-specificities and different degree of affinity of the T-cell receptors (TCRs) T cells are a product of the enormous diversity in possible V(D)J gene-rearrangements at the chromosomal loci encoding the TCR²⁹. T cells undergo positive and negative selection in the thymus. In the first round, T cells are screened which can successfully recognize self MHC class I molecules; positive selection. T cells failing to recognize MHC class I molecules are deleted. In a second screening, T cells are selected based on the affinity of their TCR for its specific epitope presented in MHC class I molecules.

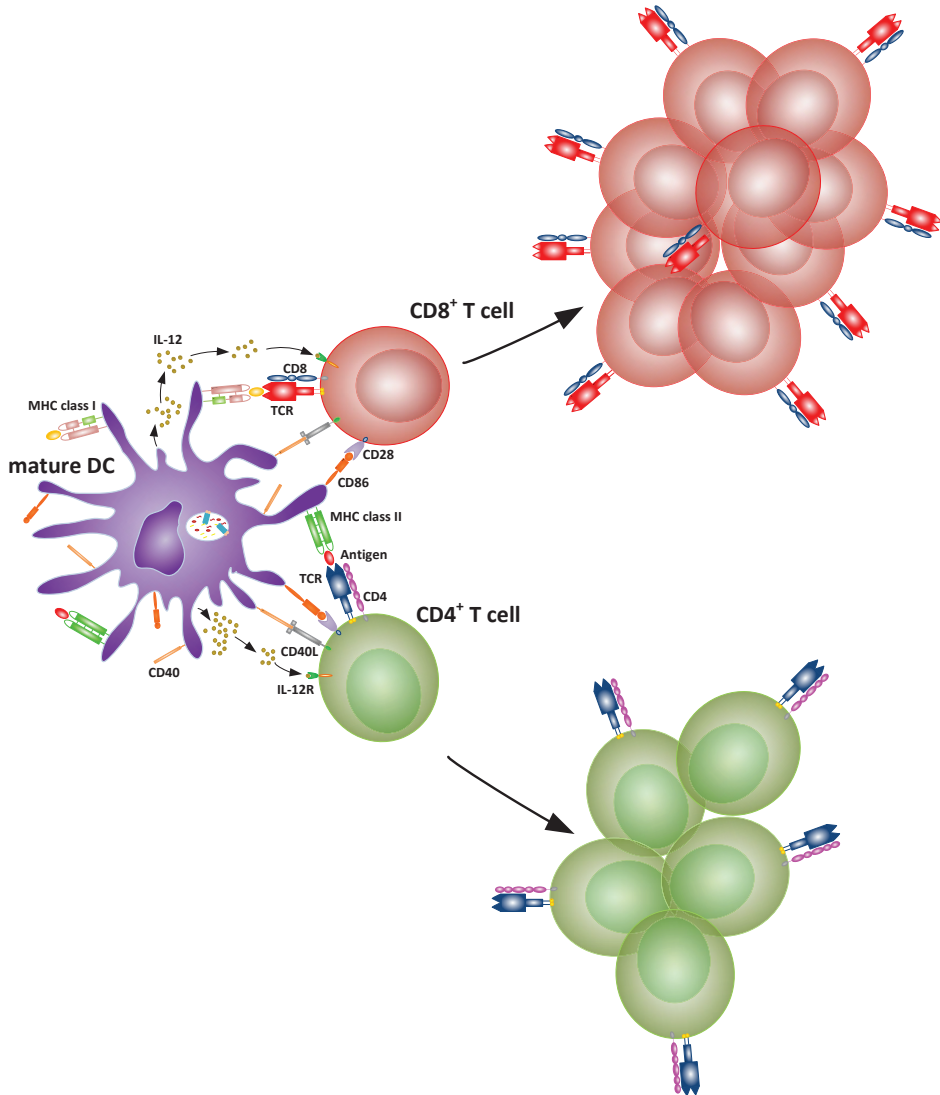


Figure 1.2 Mature DC prime and activate naïve T cells.

DC maturation leads to the up regulation of co-stimulatory molecules and production of cytokines important for an efficient activation of T cells. Mature DC acquires potent antigen processing and presentation capacity. Pathogen or vaccine specific epitopes are processed and presented in the context of MHC class I (CD8⁺ T cells) or II molecules (CD4⁺ T cells). The expression of the co-stimulatory molecules CD40, CD80 and CD86 on DC facilitates T cell activation and proliferation via the ligation of T cell expressed molecules, CD154 and CD28. In addition, IL-12 production by DC programs T cells to acquire a type 1 pro-inflammatory phenotype, characterized by high IL-2, IFN- γ and TNF- α production.

In this process, T cells showing a supra-threshold affinity TCR are deleted; negative selection. Negative selection is important for “central tolerance” and functions to prevent the release of high-affinity self-reactive T cells from the thymus into the periphery where they can cause autoimmunity³⁰⁻³².

B cell receptors (BCRs) are membrane-bound immunoglobulins which recognize conformational epitopes which can be derived from various Ags, such as protein, polysaccharides, lipids and nucleic acids. BCRs are produced in process similar to TCRs, based on the V(D)J rearrangements^{21,33}. Every B cell will express on its cell-surface BCRs with a single Ag-specificity. Ligation of BCRs initiates B cell maturation into plasma cells which secrete high amounts of soluble BCRs; antibodies³⁴. Somatic hypermutation (SHM); a process whereby the total antibody avidity to a specific Ag is increased by “affinity maturation” of the genes encoding the Ag-specific BCR and by selection of higher-affinity B cell clones, regulates the efficiency of B cell responses. The B cells with the high(er) affinity BCR will out-compete the low(er) affinity B cells for the specific Ag resulting in apoptosis of the “weak” B cells. The net result is the induction of an Ag-specific high avidity antibody response through the activation of the selected high affinity B cells²¹. Secreted antibodies have two distinct functions 1) bind specifically to pathogens or their toxins, neutralizing the pathogen and inhibit their capacity to infect cells and 2) recruitment off- and signaling to other immune cells to target, engulf and kill the invading pathogen after binding by the antibody; antibody dependent cell cytotoxicity (ADCC).

TCRs, in contrast to BCRs, are expressed only as membrane-bound molecules. TCR-triggering via its specific epitope stimulates intracellular signaling cascades leading to T cell activation. TCR differ from BCR in an important way: TCR recognizes linear epitopes of proteins, lipids or glycolipids; short (peptide) fragments derived from pathogen-associated- or tumor associated Ag in the context of classical MHC³⁵.

3.1 Immune activation to self or non-self Ag by signals of danger

The danger-model proposed by Matzinger et al.³⁶⁻³⁸ is an alternative theory to the original self-non self-theory set forward by Burnet et al who stated that an immune response can be explicitly be mounted to only “foreign” in other words, non-self-entities. In contrast, Matzinger’s theory proposes that the immune system is also possible to against self-entities as long as there is a sense of “danger” present. Both theories offer plausible explanations for the activation of the immune system, however, both theories obviously have some

limitations³⁹. Most cancers express self-Ag; in cancer patients the cancerous cells perhaps fail to trigger an adequate immune response because the (pre-)malignant lesions fail to present an imminent and acute sense of danger to the body. Considering Matzinger's danger theory from the viewpoint of vaccinology, it does offer an important basis for the use of adjuvants to enhance potency and efficacy cancer vaccines. Namely, adjuvants based on synthetic, well-defined small-molecular compounds mimicking PAMPs^{22,24,25}. The addition of an adjuvant, will cause an acute sense of "danger" as the immune system will be tricked that a harmful pathogen is present in the body and thus prime (or boost) a cancer vaccine-specific immune response.

Cancer immunotherapy based on vaccination will be discussed in more detail in the following paragraphs.

4. Ag uptake, processing and presentation to T cells by DC

DC and other myeloid cells, for example M Φ , are very efficient phagocytic cells and possess multiple endocytic mechanisms allowing internalization of vast amounts of exogenous materials for intracellular processing. DC and M Φ have several shared characteristics^{40,41}. However DC differ from M Φ as they mainly contain intracellular compartments dedicated for Ag-processing⁴² and Ag-storage⁴³ but less well equipped for Ag-degradation^{43,44}. M Φ on the contrary contain mainly intracellular compartments specialized for Ag-degradation.

Internalized Ag is cleaved, trimmed and processed in a controlled manner by various proteases present inside endo-lysosomes and the cytosol⁴⁵⁻⁴⁸. DCs are specialized Ag presentation in MHC class II molecules, which are recognized by CD4⁺ T cells (Figure 1.3), and MHC class I molecules, which are recognized by CD8⁺ T cells⁴⁹. MHC class I Ag presentation of exogenous material is known as Ag cross-presentation⁴⁶ (Figure 1.4).

Classically, exogenous materials were postulated to be processed only into MHC class II molecules whereas MHC class I molecules existed to present solely endogenous, self, produced proteins. These two processing pathways were described to function fully independent of each other. However it is now known that MHC class I and II Ag presentation consist of overlapping processing pathways^{44,46,49}. MHC class I Ag cross-presentation is a crucial pathway by which the immune system can detect and respond to bacterial, viral and parasitic infections that exclusively invade non-hematopoietic cells or reside in extracellular environments. Notably, MHC class I Ag cross-presentation is the primary mechanism how

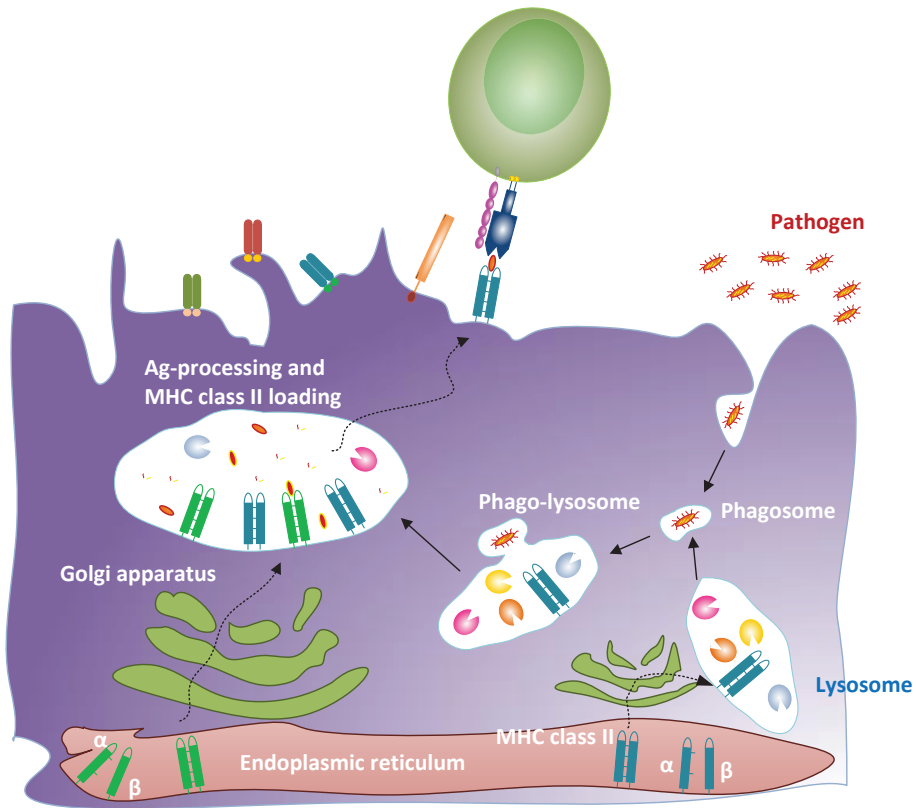


Figure 1.3 MHC class II processing and presentation of Ag by DC.

Exogenous antigens are internalized by DC inside phagosomes, or alternatively endosomes. Lysosomes inside DC, which are acidic intracellular compartments containing pH-sensitive proteases, so called cathepsins, fuse with phagosomes or endosomes. This fusion is also referred to as endo- or phagosomal maturation. This process is characterized by pH drop inside these compartments, thereby activating the cathepsins. The Ag content is degraded of into smaller peptide strands 12–20 aminoacid, epitopes. MHC class II molecules are assembled inside the endoplasmatic reticulum (ER) and translocated via the Colgi apparatus into MHC class II loading compartments. In these compartments, the epitopes are loaded on MHC class II molecules and transported to the cell-surface where they are recognized by CD4⁺ T cells.

CD8⁺ T cells are primed against tumor-associated Ags which are otherwise only presented on malignant cells⁵⁰⁻⁵².

DCs are the principal APC endowed with the capacity to cross-present Ag into MHC class I molecules. Depending on the type of Ag, DCs use phagocytosis, pinocytosis, fluid-

phase endocytosis and receptor-mediated endocytosis for Ag-internalization. It has been suggested that the mechanism of Ag-internalization dictates how the Ag is processed and presented by DC on MHC class I and II molecules⁵³.

4.1 Ag-processing by DC; mechanisms of MHC class I Ag cross-presentation

Several MHC class I Ag cross-presentation processing pathways have been reported^{52,54,55}. For simplicity these pathways can be grouped in two principal pathways, commonly referred to as the *classical/cytosolic* (Figure 1.4) and an *endosomal/vacuolar* pathway.

Ag routed via the classical pathway is processed through similar mechanisms as endogenous self-protein Ag, mediated mainly by the proteasome, located in the cytosol. This suggests that internalized exogenous material must access the cytosol from the endosomes, become ubiquitinated and transferred to the proteasome system. The mechanisms involving the translocation of an Ag into the cytosol remains a matter of debate and extensive studies and is most likely influenced by the type of Ag. Proteasome-cleaved peptides are then transported into the Endoplasmic Reticulum (ER) by the transporter associated with antigen processing (TAP) for loading on newly formed MHC class I molecules (Figure 1.4). The majority of MHC class I epitopes are loaded on MHC class I molecules inside the ER. However, there is no firm evidence that peptide loading on MHC class I molecules occurs exclusively in the ER. Therefore, the cytosolic pathway of MHC class I Ag cross-presentation refers primarily to the intracellular location where exogenous Ag is processed, the cytosol, without taking into account the compartment where the loading of MHC class I molecules occurs.

The “endosomal/vacuolar” pathway is generally independent of proteasome activity and TAP-mediated transfer of cleaved peptides into the ER. However, Ag-processing through the endosomal/vacuolar pathway, is sensitive to endo-lysosomal proteases, such as cathepsins⁴⁸, and dependent on the pH-environment inside endo-lysosomes. The key factor distinguishing the two cross-presentation pathways is thus whether the internalized exogenous material is translocated from the endolysosomes to the cytosol for processing or not⁴⁶.

5. Cancer

Cancer is the collective name given to more than 100 neoplastic diseases, which are characterized by uncontrolled growth of malignant cells, their subsequent metastasis and invasion of healthy tissues impairing their normal functioning. The development of cancer

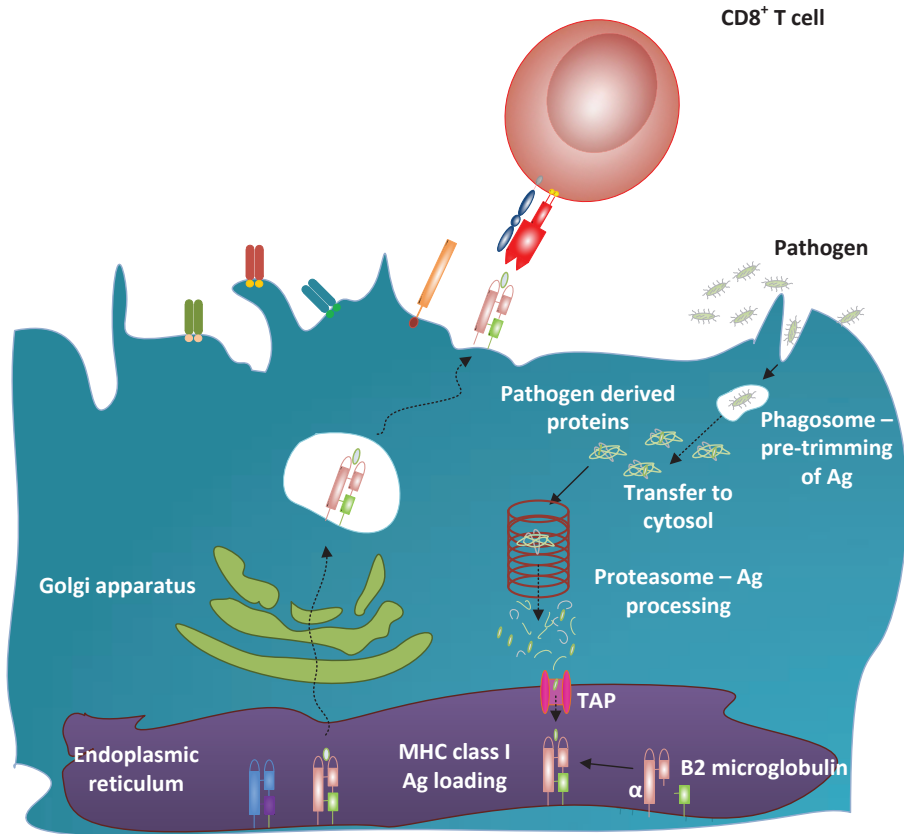


Figure 1.4 MHC class I Ag (cross-)presentation by DC.

Exogenous Ag engulfed by DC are present inside phagosomes or endosomes (Figure 1.3). The Ag content is translocated from these compartments into the cytosol by yet unknown mechanisms. Inside the cytosol, Ag-derived proteins are degraded by the cytosolic protease, the proteasome, into short 8–9 aminoacids peptide strands. The transporter associated with antigen processing (TAP) next transfers the peptide strands from the cytosol into the ER where MHC class molecules are assembled and loaded with their specific epitopes. The loaded MHC class I molecules are then transported via the Golgi apparatus to the cell surface where CD8⁺ T cells are able to triggered via the TCR.

is a multistep process originating from DNA mutations in oncogenes or tumor-suppressor genes and, importantly, failure to repair mutated damaged DNA sequences. Malignant transformation and DNA mutations can be caused by both exogenous and endogenous triggers; carcinogens⁵⁶⁻⁵⁸. Succeeding DNA mutations malignant cells acquire various

hallmarks of cancer; continuous proliferative signaling, insensitivity to growth suppressors, resistance of apoptosis, activation of replicative immortality, induction of angiogenesis, and activation of metastasis invasion of other organs^{59,60}. Cancer can partially be designated an immunological disease, already at the initial stages of carcinogenesis, (pre-)malignant lesions and the immune system are involved in a two way battle. The immune system is able to recognize tumors as implied by 1) rejection of experimental tumors 2) increased carcinogenesis in immunodeficient animals and/or 3) increased incidence of some cancers in immunodeficient patients and in the elderly. A strong evidence for potent tumor-specific immunity is provided by studies on cancer patients with paraneoplastic syndrome. For example, oncoproteins of neural origin can in some cases of breast and ovarian cancer be expressed by the tumor. In healthy individuals these (onco)proteins are expressed only in immune-privileged sites, such as neurons. However, in these cancer patients, a strong CD8⁺ T-cell response is generated which effectively controls tumor growth but also induces severe auto-immune neurological diseases. Thus, in cancer patients despite the induction of a tumor specific immune response, the tumor is not controlled and grows out; tumor escape. Mechanisms resulting in tumor escape are many. DNA mutations does not only modulate oncogenes and tumor suppressor genes but also facilitate carcinogenesis by driving tumor promoting inflammation^{61,62}, angiogenesis^{63,64} and induction of local immune suppression via the attraction/induction of T regulatory cells^{65,66} and myeloid derived suppressor cells (MDSCs)⁶⁷. Several other factors have been attributed to the overall lack of a potent anti-tumor response in cancer patients⁶⁸⁻⁷⁰ and combined these factors lead to a weak immunogenic tumor microenvironment allowing escape of the tumor from surveillance by the immune system.

5.1 Cancer; disease prevalence in the Netherlands

In the Netherlands, 100,600 new cases of cancer were diagnosed in 2011. This number is 4% higher than the previous year, 96,500. Skin cancer is the most common with 14,400 cases followed by breast cancer (14,100), colorectal cancer (13,300), lung & tracheal cancer (11,700) and 11,400 cases of prostate cancer. The steepest rise was seen with skin cancer with 1,500 new cases in 2011 compared to 2010. The expectation is that an annual increase of 3% in total cancer cases will be evident for the next ten years

Life expectancy of cancer patients has increased approximately with 3 years in the past decade. In general, the longer people live the higher their chances of being diagnosed

with cancer. Another factor contributing to the rise of cancer prevalence is the change in daily activities. For example, more women reported being a regular smoker, a habit which most likely is the cause the increase of lung cancer among women. Nowadays, the chance of getting cancer for women is 1 in 3, was 1 in 4, and for men 1 in 2, was 1 in 3. This clear increase is most evident in patients of 85 years and older. Unhealthy diets, alcohol consumption and lack of physical exercise have also been related to the increase in cancer.

In 2011, 43,139 persons in the Netherlands died from cancer or related complications. That is 42% of the the total cancer cases in the same year. Thus, it is very clear that better treatment modalities are required (Dutch Association of Comprehensive Cancer Centers).

6. Vaccines

The use of classical prophylactic vaccines dates back to the late 18th century when it was shown by Jenner and others that humans could be protected against small-pox by cross-immunity against cow-pox after inoculation with pus from cow-pox blisters. This important observation initiated the field of vaccine development. Although Jenner successfully induced immunity and protection in his patients, he was not aware of the entity causing this protection. Koch et al. then showed that infectious diseases are caused by pathogenic microorganisms, each one responsible for a particular disease. These findings led to the culture of artificially weakened strains of virulent pathogens by Pasteur, which were then used as vaccines against rabies and anthrax.

Immunostimulatory agents, adjuvants, were introduced in the 20th century by Gaston Ramon. "Adjuvant" is derived from the latin word *adjuvare* (translation "to help"). An adjuvant potentiates the working of a vaccine by hyperactivation of the immune system. The use of aluminum salts based adjuvants (alum) were one of the first to be applied in the modern era to boost immune responses elicited by prophylactic vaccines. Alum remained for decades the only clinically approved adjuvant for human use. Alum effectively enhances Type 2 (T_H2) humoral responses, prolongs antibody production and promotes the formation of memory B cells. Nowadays there are other clinically approved adjuvants based on water-in-oil (w/o) emulsions such as MF59TM (Novartis) and the adjuvant systems (AS) marketed by Glaxo-Smith-Kline. These adjuvants are used primarily as agents to enhance the efficacy of prophylactic vaccines which is based on the induction of neutralizing antibodies.

Although tumors do stimulate humoral responses and the production of tumor-specific antibodies with cytotoxic effects^{61,62,71}, tumor cell killing is primarily achieved through the mechanisms of the cellular immune system, in other words T cells. For the purpose of tumor specific vaccination, therapies are required to boost not only the antibody response but more importantly the tumor specific T cell response.

7. Cancer immunotherapy

The natural capacity of the body's own immune system to recognize and eradicate cancers allows the possibility for treatments which enhances anti-tumor effector mechanisms, cancer immunotherapy. The need for new treatments against cancer is direct consequence of the critical challenges imposed by conventional treatments against cancers, such as surgery, chemotherapy and radiotherapy. Their clinical efficacy is poor and causes significant adverse effects in treated individuals. There is a high requirement for a more personal, tumor-specific and efficacious cancer therapy with considerably lower treatment-related adverse effects.

Significant improvements in immunology have provided greater understanding of the interactions between malignant and immune cells. It is now well accepted that avoiding destruction by the immune system is a hallmark of cancer⁶⁰. This knowledge also allows the development of novel strategies and medical interventions aiming to boost the immune system against a growing tumor. Several cancer immunotherapies have been successfully devised which are currently undergoing (pre-)clinical testing or have already been approved for standard 1st line therapy. These include the enhancement of B cell responses⁷²⁻⁷⁵, antibody-based cancer immunotherapy^{71,76-78}, adoptive cell transfer of cytotoxic CD8⁺ T cells⁷⁹⁻⁸², DC based vaccines⁸³⁻⁸⁵, inhibitors of immune checkpoint blockade, such as the FDA approved anti-CTLA4 mAb, YERVOY® (Ipilumimab)⁸⁶⁻⁸⁹ or cancer vaccines based on proteins^{90,91}, short peptides encoding minimal CTL epitopes⁹²⁻⁹⁶ or the main focus of the tumor immunology group at LUMC, long peptide vaccines⁹⁷⁻¹⁰².

Vaccination against cancer represents a promising treatment modality and is based on the principle of activating or boosting specific T cell responses against a tumor-associated Ag (TAA). From the pharmaceutical point of view; vaccinations with (long) peptides offers the possibility of having an "off the shelf" product which can be manufactured in large numbers and under GMP-conditions. More and more TAA are being discovered and described¹⁰³⁻¹⁰⁶ allowing the production of long peptide vaccines for these targets.

7.1 Cancer immunotherapy; therapeutic vaccines

Successful cancer immunotherapy requires a strong pro-inflammatory Type 1 (TH1) CD4⁺ and CD8⁺ T cell responses. Advances in molecular immunology have led to the development of a broad range of novel synthetic adjuvants that are currently being explored in clinical trials in combination with vaccines ^{60,107-109}. Adjuvants, such as synthetic TLR agonists mimic PAMPs expressed by pathogen resulting in immune activation of the immune system. The Ag-composition of vaccines themselves have also undergone considerable developments; from completely undefined material such as pus from cow-pox blisters, modern immunologists aim to vaccinate with precisely defined Ag, from DNA-sequences, protein or peptides, encoding or representing a specific pathogen-associated or tumor-associated Ag (TAA). Therapeutic cancer vaccines aim to successfully activate or boost an effective anti-tumor T cell immune response. DC hold the key to this process, thus the main objective of vaccination regimens against cancer should be the specific and efficient delivery of the vaccine, encoding a TAA, to DC.

7.2 Cancer Immunotherapy; soluble Ag vaccines – pros and cons

Historically, protein and/or peptides in their soluble, native, form were the first vaccine Ag candidates tested in pre-clinical experimental tumor models or in the clinic. These vaccines have led to promising observations of enhanced tumor-specific T cells responses ¹¹⁰⁻¹¹². Nevertheless, in most, if not all, clinical trials, soluble protein and peptide vaccines have failed to induce complete and durable responses in cancer patients despite increasing tumor immunity.

Regarding soluble protein vaccines, it's suggested that their capacity to boost the CD8⁺ T-cell repertoire against a tumor to be rather poor ¹¹³⁻¹¹⁵. Efficient anti-tumor immune responses require potent cytotoxic CD8⁺ T cell responses to achieve the desired clinical benefit.

Synthetic short-peptide (SSP) vaccines, encoding minimal MHC class I molecule binding epitopes on the other hand considerably boost the CD8⁺ T cell tumor immunity which translated into improved clinical responses. But vaccinations with SSP are associated with significant limitations on the long term ¹¹⁶⁻¹¹⁹. SSP-vaccines do not directly stimulate CD4⁺ T cell responses. It is well known that the co-activation of CD4⁺ T cells is crucial in all aspects of CD8⁺ T cell responses and plays an important role during the priming, effector and memory phase CD8⁺ T cells ¹²⁰⁻¹²⁵. Thus when SSP are used as vaccines, the ensuing CD8⁺ T cell responses are short-lived ¹¹⁶ and of sub-optimal potency. Other restrictions

related to the use of SSP vaccines are the necessity for HLA-typing for each patient to be treated and tolerance induction due to SSP presentation by non-professional APC ¹¹⁶. Another disadvantage of SSP is the short-lived *in vitro* Ag presentation in comparison to SLP ¹²⁶ which, next to SSP loading on non-professional APC might underlie the vanishing CD8⁺ T-cell responses observed *in vivo* post-vaccination ¹¹⁶.

The concept of synthetic long peptide (SLP) vaccines was introduced by Melief et al. ^{114,115,127}, as way to improve the efficacy of peptide vaccines. The SLPs are overlapping synthetic peptides of 15–35 amino acids that 1) cover the entire sequence of the native protein TAA to which an immune response is targeted to, 2) SLP require DC-specific internalization and processing for optimal presentation in MHC class I and class II molecules and 3) do not require HLA-typing as ingestion by DC of overlapping strands of peptides allows epitope selection *in vivo* based on the patient's own HLA-profile 4) facilitates simultaneous priming of T-cells against multiple dominant and subdominant epitopes stimulating a broad T-cell response ¹¹⁴. Therapeutic vaccinations with SLP encoding the E6 and E7 oncoproteins of high risk HPV16 successfully boosts CD4⁺ and CD8⁺ T-cell responses in pre-clinical murine models of cervical cancer and in patients with (pre-)malignant disease of the cervix and the vulva ^{128,129}. SLP vaccines have also been used against other types of cancers ^{119,130-132} and against other immunological diseases ^{133,134}. In a direct comparison, SLP vaccines were more efficient in inducing CD8⁺ T-cell responses than protein vaccines ¹¹⁹ and lead to stronger and more effective Ag-specific immune responses.

The positive effect on the anti-tumor responses and resulting clinical benefits are well described for SLP vaccines. But still, soluble SLP vaccines carry some disadvantages especially related to the method of administration. Montanide-based water-in-oil (w/o) emulsions are mostly used to formulate SLP vaccines, but also protein vaccines, for administration to patients enrolled in clinical trials ¹³³⁻¹³⁸. Montanide w/o emulsions function as an Ag-depot and triggers inflammation at the site of injection. However, the properties of Montanide which cause inflammation are poorly described. In addition, the use of w/o formulations cause significant local side effects in treated patients because of their non-biocompatible/non-biodegradable properties. Moreover, unpredictable Ag release rates and lack of long-term stability of the w/o emulsions limit pharmaceutical scalability ^{128,129,139}.

Besides the disadvantages related to the delivery system, once released from the w/o emulsion based Ag-depot, SLPs are rapidly cleared via the kidney from the body ^{140,141} because of their typically small size of ≤ 5 kD. As a result, injected SLPs are inefficiently

target to- and internalized by DCs when administered s.c. or i.d. *in vivo*. Thus alternative methods to deliver SLP vaccines are highly required. Particulate vaccine carriers prepared from bio-degradable, biocompatible polymers offer a suitable substitute for Montanide or other w/o emulsions due to their relative ease of pharmaceutical formulation and immunological properties.

7.3 Cancer immunotherapy; particulate vaccine carriers based on PLGA-nanoparticles

To date, many particulate vaccine carriers have been successfully formulated from various types of biocompatible polymers¹⁴²⁻¹⁵⁰. These resulting “particulate vaccines” boosts Ag-specific humoral and cellular responses with higher efficiency compared to soluble vaccines. Their method of action is for a large part based on facilitated uptake of particulate Ag by APCs compared to soluble protein- and/or peptide Ag. From a cancer therapy perspective, one would desire to develop particulate carriers, carrying TAA that can efficiently target DC, either actively or passively, promote Ag processing and MHC class I and II presentation and finally generate of potent immune responses capable of tumor control¹⁵¹⁻¹⁵⁴.

Biodegradable particulate vaccine carriers prepared with the polymer Poly-(Lactic-co-Glycolic-acid) (PLGA) have yielded positive results as a carrier for various types of Ag, from DNA, proteins to peptides¹⁵²⁻¹⁵⁸. The use of PLGA-nanoparticles (PLGA-NP) offer some unique advantages over the administration of the soluble vaccine-Ag encoding TAA or the use of W/O based delivery vehicles; these include 1) PLGA is an FDA approved polymer 2) protection of the Ag cargo from premature degradation, 3) encapsulation of Ag in NP increases the total size of the vaccine and slows renal clearance, 4) enhanced uptake of the Ag by DC. 5) PLGA-NP makes it possible to accommodate both Ag and adjuvant in “one” particle to create a single immune activating “pathogen-like entity” and finally 6) PLGA-NP immunogenicity can be further modified by coupling of various ligands to- or surface coating of the NP to modulate the *in vivo* bio distribution and immune cell specific uptake of particles.

Owing to these favorable characteristics of PLGA-NP as vaccine delivery carriers and the crucial requirement to improve the immunogenicity of SLP-vaccines currently administered in Montanide a study was designed to assess several aspects of PLGA-NP as potential clinically applicable delivery vehicle/vaccine carrier for SLP-vaccines.

8. Scope of this thesis

Chapter 2 describes our studies exploring the mechanisms of long peptide-Ag-processing by DC. Understanding these mechanisms will allow further fine-tuning of SLP vaccines, with the goal to enhance their *in vivo* potency which may ultimately lead to improved treatment of cancer patients. We set out to enhance SLP-vaccine potency through the encapsulation in PLGA-NP.

In **chapter 3** we studied the feasibility to encapsulate SLP in PLGA-NP as a method to improve the immunogenicity of SLP. This study focused on the physical and formulation criteria necessary to successfully encapsulate SLP in PLGA-NP (PLGA-SLP). Subsequently, we studied the efficacy of cross-presentation by DC of PLGA-SLP in comparison to soluble SLP. We next studied the intracellular mechanisms used by DC to process PLGA-SLP in **chapter 4** and in addition describe the *in vivo* vaccine potency of PLGA-SLP in comparison to soluble SLP.

In **chapter 5** we report the application of PLGA-NP encapsulating protein Ag as a delivery vehicle to enhance DC-mediated stimulation of Ag-specific T cells *ex vivo* which could be used for adoptive T cell immunotherapy.

Because plain PLGA-particles have sub-optimal adjuvant properties *in vivo*, the optimization of PLGA-NP vaccines to achieve efficient anti-tumor responses is the topic of **chapter 6** in which nanoparticles and microparticles were studied in a head-to-head comparison in their capacity to activate B and T cell responses.

Chapter 7 continues with the optimization of PLGA-NP vaccines where PLGA-NP vaccines were formulated co-encapsulating protein Ag and TLR combined with active targeting of DC via CD40 molecules expressed on the cell-surface. In **chapter 8** a follow up study was performed to analyze different targeting strategies to enhance delivery of PLGA-NP encapsulated Ag to DC. For this purpose, PLGA-NP encapsulating TLR and Ag were targeted to CD40 (a TNF-receptor family molecule), DEC-205 (a C-type lectin receptor) and CD11c (an integrin receptor).

Finally, in **chapter 9** we will discuss the most important findings described in this thesis and present a general overview. The contribution of the results to the further understanding of the immune system and the field of cancer vaccine development will be put into context of known literature. Finally we will highlight the clinical relevancy of our findings and debate the future perspectives for particulate carriers as vehicles for SLP-vaccines.

References

1. Schenten D, Medzhitov R 2011. The control of adaptive immune responses by the innate immune system. *Adv Immunol* 109:87-124.
2. Heine H, Lien E 2003. Toll-like receptors and their function in innate and adaptive immunity. *Int Arch Allergy Immunol* 130:180-192.
3. Nibbs RJ, Graham GJ 2013. Immune regulation by atypical chemokine receptors. *Nat Rev Immunol* 13:815-829.
4. Mortier A, Van DJ, Proost P 2012. Overview of the mechanisms regulating chemokine activity and availability. *Immunol Lett* 145:2-9.
5. Zhu Y, Yao S, Chen L 2011. Cell surface signaling molecules in the control of immune responses: a tide model. *Immunity* 34:466-478.
6. Matzinger P 2002. The danger model: a renewed sense of self. *Science* 296:301-305.
7. Fujii SI, Shimizu K, Okamoto Y, Kunii N, Nakayama T, Motohashi S, Taniguchi M 2013. NKT Cells as an Ideal Anti-Tumor Immunotherapeutic. *Front Immunol* 4:409.
8. Min-Oo G, Kamimura Y, Hendricks DW, Nabekura T, Lanier LL 2013. Natural killer cells: walking three paths down memory lane. *Trends Immunol* 34:251-258.
9. Vantourout P, Hayday A 2013. Six-of-the-best: unique contributions of gammadelta T cells to immunology. *Nat Rev Immunol* 13:88-100.
10. Uematsu S, Akira S 2006. Toll-like receptors and innate immunity. *J Mol Med (Berl)* 84:712-725.
11. Pasare C, Medzhitov R 2004. Toll-like receptors: linking innate and adaptive immunity. *Microbes Infect* 6:1382-1387.
12. Elinav E, Nowarski R, Thaiss CA, Hu B, Jin C, Flavell RA 2013. Inflammation-induced cancer: crosstalk between tumours, immune cells and microorganisms. *Nat Rev Cancer* 13:759-771.
13. Fuertes MB, Woo SR, Burnett B, Fu YX, Gajewski TF 2013. Type I interferon response and innate immune sensing of cancer. *Trends Immunol* 34:67-73.
14. Canton J, Neculai D, Grinstein S 2013. Scavenger receptors in homeostasis and immunity. *Nat Rev Immunol* 13:621-634.
15. Satpathy AT, Wu X, Albring JC, Murphy KM 2012. Re(de)fining the dendritic cell lineage. *Nat Immunol* 13:1145-1154.
16. Kamphorst AO, Guermonprez P, Dudziak D, Nussenzweig MC 2010. Route of antigen uptake differentially impacts presentation by dendritic cells and activated monocytes. *J Immunol* 185:3426-3435.
17. Russo E, Nitschke M, Halin C 2013. Dendritic cell interactions with lymphatic endothelium. *Lymphat Res Biol* 11:172-182.
18. Steinman RM 2001. Dendritic cells and the control of immunity: enhancing the efficiency of antigen presentation. *Mt Sinai J Med* 68:160-166.

19. Steinman RM, Hemmi H 2006. Dendritic cells: translating innate to adaptive immunity. *Curr Top Microbiol Immunol* 311:17-58.
20. Randolph GJ, Angeli V, Swartz MA 2005. Dendritic-cell trafficking to lymph nodes through lymphatic vessels. *Nat Rev Immunol* 5:617-628.
21. Chan TD, Brink R 2012. Affinity-based selection and the germinal center response. *Immunol Rev* 247:11-23.
22. Suckow MA 2013. Cancer vaccines: harnessing the potential of anti-tumor immunity. *Vet J* 198:28-33.
23. Vanderlugt CL, Miller SD 2002. Epitope spreading in immune-mediated diseases: implications for immunotherapy. *Nat Rev Immunol* 2:85-95.
24. Demento SL, Siefert AL, Bandyopadhyay A, Sharp FA, Fahmy TM 2011. Pathogen-associated molecular patterns on biomaterials: a paradigm for engineering new vaccines. *Trends Biotechnol* 29:294-306.
25. Mahla RS, Reddy MC, Prasad DV, Kumar H 2013. Sweeten PAMPs: Role of Sugar Complexed PAMPs in Innate Immunity and Vaccine Biology. *Front Immunol* 4:248.
26. Gross CC, Wiendl H 2013. Dendritic cell vaccination in autoimmune disease. *Curr Opin Rheumatol* 25:268-274.
27. Banchereau J, Steinman RM 1998. Dendritic cells and the control of immunity. *Nature* 392:245-252.
28. Chan VS, Nie YJ, Shen N, Yan S, Mok MY, Lau CS 2012. Distinct roles of myeloid and plasmacytoid dendritic cells in systemic lupus erythematosus. *Autoimmun Rev* 11:890-897.
29. Schatz DG, Ji Y 2011. Recombination centres and the orchestration of V(D)J recombination. *Nat Rev Immunol* 11:251-263.
30. Saito T, Watanabe N 1998. Positive and negative thymocyte selection. *Crit Rev Immunol* 18:359-370.
31. Lo WL, Allen PM 2013. Self-awareness: how self-peptide/MHC complexes are essential in the development of T cells. *Mol Immunol* 55:186-189.
32. Yasutomo K, Lucas B, Germain RN 2000. TCR signaling for initiation and completion of thymocyte positive selection has distinct requirements for ligand quality and presenting cell type. *J Immunol* 165:3015-3022.
33. Schatz DG, Swanson PC 2011. V(D)J recombination: mechanisms of initiation. *Annu Rev Genet* 45:167-202.
34. Scott AM, Wolchok JD, Old LJ 2012. Antibody therapy of cancer. *Nat Rev Cancer* 12:278-287.
35. Leone P, Shin EC, Perosa F, Vacca A, Dammacco F, Racanelli V 2013. MHC class I antigen processing and presenting machinery: organization, function, and defects in tumor cells. *J Natl Cancer Inst* 105:1172-1187.

36. Matzinger P 1994. Tolerance, danger, and the extended family. *Annu Rev Immunol* 12:991-1045.
37. Matzinger P 1998. An innate sense of danger. *Semin Immunol* 10:399-415.
38. Matzinger P 2012. The evolution of the danger theory. Interview by Lauren Constable, Commissioning Editor. *Expert Rev Clin Immunol* 8:311-317.
39. Pradeu T, Cooper EL 2012. The danger theory: 20 years later. *Front Immunol* 3:287.
40. Hume DA 2008. Macrophages as APC and the dendritic cell myth. *J Immunol* 181:5829-5835.
41. Rabinovitch M 1995. Professional and non-professional phagocytes: an introduction. *Trends Cell Biol* 5:85-87.
42. Savina A, Jancic C, Hugues S, Guermonprez P, Vargas P, Moura IC, Lennon-Dumenil AM, Seabra MC, Raposo G, Amigorena S 2006. NOX2 controls phagosomal pH to regulate antigen processing during crosspresentation by dendritic cells. *Cell* 126:205-218.
43. van MN, Mangsbo SM, Camps MG, van Maren WW, Verhaart IE, Waisman A, Drijfhout JW, Melief CJ, Verbeek JS, Ossendorp F 2012. Circulating specific antibodies enhance systemic cross-priming by delivery of complexed antigen to dendritic cells in vivo. *Eur J Immunol* 42:598-606.
44. Ramachandra L, Simmons D, Harding CV 2009. MHC molecules and microbial antigen processing in phagosomes. *Curr Opin Immunol* 21:98-104.
45. Buschow SI, Nolte-'t Hoen EN, van NG, Pols MS, ten BT, Lauwen M, Ossendorp F, Melief CJ, Raposo G, Wubbolts R, Wauben MH, Stoorvogel W 2009. MHC II in dendritic cells is targeted to lysosomes or T cell-induced exosomes via distinct multivesicular body pathways. *Traffic* 10:1528-1542.
46. Joffre OP, Segura E, Savina A, Amigorena S 2012. Cross-presentation by dendritic cells. *Nat Rev Immunol* 12:557-569.
47. Kloetzel PM, Ossendorp F 2004. Proteasome and peptidase function in MHC-class-I-mediated antigen presentation. *Curr Opin Immunol* 16:76-81.
48. Rock KL, Farfan-Arribas DJ, Shen L 2010. Proteases in MHC class I presentation and cross-presentation. *J Immunol* 184:9-15.
49. Mantegazza AR, Magalhaes JG, Amigorena S, Marks MS 2013. Presentation of phagocytosed antigens by MHC class I and II. *Traffic* 14:135-152.
50. Palucka K, Ueno H, Fay J, Banchereau J 2011. Dendritic cells and immunity against cancer. *J Intern Med* 269:64-73.
51. Garbi N, Kreutzberg T 2012. Dendritic cells enhance the antigen sensitivity of T cells. *Front Immunol* 3:389.
52. Dresch C, Leverrier Y, Marvel J, Shortman K 2012. Development of antigen cross-presentation capacity in dendritic cells. *Trends Immunol* 33:381-388.
53. Burgdorf S, Kurts C 2008. Endocytosis mechanisms and the cell biology of antigen presentation. *Curr Opin Immunol* 20:89-95.

54. Joffre OP, Sancho D, Zelenay S, Keller AM, Reis e Sousa 2010. Efficient and versatile manipulation of the peripheral CD4+ T-cell compartment by antigen targeting to DNGR-1/CLEC9A. *Eur J Immunol* 40:1255-1265.
55. Segura E, Amigorena S 2013. Cross-presentation by human dendritic cell subsets. *Immunol Lett*.
56. Hullar MA, Burnett-Hartman AN, Lampe JW 2014. Gut microbes, diet, and cancer. *Cancer Treat Res* 159:377-399.
57. Fujiki H, Sueoka E, Suganuma M 2013. Tumor promoters: from chemicals to inflammatory proteins. *J Cancer Res Clin Oncol* 139:1603-1614.
58. Wullich B 2000. [Molecular genetic principles of progression of malignant diseases]. *Urologe A* 39:222-227.
59. Hanahan D, Coussens LM 2012. Accessories to the crime: functions of cells recruited to the tumor microenvironment. *Cancer Cell* 21:309-322.
60. Hanahan D, Weinberg RA 2011. Hallmarks of cancer: the next generation. *Cell* 144:646-674.
61. Candido J, Hagemann T 2013. Cancer-related inflammation. *J Clin Immunol* 33 Suppl 1:S79-S84.
62. Bondar T, Medzhitov R 2013. The origins of tumor-promoting inflammation. *Cancer Cell* 24:143-144.
63. Sakurai T, Kudo M 2011. Signaling pathways governing tumor angiogenesis. *Oncology* 81 Suppl 1:24-29.
64. Weis SM, Cheresh DA 2011. Tumor angiogenesis: molecular pathways and therapeutic targets. *Nat Med* 17:1359-1370.
65. Bright JD, Schultz HN, Byrne JA, Bright RK 2013. Injection site and regulatory T cells influence durable vaccine-induced tumor immunity to an over-expressed self tumor associated antigen. *Oncoimmunology* 2:e25049.
66. Huang XM, Liu XS, Lin XK, Yu H, Sun JY, Liu XK, Chen C, Jin HL, Zhang GE, Shi XX, Zhang Q, Yu JR 2014. Role of plasmacytoid dendritic cells and inducible costimulator-positive regulatory T cells in the immunosuppression microenvironment of gastric cancer. *Cancer Sci* 105:150-158.
67. Marigo I, Dolcetti L, Serafini P, Zanovello P, Bronte V 2008. Tumor-induced tolerance and immune suppression by myeloid derived suppressor cells. *Immunol Rev* 222:162-179.
68. Simova J, Pollakova V, Indrova M, Mikyskova R, Bieblova J, Stepanek I, Bubenik J, Reinis M 2011. Immunotherapy augments the effect of 5-azacytidine on HPV16-associated tumours with different MHC class I-expression status. *Br J Cancer* 105:1533-1541.
69. Seliger B, Massa C 2013. The Dark Side of Dendritic Cells: Development and Exploitation of Tolerogenic Activity That Favor Tumor Outgrowth and Immune Escape. *Front Immunol* 4:419.
70. Poggi A, Musso A, Dapino I, Zocchi MR 2014. Mechanisms of tumor escape from immune system: Role of mesenchymal stromal cells. *Immunol Lett* 159:55-72.

71. Scott AM, Wolchok JD, Old LJ 2012. Antibody therapy of cancer. *Nat Rev Cancer* 12:278-287.
72. Carpenter EL, Mick R, Ruter J, Vonderheide RH 2009. Activation of human B cells by the agonist CD40 antibody CP-870,893 and augmentation with simultaneous toll-like receptor 9 stimulation. *J Transl Med* 7:93.
73. DiLillo DJ, Yanaba K, Tedder TF 2010. B cells are required for optimal CD4+ and CD8+ T cell tumor immunity: therapeutic B cell depletion enhances B16 melanoma growth in mice. *J Immunol* 184:4006-4016.
74. Kornbluth RS, Stempniak M, Stone GW 2012. Design of CD40 agonists and their use in growing B cells for cancer immunotherapy. *Int Rev Immunol* 31:279-288.
75. Forte G, Sorrentino R, Montinaro A, Luciano A, Adcock IM, Maiolino P, Arra C, Cicala C, Pinto A, Morello S 2012. Inhibition of CD73 improves B cell-mediated anti-tumor immunity in a mouse model of melanoma. *J Immunol* 189:2226-2233.
76. Lianos GD, Vlachos K, Zoras O, Katsios C, Cho WC, Roukos DH 2014. Potential of antibody-drug conjugates and novel therapeutics in breast cancer management. *Onco Targets Ther* 7:491-500.
77. Naujokat C 2014. Monoclonal antibodies against human cancer stem cells. *Immunotherapy* 6:290-308.
78. Glassman PM, Balthasar JP 2014. Mechanistic considerations for the use of monoclonal antibodies for cancer therapy. *Cancer Biol Med* 11:20-33.
79. Rosenberg SA, Dudley ME 2009. Adoptive cell therapy for the treatment of patients with metastatic melanoma. *Curr Opin Immunol* 21:233-240.
80. Park TS, Rosenberg SA, Morgan RA 2011. Treating cancer with genetically engineered T cells. *Trends Biotechnol* 29:550-557.
81. Restifo NP, Dudley ME, Rosenberg SA 2012. Adoptive immunotherapy for cancer: harnessing the T cell response. *Nat Rev Immunol* 12:269-281.
82. Kalos M, June CH 2013. Adoptive T cell transfer for cancer immunotherapy in the era of synthetic biology. *Immunity* 39:49-60.
83. Butterfield LH 2013. Dendritic Cells in Cancer Immunotherapy Clinical Trials: Are We Making Progress? *Front Immunol* 4:454.
84. Gonzalez FE, Ortiz C, Reyes M, Dutzan N, Patel V, Pereda C, Gleisner MA, Lopez MN, Gutkind JS, Salazar-Onfray F 2014. Melanoma cell lysate induces CCR7 expression and in vivo migration to draining lymph nodes of therapeutic human dendritic cells. *Immunology*.
85. Gelao L, Criscitiello C, Esposito A, Laurentiis MD, Fumagalli L, Locatelli MA, Minchella I, Santangelo M, Placido SD, Goldhirsch A, Curigliano G 2014. Dendritic cell-based vaccines: clinical applications in breast cancer. *Immunotherapy* 6:349-360.
86. Vanneman M, Dranoff G 2012. Combining immunotherapy and targeted therapies in cancer treatment. *Nat Rev Cancer* 12:237-251.

87. Lipson EJ, Sharfman WH, Drake CG, Wollner I, Taube JM, Anders RA, Xu H, Yao S, Pons A, Chen L, Pardoll DM, Brahmer JR, Topalian SL 2013. Durable cancer regression off-treatment and effective reinduction therapy with an anti-PD-1 antibody. *Clin Cancer Res* 19:462-468.
88. Intlekofer AM, Thompson CB 2013. At the bench: preclinical rationale for CTLA-4 and PD-1 blockade as cancer immunotherapy. *J Leukoc Biol* 94:25-39.
89. Brahmer JR 2014. Immune checkpoint blockade: the hope for immunotherapy as a treatment of lung cancer? *Semin Oncol* 41:126-132.
90. Mischo A, Bubel N, Cebon JS, Samaras P, Petrausch U, Stenner-Liewen F, Schaefer NG, Kubuschok B, Renner C, Wadle A 2011. Recombinant NY-ESO-1 protein with ISCOMATRIX adjuvant induces broad antibody responses in humans, a RAYS-based analysis. *Int J Oncol* 39:287-294.
91. Chen Q, Jackson H, Parente P, Luke T, Rizkalla M, Tai TY, Zhu HC, Mifsud NA, Dimopoulos N, Masterman KA, Hopkins W, Goldie H, Maraskovsky E, Green S, Miloradovic L, McCluskey J, Old LJ, Davis ID, Cebon J, Chen W 2004. Immunodominant CD4+ responses identified in a patient vaccinated with full-length NY-ESO-1 formulated with ISCOMATRIX adjuvant. *Proc Natl Acad Sci U S A* 101:9363-9368.
92. Iinuma H, Fukushima R, Inaba T, Tamura J, Inoue T, Ogawa E, Horikawa M, Ikeda Y, Matsutani N, Takeda K, Yoshida K, Tsunoda T, Ikeda T, Nakamura Y, Okinaga K 2014. Phase I clinical study of multiple epitope peptide vaccine combined with chemoradiation therapy in esophageal cancer patients. *J Transl Med* 12:84.
93. Matsushita N, Aruga A, Inoue Y, Kotera Y, Takeda K, Yamamoto M 2013. Phase I clinical trial of a peptide vaccine combined with tegafur-uracil plus leucovorin for treatment of advanced or recurrent colorectal cancer. *Oncol Rep* 29:951-959.
94. Ohno S, Okuyama R, Aruga A, Sugiyama H, Yamamoto M 2012. Phase I trial of Wilms' Tumor 1 (WT1) peptide vaccine with GM-CSF or CpG in patients with solid malignancy. *Anticancer Res* 32:2263-2269.
95. Karbach J, Gnjjatic S, Pauligk C, Bender A, Maeurer M, Schultze JL, Nadler K, Wahle C, Knuth A, Old LJ, Jager E 2007. Tumor-reactive CD8+ T-cell clones in patients after NY-ESO-1 peptide vaccination. *Int J Cancer* 121:2042-2048.
96. Odunsi K, Qian F, Matsuzaki J, Mhawech-Fauceglia P, Andrews C, Hoffman EW, Pan L, Ritter G, Vilella J, Thomas B, Rodabaugh K, Lele S, Shrikant P, Old LJ, Gnjjatic S 2007. Vaccination with an NY-ESO-1 peptide of HLA class I/II specificities induces integrated humoral and T cell responses in ovarian cancer. *Proc Natl Acad Sci U S A* 104:12837-12842.
97. Chauvin JM, Larriue P, Sarrabayrouse G, Prevost-Blondel A, Lengagne R, Desfrancois J, Labarriere N, Jotereau F 2012. HLA anchor optimization of the melan-A-HLA-A2 epitope within a long peptide is required for efficient cross-priming of human tumor-reactive T cells. *J Immunol* 188:2102-2110.
98. Gnjjatic S, Atanackovic D, Matsuo M, Jager E, Lee SY, Valmori D, Chen YT, Ritter G, Knuth A, Old LJ 2003. Cross-presentation of HLA class I epitopes from exogenous NY-ESO-1 polypeptides by nonprofessional APCs. *J Immunol* 170:1191-1196.

99. Kenter GG, Welters MJ, Valentijn AR, Lowik MJ, Berends-van der Meer DM, Vloon AP, Essahsah F, Fathers LM, Offringa R, Drijfhout JW, Wafelman AR, Oostendorp J, Fleuren GJ, van der Burg SH, Melief CJ 2009. Vaccination against HPV-16 oncoproteins for vulvar intraepithelial neoplasia. *N Engl J Med* 361:1838-1847.
100. Sabbatini P, Tsuji T, Ferran L, Ritter E, Sedrak C, Tuballes K, Jungbluth AA, Ritter G, Aghajanian C, Bell-McGuinn K, Hensley ML, Konner J, Tew W, Spriggs DR, Hoffman EW, Venhaus R, Pan L, Salazar AM, Diefenbach CM, Old LJ, Gnjatich S 2012. Phase I trial of overlapping long peptides from a tumor self-antigen and poly-ICLC shows rapid induction of integrated immune response in ovarian cancer patients. *Clin Cancer Res* 18:6497-6508.
101. Tomita Y, Nishimura Y 2013. Long peptide-based cancer immunotherapy targeting tumor antigen-specific CD4 and CD8 T cells. *Oncoimmunology* 2:e25801.
102. Wada H, Isobe M, Kakimi K, Mizote Y, Eikawa S, Sato E, Takigawa N, Kiura K, Tsuji K, Iwatsuki K, Yamasaki M, Miyata H, Matsushita H, Udono H, Seto Y, Yamada K, Nishikawa H, Pan L, Venhaus R, Oka M, Doki Y, Nakayama E 2014. Vaccination with NY-ESO-1 overlapping peptides mixed with Picibanil OK-432 and montanide ISA-51 in patients with cancers expressing the NY-ESO-1 antigen. *J Immunother* 37:84-92.
103. Terashima T, Mizukoshi E, Arai K, Yamashita T, Yoshida M, Ota H, Onishi I, Kayahara M, Ohtsubo K, Kagaya T, Honda M, Kaneko S 2014. P53, hTERT, WT-1, and VEGFR2 are the most suitable targets for cancer vaccine therapy in HLA-A24 positive pancreatic adenocarcinoma. *Cancer Immunol Immunother* 63:479-489.
104. Babiak A, Steinhauser M, Gotz M, Herbst C, Dohner H, Greiner J 2014. Frequent T cell responses against immunogenic targets in lung cancer patients for targeted immunotherapy. *Oncol Rep* 31:384-390.
105. Mocellin S 2012. Peptides in melanoma therapy. *Curr Pharm Des* 18:820-831.
106. Mizukoshi E, Nakamoto Y, Arai K, Yamashita T, Sakai A, Sakai Y, Kagaya T, Yamashita T, Honda M, Kaneko S 2011. Comparative analysis of various tumor-associated antigen-specific t-cell responses in patients with hepatocellular carcinoma. *Hepatology* 53:1206-1216.
107. Wille-Reece U, Flynn BJ, Lore K, Koup RA, Miles AP, Saul A, Kedl RM, Mattapallil JJ, Weiss WR, Roederer M, Seder RA 2006. Toll-like receptor agonists influence the magnitude and quality of memory T cell responses after prime-boost immunization in nonhuman primates. *J Exp Med* 203:1249-1258.
108. Celis E 2007. Toll-like Receptor Ligands Energize Peptide Vaccines through Multiple Paths. *Cancer Research* 67:7945-7947.
109. Perez O, Romeu B, Cabrera O, Gonzalez E, Batista-Duharte A, Labrada A, Perez R, Reyes LM, Ramirez W, Sifontes S, Fernandez N, Lastre M 2013. Adjuvants are Key Factors for the Development of Future Vaccines: Lessons from the Finlay Adjuvant Platform. *Front Immunol* 4:407.

110. Adams S, O'Neill DW, Nonaka D, Hardin E, Chiriboga L, Siu K, Cruz CM, Angiulli A, Angiulli F, Ritter E, Holman RM, Shapiro RL, Berman RS, Berner N, Shao Y, Manches O, Pan L, Venhaus RR, Hoffman EW, Jungbluth A, Gnjatic S, Old L, Pavlick AC, Bhardwaj N 2008. Immunization of malignant melanoma patients with full-length NY-ESO-1 protein using TLR7 agonist imiquimod as vaccine adjuvant. *J Immunol* 181:776-784.
111. Welters MJ, Filippov DV, van den Eeden SJ, Franken KL, Nouta J, Valentijn AR, van der Marel GA, Overkleef HS, Lipford G, Offringa R, Melief CJ, van Boom JH, van der Burg SH, Drijfhout JW 2004. Chemically synthesized protein as tumour-specific vaccine: immunogenicity and efficacy of synthetic HPV16 E7 in the TC-1 mouse tumour model. *Vaccine* 23:305-311.
112. Davis ID, Chen W, Jackson H, Parente P, Shackleton M, Hopkins W, Chen Q, Dimopoulos N, Luke T, Murphy R, Scott AM, Maraskovsky E, McArthur G, Macgregor D, Sturrock S, Tai TY, Green S, Cuthbertson A, Maher D, Miloradovic L, Mitchell SV, Ritter G, Jungbluth AA, Chen YT, Gnjatic S, Hoffman EW, Old LJ, Cebon JS 2004. Recombinant NY-ESO-1 protein with ISCOMATRIX adjuvant induces broad integrated antibody and CD4(+) and CD8(+) T cell responses in humans. *Proc Natl Acad Sci U S A* 101:10697-10702.
113. Zhang H, Hong H, Li D, Ma S, Di Y, Stoten A, Haig N, Di GK, Yu Z, Xu XN, McMichael A, Jiang S 2009. Comparing pooled peptides with intact protein for accessing cross-presentation pathways for protective CD8+ and CD4+ T cells. *J Biol Chem* 284:9184-9191.
114. Melief CJ, van der Burg SH 2008. Immunotherapy of established (pre)malignant disease by synthetic long peptide vaccines. *Nat Rev Cancer* 8:351-360.
115. Melief CJ 2011. Synthetic vaccine for the treatment of lesions caused by high risk human papilloma virus. *Cancer J* 17:300-301.
116. Bijker MS, van den Eeden SJ, Franken KL, Melief CJ, Offringa R, van der Burg SH 2007. CD8+ CTL priming by exact peptide epitopes in incomplete Freund's adjuvant induces a vanishing CTL response, whereas long peptides induce sustained CTL reactivity. *J Immunol* 179:5033-5040.
117. Bijker MS, Melief CJ, Offringa R, van der Burg SH 2007. Design and development of synthetic peptide vaccines: past, present and future. *Expert Rev Vaccines* 6:591-603.
118. Bijker MS, van den Eeden SJ, Franken KL, Melief CJ, van der Burg SH, Offringa R 2008. Superior induction of anti-tumor CTL immunity by extended peptide vaccines involves prolonged, DC-focused antigen presentation. *Eur J Immunol* 38:1033-1042.
119. Zhang H, Hong H, Li D, Ma S, Di Y, Stoten A, Haig N, Di GK, Yu Z, Xu XN, McMichael A, Jiang S 2009. Comparing pooled peptides with intact protein for accessing cross-presentation pathways for protective CD8+ and CD4+ T cells. *J Biol Chem* 284:9184-9191.
120. Feau S, Garcia Z, Arens R, Yagita H, Borst J, Schoenberger SP 2012. The CD4(+) T-cell help signal is transmitted from APC to CD8(+) T-cells via CD27-CD70 interactions. *Nat Commun* 3:948.
121. Toes RE, Schoenberger SP, van der Voort EI, Offringa R, Melief CJ 1998. CD40-CD40Ligand interactions and their role in cytotoxic T lymphocyte priming and anti-tumor immunity. *Semin Immunol* 10:443-448.

122. Bos R, Sherman LA 2010. CD4+ T-cell help in the tumor milieu is required for recruitment and cytolytic function of CD8+ T lymphocytes. *Cancer Res* 70:8368-8377.
123. Sokke UC, Hebbandi NR, Xie Y, Freywald A, Deng Y, Ma H, Xiang J 2012. CD154 and IL-2 signaling of CD4+ T cells play a critical role in multiple phases of CD8+ CTL responses following adenovirus vaccination. *PLoS One* 7:e47004.
124. Novy P, Quigley M, Huang X, Yang Y 2007. CD4 T cells are required for CD8 T cell survival during both primary and memory recall responses. *J Immunol* 179:8243-8251.
125. Matloubian M, Concepcion RJ, Ahmed R 1994. CD4+ T cells are required to sustain CD8+ cytotoxic T-cell responses during chronic viral infection. *J Virol* 68:8056-8063.
126. Faure F, Mantegazza A, Sadaka C, Sedlik C, Jotereau F, Amigorena S 2009. Long-lasting cross-presentation of tumor antigen in human DC. *Eur J Immunol* 39:380-390.
127. Melief CJ 2008. Cancer immunotherapy by dendritic cells. *Immunity* 29:372-383.
128. Kenter GG, Welters MJ, Valentijn AR, Lowik MJ, Berends-van der Meer DM, Vloon AP, Drijfhout JW, Wafelman AR, Oostendorp J, Fleuren GJ, Offringa R, van der Burg SH, Melief CJ Phase I immunotherapeutic trial with long peptides spanning the E6 and E7 sequences of high-risk human papillomavirus 16 in end-stage cervical cancer patients shows low toxicity and robust immunogenicity.
129. Kenter GG, Welters MJ, Valentijn AR, Lowik MJ, Berends-van der Meer DM, Vloon AP, Essahsah F, Fathers LM, Offringa R, Drijfhout JW, Wafelman AR, Oostendorp J, Fleuren GJ, van der Burg SH, Melief CJ 2009. Vaccination against HPV-16 oncoproteins for vulvar intraepithelial neoplasia. *N Engl J Med* 361:1838-1847.
130. Eikawa S, Kakimi K, Isobe M, Kuzushima K, Luescher I, Ohue Y, Ikeuchi K, Uenaka A, Nishikawa H, Udono H, Oka M, Nakayama E 2013. Induction of CD8 T-cell responses restricted to multiple HLA class I alleles in a cancer patient by immunization with a 20-mer NY-ESO-1f (NY-ESO-1 91-110) peptide. *Int J Cancer* 132:345-354.
131. Speetjens FM, Kuppen PJ, Welters MJ, Essahsah F, Voet van den Brink AM, Lantrua MG, Valentijn AR, Oostendorp J, Fathers LM, Nijman HW, Drijfhout JW, van d, V, Melief CJ, van der Burg SH 2009. Induction of p53-specific immunity by a p53 synthetic long peptide vaccine in patients treated for metastatic colorectal cancer. *Clin Cancer Res* 15:1086-1095.
132. Sabbatini P, Tsuji T, Ferran L, Ritter E, Sedrak C, Tuballes K, Jungbluth AA, Ritter G, Aghajanian C, Bell-McGuinn K, Hensley ML, Konner J, Tew W, Spriggs DR, Hoffman EW, Venhaus R, Pan L, Salazar AM, Diefenbach CM, Old LJ, Gnjjatic S 2012. Phase I trial of overlapping long peptides from a tumor self-antigen and poly-ICLC shows rapid induction of integrated immune response in ovarian cancer patients. *Clin Cancer Res* 18:6497-6508.
133. Arevalo-Herrera M, Soto L, Perlaza BL, Cespedes N, Vera O, Lenis AM, Bonelo A, Corradin G, Herrera S 2011. Antibody-mediated and cellular immune responses induced in naive volunteers by vaccination with long synthetic peptides derived from the *Plasmodium vivax* circumsporozoite protein. *Am J Trop Med Hyg* 84:35-42.

134. Olugbile S, Villard V, Bertholet S, Jafarshad A, Kulangara C, Roussilhon C, Frank G, Agak GW, Felger I, Nebie I, Konate K, Kajava AV, Schuck P, Druilhe P, Spertini F, Corradin G 2011. Malaria vaccine candidate: Design of a multivalent subunit alpha-helical coiled coil poly-epitope. *Vaccine* 29:7090-7099.
135. Vesikari T, Groth N, Karvonen A, Borkowski A, Pellegrini M 2009. MF59-adjuvanted influenza vaccine (FLUAD) in children: safety and immunogenicity following a second year seasonal vaccination. *Vaccine* 27:6291-6295.
136. Durando P, Icardi G, Ansaldi F 2010. MF59-adjuvanted vaccine: a safe and useful tool to enhance and broaden protection against seasonal influenza viruses in subjects at risk. *Expert Opin Biol Ther* 10:639-651.
137. ELSH 2010. MF59 as a vaccine adjuvant: a review of safety and immunogenicity. *Expert Rev Vaccines* 9:1135-1141.
138. Aucouturier J, Dupuis L, Deville S, Ascarateil S, Ganne V 2002. Montanide ISA 720 and 51: a new generation of water in oil emulsions as adjuvants for human vaccines. *Expert Rev Vaccines* 1:111-118.
139. Murray R, Cohen P, Hardegree MC 1972. Mineral oil adjuvants: biological and chemical studies. *Ann Allergy* 30:146-151.
140. Longmire M, Choyke PL, Kobayashi H 2008. Clearance properties of nano-sized particles and molecules as imaging agents: considerations and caveats. *Nanomedicine (Lond)* 3:703-717.
141. Maack T 1975. Renal handling of low molecular weight proteins. *Am J Med* 58:57-64.
142. Elamanchili P, Lutsiak CM, Hamdy S, Diwan M, Samuel J "Pathogen-mimicking" nanoparticles for vaccine delivery to dendritic cells.
143. Mohanan D, Slutter B, Henriksen-Lacey M, Jiskoot W, Bouwstra JA, Perrie Y, Kundig TM, Gander B, Johansen P 2010. Administration routes affect the quality of immune responses: A cross-sectional evaluation of particulate antigen-delivery systems. *J Control Release* 147:342-349.
144. Mahapatro A, Singh DK 2011. Biodegradable nanoparticles are excellent vehicle for site directed in-vivo delivery of drugs and vaccines. *J Nanobiotechnology* 9:55.
145. Joshi VB, Geary SM, Salem AK 2013. Biodegradable particles as vaccine delivery systems: size matters. *AAPS J* 15:85-94.
146. Todd CW, Pozzi LA, Guarnaccia JR, Balasubramanian M, Henk WG, Younger LE, Newman MJ 1997. Development of an adjuvant-active nonionic block copolymer for use in oil-free subunit vaccines formulations. *Vaccine* 15:564-570.
147. Brey RN 1995. Development of vaccines based on formulations containing nonionic block copolymers. *Pharm Biotechnol* 6:297-311.
148. Oyewumi MO, Kumar A, Cui Z Nano-microparticles as immune adjuvants: correlating particle sizes and the resultant immune responses.

149. Danhier F, Ansorena E, Silva JM, Coco R, Le BA, Preat V 2012. PLGA-based nanoparticles: an overview of biomedical applications. *J Control Release* 161:505-522.
150. Waeckerle-Men Y, Groettrup M 2005. PLGA microspheres for improved antigen delivery to dendritic cells as cellular vaccines. *Adv Drug Deliv Rev* 57:475-482.
151. Zhang Z, Tongchusak S, Mizukami Y, Kang YJ, Ioji T, Touma M, Reinhold B, Keskin DB, Reinherz EL, Sasada T 2011. Induction of anti-tumor cytotoxic T cell responses through PLGA-nanoparticle mediated antigen delivery. *Biomaterials* 32:3666-3678.
152. Hamdy S, Molavi O, Ma Z, Haddadi A, Alshamsan A, Gobti Z, Elhasi S, Samuel J, Lavasanifar A 2008. Co-delivery of cancer-associated antigen and Toll-like receptor 4 ligand in PLGA nanoparticles induces potent CD8+ T cell-mediated anti-tumor immunity. *Vaccine* 26:5046-5057.
153. Ghotbi Z, Haddadi A, Hamdy S, Hung RW, Samuel J, Lavasanifar A 2011. Active targeting of dendritic cells with mannan-decorated PLGA nanoparticles. *J Drug Target* 19:281-292.
154. Mueller M, Schlosser E, Gander B, Groettrup M 2011. Tumor eradication by immunotherapy with biodegradable PLGA microspheres--an alternative to incomplete Freund's adjuvant. *Int J Cancer* 129:407-416.
155. Demento SL, Eisenbarth SC, Foellmer HG, Platt C, Caplan MJ, Mark SW, Mellman I, Ledizet M, Fikrig E, Flavell RA, Fahmy TM 2009. Inflammasome-activating nanoparticles as modular systems for optimizing vaccine efficacy. *Vaccine* 27:3013-3021.
156. Gutierrez I, Hernandez RM, Igartua M, Gascon AR, Pedraz JL 2002. Size dependent immune response after subcutaneous, oral and intranasal administration of BSA loaded nanospheres. *Vaccine* 21:67-77.
157. San RB, Irache JM, Gomez S, Tsapis N, Gamazo C, Espuelas MS 2008. Co-encapsulation of an antigen and CpG oligonucleotides into PLGA microparticles by TROMS technology. *Eur J Pharm Biopharm* 70:98-108.
158. Walter E, Dreher D, Kok M, Thiele L, Kiama SG, Gehr P, Merkle HP 2001. Hydrophilic poly(DL-lactide-co-glycolide) microspheres for the delivery of DNA to human-derived macrophages and dendritic cells. *J Control Release* 76:149-168.



Chapter 2

Dendritic cells process synthetic long peptides better than whole protein, improving antigen presentation and T-cell activation

Rodney A. Rosalia, Esther D. Quakkelaar, Anke Redeker, Selina Khan, Marcel Camps, Jan W. Drijfhout, Ana Luisa Silva, Wim Jiskoot, Thorbald van Hall, Peter A. van Veelen, George Janssen, Kees Franken, Luis J. Cruz, Angelino Tromp, Jaap Oostendorp, Sjoerd H. van der Burg, Ferry Ossendorp & Cornelis J.M. Melief

Abstract

The efficiency of antigen (Ag) processing by dendritic cells (DCs) is vital for the strength of the ensuing T-cell responses. Previously we and others have shown that in comparison to protein vaccines, vaccination with synthetic long peptides (SLPs) has shown more promising (pre-)clinical results. Here we studied the unknown mechanisms underlying the observed vaccine efficacy of SLPs. We report an in vitro processing analysis of SLPs for MHC class I and class II presentation by murine DCs and human monocyte-derived DC (MoDCs). Compared to protein, SLPs were rapidly and much more efficiently processed by DCs, resulting in an increased presentation to CD4⁺ and CD8⁺ T cells. The mechanism of access to MHC class I loading appeared to differ between the two forms of Ag. Whereas whole soluble protein Ag ended up largely in endo-lysosomes, SLPs were detected very rapidly outside the endo-lysosomes after internalization by DCs, followed by proteasome- and TAP-dependent MHC class I presentation. Compared to the slower processing route taken by whole protein Ags, our results indicate that the efficient internalization of SLPs, accomplished by DCs but not by B or T cells and characterized by a different and faster intracellular routing, leads to enhanced CD8⁺ T-cell activation.

Introduction

DCs are the major antigen (Ag) presenting cells (APCs) of the immune system and initiate adaptive T-cell responses¹. Therapeutic vaccination in cancer immunotherapy aims at the induction of potent effector CD4⁺ and CD8⁺ T-cell responses able to target and eradicate malignant cells. Vaccination with properly folded protein Ag efficiently induces CD4⁺ T helper cell responses that can exert effector function by themselves, and strongly promotes (neutralizing) antibody formation and has therefore successfully been applied for prophylactic vaccination against viral infections²⁻⁴. Although protein vaccines can induce CD8⁺ T-cell responses⁵, efficient anti-tumor immune responses require a more robust and efficient induction of potent cytotoxic CD8⁺ T cells. However, improvement of the quality and quantity of CD8⁺ T-cell responses by vaccination remains a major challenge^{6,7}. Our group has previously reported successful induction of potent CD4⁺ and CD8⁺ T-cell responses in preclinical models and patients with (pre-)malignant disease of the cervix via therapeutic vaccination with synthetic long peptides (SLPs) of the E6 and E7 oncoproteins of high risk HPV16⁸⁻¹⁰. The SLPs used as vaccines in these studies are overlapping synthetic peptides of 15–35 amino acids that i) Cover the entire sequence of the native protein Ag to which an immune response is targeted and ii) Require internalization and processing by DCs for optimal presentation in MHC class I and class II molecules¹¹ iii) Do not require HLA-typing as ingestion by antigen-presenting cells of overlapping strands of peptides allows epitope selection *in vivo* based on the patient's own HLA-profile iv) Facilitates simultaneous priming of T cells against multiple dominant and subdominant epitopes stimulating a broad T-cell response¹². SLP vaccines have also been used against other types of cancers. T-cell immunity was induced against p53 in patients with metastatic colorectal cancer using SLP vaccines¹³ and robust immune responses were similarly induced against NY-ESO-1 in patients with ovarian cancer¹⁴. In addition, SLP vaccines have shown promising results against other immunological diseases¹⁵⁻¹⁸. In a direct comparison, SLP vaccines were more efficient in inducing CD8⁺ T-cell responses than protein vaccines^{6,17} and lead to stronger and more effective Ag-specific immune responses¹⁹⁻²¹. The positive effects of SLP vaccines in pre-clinical models and in patients are well described, but little is known concerning the mechanisms underlying the vaccine efficacy and the intracellular processing and efficiency of MHC class I and class II presentation of SLPs. It is believed that substitution of whole protein Ag by overlapping long peptide Ag facilitates the internalization, processing and presentation of the relevant epitopes by DC¹¹. We now report studies on the uptake, intracellular localization, and efficiency of processing and MHC presentation of SLPs by

murine and human DCs, including scrutiny of the role of the proteasome, TAP and endo-lysosomal processing in MHC class I cross-presentation of SLPs. To our knowledge this is the first report presenting how DC efficiently process SLPs, for presentation to CD8⁺ T cells. We observed a distinct cellular localization of SLPs compared to protein in DC following exposure to Ag, compatible with the different kinetics and efficiency of cross-presentation and subsequent CD8⁺ T-cell activation. These results highlight the fact that SLPs behave fundamentally different from proteins as an Ag for T-cell response induction. This insight can serve as a starting point for further optimization of SLP-based vaccines.

RESULTS

Superior Ag presentation of SLPs by DCs compared with that of protein

The capacity of DCs to process and present different forms of exogenous Ag in MHC class I and II was studied by loading BMDCs with SLP-OVA_{24aa} or soluble OVA protein (OVA-protein) for 24 h and measuring B3Z CD8⁺ T-cell and KZO CD4⁺ T-cell activation. DCs loaded with SLPs potently activate B3Z and KZO T cells suggesting that SLPs is internalized and efficiently routed into the MHC class I and II Ag presentation pathways (Figure 2.1A and B). In contrast, DCs loaded with protein completely failed to activate CD8⁺ T cells but did successfully activate KZO CD4⁺ T cells, albeit with at least 64-fold lower efficiency compared to SLP-loaded DCs (Figure 2.1B). Pre-stimulation of DCs with the TLR4 ligand LPS had no effect on the MHC class I presentation of OVA-protein but improved Ag presentation of SSP-OVA_{8aa} (data not shown) and long peptide Ag (Figure 2.1C). HLA-B7-restricted presentation by human MoDCs of HIV-derived protein and SLPs was also studied. We were unable to detect cytokine production by CD8⁺ T cells co-cultured with GAG-protein-loaded DCs. In contrast, SLP-GAG_{22aa} induced significant CD8⁺ T-cell activation (see Figure 2.2 and below). Together, these data show that cross-presentation of SLPs is superior to that of proteins as examined with both mouse and human DCs.

Rapid Ag presentation of SLPs by murine and human DCs

The efficiency of SLP-processing was assessed by studying the time required for DCs to present Ag on MHC class I (H2-K^b) molecules. Murine DCs were incubated with a single concentration of SLPs, SSPs or protein for the indicated time-periods. The minimal peptide, SSPs, was rapidly presented to CD8⁺ T cells resulting in strong activation already after 1

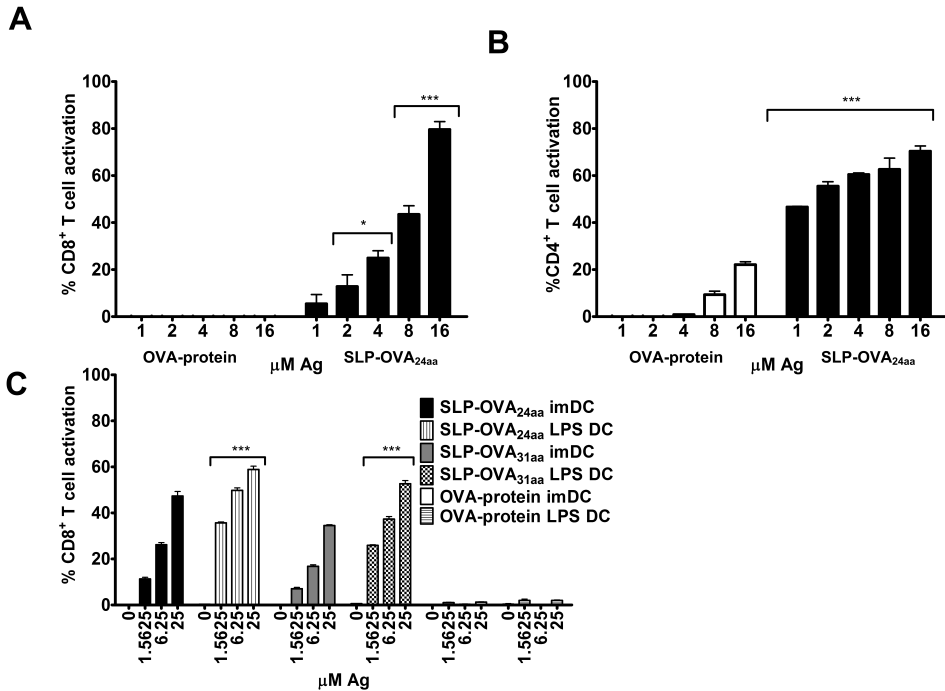


Figure 2.1 Efficient MHC class I and class II presentation by mouse DCs incubated with SLPs.

C57BL/6 x C3H F₁ BMDCs were incubated for 24 h with titrated amounts of SLP-OVA_{24aa} or OVA-protein and co-cultured overnight in the presence of (A) B3Z CD8⁺ T cells or (B) KZO CD4⁺ T cells. T-cell activation was determined as described in Materials and Methods. (C) D1 cells were pre-cultured with 10 μ g/ml LPS (LPS DC) and compared with immature DCs (imDC) in their capacity to activate B3Z T cells after 24 h incubation with Ag. Data are shown as mean + SD of 3 samples from one representative experiment representative of four (A), two (B) and three (C) experiments performed. ***P < 0.001, *P < 0.05, two-way ANOVA and Bonferroni posttests.

h. DCs loaded with SLP- also activated CD8⁺ T cells 1 h after Ag loading but with lower potency. We excluded that SLPS- were cleaved extra-cellularly, processed and loaded on MHC class I and II molecules by incubating PFA-fixed cells for with the peptide Ag and observed no cross-presentation (data not shown). DCs loaded with 10 μ M OVA-protein failed to induce significant CD8⁺ T-cell activation (Figure 2.2A). I-A^b-restricted MHC class II presentation was next studied and we observed that within 1 h of Ag incubation DC loaded with SLP-OVA_{17aa} and SLP-OVA_{31aa} activated CD4⁺ T cells with similar efficiency even though the peptides varied in length. In contrast, DC loaded with OVA-protein stimulated OT-II/CD4⁺ T cells with lower potency and it took at least 3 h of Ag loading, suggesting

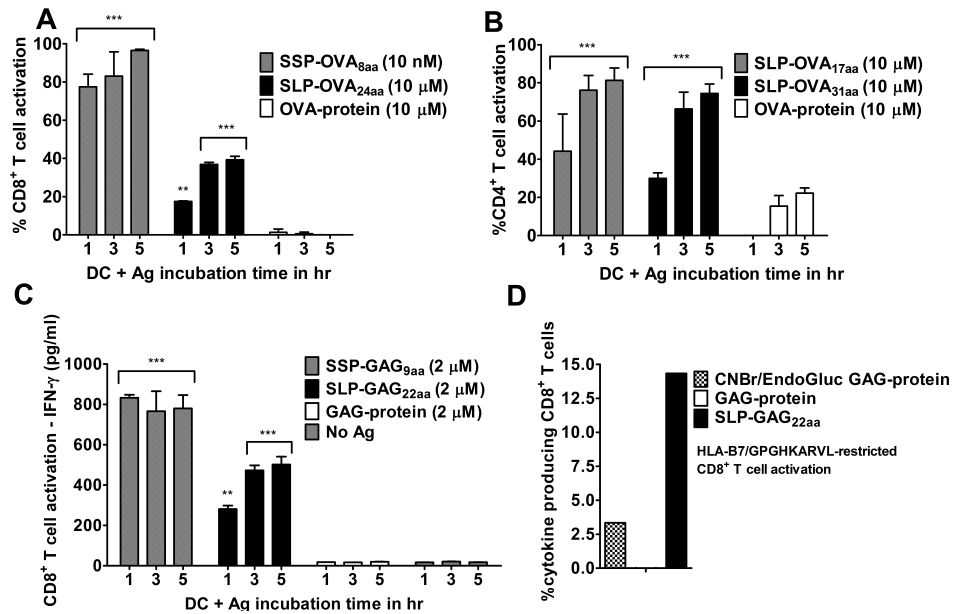


Figure 2.2 Rapid cross-presentation by mouse and human DCs loaded with SLPs compared with soluble protein.

Murine DCs were pulsed for 1, 3 or 5 h with 10 nM SSP-OVA_{8aa}, 10 μM SLP-OVA_{17aa}, SLP-OVA_{24aa}, SLP-OVA_{31aa} or OVA-protein, washed 3x times with PBS/0.2% FCS and fixed with 0.4% paraformaldehyde. Ag-loaded DCs were cultured overnight with (A) B3Z CD8⁺ T cells or (B) OT-I/II CD4⁺ T cells. (C) Human MoDCs were incubated for 1, 3 or 5 h with GAG protein, SLP-GAG_{22aa} or SLP-GAG_{9aa} (2 μM), cells fixed, and HIV-specific CD8⁺ T cells added overnight. IFN-γ production measured by ELISA was used to determine CD8⁺ T-cell activation. MoDCs were incubated for 24 h with SLP-GAG_{22aa}, soluble GAG-protein and a CNBr/EndoGluc-treated GAG-protein digest. (D) HIV-specific T cells were added and total IFN-γ- or TNF-α-producing cells were determined by flow cytometry. Data are shown as mean + SD of 3 samples from one experiment representative of three (A) or two (B, C) or from one single experiment (D). (A-C) Data were analyzed with two-way ANOVA and Bonferroni posttests, ***P < 0.001, **P < 0.01.

slower uptake and processing mechanisms involved for the MHC class II processing of protein compared to SLPs (Figure 2.2B). The rapid and efficient processing of SLPs into MHC class I molecules was also observed with human DCs (Figure 2.2C). MoDCs loaded with SLPs activated CD8⁺ T cells already 1 h post-incubation. Ag presentation increased further with longer incubation periods and appeared to reach plateau levels at 3 h post-incubation. In line with the experiment shown in Figure 2.1A, no Ag presentation could be detected after incubation of MoDCs with GAG-protein, even when the concentration of the

protein was increased five-fold (data not shown). SSPs showed robust cytokine production, within 1 hour of Ag-loading. In general, the percentages of IFN- γ -producing CD8⁺ T cells stimulated by SLP-loaded DCs were lower compared to stimulation by DCs loaded with SSPs. GAG-protein could be cross-presented, however, if offered in an alternative way to APC. DCs loaded with protein fragments obtained by treatment with cyanogen bromide (CNBr) and Endo-Glu-C cross-presented the protein digest and activated HIV-specific CD8⁺ T cells, but with lower potency compared to SLP-GAG_{22aa} (Figure 2.2D). The CNBr and Endo-Glu-C generated GAG-protein digest was analyzed and yielded the specific fragments highlighted in Supporting Information Figure S2.1. HIV-specific CD8⁺ T cells readily recognized processed GAG-protein in its native conformation. DCs were incubated with NYVAC-C-infected apoptotic HeLa cells expressing among other viral proteins the GAG-protein⁵⁸, inducing potent activation of CD8⁺ T cells. DCs incubated with HeLa cells infected with NYVAC-WT (HIV GAG-negative) failed to activate HIV-specific CD8⁺ T cells. (Supporting Information Figure S2.2) Taken together, our data suggest that the method of Ag delivery is crucial for cross-presentation to be efficient and indicate that both murine and human DCs more efficiently internalize and process SLPs compared to soluble protein.

SLPs are primarily located outside endo-lysosomes upon internalization

To assess the internalization of SLPs by DCs, murine DCs were incubated for indicated time periods with fluorescently labeled SLP-OVA_{24aa}-Bodipy-FL (Figure 2.3A) or SLP-OVA_{17aa}-Bodipy-FL (Figure 2.3B) and the uptake was analyzed by confocal imaging. SLPs were internalized by DCs within 2 h of incubation. The fluorescence intensity increased with longer incubation, indicating continuous uptake of SLPs during 24 h. The integrity of the Bodipy-labeled SLPs was confirmed by analysis on Tricine-gel, excluding that Bodipy-dye was intracellularly cleaved from the SLPs resulting in free dye and SLP inside the cells (Supporting Information Figure S2.3). Next, the intracellular localization of SLPs and protein was compared. To this purpose, DCs were incubated with Ag and LysoTracker red and the co-localization between the Ag (green) and endo-lysosomes (red) was studied. Although SLPs is internalized within 2 h, we observed that DCs internalized SLP-OVA_{24aa}-Bodipy-FL and, the much slower endocytosed, OVA-protein-Alexa488 in sufficient amounts to be accurately detected and quantified after 24 h. The disparity in green fluorescence intensity is related to the intrinsic differences in the green dyes (1 Bodipy-FL dye per SLP molecule versus 4 – 5 Alexa488 dye's per protein molecule) used in the analysis. We have confirmed previously that Alexa488 and Bodipy-FL dyes do not differentially modulate

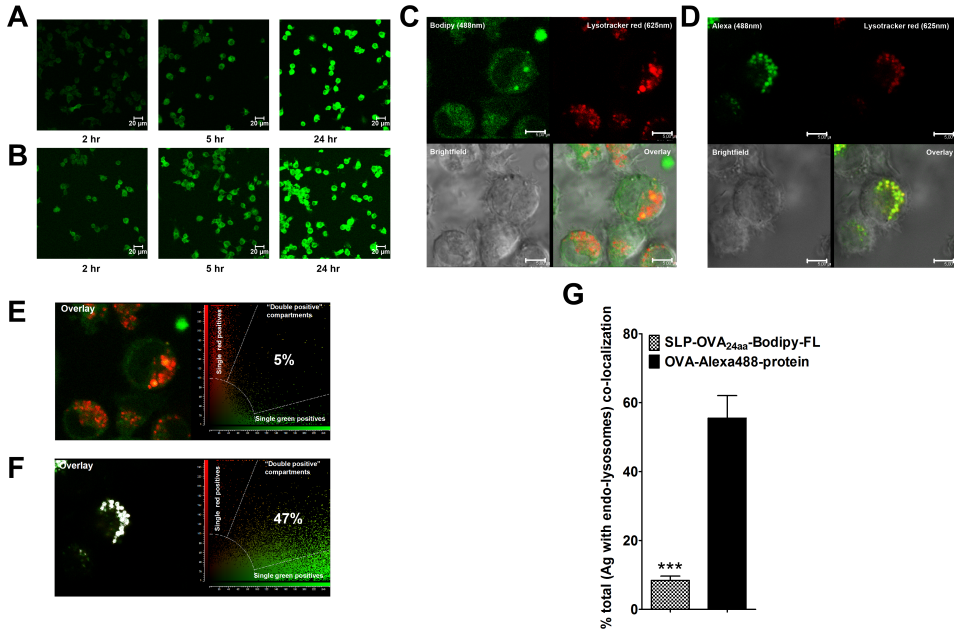


Figure 2.3 Distinct intracellular localization of SLPs and protein Ag in DCs.

DCs were incubated with 20 μ M **(A)** SLP-OVA_{24aa}-Bodipy-FL or **(B)** SLP-OVA_{17aa}-Bodipy-FL for 2, 5 and 24 h and analyzed by confocal microscopy (63x objective, scale bar, 20 μ m). **(C, D)** DCs loaded with 10 μ M SLP-OVA_{24aa}-Bodipy-FL or 10 μ M OVA-Alexa488-protein for 24 h were co-stained with LysoTracker red for visualization of endo-lysosomes. Confocal images of DCs incubated with **(C)** SLP-OVA_{24aa}-Bodipy-FL and **(D)** OVA-Alexa488 are shown as Bodipy/Alexa488/green fluorescence (top left), LysoTracker/red fluorescence (top right), bright field (bottom left) and overlay image (bottom right). **(C, D)** All scale bars, 5 μ m. **(E, F)** Co-localization of the green-fluorescence of **(E)** SLP-OVA_{24aa}-Bodipy-FL and **(F)** OVA-Alexa488 with endo-lysosomes was analyzed using Leica software (scatter plots) and **(G)** quantified results are depicted as mean + SEM of 10-20 samples from one experiment representative of two performed. Results are representative of four **(A, B)** or two **(C-G)** independent experiments analyzing 10-20 images per experiment. The Mann-Whitney test was applied to determine the difference between SLP-OVA_{24aa}-Bodipy-FL vs. OVA-Alexa488, ***P < 0.001.

uptake, intracellular routing and processing of Ag²². Internalized SLPs was detectable diffusely inside DCs (Figure 2.3C). The use of the lysotracker red allowed the identification of distinct round (red fluorescent) organelles which represented endo-lysosomes. Upon overlay of the green and red fluorescent images, a low level of co-localization of the two colors was detected in DCs that were cultured with SLPs, indicating that SLPs was primarily outside the endo-lysosomes. In contrast, DCs which had internalized protein contained

distinct green-fluorescent hot spots within the cell which in addition had a high degree of co-localization with LysoTracker red resulting in a nearly complete absence of single red fluorescent compartments and appearance of yellow(ish) spots (Figure 2.3D). The results indicate that most, if not all, endo-lysosomes contained protein upon internalization by DCs. Co-localization was quantified by analyzing DCs which internalized SLPs (Figure 2.3E) or protein (Figure 2.3F). On average, in DCs cultured with SLPs, $8 \pm 3\%$ of the green signal detected co-localized with the red fluorescence detected. In comparison, in DCs loaded with protein (Figure 2.3F) as much as $56 \pm 18\%$ of the green signal detected co-localized with the red fluorescence (Figure 2.3G). In summary, after 24 h of Ag uptake, the majority of SLPs is localized outside of the endo-lysosomes whereas the majority of protein is present inside endo-lysosomes.

MHC class I Ag cross-presentation by DCs loaded with SLPs is proteasome- and TAP- dependent

The contribution of the proteasome, the transporter associated with Ag processing (TAP) and endosomal processing in the MHC class I cross-presentation of SLPs by DCs was investigated with SLP-OVA_{24aa} as model Ag. To this purpose, WT BMDCs were incubated with titrated amounts of SLPs (Figure 2.4A) or alternatively, the proteasome inhibitor epoxomicin was added during culture of DCs and SLPs (Figure 2.4B). We observed a nearly complete loss in MHC class I cross-presentation of SLPs when the proteasome function was inhibited, indicating that intracellular processing of SLPs is dependent on proteasome functionality. Epoxomicin-treated DCs cross-presented particulate forms of SLPs under similar conditions (Supporting Information Figure S2.4B), suggesting that the decrease of MHC class I cross-presentation via inhibition of the proteasome was mainly associated with the processing of soluble SLPs.

In comparison to WT BMDC, TAP1 KO BMDCs were largely deficient in activating CD8⁺T cells (Figure 2.4C). All DC conditions used to study MHC class I presentation of SLP efficiently presented SSP-OVA_{8aa} on MHC class I molecules indicating that epoxomicin or the absence of functional TAP did not affect the general MHC class I presentation machinery of DCs (Figure 2.4D). A potential role of endo-lysosomal acidification in the processing by DCs of SLPs was assessed by Ag-loading in the presence of titrated amounts of bafilomycin A (Baf A), a lysotropic reagent which inhibits acidification of endo-lysosomes thereby influencing the activity of pH-sensitive proteases present in these compartments. Only a moderate effect of Baf A on MHC class I cross-presentation was observed, reflected by

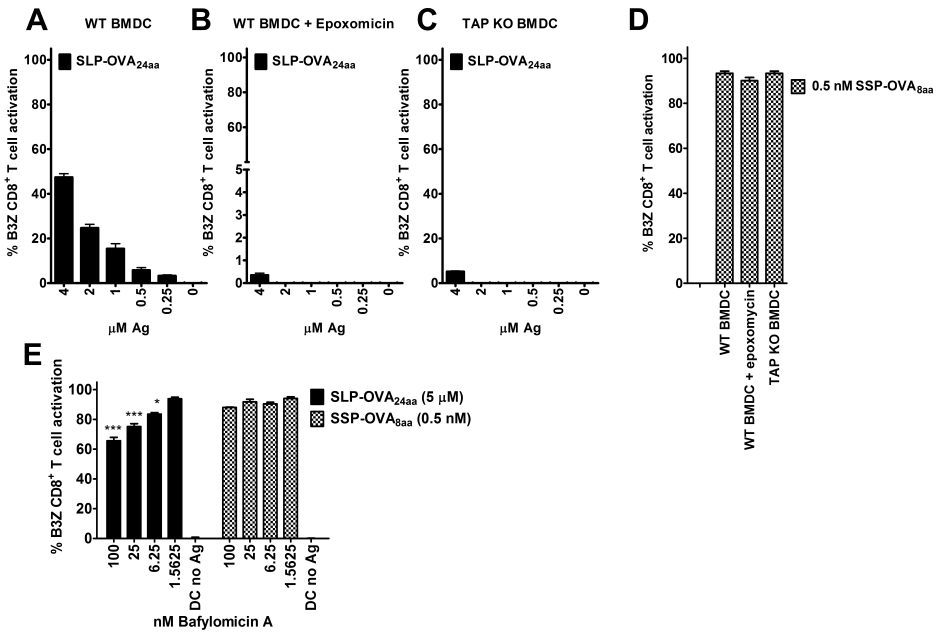


Figure 2.4 MHC class I Ag cross-presentation of SLPs depends on proteasome activity and TAP translocation.

WT C57BL/6 BMDCs were (A) left untreated or (B) pretreated for 60 min with 1 μM epoxomicin before culture with titrated amounts of SLP-OVA_{24aa} or (D) 0.5 nM SSP-OVA_{8aa}. (C, D) TAP1- KO BMDCs were loaded with titrated amounts of SLP-OVA_{24aa} or 0.5 nM SSP-OVA_{8aa}. (E) D1 cells were cultured with the indicated amounts of Baf A for 1 h and then loaded with 5 μM SLP-OVA_{24aa} and 0.5 nM SSP-OVA_{8aa} in continuous presence of Baf A. Ag incubation was carried out for 24 h, cells washed 3x times with complete medium and B3Z CD8⁺ T-cell activation determined after stimulation with Ag-loaded DCs. Data are shown as mean + SD of 3 samples from one experiment representative of three performed. (E) Statistical significance determined with two-way ANOVA and Bonferroni posttests, ***P < 0.001 & *P < 0.05.

a maximally 35% decrease in CD8⁺ T-cell activation at the highest concentration of the compound used (Figure 2.4E). DCs cross-presented SLPs with similar efficiency over a range of Ag-concentrations in the presence of Baf A comparable with that of untreated DCs whereas the cross-presentation of particulate SLPs was considerably decreased (Supporting Information Figure S2.4C, D and E). Lack of Cathepsin S did not modulate MHC class I cross-presentation of SLPs (Supporting Information 4C and E). Collectively, the results suggest that SLPs, upon internalization are most likely cross-presented into MHC class I molecules via classical cytosolic Ag presentation pathways.

SLPs are efficiently cross-presented by murine DCs but poorly by other cell types

Freshly isolated B and T cells were incubated with SLP-OVA_{24aa}, their MHC class I presentation capacity of SLPs compared to DCs. Maximum MHC class I presentation by the different cell types was based on the presentation of SSP-OVA_{8aa}. DCs (Figure 2.5A-C) were superior in cross-presentation of SLPs in comparison to B or T cells. Within this setting, B and T cells failed to activate CD8⁺ T cells upon loading with protein (data not shown). To better mimic the *in vivo* ratio of DC, B and T cells present in the draining lymph nodes (DLN)^{23,24}, MHC

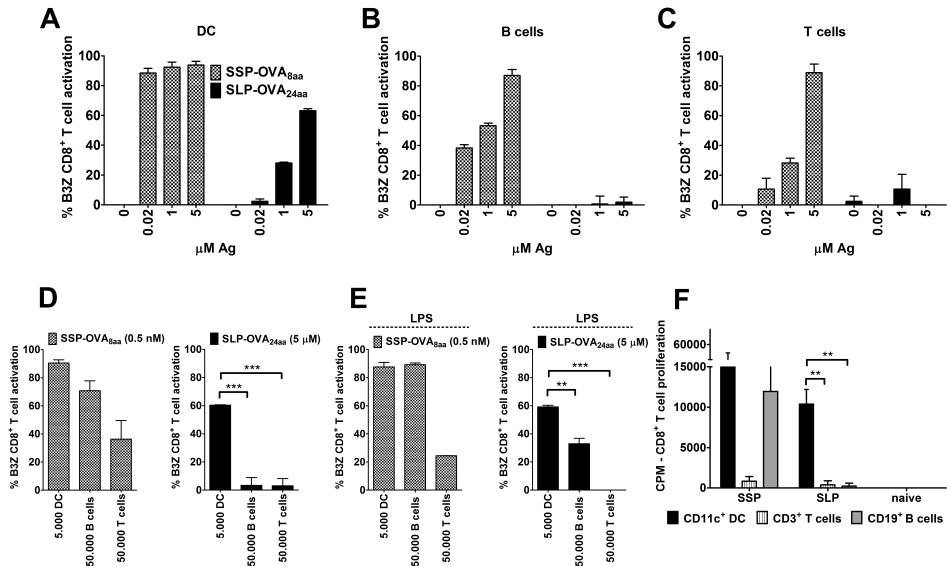


Figure 2.5 DCs specifically and more efficiently cross-present SLPs than B and T cells to CD8⁺ T cells.

(A-C) Five thousand (A) DCs, (B) B cells and (C) T cells were loaded with titrated amounts SLP-OVA_{24aa} and SSP-OVA_{8aa}. B and T-cell numbers were increased 10-fold (50,000 cells) and subsequently loaded with (D) 0.5 μM SSPs and 5 μM SLPs or with (E) LPS (10 μg/ml) added to the cultures. Ag incubation was carried out for 24 h, followed by washing steps and incubation with B3Z T cells. Mice were vaccinated with mixtures of 40 nmol SLP-OVA_{24aa} and 5 nmol CpG ODN 1826. 24 h after vaccination, animals were sacrificed, DLNs removed and CD11c⁺, CD19⁺ and CD3⁺ cells FACS-sorted out and used as APCs in a 72 h *ex vivo* culture with OT-I splenocytes. CD8⁺ OT-I proliferation was determined by ³H-thymidine incorporation. (A-E) Data are shown as mean + SD of 3 samples from one out of two independent cell isolations/experiments performed. (F) The averages ± SEM from two independent experiment/injections are shown. (D, E) Statistical significance determined with one-way ANOVA and Bonferroni posttests; (F) data compared using a Student's t-test. ***P < 0.001, **P < 0.01.

class I Ag presentation by 10-fold higher numbers of B and T cells were also compared to DCs. However, no improvement of CD8⁺ T-cell activation was observed (Figure 2.5D). LPS stimulation of B cells resulted in comparable presentation of SSPs to CD8⁺ T cells as by DCs, but DCs were still superior APC in cross-presenting SLPs even in the presence of LPS (Figure 2.5E). Finally, direct vaccinations with SLPs resulted in preferential internalization *in vivo* and presentation by DCs whereas SSPs can also be presented by B cells (Figure 2.5F). Collectively, these results point to DCs as the primary and most efficient APC to cross-present SLPs in MHC class I molecules.

Discussion

Using two distinct experimental Ag models, we show that both mouse and human DCs more efficiently cross-present SLPs in MHC class I molecules in contrast to whole protein Ag, which poorly induces MHC class I cross-presentation and under the conditions tested fails to activate CD8⁺ T cells. The improved MHC class I cross-presentation of SLPs is possibly related to the distinct intracellular localization of SLPs compared with that of protein Ag upon uptake by DCs. SLPs were shown to be located primarily outside the endo-lysosomes as early as 2 h after Ag incubation. The role of the proteasome and TAP next to the cytosolic presence suggest that SLP Ag is rapidly cross-presented into MHC class I molecules via the classical MHC class I Ag processing pathway^{25,26}, leading to efficient and potent activation of CD8⁺ T cells. Employing a faster cytosolic route upon internalization of SLPs, in contrast to the slower lysosomal route traveled by protein Ag^{27,28}, is compatible with the shorter time span needed for SLPs cross-presentation by DCs.

The advantages of substituting proteins or short peptides by SLPs in active immunization protocols, to enhance *in vivo* priming of anti-tumor CD4⁺ and CD8⁺ T cells have been shown and published before by our group²⁹ and also by others⁶. In these reports, mostly (pre-) clinical *in vivo* observations were described but not the processing mechanisms of SLPs by DCs and the efficiency of the ensuing MHC class I and class II presentation. We have now analyzed the mechanistic aspects of SLP processing and presentation by DCs and show in direct comparisons that SLPs facilitated MHC class I and II Ag presentation by DCs compared with that of equimolar concentrations of protein Ag. These results are in accordance with the study by Zhang et al.⁶ who showed that, in comparison to long peptide vaccines, vaccinations with soluble protein led to poor protection of mice against a lethal viral challenge which was associated with insufficient CD4⁺ T-cell responses and low specific CD8⁺ T-cell responses.

Relatively poor potency of protein based vaccines to induce CD8⁺ T-cell responses *in vitro* and *in vivo* can be enhanced by coupling of targeting moieties³⁰⁻³³ or via encapsulation in PLGA-particles³⁴. These methods are all believed to improve uptake and processing by professional APCs. Likewise, potency of SLPs can be further enhanced, via encapsulation in PLGA-particles³⁵, by antibody-targeting strategies³² and as published previously by our group, production of SLP-TLRL peptide-conjugates²² that will undergo phase I clinical trial testing in the near future.

Our data at face value might contradict other pre-clinical studies showing better MHC class I Ag presentation and CD8⁺ T-cell activation using OVA-protein as Ag²⁷. This discrepancy can be explained by the fact that the B3Z CD8⁺ T-cell clone used in our study to analyze MHC class I Ag presentation is co-stimulation independent and is purely dependent on the recognition of the H2-k^b/SIINFEKL complexes. Using co-stimulation dependent OT-I CD8⁺ T cells MHC class I cross-presentation of OVA was detected at concentrations starting from 0.0025 μ M (data not shown) in accordance with other published reports³⁶. However, the use of co-stimulation-independent T-cell clones was vital in the current study to accurately analyze the efficiency of MHC-restricted Ag processing and presentation without interference by additional stimuli modulating T-cell activation.

In the human model, no MHC class I cross-priming of HIV-specific CD8⁺ T cells was detected using whole soluble GAG-protein. MHC class I presentation could be induced by loading DCs with pre-cleaved protein fragments. This observation suggests that the intracellular processing of internalized whole soluble GAG-protein is very inefficient and that pre-cleaved protein fragments facilitate internalization and intracellular Ag processing.

SLPs were clearly present inside DCs after 2 h of incubation. Previous work by our group revealed that DCs required more than 30 min to internalize the SLPs²². As observed before, internalized soluble intact protein ended up mainly in the endosomes of DCs^{37,38}, whereas most of the internalized SLPs was localized outside the endo-lysosomal compartments at all the time points analyzed. Our results partially differ from an earlier published study reporting a larger fraction of internalized long peptides inside the lysosomes. In this study internalized long peptides were detected outside lysosomes at early- but not at late time points⁶. In addition, the authors reported dotted patterns of long peptide Ag inside DCs in contrast to the diffuse pattern of internalized SLPs, mainly located outside the endo-lysosomes, as we show here. These differences might be related to the DCs used in the respective studies with possibly different functional properties. Zhang et al. used the

DC2.4 murine bone marrow-derived DCs cell line³⁹. We used D1 cells, a cell line closely resembling primary DCs⁴⁰. Confocal analysis with freshly cultured BMDCs confirmed that internalized SLPs were present throughout the cell (data not shown). Importantly, both our results and those of Zhang et al.⁶ show that protein Ag does not or poorly access the cytosol upon internalization by DCs. Therefore, we can conclude that (synthetic) long peptide Ag and protein Ag are routed differently in DCs.

Lack of specific markers for the cytosol thwarted our attempts to conclusively show that SLPs are in the cytosol. Nevertheless, the proteasome inhibition experiments and experiments with TAP1 KO DCs provide important evidence that ingested SLPs end up in the cytosol for processing and presentation.

Some recent reports have indicated that some proteases associated with MHC class II Ag presentation could also play a role in class I cross-presentation^{25,26}. Ag trimming in endo-lysosomes by proteases are pH-dependent. A significant role for Cathepsin S, which has optimal activity at neutral pH⁴¹, in the processing of SLPs into MHC class I molecules was excluded. Inhibitors of endo-lysosomal acidification have been shown to block the translocation of protein from the endosomes to the cytosol⁴². The minor decrease in MHC class I presentation of SLPs by DCs in the presence of Baf A might be due to decreased translocation of internalized SLPs from the endo-lysosomes to the cytosol, limiting the amount of SLPs cleaved by the proteasome..

DCs incubated with SSPs resulted in the most rapid and vigorous T-cell activation in comparison to the SLPs. However, immunizations with SSPs are associated with considerable limitations^{43,44}; for example the lack of CD4⁺ T-cell help characterizing the use of short peptides representing minimal CD8⁺ T-cell epitopes. Other restrictions are the necessity for HLA-typing for each patient to be treated and tolerance induction due to SSP presentation by non-professional APC¹¹. Another disadvantage of SSPs is the short-lived *in vitro* Ag presentation in comparison to SLPs⁴⁵ which, next to SSP loading on non-professional APCs might underlie the vanishing CD8⁺ T-cell responses observed *in vivo* following vaccination with SSPs⁴⁶. SLPs are not able to bind directly to MHC class I and their presentation to CD8⁺ T cells therefore requires uptake and processing by DCs before they are presented^{43,47}. Interestingly, Eikawa et al showed that MHC class I presentation by human APC of NY-ESO-1 long peptides could be blocked by inhibiting actin filament formation⁴⁷.

A vital aspect of efficient T-cell priming *in vivo* is specific Ag presentation by DCs and not by other immune cells that lack the capacity to provide adequate co-stimulation and thus

may cause T-cell tolerance^{48,49}. DCs are present in lower numbers in human blood but also in lymphoid tissues^{23,24}. In addition, s.c. or intradermally administered SLP-vaccines do not require active transport by phagocytic cells due to their small size (1.5 – 5 kD). Most likely SLP-vaccines enter the DLN through passive transport⁵⁰ where they encounter abundant numbers of B cells in the B-cell follicles before accessing resident or migrating DCs present in the T-cell zone^{51,52}. But B cells isolated from vaccinated animals were not capable of priming naïve CD8⁺ T cells *ex vivo* 1 day post subcutaneous vaccination with SLPs (Figure 2.5), whereas CD11c⁺ DCs isolated from the same DLN showed potent capacity to prime naïve CD8⁺ T cells. in accordance with the data of Bijker et al.⁸.

Previous reports describing the *in vivo* potency of vaccinations with SLPs have not revealed a mechanistic basis for the observed enhanced anti-tumor T-cell responses in cancer patients^{9,53}.

Our novel findings, involving a head to head comparison show conclusively that SLPs are far more efficiently processed into both the MHC class I and class II Ag presentation pathways by DCs in comparison with soluble protein. MHC class I cross-presentation of SLPs is accomplished via processing mechanisms most commonly associated with the classical cytosolic MHC class I Ag cross-presentation pathways⁵⁴. In addition, DCs loaded with SLPs potently activate CD4⁺ T cells. Dual priming of both CD4⁺ and CD8⁺ T cells by the same DCs likely underlies the potent and efficient adaptive cellular immune responses observed upon therapeutic vaccinations with SLPs in patients with (pre-)malignant diseases.

Material and methods

Mice

WT C57BL/6 (CD45.2/Thy1.2; H2-K^b) mice were obtained from Charles River Laboratories (France). F1 progeny of C57BL/6 x C3H (H2-K^k) and OT-I/Thy1.1/CD45.2 were bred in the specific pathogen-free animal facility of the Leiden University Medical Center. TAP1 KO mice (C57BL/6 CD45.2/Thy1.2; H2-K^b) were purchased from the Jackson laboratory (Bar Harbor, ME). All mice were used at 8–12 weeks of age in accordance with national legislation and under supervision of the animal experimental committee of the University of Leiden.

Peptides and proteins

For the murine OVA-experimental model, peptides were generated, purified, dissolved and stored as described previously⁵⁵. Fluorescent labeling of SLP-OVA_{24aa} with BODIPY-FL N-(2-aminoethyl) maleimide was performed as described before (Table 2.1)⁵⁵ and endotoxin-free ovalbumin (OVA, Worthington LS003048) used. Ovalbumin-Alexa Fluor® 488 was purchased from Invitrogen. Table 2.1 also describes the peptides used for the experiments with human cells. HIV-1 GAG-protein was generated as described before⁵⁶, over-expressed in Escherichia coli BL21 (DE3) and purified as described before⁵⁷.

Cells

Human monocyte derived DC (MoDC) were obtained from freshly isolated peripheral blood mononuclear cells (PBMCs) in buffy coats of healthy blood donors and generated by isolating CD14⁺ monocytes. The generation of the HIV-specific CD8⁺ T-cell line has been

Table 2.1 List of peptides used

Abbreviation	Location in protein (begin-end)	Chemical modifications	Sequence
SSP-OV _{A8a} a	257–264	SSP-OVA _{257–264}	<u>SIINFEKL</u>
SSP-OVA _{8aa}	257–264	SSP-OVA _{257–264} -Bodipy	<u>SIINFEKL</u> -Bodipy
SLP-OV _{A24a} a	247–264	SLP-OVA _{247–264} ASK	DEVSGLEQLES <u>SIINFEKL</u> AAAAAK
SLP-OVA _{24aa} - Bodipy	247–264	SLP-OVA _{247–264} ASK -Bodipy	DEVSGLEQLES <u>SIINFEKL</u> AAAAAK-Bodipy
SLP-OVA _{31aa}	240–264	SLP-OVA _{240–264} ASK	SMLVLLPDEVSGLEQLES <u>SIINFEKL</u> AAAAAK
SLP-OVA _{31aa} - Bodipy	240–264	SLP-OVA _{240–264} ASK -Bodipy	SMLVLLPDEVSGLEQLES <u>SIINFEKL</u> AAAAAK-Bodipy
SLP-OVA _{17aa}	323–339	SLP-OVA _{323–339}	<u>ISOAVHAAHAEINEAGR</u>
SLP-OVA _{17aa} - Bodipy	323–339	SLP-OVA _{323–339} -Bodipy	<u>ISOAVHAAHAEINEAGR</u> -Bodipy
SLP-OVA _{31aa}	316–346	SLP-OVA _{316–346}	SSAESLK <u>ISQAVHAAHAEINEAGRE</u> VVGSAE
SLP-OVA _{31aa} - Bodipy	316–346	SLP-OVA _{316–346} -Bodipy	SSAESLK <u>ISQAVHAAHAEINEAGRE</u> VVGSAE-Bodipy
SSP-GA _{G9a} a	223–231	SSP-GAG _{223–231}	<u>GPGHKARVL</u>
SLP-GA _{G22a} a	216–237	SLP-GAG _{216–237}	TACQGVGG <u>GPGHKARVL</u> AEAMSQ

described before⁵⁸. Freshly isolated murine DC were cultured from mouse bone marrow (BM) cells, as described before⁵⁹. The D1 cell line, an immature primary splenic DC line (C57BL/6-derived), was cultured as described elsewhere⁶⁰. B3Z CD8⁺ T cells, OT-IIZ and KZO CD4⁺ T-cells are hybridoma cell lines expressing a β -galactosidase construct which upon T-cell activation can be measured by a colorimetric assay²².

Murine MHC class I and class II Ag presentation assays

Unless otherwise indicated, 100,000 DC were plated out in triplicate using Greiner flat bottom 96-wells plate (#655101) and incubated for 24 hr with the Ags at the indicated concentrations. In some experiments, DCs were cultured in the presence of 10 μ g/ml LPS prior to Ag incubation. Cells were washed 3x times with complete medium to remove excess Ag before the T-cell hybridoma B3Z CD8⁺ T cells (H2-k^b/SIINFEKL), KZO CD4⁺ T cells (I-A^k/DEVSGLEQLESI) or OT-IIZ CD4⁺ T cells (I-A^{kb}/ISQAVHAAHAEINEAGR) were added. T cells were cultures in the presence of Ag-loaded DC O/N at 37°C. To study kinetics of MHC class I and class II presentation, DCs were incubated with 10 nM SSPs, 10 μ M SLPs or 10 μ M protein for 1, 3 or 5 hr. After 3x washing, DCs were fixated by adding 50 μ l/well of 0.2% PFA for 15 min. Fixation was blocked by adding 150 μ l/well complete medium. In experiments aimed to study intracellular processing pathways involved in SLP-cross presentation in MHC class I molecules, BMDC or D1 cells were pre-incubated with epoxomicin (324800, Merck) or bafilomycin A1 (196000, Merck) followed by Ag-incubation as described above in the presence of the compounds. To assess Ag presentation by other cells in comparison to DC, B and T cells were isolated from total spleen single cell suspensions, FACS-sorted, and incubated with titrated amounts of SLP-OVA_{24aa'}, SSP-OVA_{8aa} or OVA and subsequently used as APC in co-cultures with B3Z CD8⁺ T cells as described above.

***In vitro* analysis of human T-cell activation**

Human CD8⁺ T-cell activation was studied using MoDC cross-presenting Ags to human HIV-specific CD8 T cells. The cytokine production of HIV-specific CD8⁺ T cells was used as read out. To this purpose, MoDC were incubated for the indicated time with Gag-protein, SLP-GAG_{22aa'}, SSP-GAG_{9aa} or medium as a control. After the indicated incubation, MoDC were fixed with 0.2% paraformaldehyde (PFA) to prevent further processing and HIV-specific CD8 T cells were added (at approximately 5 T-cell: 1 DC ratio) followed by

overnight culture at 37°C/5%CO₂. After 18 hr, supernatant was harvested to determine IFN-γ production by ELISA according to the manufacturer's protocol (Sanquin, Amsterdam, The Netherlands).

***In vitro* analysis of human T-cell activation by MoDC incubated with EndoGluc-CNBr GAG-protein fragments**

Human CD8⁺ T-cell activation was studied using MoDC cross-presenting EndoGluc-CNBr GAG-protein fragments, which were generated as described above, to human HIV-specific CD8 T cells. The cytokine production of HIV-specific CD8⁺ T cells was used as read out. For this purpose, MoDC were incubated with GAG-protein, SLP-GAG_{22aa} and EndoGluc-CNBr GAG-protein fragments. After 24 hr incubation, HIV-specific CD8 T-cells were added (at approximately 5 T-cell: 1 DC ratio) followed by overnight culture at 37°C/5%CO₂. Brefeldin A (10 µg/ml, Sigma-Aldrich) was added to retain cytokines within the T-cells allowing the detection of multiple cytokines. After 18 hr, intracellular cytokine staining (ICS) was performed as described⁶¹. Cells were fixed and permeabilized using Cytofix/Cytoperm™ Fixation/Permeabilization Solution Kit (BD). Cells were then incubated with α-TNF PE-Cy7 (clone MAb11, eBiosciences), α-IFN-γ FITC, α-IL-2 APC, α-MIP-1β PE (all three from BD) and α-CD8 PerCP (Dako). After washing, cells were analyzed by flow cytometry using a LSRII flow cytometer (BD Pharmingen) and analyzed with FlowJo software (Treestar). Cells were first gated based on the characteristics forward and side scatter properties, followed by identification of CD3⁺CD8⁺ T cells followed by intracellular analysis of cytokines produced within the gated CD8⁺ T cells. Net accumulation of activated GAG-specific CD8⁺ T-cells is the percentage of live CD8⁺ cells expressing one or more of the analyzed cytokines upon stimulation with MoDC loaded with Ag.

Confocal microscopy

DC were incubated for 2, 5 and 24 hr with 20 µM SLP-OVA_{17aa}-Bodipy and SLP-OVA_{24aa}-Bodipy at 37°C. After incubation cells were washed 3 times to remove excess and unbound Ag, resuspended at a concentration of 2x10⁵ cells in 200 µl complete medium and plated into poly-d-lysine coated glass-bottom dishes (MatTek) followed by mild centrifugation to allow the cells to adhere. Adhered cells were then fixed with 0.2% paraformaldehyde. All experiments were carried out on a Leica TCS SP5 confocal microscope (HCX PL APO 63x/1.4 NA oil-immersion objective, 12 bit resolution, 1024x1024 pixels, pinhole 2.1 Airy

discs, zoomfactor 1 or 7). Imaging was performed using the 488 nm line from an Argon laser collecting emission between 500 and 600 nm.

Alternatively, DC were incubated for 24 hr with 10 μ M OVA-protein-Alexa488 or SLP-OVA_{24aa}-Bodipy at 37°C. After incubation cells were washed 3 times to remove excess and unbound Ag followed by 30 min incubation with 300 nM LysoTracker® red (Invitrogen) to stain endo-lysosomal compartments. After incubation, cells were washed and resuspended at a concentration of 2×10^5 cells 200 μ l and plated into poly-d-lysine coated glass-bottom dishes (MatTek) 2 hr before analysis to allow cells to adhere. Cells were imaged using an inverted Leica TCS SP5 confocal microscope. Dual color images were acquired by sequential scanning, with only one laser per scan to avoid cross talk. The images were analyzed using the Leica software program (LAS AF).

Vaccination and *ex vivo* Ag presentation

Animals were injected subcutaneously (s.c.) with 40 nmol of SLPs or SSPs mixed with 5 nmol CpG (Invivogen). One day later, sacrificed and draining lymph nodes (DLN) harvested and single cell suspensions prepared. To assess *ex vivo* Ag presentation, CD11c⁺ DC, CD19⁺ B and CD3⁺ T cells were isolated purified using FACS-sorting from DLN cell suspensions and subsequently used as APC in co-cultures with OT-I CD8⁺ T cells.

Statistics

Statistical analyses applied to determine the significance of differences are described in the figure legends.

Acknowledgements

We acknowledge the support of Ing. A. van der Laan from the Dept of Molecular Cell biology and Imaging Facility of the LUMC. We thank Dr. Nilabh Shastri for his kind gift of the KZO T-cell hybridoma. The following reagent was obtained through the NIH AIDS Research and Reference Reagent Program, Division of AIDS, NIAID, NIH: pGag-EGFP (Cat#11468) from Dr. Marilyn Resh. The PBMCs from which the HIV-specific CD8⁺ T cells were generated were kindly provided by Prof. G. Pantaleo. This study was supported by grants from Immune System Activation (ISA) Pharmaceuticals, University of Leiden and the Leiden University Medical Center.

References

1. Banchereau J, Steinman RM 1998. Dendritic cells and the control of immunity. *Nature* 392:245-252.
2. Huang LM, Lu CY, Chen DS 2011. Hepatitis B virus infection, its sequelae, and prevention by vaccination. *Curr Opin Immunol* 23:237-243.
3. Frazer IH, Lowy DR, Schiller JT 2007. Prevention of cancer through immunization: Prospects and challenges for the 21st century. *Eur J Immunol* 37 Suppl 1:S148-S155.
4. Schiller JT, Lowy DR 2010. Vaccines to prevent infections by oncoviruses. *Annu Rev Microbiol* 64:23-41.
5. Atanackovic D, Altorki NK, Stockert E, Williamson B, Jungbluth AA, Ritter E, Santiago D, Ferrara CA, Matsuo M, Selvakumar A, Dupont B, Chen YT, Hoffman EW, Ritter G, Old LJ, Gnjatic S 2004. Vaccine-induced CD4+ T cell responses to MAGE-3 protein in lung cancer patients. *J Immunol* 172:3289-3296.
6. Zhang H, Hong H, Li D, Ma S, Di Y, Stoten A, Haig N, Di GK, Yu Z, Xu XN, McMichael A, Jiang S 2009. Comparing pooled peptides with intact protein for accessing cross-presentation pathways for protective CD8+ and CD4+ T cells. *J Biol Chem* 284:9184-9191.
7. Chua BY, Pejoski D, Turner SJ, Zeng W, Jackson DC 2011. Soluble proteins induce strong CD8+ T cell and antibody responses through electrostatic association with simple cationic or anionic lipopeptides that target TLR2. *J Immunol* 187:1692-1701.
8. Bijker MS, van den Eeden SJ, Franken KL, Melief CJ, van der Burg SH, Offringa R 2008. Superior induction of anti-tumor CTL immunity by extended peptide vaccines involves prolonged, DC-focused antigen presentation. *Eur J Immunol* 38:1033-1042.
9. Kenter GG, Welters MJ, Valentijn AR, Lowik MJ, Berends-van der Meer DM, Vloon AP, Essahsah F, Fathers LM, Offringa R, Drijfhout JW, Wafelman AR, Oostendorp J, Fleuren GJ, van der Burg SH, Melief CJ 2009. Vaccination against HPV-16 oncoproteins for vulvar intraepithelial neoplasia. *N Engl J Med* 361:1838-1847.
10. Kenter GG, Welters MJ, Valentijn AR, Lowik MJ, Berends-van der Meer DM, Vloon AP, Drijfhout JW, Wafelman AR, Oostendorp J, Fleuren GJ, Offringa R, van der Burg SH, Melief CJ 2008. Phase I immunotherapeutic trial with long peptides spanning the E6 and E7 sequences of high-risk human papillomavirus 16 in end-stage cervical cancer patients shows low toxicity and robust immunogenicity. *Clin Cancer Res* 14:169-177.
11. Melief CJ, van der Burg SH 2008. Immunotherapy of established (pre)malignant disease by synthetic long peptide vaccines. *Nat Rev Cancer* 8:351-360.
12. Welters MJ, Kenter GG, de Vos van Steenwijk PJ, Lowik MJ, Berends-van der Meer DM, Essahsah F, Stynenbosch LF, Vloon AP, Ramwadhoebe TH, Piersma SJ, van der Hulst JM, Valentijn AR, Fathers LM, Drijfhout JW, Franken KL, Oostendorp J, Fleuren GJ, Melief CJ, van der Burg SH 2010. Success or failure of vaccination for HPV16-positive vulvar lesions correlates with kinetics and phenotype of induced T-cell responses. *Proc Natl Acad Sci U S A* 107:11895-11899.

13. Speetjens FM, Kuppen PJ, Welters MJ, Essahsah F, Voet van den Brink AM, Lantrua MG, Valentijn AR, Oostendorp J, Fathers LM, Nijman HW, Drijfhout JW, van de V, Melief CJ, van der Burg SH 2009. Induction of p53-specific immunity by a p53 synthetic long peptide vaccine in patients treated for metastatic colorectal cancer. *Clin Cancer Res* 15:1086-1095.
14. Sabbatini P, Tsuji T, Ferran L, Ritter E, Sedrak C, Tuballes K, Jungbluth AA, Ritter G, Aghajanian C, Bell-McGuinn K, Hensley ML, Konner J, Tew W, Spriggs DR, Hoffman EW, Venhaus R, Pan L, Salazar AM, Diefenbach CM, Old LJ, Gnjatic S 2012. Phase I Trial of Overlapping Long Peptides from a Tumor Self-Antigen and Poly-ICLC Shows Rapid Induction of Integrated Immune Response in Ovarian Cancer Patients. *Clinical Cancer Research* 18:6497-6508.
15. Arevalo-Herrera M, Soto L, Perlaza BL, Cespedes N, Vera O, Lenis AM, Bonelo A, Corradin G, Herrera S 2011. Antibody-mediated and cellular immune responses induced in naive volunteers by vaccination with long synthetic peptides derived from the Plasmodium vivax circumsporozoite protein. *Am J Trop Med Hyg* 84:35-42.
16. Olugbile S, Villard V, Bertholet S, Jafarshad A, Kulangara C, Roussillon C, Frank G, Agak GW, Felger I, Nebie I, Konate K, Kajava AV, Schuck P, Druilhe P, Spertini F, Corradin G 2011. Malaria vaccine candidate: Design of a multivalent subunit alpha-helical coiled coil poly-epitope. *Vaccine* 29:7090-7099.
17. Rosario M, Bridgeman A, Quakkelaar ED, Quigley MF, Hill BJ, Knudsen ML, Ammendola V, Ljungberg K, Borthwick N, Im EJ, McMichael AJ, Drijfhout JW, Greenaway HY, Venturi V, Douek DC, Colloca S, Liljestrom P, Nicosia A, Price DA, Melief CJ, Hanke T 2010. Long peptides induce polyfunctional T cells against conserved regions of HIV-1 with superior breadth to single-gene vaccines in macaques. *Eur J Immunol* 40:1973-1984.
18. Rosario M, Borthwick N, Stewart-Jones GB, Mbewe-Mvula A, Bridgeman A, Colloca S, Montefiori D, McMichael AJ, Nicosia A, Quakkelaar ED, Drijfhout JW, Melief CJ, Hanke T 2012. Prime-boost regimens with adjuvanted synthetic long peptides elicit T cells and antibodies to conserved regions of HIV-1 in macaques. *AIDS* 26:275-284.
19. Zeng G, Li Y, El-Gamil M, Sidney J, Sette A, Wang Rf, Rosenberg SA, Robbins PF 2002. Generation of NY-ESO-1-specific CD4+ and CD8+ T Cells by a Single Peptide with Dual MHC Class I and Class II Specificities. *Cancer Research* 62:3630-3635.
20. Knutson KL, Schiffman K, Disis ML 2001. Immunization with a HER-2/neu helper peptide vaccine generates HER-2/neu CD8 T-cell immunity in cancer patients. *J Clin Invest* 107:477-484.
21. van der Burg SH, Melief CJ 2011. Therapeutic vaccination against human papilloma virus induced malignancies. *Curr Opin Immunol* 23:252-257.
22. Khan S, Bijker MS, Weterings JJ, Tanke HJ, Adema GJ, van HT, Drijfhout JW, Melief CJ, Overkleef HS, van der Marel GA, Filippov DV, van der Burg SH, Ossendorp F 2007. Distinct uptake mechanisms but similar intracellular processing of two different toll-like receptor ligand-peptide conjugates in dendritic cells. *J Biol Chem* 282:21145-21159.
23. Baldazzi V, Paci P, Bernaschi M, Castiglione F 2009. Modeling lymphocyte homing and encounters in lymph nodes. *BMC Bioinformatics* 10:387.

24. von Andrian UH, Mempel TR 2003. Homing and cellular traffic in lymph nodes. *Nat Rev Immunol* 3:867-878.
25. Singh R, Cresswell P 2010. Defective cross-presentation of viral antigens in GILT-free mice. *Science* 328:1394-1398.
26. Rock KL, Farfan-Arribas DJ, Shen L 2010. Proteases in MHC class I presentation and cross-presentation. *J Immunol* 184:9-15.
27. Burgdorf S, Scholz C, Kautz A, Tampe R, Kurts C 2008. Spatial and mechanistic separation of cross-presentation and endogenous antigen presentation. *Nat Immunol* 9:558-566.
28. Chen L, Jondal M 2004. Endolysosomal processing of exogenous antigen into major histocompatibility complex class I-binding peptides. *Scand J Immunol* 59:545-552.
29. Zwaveling S, Ferreira Mota SC, Nouta J, Johnson M, Lipford GB, Offringa R, van der Burg SH, Melief CJ 2002. Established human papillomavirus type 16-expressing tumors are effectively eradicated following vaccination with long peptides. *J Immunol* 169:350-358.
30. Bonifaz LC, Bonnyay DP, Charalambous A, Darguste DI, Fujii S, Soares H, Brimnes MK, Moltedo B, Moran TM, Steinman RM 2004. In vivo targeting of antigens to maturing dendritic cells via the DEC-205 receptor improves T cell vaccination. *J Exp Med* 199:815-824.
31. Rudd BD, Brien JD, Davenport MP, Nikolich-Zugich J 2008. Cutting edge: TLR ligands increase TCR triggering by slowing peptide-MHC class I decay rates. *J Immunol* 181:5199-5203.
32. Kreutz M, Giquel B, Hu Q, Abuknesha R, Uematsu S, Akira S, Nestle FO, Diebold SS 2012. Antibody-antigen-adjuvant conjugates enable co-delivery of antigen and adjuvant to dendritic cells in cis but only have partial targeting specificity. *PLoS One* 7:e40208.
33. Singh SK, Streng-Ouwehand I, Litjens M, Kalay H, Burgdorf S, Saeland E, Kurts C, Unger WW, van KY 2011. Design of neo-glycoconjugates that target the mannose receptor and enhance TLR-independent cross-presentation and Th1 polarization. *Eur J Immunol* 41:916-925.
34. Shen H, Ackerman AL, Cody V, Giodini A, Hinson ER, Cresswell P, Edelson RL, Saltzman WM, Hanlon DJ 2006. Enhanced and prolonged cross-presentation following endosomal escape of exogenous antigens encapsulated in biodegradable nanoparticles. *Immunology* 117:78-88.
35. Silva AL, Rosalia RA, Sazak A, Carstens MG, Ossendorp F, Oostendorp J, Jiskoot W Optimization of encapsulation of a synthetic long peptide in PLGA nanoparticles: low burst release is crucial for efficient CD8+ T cell activation. *European Journal of Pharmaceutics and Biopharmaceutics*.
36. Burgdorf S, Schuette V, Semmling V, Hochheiser K, Lukacs-Kornek V, Knolle PA, Kurts C 2010. Steady-state cross-presentation of OVA is mannose receptor-dependent but inhibitable by collagen fragments. *Proc Natl Acad Sci U S A* 107:E48-E49.
37. Chen L, Jondal M 2004. Endolysosomal processing of exogenous antigen into major histocompatibility complex class I-binding peptides. *Scand J Immunol* 59:545-552.
38. Burgdorf S, Scholz C, Kautz A, Tampe R, Kurts C 2008. Spatial and mechanistic separation of cross-presentation and endogenous antigen presentation. *Nat Immunol* 9:558-566.

39. Hargadon KM, Forrest OA, Reddy PR 2012. Suppression of the maturation and activation of the dendritic cell line DC2.4 by melanoma-derived factors. *Cellular Immunology* 272:275-282.
40. van Helden SFG, van Leeuwen FN, Figdor CG 2008. Human and murine model cell lines for dendritic cell biology evaluated. *Immunology Letters* 117:191-197.
41. Claus V, Jahraus A, Tjelle T, Berg T, Kirschke H, Faulstich H, Griffiths G 1998. Lysosomal enzyme trafficking between phagosomes, endosomes, and lysosomes in J774 macrophages. Enrichment of cathepsin H in early endosomes. *J Biol Chem* 273:9842-9851.
42. Horiguchi M, Arita M, Kaempf-Rotzoll DE, Tsujimoto M, Inoue K, Arai H 2003. pH-dependent translocation of alpha-tocopherol transfer protein (alpha-TTP) between hepatic cytosol and late endosomes. *Genes Cells* 8:789-800.
43. Melief CJ 2008. Cancer immunotherapy by dendritic cells. *Immunity* 29:372-383.
44. van HT, van der Burg SH 2012. Mechanisms of peptide vaccination in mouse models: tolerance, immunity, and hyperreactivity. *Adv Immunol* 114:51-76.
45. Faure F, Mantegazza A, Sadaka C, Sedlik C, Jotereau F, Amigorena S 2009. Long-lasting cross-presentation of tumor antigen in human DC. *Eur J Immunol* 39:380-390.
46. Bijker MS, van den Eeden SJ, Franken KL, Melief CJ, Offringa R, van der Burg SH 2007. CD8+ CTL priming by exact peptide epitopes in incomplete Freund's adjuvant induces a vanishing CTL response, whereas long peptides induce sustained CTL reactivity. *J Immunol* 179:5033-5040.
47. Eikawa S, Kakimi K, Isobe M, Kuzushima K, Luescher I, Ohue Y, Ikeuchi K, Uenaka A, Nishikawa H, Uono H, Oka M, Nakayama E 2013. Induction of CD8 T-cell responses restricted to multiple HLA class I alleles in a cancer patient by immunization with a 20-mer NY-ESO-1f (NY-ESO-1 91-110) peptide. *Int J Cancer* 132:345-354.
48. Guermonprez P, Valladeau J, Zitvogel L, Thery C, Amigorena S 2002. Antigen presentation and T cell stimulation by dendritic cells. *Annu Rev Immunol* 20:621-667.
49. Bennett SR, Carbone FR, Toy T, Miller JF, Heath WR 1998. B cells directly tolerize CD8(+) T cells. *J Exp Med* 188:1977-1983.
50. Manolova V, Flace A, Bauer M, Schwarz K, Saudan P, Bachmann MF 2008. Nanoparticles target distinct dendritic cell populations according to their size. *Eur J Immunol* 38:1404-1413.
51. Jenkins MK, Khoruts A, Ingulli E, Mueller DL, McSorley SJ, Reinhardt RL, Itano A, Pape KA 2001. In vivo activation of antigen-specific CD4 T cells. *Annu Rev Immunol* 19:23-45.
52. Gretz JE, Norbury CC, Anderson AO, Proudfoot AE, Shaw S 2000. Lymph-borne chemokines and other low molecular weight molecules reach high endothelial venules via specialized conduits while a functional barrier limits access to the lymphocyte microenvironments in lymph node cortex. *J Exp Med* 192:1425-1440.

53. de Vos van Steenwijk PJ, Ramwadhoebe TH, Lowik MJ, van der Minne CE, Berends-van der Meer DM, Fathers LM, Valentijn AR, Oostendorp J, Fleuren GJ, Hellebrekers BW, Welters MJ, van Poelgeest MI, Melief CJ, Kenter GG, van der Burg SH 2012. A placebo-controlled randomized HPV16 synthetic long-peptide vaccination study in women with high-grade cervical squamous intraepithelial lesions. *Cancer Immunol Immunother* 61:1485-1492.
54. Joffre OP, Segura E, Savina A, Amigorena S 2012. Cross-presentation by dendritic cells. *Nat Rev Immunol* 12:557-569.
55. Feltkamp MC, Smits HL, Vierboom MP, Minnaar RP, de Jongh BM, Drijfhout JW, ter Schegget J, Melief CJ, Kast WM 1993. Vaccination with cytotoxic T lymphocyte epitope-containing peptide protects against a tumor induced by human papillomavirus type 16-transformed cells. *Eur J Immunol* 23:2242-2249.
56. Schwartz S, Campbell M, Nasioulas G, Harrison J, Felber BK, Pavlakis GN 1992. Mutational inactivation of an inhibitory sequence in human immunodeficiency virus type 1 results in Rev-independent gag expression. *Journal of Virology* 66:7176-7182.
57. Franken KL, Hiemstra HS, van Meijgaarden KE, Subronto Y, den Hartigh J, Ottenhoff TH, Drijfhout JW 2000. Purification of his-tagged proteins by immobilized chelate affinity chromatography: the benefits from the use of organic solvent. *Protein Expr Purif* 18:95-99.
58. Quakkelaar ED, Redeker A, Haddad EK, Harari A, McCaughey SM, Duhon T, Filali-Mouhim A, Goulet JP, Loof NM, Ossendorp F, Perdiguero B, Heinen P, Gomez CE, Kibler KV, Koelle DM, Sekaly RP, Sallusto F, Lanzavecchia A, Pantaleo G, Esteban M, Tartaglia J, Jacobs BL, Melief CJ 2011. Improved innate and adaptive immunostimulation by genetically modified HIV-1 protein expressing NYVAC vectors. *PLoS One* 6:e16819.
59. van Montfoort N, Camps MG, Khan S, Filippov DV, Weterings JJ, Griffith JM, Geuze HJ, van Hall T, Verbeek JS, Melief CJ, Ossendorp F 2009. Antigen storage compartments in mature dendritic cells facilitate prolonged cytotoxic T lymphocyte cross-priming capacity. *Proc Natl Acad Sci U S A* 106:6730-6735.
60. Schuurhuis DH, Ioan-Facsinay A, Nagelkerken B, van Schip JJ, Sedlik C, Melief CJ, Verbeek JS, Ossendorp F 2002. Antigen-antibody immune complexes empower dendritic cells to efficiently prime specific CD8+ CTL responses in vivo. *J Immunol* 168:2240-2246.
61. Jing L, McCaughey SM, Davies DH, Chong TM, Felgner PL, De Rosa SC, Wilson CB, Koelle DM 2009. ORFeome approach to the clonal, HLA allele-specific CD4 T-cell response to a complex pathogen in humans. *J Immunol Methods* 347:36-45.

Supporting Information – Material and methods

HIV-1 GAG-protein Identification by Mass Spectrometry (MS)

HIV-GAG protein was digested with CNBr and endoproteinase GluC as follows: 400 µg HIV-GAG was reduced with DTT and alkylated with iodoacetamide. Chemical cleavage at methionine with CNBr in 70% formic acid was performed as described by ¹. After lyophilization, the protein was additionally digested for 16 h at ambient temperature with 40 µg endoproteinase GluC (Worthington) in ammonium bicarbonate pH 7.8. The mixture was passed through a 30 kD Microcon (Millipore) filter and peptides recovered from the filtrate (flow-through). The filtrate was lyophilized, dissolved in 95/3/0.1 v/v/v water/acetonitril/formic acid and subsequently analyzed by on-line nanoHPLC MS/MS using an 1100 HPLC system (Agilent Technologies), as previously described ². Peptides were trapped at 10 µL/min on a 15-mm column (100-µm ID; ReproSil-Pur C18-AQ, 3 µm, Dr. Maisch GmbH) and eluted to a 200 mm column (50-µm ID; ReproSil-Pur C18-AQ, 3 µm) at 150 nL/min. All columns were packed in house. The column was developed with a 30-min gradient from 0 to 50% acetonitrile in 0.1% formic acid. The end of the nanoLC column was drawn to a tip (ID ~5 µm), from which the eluent was sprayed into a 7-tesla LTQ-FT Ultra mass spectrometer (Thermo Electron). The mass spectrometer was operated in data-dependent mode, automatically switching between MS and MS/MS acquisition. Full scan MS spectra were acquired in the FT-ICR with a resolution of 25,000 at a target value of 3,000,000. The two most intense ions were then isolated for accurate mass measurements by a selected ion monitoring scan in FT-ICR with a resolution of 50,000 at a target accumulation value of 50,000. Selected ions were fragmented in the linear ion trap using collision-induced dissociation at a target value of 10,000. In a post-analysis process, raw data were first converted to peak lists using Bioworks Browser software v 3.2 (Thermo Electron), then submitted to the Swissprot database using Mascot v. 2.2.04 (www.matrixscience.com) for protein identification. Mascot searches were with 2 ppm and 0.8 Da deviation for precursor and fragment mass, respectively, and no enzyme specified. Collision-induced dissociation spectra were manually inspected (see Supporting Information Figure S2.1B)

Human Ag presentation assays with apoptotic HeLa cells

Ag presentation to HIV- and vaccinia-specific human CD8 T-cells was studied using MoDC cross-presenting Ag from HeLa cells that were infected with NYVAC-C as described by

Quakkelaar et al. ³. The cytokine production of HIV-specific CD8 T-cells was assessed. In brief, HeLa cells were harvested by EDTA and infected with NYVAC-C or NYVAC-WT at a MOI of 5 for 1 hour. Cells were extensively washed to remove residual virus. After overnight incubation, cells were irradiated with UV-C (200 $\mu\text{W}/\text{cm}^2$) to ensure that no residual virus and no viable cells were present and thus exclude direct presentation. Apoptotic virus-infected HeLa cells were harvested and added to MoDC at a 2:1 ratio. After 6 hr incubation, HIV- or vaccinia-specific CD8 T-cells were added (at approximately 5 T-cell: 1 DC ratio) followed by overnight culture at 37°C/5%CO₂. Brefeldin A (10 $\mu\text{g}/\text{ml}$, Sigma-Aldrich) was added to retain cytokines within the T-cells allowing the detection of multiple cytokines. After 18 hr, intracellular cytokine staining (ICS) was performed as described ⁴. Cells were fixed and permeabilized using Cytofix/Cytoperm™ Fixation/Permeabilization Solution Kit (BD). Cells were then incubated with α -TNF PE-Cy7 (clone MAb11, eBiosciences), α -IFN- γ FITC, α -IL-2 APC, α -MIP-1 β PE (all three from BD) and α -CD8 PerCP (Dako). After washing, cells were analyzed by flow cytometry using a LSRII flow cytometer (BD Pharmingen) and analyzed with FlowJo software (Treestar). Cells were first gated based on the characteristics forward and side scatter properties, followed by identification of CD3⁺CD8⁺ T cells followed by intracellular analysis of cytokines produced within the gated CD8⁺ T cells. Net accumulation of activated GAG-specific CD8⁺ T-cells is the percentage of live CD8⁺ cells expressing one or more of the analyzed cytokines upon stimulation with MoDC loaded with apoptotic NYVAC-C-infected HeLa cells. Background levels of cytokine production were determined, and subtracted from percentages obtained by GAG-specific stimulation, by culturing GAG-specific CD8⁺ T-cells with MoDC incubated with NYVAC-WT infected HeLa.

Analysis of dendritic cell lysates incubated with fluorescent SLP by Tricine-SDS-PAGE

DC in 2 ml medium containing 2×10^6 cells were incubated with SLP-OVA_{31aa}-Bodipy for 24 hr. After incubation, cells were harvested and washed twice with PBS to remove non-internalized excess Ag. Supernatant was removed, the cell pellet resuspended in 50 μl lysis buffer (LB) (pH 7,4) and stored in eppendorf tubes at -80°C till further use. Cell lysates were subsequently obtained by repetitive freeze-thaw cycles by placing tubes for 30 sec in liquid nitrogen followed by 30 sec in heating blocks (eppendorf thermostat plus) set at 60°C. Cell lysates were analyzed using Tricine-SDS-PAGE gel as described before ⁵ with minor modifications. Briefly, 15 μl cell lysate was then mixed in a 1:1 ratio with *reducing* sample buffer and heated to 95°C for 10 minutes. Samples were next loaded onto a 1.5

mm SDS-PAGE gel (49.5%T 3%C stacking gel and 49.5%T 6%C separating gel). Samples were ran at 90 V through the stacking gel and followed by 5 hr run at 35 V through the separating gel (Biorad systems). Protein and peptides fragments where visualized using Coomassie (Supporting Information Figure S2.3A). Green-fluorescent fragments were imaged and analyzed for *EPI fluorescence intensity* applying *IVIS Imaging Systems*, measuring the fluorescence at 520nm emission wavelength (Supporting Information Figure S2.3B).

PLGA-SLP preparation

Poly-(lactic-co-glycolic-acid) (PLGA) nanoparticles loaded with SLP-OVA_{24aa} were prepared using a double emulsion with solvent evaporation method ⁶.

MHC class I Ag presentation by soluble SLP compared to SLP encapsulated in PLGA-NP in the presence of epoxomicin

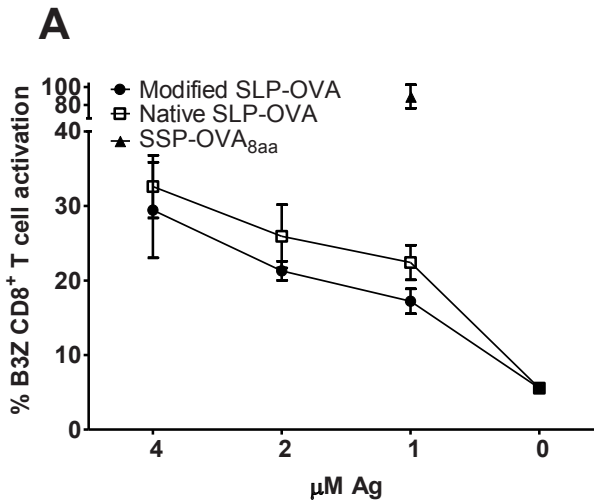
BMDC were left untreated or pre-incubated with 1 μ M *epoxomicin* (324800, Merck) incubated for 24 hr with SSP, SLP or protein or SLP encapsulated in PLGA-NP at the indicated concentrations. Cells were washed three times with medium before the T-cell hybridoma B3Z CD8⁺ T-cells were added followed by O/N incubation at 37°C. MHC class I Ag presentation of OVA₂₅₇₋₂₆₄ in H-2K^b was detected by activation of B3Z cells.

MHC class I Ag presentation by DC in the presence of Bafilomycin or in the absence of Cathepsin S

BMDC were left untreated (A) or pre-incubated with 50 nM of bafilomycin A1 (196000, Merck) followed by Ag-incubation as described above in the presence of the compound (B). Cells were washed three times with medium before the T-cell hybridoma B3Z CD8⁺ T-cells were added followed by O/N incubation at 37°C. BMDC from cathepsin S-deficient (Cathepsin KO) mice were cultured in the presence of titrated amounts of SLP-OVA_{24aa} and SSP-OVA_{8aa} followed by analysis of B3Z CD8⁺ T-cell activation after co-culture with Ag loaded BMDC (C). MHC class I Ag presentation of OVA₂₅₇₋₂₆₄ in H-2K^b was detected by activation of B3Z CD8⁺ T cells.

References

1. Crimmins DL, Mische SM, Denslow ND 2005. Chemical cleavage of proteins in solution. *Curr Protoc Protein Sci.* Chapter 11: Unit.
2. Meiring HD, van der Heeft E, ten Hove GJ, de Jong APJM 2002. Nanoscale LC μ MS(n): technical design and applications to peptide and protein analysis. *J Sep Science* 25:557-568.
3. Quakkelaar ED, Redeker A, Haddad EK, Harari A, McCaughey SM, Duhon T, Filali-Mouhim A, et al. 2011. Improved innate and adaptive immunostimulation by genetically modified HIV-1 protein expressing NYVAC vectors. *PLoS One* 6:e16819.
4. Jing L, McCaughey SM, Davies DH, Chong TM, Felgner PL, De Rosa SC, et al. 2009. ORFeome approach to the clonal, HLA allele-specific CD4 T-cell response to a complex pathogen in humans. *J Immunol Methods* 347:36-45.
5. Schagger H 2006. Tricine-SDS-PAGE. *Nat Protoc* 1:16-22.
6. Silva AL, Rosalia RA, Sazak A, Carstens MG, Ossendorp F, Oostendorp J, Jiskoot W 2013. Optimization of encapsulation of a synthetic long peptide in PLGA nanoparticles: low burst release is crucial for efficient CD8⁺ T cell activation. *Eur J Pharm Biopharm* 83:338-345.



Supporting Information Figure S2.1A Similar processing and MHC class I presentation by DC of native and modified SLP-OVA_{24aa}*

WT BMDC were incubated for 24 hr with titrated amounts of native SLP-OVA with C-terminus sequence TEWTS or the SLP-OVA_{24aa} (see Table 2.1 in manuscript), washed 3x to remove excess Ag and co-cultured overnight in the presence of B3Z CD8⁺ T cells. T-cell activation was determined as described in M&M.

B

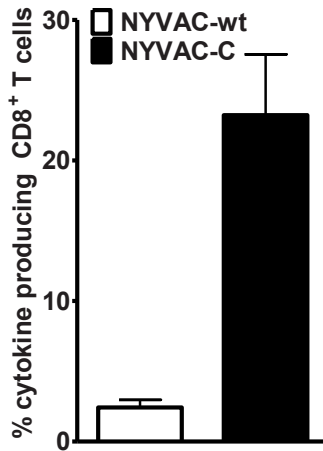
```

1  MGARASVLSG  GE LDRWEKIR  LRPGGKKKYK  LKHIVWASRE  LERFAVNPGL
51  LETSEGCVRQI  LGQLQPSLQT  GSEELRSLYN  TVATLYCVHQ  RIEIKDTKEA
101 LDKIEEEQNK  SKKKAQQAAA  DTGHSNQVSQ  NYPIVQNIQG  QMVHQAI SPR
151 TLNAWVKVVE  EKAFSPEVIP  MFSALSEGAT  PQDLNTMLNT  VGGHQAAQM
201 LKETINEEAA  EWDRVHPVHA  GPIAPGQMR  PRGSDIAGTT  STLQE QIGWM
251 TNNPPIPVGE  IYKRWII LGL  NKIVRMYSP  T  SILDIRQGPK  EPFRDYVDRF
301 YKTLRAEQAS  QEVKNWMTET  LLVQANPDC  KTILKALGPA  ATLEEMMTAC
351 QGVGGPGHKA  RVLAEAMSQV  TNSATIMMQR  GNFRNQRKIV  KCFNCGKEGH
401 TARNCRAPRK  KGCWKCGKEG  HQMKDCTERQ  ANFLGKIWPS  YKGRPGNFLQ
451 SRPEPTAPPE  ESFRSGVETT  TPPQKQEPID  KELYPLTSLR  SLFGNDPSSQ
501
..... = GPGHKARVL-epitope sequence presented in HLA-B7 and
recognized by the HIV-specific CD8+ T cell clone

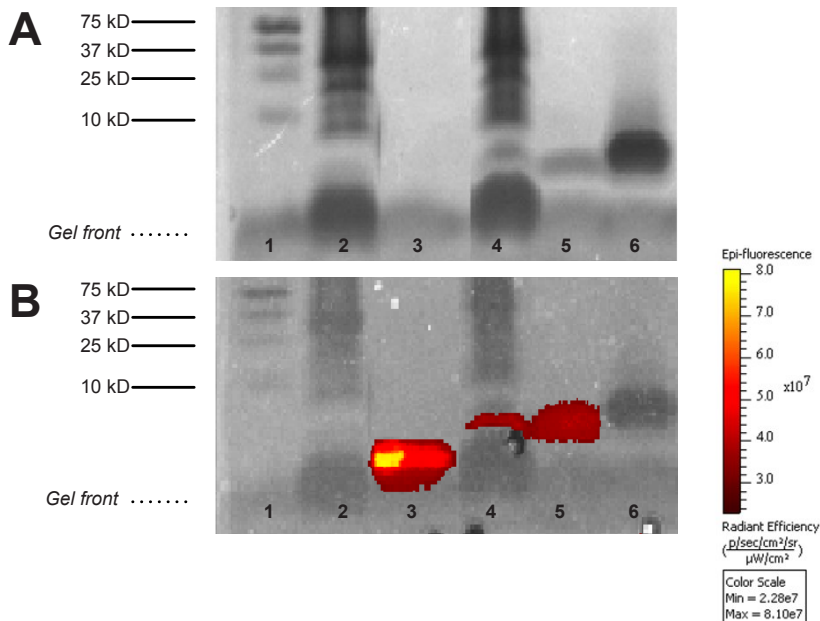
```

Supporting Information Figure S2.1B HIV-1 GAG-protein Identification by Mass Spectrometry.

HIV-GAG protein was digested with CNBr and endoproteinase GluC and analyzed by mass spectrometry (MS) as described in Supporting Information M&M. Full scan MS spectra were acquired. In a post-analysis process, raw data were first converted to peak lists using Bioworks Browser software v 3.2 (Thermo Electron), then submitted to the Swissprot database using Mascot v. 2.2.04 (www.matrixscience.com) for protein identification.

HLA-B7/GPGHKARVL CD8⁺ T cell activation**Supporting Information Figure S2.2 CD8⁺ T cell recognition of processed native GAG-protein presented by human DC loaded with apoptotic HeLa cells.**

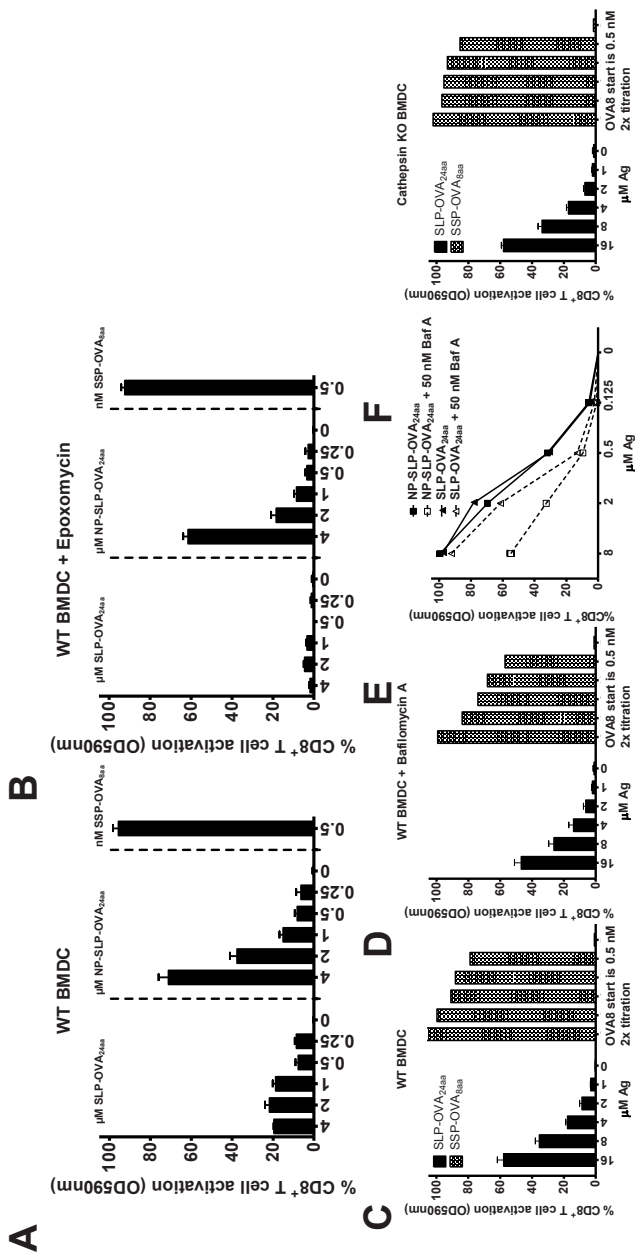
HeLa cells were harvested by EDTA and infected with NYVAC-C or NYVAC-WT at a MOI of 5 for 1 hour. Cells were extensively washed to remove residual virus. After overnight incubation, cells were irradiated with UV-C (200 $\mu\text{W}/\text{cm}^2$) to ensure that no residual virus and no viable cells were present and thereby excluding direct presentation. Apoptotic virus-infected HeLa cells were harvested and added to MoDC at a 2:1 ratio. After 6 hr incubation, HIV- or vaccinia-specific CD8 T-cells were added (at approximately 5 T-cell: 1 DC ratio) followed by overnight culture at 37°C/5%CO₂. Brefeldin A (10 $\mu\text{g}/\text{ml}$, Sigma-Aldrich) was added to retain cytokines within the T-cells allowing the detection of multiple cytokines. After 18 hr, intracellular cytokine staining was performed. Cells were fixed and permeabilized using Cytotfix/Cytoperm™ Fixation/Permeabilization Solution Kit (BD). Cells were then incubated with anti-TNF PE-Cy7 (clone MAb11, eBiosciences), anti-IFN- γ FITC, anti-IL-2 APC, anti-MIP-1 β PE (all three from BD) and anti-CD8 PerCP (Dako). After washing, cells were analyzed by flow cytometry using a LSRII flow cytometer (BD Pharmingen) and analyzed with FlowJo software (Treestar).



- 1) Resolution of the Bio Rad Precision plus Protein all blue standard protein kit 250 kD- 10 kD in 49,5%T, 3%C gel.
- 2) Cellysate of DC mock incubation
- 3) soluble SLP-OVA_{8aa}-Bodipy-FL
- 4) Cellysate of DC incubated with SLP-OVA_{31aa}-Bodipy-FL for 24 hr
- 5) soluble SLP-OVA_{31aa}-Bodipy-FL
- 6) soluble SLP-OVA_{31aa}

Supporting Information Figure S2.3 SLP-Bodipy-FL are intact upon internalization by DC.

DC in 2 ml medium containing 2×10^6 cells were incubated with SLP-OVA_{31aa}-Bodipy for 24 hr. After incubation, cells were harvested and washed twice with PBS to remove non-internalized excess Ag. Supernatant was removed, the cell pellet resuspended in 50 μ l lysis buffer (LB) (pH 7,4) and stored in eppendorf tubes at -80°C till further use. Cell lysates were subsequently obtained by repetitive freeze-thaw cycles by placing tubes for 30 sec in liquid nitrogen followed by 30 sec in heating blocks (eppendorf thermostat plus) set at 60°C . Cell lysates were analyzed using Tricine-SDS-PAGE gel as described before (35) with minor modifications. Briefly, 15 μ l cell lysate was then mixed in a 1:1 ratio with *reducing* sample buffer and heated to 95°C for 10 minutes. Samples were next loaded onto a 1.5 mm SDS-PAGE gel (49.5%T 3%C stacking gel and 49.5%T 6%C separating gel). Samples were ran at 90 V through the stacking gel and followed by 5 hr run at 35 V through the separating gel (Biorad systems). Protein and peptides fragments where visualized using Coomassie (Supporting Information Figure S2.2A). Green-fluorescent fragments were imaged and analyzed for *EPI fluorescence intensity* applying *IVIS Imaging Systems*, measuring the fluorescence at 520nm emission wavelength.



Supporting Information Figure S2.4 MHC class I presentation of soluble SLP is modulated by epoxomicin but not by Bafilomycin A and Cathepsin S.

BMDC were left untreated or pre-incubated with 1 μM *epoxomicin* (324800, Merck) incubated for 24 hr with SSP, SLP (A) or protein or SLP encapsulated in PLGA-NP (B) at the indicated concentrations. BMDC were left untreated (C) or pre-incubated with 50 nM of bafilomycin A1 (196000, Merck) followed by Ag-incubation as described above in the presence of the compound (D & E). Cells were washed three times with medium before the T-cell hybridoma B3Z CD8⁺ T-cells were added followed by O/N incubation at 37°C. BMDC from cathepsin S-deficient (Cathepsin KO) mice were cultured in the presence of titrated amounts of SLP-OVA_{24aa} and SSP-OVA_{24aa} followed by analysis of B3Z CD8⁺ T-cell activation after co-culture with Ag loaded BMDC (F). Cells were washed three times with medium before the T-cell hybridoma B3Z CD8⁺ T-cells were added followed by O/N incubation at 37°C. MHC class I Ag presentation of OVA₂₅₇₋₂₆₄ in H-2K^b was detected by activation of B3Z cells.



Chapter 3

Optimization of encapsulation of a synthetic long peptide in PLGA nanoparticles: low burst release is crucial for efficient CD8⁺ T cell activation

Ana Luisa Silva, Rodney A. Rosalia, Arzu Sazak, Myrra G. Carstens,
Ferry Ossendorp, Jaap Oostendorp & Wim Jiskoot

Abstract

Overlapping synthetic long peptides (SLP) hold great promise for immunotherapy of cancer. Poly(lactic-co-glycolic acid) (PLGA) nanoparticles (NP) are being developed as delivery systems to improve the potency of peptide-based therapeutic cancer vaccines. Our aim was to optimize PLGA NP for SLP delivery with respect to encapsulation and release, using OVA₂₄, a 24-residue long synthetic Agic peptide covering a CTL epitope of ovalbumin (SIINFEKL), as a model antigen (Ag). Peptide-loaded PLGA NP were prepared by a double emulsion/solvent evaporation technique. Using standard conditions (acidic inner aqueous phase), we observed that either encapsulation was very low (1–30%), or burst release extremely high (> 70%) upon resuspension of NP in physiological buffers. By adjusting formulation and process parameters, we uncovered that the pH of the first emulsion was critical to efficient encapsulation and controlled release. In particular, an alkaline inner aqueous phase resulted in circa 330 nm sized NP with approximately 40% encapsulation efficiency and low (< 10%) burst release. These NP showed enhanced MHC class I restricted T cell activation *in vitro* when compared to high-burst releasing NP and soluble OVA₂₄, proving that efficient entrapment of the Ag is crucial to induce a potent cellular immune response.

Introduction

In recent years there is an increased interest in the application of therapeutic vaccination for treatment of cancer¹. Therapeutic cancer vaccines aim to induce a strong cellular response against tumor associated Ags². Dendritic cells (DC) are professional Ag presenting cells (APCs) that play a major role in the initiation of such an immune response, by continuously sampling the environment for foreign Ags and establishing the communication between the innate and adaptive immune system^{3,4}. Only appropriately activated DC are capable of inducing a robust cytotoxic T cell (CTL) response, which is required for effective immunotherapy of established tumors⁵⁻⁸. For this purpose, DC are the major target cells for cancer immunotherapy vaccines^{2,8}.

Therapeutic vaccination with overlapping synthetic long peptides (SLP), covering the entire amino acid sequence of tumor associated protein Ags and thus containing all possible MHC class I and II epitopes, has been successfully applied in murine models and clinical therapeutic vaccination trials⁹⁻¹³. Moreover, vaccination of patients suffering from human papillomavirus 16 (HPV16) induced premalignant vulvar intraepithelial neoplasia with an HPV16-based SLP vaccine resulted in complete clinical regression of the lesions in some cases¹¹⁻¹³.

So far, Montanide-based water-in-oil (w/o) emulsions have been applied to formulate SLP in the majority of clinical therapeutic cancer vaccination trials¹²⁻¹⁸. The use of Montanide-based formulations has some important limitations, including non-biodegradability, causing significant local side effects, poorly controlled Ag release rates and limited scalability because of lack of long-term stability¹⁹⁻²¹. Biodegradable delivery systems based on poly(lactic-co-glycolic acid) (PLGA) offer a promising alternative strategy for peptide-based cancer vaccines. PLGA is well suited for the preparation of micro- and nanoparticles (NP)²²⁻²⁵, which can protect Ag from proteolytic enzymatic degradation and rapid clearance²⁶⁻²⁹, allow co-encapsulation and simultaneous delivery of both Ag and adjuvants, and facilitate Ag uptake by DC³⁰⁻³³. PLGA has a long safety record and is Food and Drug Administration (FDA) approved as an excipient, owing to its biodegradability and biocompatibility, with several slow-release formulations currently on the market^{31,34}. PLGA undergoes hydrolysis in the body to produce the original monomers, lactic acid and glycolic acid, which are natural by-products of metabolic pathways. Ag release can be regulated e.g. by varying the lactic acid/glycolic acid ratio³⁵⁻³⁷. PLGA-based particulate systems can be manufactured reproducibly according to Good Manufacturing Practice conditions

and have been studied extensively for the delivery of a wide variety of Ags^{24,34,38-40}. Ags encapsulated in PLGA microparticles have shown to induce immune responses comparable to those of Ags adjuvanted with Montanide 51^{37,41}. PLGA is also known to have several disadvantages regarding instability of protein Ags, e.g., due to the hydrophobicity of the polymer and the local acidification of the microenvironment that occurs during degradation of the polymer at physiological pH⁴²⁻⁴⁴. However, for synthetic peptides, which do not possess a tertiary structure, this is less problematic and several peptides in PLGA microspheres have been successfully launched on the market^{34,40,44}.

The aim of this study was the pharmaceutical characterization of PLGA NP as a suitable delivery system for encapsulation of SLP for cancer immunotherapy. OVA_{24'}, a 24-residue long synthetic Agic peptide covering a CTL epitope of ovalbumin (OVA; SIINFEKL), was studied as a model SLP, because of its proven capability to induce CTL responses *in vitro* and *in vivo*⁴⁵. Efficient entrapment of OVA_{24'} SLP in the polymeric matrix was obtained by exploring and fine tuning of formulation and process parameters. OVA_{24'}-loaded PLGA NP were characterized for Ag encapsulation efficiency, Ag burst release, particle size and zeta-potential, and the obtained formulations were immunologically evaluated *in vitro* for their potency to induce CD8⁺ T cell activation.

Materials and methods

Materials

Synthetic long peptide 24-mer OVA_{24'} (DEVSGLEQLESIIINFEKLAAAAAK)⁴⁶, covering the cytotoxic T lymphocyte (CTL) epitope SIINFEKL of ovalbumin (OVA) was synthesized at the interdepartmental GMP facility of the Department of Clinical Pharmacy and Toxicology of Leiden University Medical Center as described previously¹⁰. Poly(D,L-lactic-co-glycolic acid) [PLGA], Resomer® RG 502H was purchased from Boehringer Ingelheim (Ingelheim, Germany). 4-(2-hydroxyethyl)-1-piperazine-ethanesulfonic acid (HEPES), sodium cholate, dichloromethane (DCM), dimethyl sulfoxide (DMSO), and trifluoroacetic acid (TFA) were purchased from Sigma-Aldrich (Steinheim, Germany). Acetonitrile (ACN) and methanol (MeOH) were obtained from Biosolve BV (Valkenswaard, the Netherlands), Polyvinyl alcohol (PVA) 4-88 (31 kDa) was purchased from Fluka (Steinheim, Germany). Tween 20 was purchased from Merck Schuchardt (Hohenbrunn, Germany). Sodium hydroxide was purchased from Boom (Meppel, Netherlands). Reversed phase HPLC column ReproSil-Pur

C18-AQ 3 μm (150x4 mm) was purchased from Dr. Maisch HPLC GmbH (Ammerbuch-Entringen, Germany). Phosphate-buffered saline (NaCl 8.2 g/L; $\text{Na}_2\text{HPO}_4 \cdot 12 \text{H}_2\text{O}$ 3.1 g/L; $\text{NaH}_2\text{PO}_4 \cdot 2\text{H}_2\text{O}$ 0.3 g/L) (PBS) was purchased from B. Braun (Melsungen, Germany). Iscove's Modified Dulbecco's Medium (IMDM) was purchased from Lonza (Walkersville, USA). All other chemicals were of analytical grade and all aqueous solutions were prepared with milli Q water.

Nanoparticle preparation

General particle preparation process

Nanoparticles loaded with OVA₂₄ were prepared using a double emulsion with solvent evaporation method⁴⁷. In brief, 50 mg of PLGA dissolved in 1 ml of dichloromethane was emulsified under sonication (30 s, 20 W) with a solution containing 1.4 mg OVA₂₄ (for solution compositions, see results). To this first emulsion (w1/o), 2 ml of an aqueous surfactant solution (for surfactant types, see results) were added immediately, and the mixture was emulsified again by sonication (30 s, 20 W), creating a double emulsion (w1/o/w2). The emulsion was then added dropwise to 25 ml of extraction medium (0.3% w/v surfactant) previously heated to 40°C under agitation, to allow quick solvent evaporation, while stirring, which was continued for 1 h. The particles were then collected by centrifugation for 15 min at 15000 g at 10°C, washed, and resuspended in deionized water, aliquoted and freeze-dried at -55°C in a Christ Alpha 1-2 freeze-drier (Osterode am Harz, Germany) for 12 hours.

As starting conditions, the method described by Slütter et al.⁴⁷ was used, with 1% v/v Tween 20 in 25 mM Hepes pH 7.4 as the aqueous phase for second emulsion, with the following modifications: DMSO used as inner phase instead of PBS pH 7.4 and 5% (w/v) PLGA was used instead of 2.5%.

Optimization of formulation parameters

In order to achieve an optimum formulation, the following parameters involved in the particle preparation were varied, and their effect on peptide encapsulation efficiency was investigated.

- a) Surfactant type: investigated by dissolving different surfactant types (PVA; Tween 20; sodium cholate) in the second aqueous phase (w2) during the second emulsion step.

- b) Inner solvent: investigated by dissolving the peptide in different solutions (w1), i.e. DMSO; 50% ACN + 0.1% TFA; 50% ACN in 25 mM NaOH; and 50% ACN in 0.25 mM NaOH + 400 μ L Hepes pH 8.0 at different concentrations).
- c) Volume ratio (w1/o): investigated by varying the volume of the inner aqueous phase w1 (50 μ L, 100 μ L; 500 μ L).

Nanoparticle characterization

Dynamic light scattering and zeta-potential

The Z-average size and polydispersity index (PDI) of NP were measured by dynamic light scattering, using a Zetasizer (Nano ZS, Malvern Ltd., United Kingdom). The zeta-potential was measured by laser Doppler electrophoresis, using the same device. For that purpose, NP were diluted to 2.5 mg/ml in 1 mM Hepes pH 7.4.

Ag content and encapsulation efficiency

Peptide encapsulation efficiency was determined by measuring the peptide content of digested particles by reversed phase HPLC. For that purpose, 200 μ L NP suspension (containing 10 mg NP) was freeze-dried overnight. The lyophilizate was then dissolved in 250 μ L DMSO and the solution was agitated at 50°C for 30 min. Next, 750 μ L 50% ACN with 0.1% TFA were added and the mixture was agitated at 50°C for an extra 60 min, to allow dissolution of the peptide and degradation/precipitation of PLGA, which was then eliminated by centrifugation for 10 min at 18000 *g*. The supernatant containing the peptide was collected and 50 μ L were injected into a HPLC system equipped with a C18 column (Dr. Maisch Reprosil-Pur C18-AQ, 3 mg, 150 x 4.6 mm) and an ultraviolet detector (Waters 486). Mobile phases applied were 5% ACN in water with 0.1% TFA (solvent A), and 95% ACN in water with 0.085% TFA (solvent B). Separation was performed by applying a linear gradient from 0% to 78% solvent B over 20 min, at a flow rate of 1 ml/min, and peptide detection was performed by absorbance at 220 nm. Peptide concentration in each sample was calculated using a calibration curve created with known concentrations of OVA₂₄.

In vitro release studies

To determine burst release (BR) at time zero (t₀), freeze-dried NP were resuspended in 1x PBS, 1x IMDM cell culture medium, or 5% w/v glucose solution at a concentration of 10

mg PLGA NP/mL and the mixture was vortexed for 30 seconds at room temperature to allow complete resuspension of the particles. Then particles were centrifuged for 10 min at 18000 *g*, the supernatant recovered and the pellet resuspended. Both fractions were freeze-dried overnight, and extraction was performed as described previously, before being analyzed by HPLC for peptide quantification.

For longer release studies, peptide-loaded PLGA NP were prepared as described, resuspended in 1x PBS pH 7.4 at a concentration of 10 mg and maintained at 37°C in a water bath under constant tangential shaking at 100/min in a GFL 1086 shaking water bath (Burgwedel, Germany). At regular time intervals, 250 μ L samples of the suspension were taken, centrifuged for 10 min at 18000 *g*, and the supernatant recovered. To eliminate undesirable PLGA degradation products affecting detection by HPLC, the supernatant was freeze-dried over night, and extraction was performed as described, with the final supernatant being analyzed by HPLC for peptide quantification. Peptide release profiles were generated for each NP formulation in terms of cumulative Ag release (%) over time.

***In vitro* Ag presentation**

D1 cells, a long term growth factor-dependent immature splenic DC line derived from C57BL/6 (H-2K^b) mice, were cultured as described previously⁴⁸. B3Z, cultured as described before, is a CD8⁺ T-cell hybridoma cell line, specific for the H-2K^b-restricted ovalbumin derived CTL epitope SIINFEKL, that expresses a β -galactosidase construct under the regulation of the NF-AT element from the IL-2 promoter⁴⁹. DC were incubated for 2.5 h with soluble OVA₂₄ (sOVA₂₄) or OVA₂₄ encapsulated in PLGA NP at the indicated concentrations. Cells were washed three times with medium before the T-cell hybridoma B3Z cells were added followed by overnight incubation at 37°C. MHC class I Ag presentation of SIINFEKL (OVA₂₅₇₋₂₆₄) in H-2K^b was detected by activation of SIINFEKL-specific CD8⁺ B3Z T cells. Upon T-cell receptor (TCR) ligation, lacZ protein is produced under the control of the IL-2 promoter thus allowing measurement of the IL-2 production indirectly by a colorimetric assay using chlorophenol red- β -d-galactopyranoside (CPRG) as substrate to detect lacZ activity in cell lysates. Color conversion is determined by measuring absorbance (optical density, OD) at 590 nm.

Statistical analysis

Graph Pad Prism software was used for statistical analysis. Burst release in different physiological media and the effect of inner solvent and emulsion volume on burst release between different formulations in PBS were analyzed by two-tailed unpaired Student's t-test. CD8⁺ T cell activation of SIINFEKL-specific CD8⁺ T cells by a two-tailed paired Student's t-test. Effect of the inner phase composition on apparent pH and the effect of Hepes concentration in the inner phase on release were analyzed using two-way ANOVA.

RESULTS

Ag encapsulation and burst release in PLGA NP

In this study, a 24-mer SLP covering a well-known CTL epitope (SIINFEKL) of ovalbumin, here designated as OVA₂₄, was used as a model Ag to study the encapsulation of SLP in PLGA NP by a double emulsion with solvent evaporation method, as function of formulation and process parameters. As starting point, a slightly modified version of the standard double emulsion method described by Slütter et al.⁴⁷ was applied (see section 2.2.1), in which OVA₂₄ was dissolved in DMSO and Tween 20 used as surfactant in the outer phase (Table 3.1, formulation 1). Since this method led to very low encapsulation efficiencies (ca. 1%), DMSO as inner phase was replaced by 50% ACN/0.1% TFA, which resulted in a marginal improvement (see Table 3.1, formulation 2). Attempts to dissolve OVA₂₄ in the PLGA-containing dichloromethane phase failed (results not shown). Therefore, several process parameters were investigated in order to increase the encapsulation efficiency of OVA₂₄ in PLGA NP. First, commonly used surfactants for making NP, sodium cholate and PVA^{23,47}, were tested in replacement of Tween 20 (Table 3.1, formulations 3–7). The type of surfactant used to stabilize the second emulsion had a dramatic positive effect on the encapsulation efficiency. Using 50% ACN/0.1% TFA (with an apparent pH of 2.0) as first emulsion medium and PVA as surfactant in the second emulsion step resulted in the highest encapsulation efficiency (EE) (up to about 30%, see Table 3.1, formulations 4–7). PVA concentrations of 1% and 2% (w/v) PVA yielded comparable EE and particle size (Table 3.1, formulations 6 and 7). PVA concentrations below 1% led to a lower encapsulation efficiency and a larger particle size (Table 3.1, formulations 4 and 5). For our further studies, OVA₂₄-loaded PLGA NP prepared with 50% ACN/0.1% TFA as inner solvent and 1% PVA as surfactant in the second emulsion (Table 3.1, formulation 6) were selected.

Table 3.1 Effect of first and second emulsion compositions on encapsulation efficiency of OVA₂₄ SLP in PLGA NP

Formulation	1 st emulsion medium	2 nd emulsion medium	DL (%) *	EE (%)	Z-average size (nm)	PDI	ZP (mV)
1	DMSO	1% Tween 20	0.01 ± 0.004	1 ± 0.3	319 ± 90	0.23 ± 0.07	-36 ± 7.0
2	50 µL 50% ACN 0.1% TFA	1% Tween 20	0.06 ± 0.02	4 ± 1	277 ± 5	0.20 ± 0.01	-27 ± 2.0
3	50 µL 50% ACN 0.1% TFA	1% Sodium cholate	0.17 ± 0.04	9 ± 2	203 ± 3	0.10 ± 0.03	-32 ± 1.1
4	50 µL 50% ACN 0.1% TFA	0.3 % PVA	0.37 ± 0.08	16 ± 1	606 ± 4	0.17 ± 0.02	-6 ± 1.5
5	50 µL 50% ACN 0.1% TFA	0.5 % PVA	0.62 ± 0.20	22 ± 7	470 ± 36	0.22 ± 0.05	-12 ± 2.1
6	50 µL 50% ACN 0.1% TFA	1 % PVA	0.86 ± 0.31	26 ± 11	372 ± 44	0.17 ± 0.01	-10 ± 1.9
7	50 µL 50% ACN 0.1% TFA	2 % PVA	0.61 ± 0.27	22 ± 3	345 ± 28	0.15 ± 0.03	-10 ± 2.4
8	100 µL 50% ACN 25 mM NaOH	1 % PVA	0.26 ± 0.22	9 ± 8	360 ± 45	0.22 ± 0.01	-12 ± 0.8
9	100 µL 50% ACN 0.25 mM NaOH	1 % PVA	0.71 ± 25	26 ± 9	379 ± 25	0.19 ± 0.02	-12 ± 0.7
10	500 µL 50% ACN 0.1% TFA	1 % PVA	0.82 ± 0.34	29 ± 12	234 ± 3	0.11 ± 0.03	-15 ± 1.3
11	500 µL 50% ACN 25 mM NaOH	1 % PVA	1.03 ± 0.15	37 ± 5	303 ± 68	0.11 ± 0.05	-11 ± 0.1
12	100 µL 50% ACN 0.25 mM NaOH + 400 µL 1 mM Hepes pH 8.0	1 % PVA	0.55 ± 0.21	20 ± 8	384 ± 7	0.18 ± 0.03	-11 ± 0.2
13	100 µL 50% ACN 0.25 mM NaOH + 400 µL 5 mM Hepes pH 8.0	1 % PVA	0.50 ± 0.20	18 ± 6	427 ± 46	0.20 ± 0.05	-10 ± 1.7
14	100 µL 50% ACN 0.25 mM NaOH + 400 µL 10 mM Hepes pH 8.0	1 % PVA	0.44 ± 0.21	16 ± 7	382 ± 69	0.18 ± 0.05	-10 ± 0.6
15	100 µL 50% ACN 0.25 mM NaOH + 400 µL 25 mM Hepes pH 8.0	1 % PVA	0.70 ± 0.09	25 ± 3	298 ± 27	0.12 ± 0.03	-10 ± 0.9
16	100 µL 50% ACN 0.25 mM NaOH + 400 µL 50 mM Hepes pH 8.0	1 % PVA	1.07 ± 0.07	38 ± 3	328 ± 50	0.22 ± 0.07	-14 ± 0.3

* DL = drug loading, EE = encapsulation efficiency, calculated as described in section 2.3.2. PDI = polydispersity index, ZP = zeta-potential. Data are presented as average ± standard deviation of n = 3 independent batches.

Formulation 6 was tested for burst release of the peptide in PBS and IMDM (cell culture medium), which are commonly used for *in vitro* and *in vivo* applications. Directly upon resuspension ($t = 0$) in either PBS or IMDM, OVA₂₄-loaded PLGA NP showed a very high release, ranging from 80 to 90% (Figure 3.1), indicating that initial encapsulation results were misleading. In contrast, a release study in isotonic 5% glucose solution (Figure 3.1), did not induce substantial peptide release.

With the purpose to decrease the very high burst release, new solutions were tested as inner phase (w1) in the NP preparation process, where the effect of pH was studied. Instead of using pHs below the isoelectric point (pI) of the peptide (pI = 4.3), we decided to use pHs above it, which would change the charge distribution in the peptide and thereby could affect encapsulation, as well as inner phase volume, which might affect the peptide's distribution between the inner and outer aqueous phases present during formation of the double emulsion. Therefore, instead of 50% ACN/0.1% TFA (apparent pH 2.0), OVA₂₄ was dissolved in 50% ACN/25 mM NaOH (apparent pH 12.5).

Improvement was observed in neither encapsulation efficiency nor burst release when using an inner alkaline phase volume of 100 μ l (Table 3.1, formulation 9; Figure 3.2a). However, a concomitant increase of inner emulsion volume, by using an inner phase volume of 500 μ l (Table 3.1, formulation 11), drastically reduced burst release from circa 90% to less than 10%, while improving encapsulation efficiency. Still, when at acidic pH,

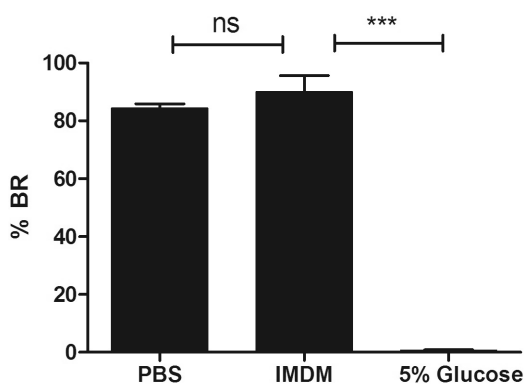


Figure 3.1 Burst release of OVA₂₄ in different physiological media (PBS, IMDM cell culture medium, 5% glucose) from PLGA NP (Table 3.1, formulation 6). Data are presented as average \pm standard deviation of $n = 3$ independent batches. Data was analyzed by two-tailed unpaired Student's t-test. P values are presented as non-significant (ns) = $P > 0.05$; * = $P < 0.05$; ** = $P < 0.01$; *** = $P < 0.0001$.

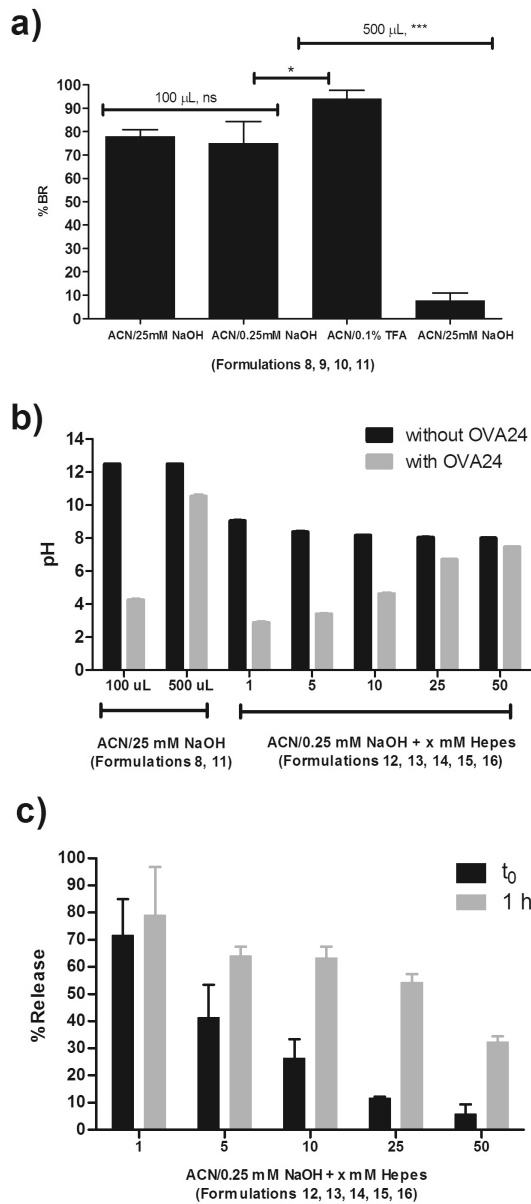


Figure 3.2 (A) Effect of inner solvent and emulsion volume on burst release of OVA₂₄ in PLGA NP, assessed upon resuspension in PBS (Formulations 8–11). (B) Effect of the inner phase composition on apparent pH before and after the addition of OVA₂₄ ($P < 0.0001$) (formulations 8, 11–16). (C) Effect of Hepes concentration in the inner phase on release, assessed at t_0 (burst release) and 1 h after resuspension ($P < 0.0001$) (formulations 12–16). Data are presented as average \pm standard deviation of $n=3$ independent batches. Formulation numbers are according to Table 3.1. P values are presented as non-significant (ns) = $P > 0.05$; * = $P < 0.05$; ** = $P < 0.01$; *** = $P < 0.0001$.

a higher inner emulsion volume (Table 3.1, formulation 10) did not affect encapsulation efficiency or burst release compared to previous values, confirming the central effect of pH in the matter. Indeed we observed that the peptide was very acidic, most likely due to remaining TFA from synthesis, drastically decreasing pH of solutions upon dissolution, with only the higher volumes containing enough base/buffer molecules to neutralize the acid contained in the peptide (Figure 3.2b), and keep the pH above 7.

The size and zeta-potential of the prepared OVA₂₄-loaded NP was measured in 1 mM Hepes pH 7.4. Irrespective of the preparation method, the particles were negatively charged, with zeta-potentials ranging from -10 to -15 mV (see Table 3.1), when prepared using 1% PVA as surfactant. Though the inner emulsion ratio is generally thought to influence final particle size, with a larger ratio typically yielding bigger particles²², we did not observe significant differences in average size (Table 3.1), with final particle sizes ranging from 300 to 400 nm for higher inner phase volumes and polydispersity indices below 0.3.

Since it is well known that extreme pH values may harm peptide structure and stability, we decided to lower the working pH. Therefore, NaOH concentrations were decreased from 25 mM (apparent pH 12.5) to 0.25 mM NaOH (yielding an apparent pH of 10.5), and after dissolving the peptide in 50% ACN 0.25 mM NaOH, pH was adjusted by diluting 5 fold in Hepes buffer pH 8.0 at different Hepes concentrations (Table 3.1, formulations 12–16). We observed that a buffer concentration of at least 50 mM was necessary to maintain a basic pH in presence of peptide (Figure 3.2b), with the final pH having a direct effect on burst release (Figure 3.2c). Since the formulation with a relatively mild inner phase with an apparent pH of 8.0 (see Table 3.1, formulation 16) showed a comparable EE and burst release as the formulation with an apparent inner phase pH of 10.5 (Table 3.1, formulation 11), formulation 16 was adopted for further functional studies. With this formulation we obtained particles with an encapsulation efficiency of 38%, with an average size of 328 nm, and zeta potential of -13.6 mV.

Release kinetics

Since the particles are meant to be delivered to DC and taken up by DC rapidly after administration, short term release properties of the peptide-loaded particles (Table 3.1, formulation 16) were assessed for 24 h. It can be observed that after 1 h OVA₂₄ shows approximately 30% release in PBS at 37°C under shaking 100/min (Figure 3.3). Over the next 24 h, no further release was observed. The slight decline in initial concentration of

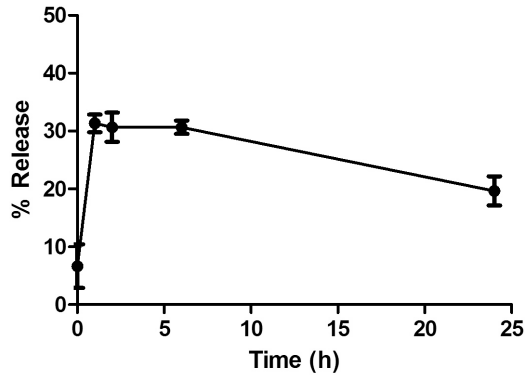


Figure 3.3 Release kinetics of OVA₂₄ from PLGA NP (Table 3.1, formulation 16) in PBS at 37°C under shaking 100/min. Data are presented as average \pm standard deviation of $n = 3$ independent batches.

OVA₂₄ was due to aggregation and, hence, partial precipitation during the centrifugation step. Indeed, free OVA₂₄ dissolved in PBS at 37°C under agitation aggregated over time, as detected by DLS (results not shown). Adding Tween 80 (0.1 % w/v) to the release medium did not help. We did not further study this phenomenon, but it obviously limited the duration of the release study.

***In vitro* Ag presentation of SLP Ag encapsulated in NP**

The effect of encapsulation of OVA₂₄ on the efficiency of DC uptake and processing into MCH class I for Ag cross-presentation resulting into activation of CD8⁺ T cells was tested *in vitro* (Figure 3.4). For that purpose, the different formulations were incubated with DC for 2.5 h, washed to remove excess unbound Ag, followed by co-culture in the presence of OVA-specific B3Z CD8⁺ T cells. OVA₂₄-containing PLGA NP with low (< 10%) burst release (Table 3.1, formulation 16) were compared with those exhibiting high (> 75%) burst release (Table 3.1, formulation 9), against soluble OVA₂₄, empty particles, and a mixture of soluble OVA₂₄ and empty particles. Encapsulation of OVA₂₄ in PLGA-NP resulted in significantly enhanced activation of B3Z CD8⁺ T cells compared to soluble OVA₂₄. Although both tested NP formulations enhanced MHC class I Ag cross-presentation, we observed that delivery of OVA₂₄ via encapsulation in PLGA NP with low (< 10%) burst release resulted in improved T cell responses in comparison to OVA₂₄-containing PLGA NP with high (ca. 75%) burst release. The addition of empty NP to soluble OVA₂₄ did not show an effect on T cell

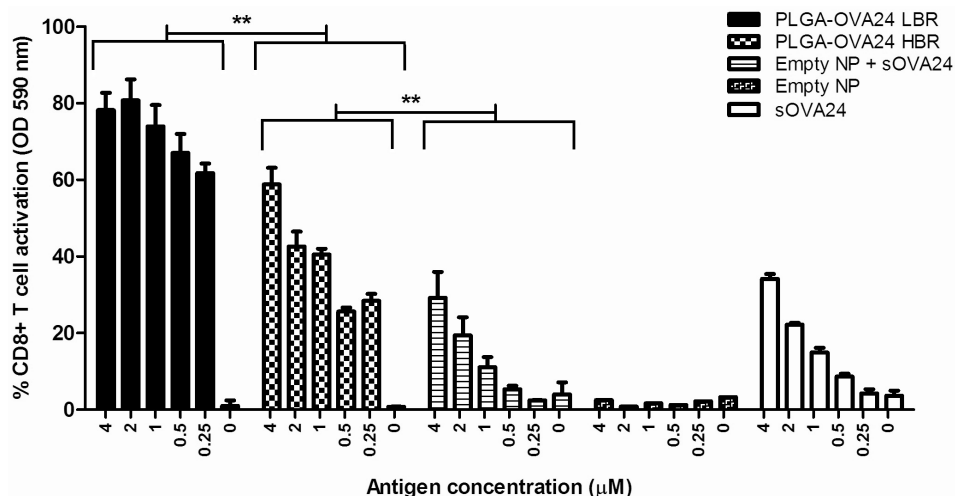


Figure 3.4 Normalized CD8⁺ T cell activation of SIINFEKL-specific CD8⁺ T cells (B3Z) after co-culturing with DC incubated for 2.5 hours with titrated amounts of different OVA₂₄ SLP formulations: low-burst releasing (LBR) PLGA NP loaded with OVA₂₄ (Table 3.1, formulation 16), high-burst releasing (HBR) PLGA NP loaded with OVA₂₄ (Table 3.1, formulation 9), soluble OVA₂₄ mixed with empty NP (OVA₂₄ + Empty NP), empty NP, and soluble OVA₂₄ (sOVA₂₄). Data are presented as average ± SD of triplicate measurements. Representative results from one out of 3 experiments are shown. Graphs depict normalized T cell activation data based on the maximal OD 590 nm value/T cell activation measured upon incubation of DC with 1 μM of the minimal H2-K^b epitope OVA₈/SIINFEKL-peptide (OD 590 nm value of 0.918 = 100%) as positive control. P values are presented as * = P < 0.05; ** = P < 0.01.

activation in comparison to soluble OVA₂₄ alone, indicating the strict necessity of peptide encapsulation in NP for enhanced processing in MHC class I Ag presentation pathways. Taken together, these data demonstrate that effective entrapment of Ag in PLGA with low burst release is crucial for efficient Ag cross-presentation by DC.

Discussion

The aim of this study was to develop a method to efficiently encapsulate OVA₂₄ in PLGA, and perform a full characterization of the obtained formulation. This approach may result in Ag-bearing biodegradable particles that can be actively taken up by DC, generating specific T cell immunity and improving the efficacy of synthetic peptide-based cancer vaccines.

Whereas hydrophilic and hydrophobic peptides have been successfully encapsulated in PLGA NP and/or microparticles in the past^{23,37,40,50}, efficient entrapment of the moderately hydrophobic OVA₂₄ proved to be challenging. OVA₂₄ does not readily dissolve in aqueous solutions and is insoluble in solvents like DCM or chloroform. However, it can be dissolved in a suitable matrix such as 50% v/v ACN in water, as well as in the commonly used solvent DMSO, prior to dilution in aqueous solutions. Standard encapsulation procedures generally used for encapsulation of hydrophilic or hydrophobic Ags led to low encapsulation efficiencies and high burst release once NP were resuspended in isotonic solutions at physiological pH. Therefore, several formulation parameters, particularly inner and outer emulsion compositions, were studied in order to increase encapsulation. The positive effect of using PVA in the outer aqueous phase on EE may be due to fact that it is not a classical surfactant with a distinct hydrophobic tail and hydrophilic headgroup, but a polymer that coats the surface, stabilizing the emulsion. In contrast, both Tween 20 and cholate are able to form micelles at concentrations above their critical micelle concentrations (0.07 and 0.6% w/v for Tween 20 and cholate, respectively), that may capture and solubilize the peptide during the emulsification process and thereby favor its extraction in the external water phase. A measurable difference between NP formulated with Tween 20 or sodium cholate (Table 3.1, formulations 1–3) and those formulated with PVA (Table 3.1, formulations 5–16) was that the negative zeta-potential of the former formulations was significantly higher. While the relatively high zeta-potential values obtained with cholate can be explained by the negative charge of the surfactant, we can only speculate that the nonionic surfactant Tween 20, due to its lower molecular size, does not shield the negative charge of the PLGA as much as PVA coating does.

The observed high burst release in the formulations with acidic inner phase led us to the notion that the majority of the OVA₂₄ molecules might not be encapsulated in the NP's polymeric matrix, but instead were adsorbed to their surface, masking real encapsulation efficiencies. This would explain the rapid release of peptide from the NP in presence of salt by disruption of electrostatic interactions between the peptide and the PLGA surface, due to the presence of counter ions that may shield the charges, and/or alter the peptide's solubility. Indeed, the high burst release is highly consistent with observed release profiles for a tumor necrosis factor alpha blocking peptide adsorbed to PLGA NP³⁹, occurring once exposed to salt-based isotonic solutions at physiological pH. Increasing particle hydrophobicity by using different types of PLGA with higher molecular weights and lactic acid/glycolic acid ratio (PLGA 75:25), as well as using DMSO as solvent, creating

an oil-in-water emulsion, instead of water-in-oil-in-water to reduce porosity^{51,52}, did not result in a decrease of the burst release (data not shown), concurring with the adsorption hypothesis, in opposition to diffusion due to high porosity. Moreover, resuspension in either water or isotonic 5% (w/v) glucose solution did not lead to substantial burst release (Figure 3.1), which provides further evidence that the instant release was not due to high particle porosity and peptide diffusion due to osmosis.

A clear correlation between burst release and pH of the inner phase was observed (Figure 3.2), confirming that the pH of the inner phase is of primary importance for efficient peptide encapsulation. The effect of the higher inner phase volume on the burst release is mainly pH related, by providing a higher number of base/buffer molecules able to neutralize the acidic peptide and maintain an alkaline pH, whereas a higher acidic inner volume showed no effect (Table 3.1, formulation 10).

In order to better understand the physicochemical characteristics of the peptide and the effect of pH of the inner (w1) phase on the observed encapsulation efficiency and burst release, the sequence of the peptide was analyzed using ProtParam, the online protein identification and analysis software that is available through the ExPASy World Wide Web server⁵³. Using this tool, the theoretical isoelectric point of the OVA₂₄ peptide was determined as 4.3, and the grand average of hydropathicity (GRAVY) as 0.087⁵⁴. According to this index, amino acids are separated into hydrophilic (negative GRAVY value) and hydrophobic (positive GRAVY value). The amino acids with GRAVY values closer to zero correspond to the least hydrophobic and hydrophilic ones, which are respectively alanine (1.8) and glycine (-0.4). The slightly positive value of the OVA₂₄ peptide confirms its slight hydrophobic nature.

Hydrophobic protein domains have shown to adsorb to polymer surfaces by electrostatic and/or hydrophobic interactions, and particle surface properties can influence adsorption⁵⁵. Though for the OVA₂₄/PLGA system the mechanism of encapsulation versus surface localization is still not clear, we hypothesize that efficient encapsulation at a higher pH of the inner phase may result from a more favorable partitioning of the peptide between internal/external aqueous phases and interfaces. A closer look at the peptide sequence and position of its charged residues (D'EVSGL⁻QLE⁻SIIN⁻FE⁻K⁺LAAAAAK⁺) allows us to divide it into two sections, with distinct characteristics. At low pHs, below the peptide's pI, the DEVSGLEQLESIIINFE part should be mostly neutral, with the exception of the N-terminal amine group, and therefore rather hydrophobic. On the other hand, the K⁺LAAAAAK⁺

sequence might act as a charged headgroup, thereby rendering the molecule surface active and prone to migrate to the surface. Free peptide in the external phase may also adsorb to the particles through electrostatic interactions between positively charged residues and negatively charged PLGA NP surfaces. Once exposed to saline solutions at higher pHs, the 'hydrophobic tail' will become negatively charged, hence more hydrophilic, by which the molecule may lose its surface activity, as well as repel from negatively charged PLGA, whereas the electrostatic interactions between the positively charged residues and PLGA may also be displaced by the presence of counter ions, which could explain the release in PBS pH 7.4, but not in water (i.e., during washing of the particles during preparation) or isotonic glucose solutions with acidic pHs.

Previous studies with the short synthetic peptide SIINFEKL in PLGA microparticles showed nearly total release of the peptide within 24 hours in PBS²⁴. Studies with longer peptides (13 to 43 amino acids) or recombinant human growth hormone in microparticles showed 20–70% release over the first 24 h⁵⁶⁻⁵⁹, whereas insulin also shows 30–40% release from PLGA NP within 24 h⁶⁰. With our method we were able to encapsulate OVA₂₄ with nearly 40% EE in NP showing minimal burst release and a total peptide release of circa 30% over 24 h. The better retention of SLP will allow delivery of encapsulated peptide to DC, which is a great improvement compared to release over the same period of time of high releasing formulations. This is especially important if we consider subsequent development of this particulate system for delivery of SLP, which may include co-encapsulation of adjuvants, such as Toll-like receptor ligands (TLRL), or even surface modification with targeting moieties that require covalent binding to the particles at controlled pH such as described by Cruz et al.²³ without losing most of the Ag during the manufacturing process or shortly after administration.

The effect of OVA₂₄ encapsulation on Ag cross-presentation to activate CD8⁺ T cells was tested *in vitro* with conclusive results. OVA₂₄-containing PLGA NP with low burst release showed significantly higher capacity of CD8⁺ T cell activation comparing to those with high burst release (Figure 3.4). Likewise, soluble peptide mixed with empty particles did not show any improvement when compared to soluble peptide, further proving the need of effective entrapment of Ag in PLGA to increase Ag cross presentation by DC. Furthermore, we showed that not only encapsulation of OVA₂₄ in PLGA NP is required, but also the release characteristics are of vital importance, with low burst release being fundamental to induce a potent cellular immune response. This is probably due to enhanced uptake and/or processing by DC of particulate Ag. When incubated with low-burst releasing particles,

DC may efficiently uptake the Ag cargo still encapsulated in PLGA particles, whereas with high-burst releasing particles, DC will take up less encapsulated peptide, thereby lowering the overall efficiency by which the peptide is internalized and routed into MHC class I Ag presentation pathways. The improved MHC class I Ag presentation observed with low-burst releasing particles is indicative of sustained release of the peptide inside the DC, similar to other Ag delivery systems to DC ⁶¹.

Conclusion

In this study we described a method for efficient encapsulation of a model SLP in PLGA NP, resulting in a particle delivery system able to enhance CD8⁺ T cell activation *in vitro*. This encapsulation method, employing an apparent inner phase pH above the pI of the encapsulated SLP, may be a promising approach for encapsulation of peptides with amphiphilic and/or hydrophilic properties, and may be considered as a firm basis for the development of NP formulations for SLP-based immunotherapy of cancer. Preliminary studies showed that the method is applicable to other SLP as well (unpublished results). Additionally, this study shows the importance of thorough characterization of peptide encapsulation process in PLGA NP to achieve a successful formulation. In conclusion, this study has shown that encapsulation and release characteristics are strongly dependent on the pH of the first emulsion, whereas a direct comparison between NP with similar physicochemical characteristics in terms of charge, size and Ag loading, but different release profiles, uncovered the importance of low burst release to induce a potent cellular immune response.

Acknowledgements

This study was supported by grants from Immune System Activation (ISA) Pharmaceuticals and the Leiden University Medical Center. We thank Jeroen van Smeden for his help with the statistical analysis.

References

1. Perrie Y, Mohammed AR, Kirby DJ, McNeil SE, Bramwell VW 2008. Vaccine adjuvant systems: enhancing the efficacy of sub-unit protein Ags. *Int J Pharm* 364(2):272-280.
2. Melief CJ, van der Burg SH 2008. Immunotherapy of established (pre)malignant disease by synthetic long peptide vaccines. *Nat Rev Cancer* 8(5):351-360.
3. Steinman R, Inaba K 1989. Immunogenicity: role of dendritic cells. *Bioessays* 10(5):145-152.
4. Steinman RM 1991. The dendritic cell system and its role in immunogenicity. *Annu Rev Immunol* 9:271-296.
5. Inaba K, Young JW, Steinman RM 1987. Direct activation of CD8+ cytotoxic T lymphocytes by dendritic cells. *J Exp Med* 166(1):182-194.
6. Trunpfheller C, Longhi MP, Caskey M, Idoyaga J, Bozzacco L, Keler T, Schlesinger SJ, Steinman RM 2012. Dendritic cell-targeted protein vaccines: a novel approach to induce T-cell immunity. *J Intern Med* 271(2):183-192.
7. Vulink A, Radford KJ, Melief C, Hart DN 2008. Dendritic cells in cancer immunotherapy. *Adv Cancer Res* 99:363-407.
8. Melief CJ 2008. Cancer immunotherapy by dendritic cells. *Immunity* 29(3):372-383.
9. Zwaveling S, Ferreira Mota SC, Nouta J, Johnson M, Lipford GB, Offringa R, van der Burg SH, Melief CJ 2002. Established human papillomavirus type 16-expressing tumors are effectively eradicated following vaccination with long peptides. *J Immunol* 169(1):350-358.
10. Ossendorp F, Mengede E, Camps M, Filius R, Melief CJ 1998. Specific T helper cell requirement for optimal induction of cytotoxic T lymphocytes against major histocompatibility complex class II negative tumors. *J Exp Med* 187(5):693-702.
11. Welters MJ, Kenter GG, Piersma SJ, Vloon AP, Lowik MJ, Berends-van der Meer DM, Drijfhout JW, Valentijn AR, Wafelman AR, Oostendorp J, Fleuren GJ, Offringa R, Melief CJ, van der Burg SH 2008. Induction of tumor-specific CD4+ and CD8+ T-cell immunity in cervical cancer patients by a human papillomavirus type 16 E6 and E7 long peptides vaccine. *Clin Cancer Res* 14(1):178-187.
12. Pieterse QD, Ter Kuile MM, Maas CP, Kenter GG 2008. The Gynaecologic Leiden Questionnaire: psychometric properties of a self-report questionnaire of sexual function and vaginal changes for gynaecological cancer patients. *Psychooncology* 17(7):681-689.
13. Randerath WJ, Galetke W, Kenter M, Richter K, Schafer T 2009. Combined adaptive servo-ventilation and automatic positive airway pressure (anticyclic modulated ventilation) in co-existing obstructive and central sleep apnea syndrome and periodic breathing. *Sleep Med* 10(8):898-903.
14. Melief CJ 2011. Synthetic vaccine for the treatment of lesions caused by high risk human papilloma virus. *Cancer J* 17(5):300-301.

15. Melief CJ 2012. Treatment of established lesions caused by high-risk human papilloma virus using a synthetic vaccine. *J Immunother* 35(3):215-216.
16. Chiang CL, Kandalaf LE, Coukos G 2011. Adjuvants for enhancing the immunogenicity of whole tumor cell vaccines. *Int Rev Immunol* 30(2-3):150-182.
17. van Driel WJ, Rensing ME, Kenter GG, Brandt RM, Krul EJ, van Rossum AB, Schuurung E, Offringa R, Bauknecht T, Tamm-Hermelink A, van Dam PA, Fleuren GJ, Kast WM, Melief CJ, Trimbos JB 1999. Vaccination with HPV16 peptides of patients with advanced cervical carcinoma: clinical evaluation of a phase I-II trial. *Eur J Cancer* 35(6):946-952.
18. Slingluff CL, Jr., Yamshchikov G, Neese P, Galavotti H, Eastham S, Engelhard VH, Kittlesen D, Deacon D, Hibbitts S, Grosh WW, Petroni G, Cohen R, Wiernasz C, Patterson JW, Conway BP, Ross WG 2001. Phase I trial of a melanoma vaccine with gp100(280-288) peptide and tetanus helper peptide in adjuvant: immunologic and clinical outcomes. *Clin Cancer Res* 7(10):3012-3024.
19. Aucouturier J, Ascarateil S, Dupuis L 2006. The use of oil adjuvants in therapeutic vaccines. *Vaccine* 24 Suppl 2:S2-44-45.
20. Aucouturier J, Dupuis L, Deville S, Ascarateil S, Ganne V 2002. Montanide ISA 720 and 51: a new generation of water in oil emulsions as adjuvants for human vaccines. *Expert Rev Vaccines* 1(1):111-118.
21. Leenaars PP, Koedam MA, Wester PW, Baumans V, Claassen E, Hendriksen CF 1998. Assessment of side effects induced by injection of different adjuvant/Ag combinations in rabbits and mice. *Lab Anim* 32(4):387-406.
22. Astete CE, Sabliov CM 2006. Synthesis and characterization of PLGA nanoparticles. *J Biomater Sci Polym Ed* 17(3):247-289.
23. Cruz LJ, Tacke PJ, Fokkink R, Joosten B, Stuart MC, Albericio F, Torensma R, Figdor CG 2010. Targeted PLGA nano- but not microparticles specifically deliver Ag to human dendritic cells via DC-SIGN in vitro. *J Control Release* 144(2):118-126.
24. Fischer S, Schlosser E, Mueller M, Csaba N, Merkle HP, Groettrup M, Gander B 2009. Concomitant delivery of a CTL-restricted peptide Ag and CpG ODN by PLGA microparticles induces cellular immune response. *J Drug Target* 17(8):652-661.
25. Mundargi RC, Babu VR, Rangaswamy V, Patel P, Aminabhavi TM 2008. Nano/micro technologies for delivering macromolecular therapeutics using poly(D,L-lactide-co-glycolide) and its derivatives. *J Control Release* 125(3):193-209.
26. Vlieghe P, Lisowski V, Martinez J, Khrestchatsky M 2010. Synthetic therapeutic peptides: science and market. *Drug Discov Today* 15(1-2):40-56.
27. Woodley JF 1994. Enzymatic barriers for GI peptide and protein delivery. *Crit Rev Ther Drug Carrier Syst* 11(2-3):61-95.
28. Schall N, Page N, Macri C, Chaloin O, Briand JP, Muller S 2012. Peptide-based approaches to treat lupus and other autoimmune diseases. *J Autoimmun* 39(3):143-153.

29. Witt KA, Gillespie TJ, Huber JD, Egleton RD, Davis TP 2001. Peptide drug modifications to enhance bioavailability and blood-brain barrier permeability. *Peptides* 22(12):2329-2343.
30. De Temmerman ML, Rejman J, Demeester J, Irvine DJ, Gander B, De Smedt SC 2011. Particulate vaccines: on the quest for optimal delivery and immune response. *Drug Discov Today* 16(13-14):569-582.
31. Fahmy TM, Demento SL, Caplan MJ, Mellman I, Saltzman WM 2008. Design opportunities for actively targeted nanoparticle vaccines. *Nanomedicine (Lond)* 3(3):343-355.
32. Elamanchili P, Lutsiak CM, Hamdy S, Diwan M, Samuel J 2007. "Pathogen-mimicking" nanoparticles for vaccine delivery to dendritic cells. *J Immunother* 30(4):378-395.
33. Schlosser E, Mueller M, Fischer S, Basta S, Busch DH, Gander B, Groettrup M 2008. TLR ligands and Ag need to be coencapsulated into the same biodegradable microsphere for the generation of potent cytotoxic T lymphocyte responses. *Vaccine* 26(13):1626-1637.
34. Jain S, O'Hagan DT, Singh M 2011. The long-term potential of biodegradable poly(lactide-co-glycolide) microparticles as the next-generation vaccine adjuvant. *Expert Rev Vaccines* 10(12):1731-1742.
35. van der Lubben IM, Verhoef JC, Borchard G, Junginger HE 2001. Chitosan and its derivatives in mucosal drug and vaccine delivery. *Eur J Pharm Sci* 14(3):201-207.
36. Jiang W, Gupta RK, Deshpande MC, Schwendeman SP 2005. Biodegradable poly(lactic-co-glycolic acid) microparticles for injectable delivery of vaccine Ags. *Adv Drug Deliv Rev* 57(3):391-410.
37. Mata E, Igartua M, Hernandez RM, Rosas JE, Patarroyo ME, Pedraz JL 2010. Comparison of the adjuvanticity of two different delivery systems on the induction of humoral and cellular responses to synthetic peptides. *Drug Deliv* 17(7):490-499.
38. Slutter B, Plapied L, Fievez V, Sande MA, des Rieux A, Schneider YJ, Van Riet E, Jiskoot W, Preat V 2009. Mechanistic study of the adjuvant effect of biodegradable nanoparticles in mucosal vaccination. *J Control Release* 138(2):113-121.
39. Yang A, Yang L, Liu W, Li Z, Xu H, Yang X 2007. Tumor necrosis factor alpha blocking peptide loaded PEG-PLGA nanoparticles: preparation and in vitro evaluation. *Int J Pharm* 331(1):123-132.
40. Wischke C, Schwendeman SP 2008. Principles of encapsulating hydrophobic drugs in PLA/PLGA microparticles. *Int J Pharm* 364(2):298-327.
41. Mueller M, Schlosser E, Gander B, Groettrup M 2011. Tumor eradication by immunotherapy with biodegradable PLGA microspheres--an alternative to incomplete Freund's adjuvant. *Int J Cancer* 129(2):407-416.
42. Liu Y, Schwendeman SP 2012. Mapping Microclimate pH Distribution inside Protein-Encapsulated PLGA Microspheres Using Confocal Laser Scanning Microscopy. *Mol Pharm* 9(5):1342-1350.
43. van de Weert M, Hennink WE, Jiskoot W 2000. Protein instability in poly(lactic-co-glycolic acid) microparticles. *Pharm Res* 17(10):1159-1167.

44. Jiskoot W, Randolph TW, Volkin DB, Middaugh CR, Schoneich C, Winter G, Friess W, Crommelin DJ, Carpenter JF 2012. Protein instability and immunogenicity: roadblocks to clinical application of injectable protein delivery systems for sustained release. *J Pharm Sci* 101(3):946-954.
45. Bijker MS, van den Eeden SJ, Franken KL, Melief CJ, Offringa R, van der Burg SH 2007. CD8+ CTL priming by exact peptide epitopes in incomplete Freund's adjuvant induces a vanishing CTL response, whereas long peptides induce sustained CTL reactivity. *J Immunol* 179(8):5033-5040.
46. Khan S, Bijker MS, Weterings JJ, Tanke HJ, Adema GJ, van Hall T, Drijfhout JW, Melief CJ, Overkleef HS, van der Marel GA, Filippov DV, van der Burg SH, Ossendorp F 2007. Distinct uptake mechanisms but similar intracellular processing of two different toll-like receptor ligand-peptide conjugates in dendritic cells. *J Biol Chem* 282(29):21145-21159.
47. Slutter B, Bal S, Keijzer C, Mallants R, Hagenaaers N, Que I, Kaijzel E, van Eden W, Augustijns P, Lowik C, Bouwstra J, Broere F, Jiskoot W 2010. Nasal vaccination with N-trimethyl chitosan and PLGA based nanoparticles: nanoparticle characteristics determine quality and strength of the antibody response in mice against the encapsulated Ag. *Vaccine* 28(38):6282-6291.
48. Winzler C, Rovere P, Rescigno M, Granucci F, Penna G, Adorini L, Zimmermann VS, Davoust J, Ricciardi-Castagnoli P 1997. Maturation stages of mouse dendritic cells in growth factor-dependent long-term cultures. *J Exp Med* 185(2):317-328.
49. Sanderson S, Shastri N 1994. LacZ inducible, Ag/MHC-specific T cell hybrids. *Int Immunol* 6(3):369-376.
50. Lang M, Seifert MH, Wolf KK, Aschenbrenner A, Baumgartner R, Wieber T, Trentinaglia V, Blisse M, Tajima N, Yamashita T, Vitt D, Noda H 2011. Discovery and hit-to-lead optimization of novel allosteric glucokinase activators. *Bioorg Med Chem Lett* 21(18):5417-5422.
51. Luan X, Bodmeier R 2006. Influence of the poly(lactide-co-glycolide) type on the leuprolide release from in situ forming microparticle systems. *J Control Release* 110(2):266-272.
52. Bao W, Zhou J, Luo J, Wu D 2006. PLGA microspheres with high drug loading and high encapsulation efficiency prepared by a novel solvent evaporation technique. *J Microencapsul* 23(5):471-479.
53. Gasteiger E, Gattiker A, Hoogland C, Ivanyi I, Appel RD, Bairoch A 2003. ExPASy: The proteomics server for in-depth protein knowledge and analysis. *Nucleic Acids Research* 31(13):3784-3788.
54. Kyte J, Doolittle RF 1982. A simple method for displaying the hydrophobic character of a protein. *J Mol Biol* 157(1):105-132.
55. Jung T, Kamm W, Breitenbach A, Klebe G, Kissel T 2002. Loading of tetanus toxoid to biodegradable nanoparticles from branched poly(sulfobutyl-polyvinyl alcohol)-g-(lactide-co-glycolide) nanoparticles by protein adsorption: a mechanistic study. *Pharm Res* 19(8):1105-1113.
56. Sales-Junior PA, Guzman F, Vargas MI, Sossai S, Patarroyo VA, Gonzalez CZ, Patarroyo JH 2005. Use of biodegradable PLGA microspheres as a slow release delivery system for the Boophilus microplus synthetic vaccine SBm7462. *Vet Immunol Immunopathol* 107(3-4):281-290.

57. Rafi M, Singh SM, Kanchan V, Anish CK, Panda AK 2010. Controlled release of bioactive recombinant human growth hormone from PLGA microparticles. *J Microencapsul* 27(6):552-560.
58. Burton KW, Shameem M, Thanoo BC, DeLuca PP 2000. Extended release peptide delivery systems through the use of PLGA microsphere combinations. *J Biomater Sci Polym Ed* 11(7):715-729.
59. Buyuktimkin B, Wang Q, Kiptoo P, Stewart JM, Berkland C, Siahaan TJ 2012. Vaccine-like controlled-release delivery of an immunomodulating peptide to treat experimental autoimmune encephalomyelitis. *Mol Pharm* 9(4):979-985.
60. Yang J, Sun H, Song C 2012. Preparation, characterization and in vivo evaluation of pH-sensitive oral insulin-loaded poly(lactic-co-glycolic acid) nanoparticles. *Diabetes Obes Metab* 14(4):358-364.
61. van Montfoort N, Camps MG, Khan S, Filippov DV, Weterings JJ, Griffith JM, Geuze HJ, van Hall T, Verbeek JS, Melief CJ, Ossendorp F 2009. Ag storage compartments in mature dendritic cells facilitate prolonged cytotoxic T lymphocyte cross-priming capacity. *Proc Natl Acad Sci U S A* 106(16):6730-6735.



Chapter 4

Co-encapsulation of synthetic long peptide antigen and Toll like receptor 2 ligand in poly-(lactic-co-glycolic-acid) particles results in sustained MHC class I cross-presentation by dendritic cells

Rodney A. Rosalia, Ana Luisa Silva, Ivan Stepanek, Annelies van der Laan, Jaap Oostendorp, Wim Jiskoot, Sjoerd H. Van der Burg, Ferry Ossendorp

Manuscript in preparation

Abstract

We previously reported the successful incorporation of synthetic long peptides (SLPs) in poly(lactic-co-glycolic acid) (PLGA) nanoparticles (NP) as a vaccine delivery vehicle. We showed that the burst release of the encapsulated SLP was crucial to improve MHC class I presentation and CD8⁺ T cell activation in comparison to soluble SLP (sSLP). Using SLP-OVA24_{aa} as vaccine antigen (Ag) and Pam3CSK4 as an adjuvant encapsulated in PLGA-NP (PLGA-SLP and PLGA-SLP/TLR2L), we show in this report that toll like receptor (TLR) 2 stimulation enhances MHC class I presentation of PLGA-SLP by dendritic cells (DCs), however co-encapsulation of the TLR ligand was not required for this effect. DC loaded with PLGA-SLP(/TLR2L), route internalized NP into endo-lysosomal compartments and not the cytosol as occurs with sSLP. Moreover, PLGA-NP encapsulated SLP could be detected for prolonged periods inside endo-lysosomal compartments. Prolonged presence of NP inside DC resulted in MHC class I presentation of PLGA-NP encapsulated SLP for up to 96 hr, which led to sustained CD8⁺ T cell proliferation *in vivo* adoptive transfer of PLGA-SLP loaded DC. These findings explain the *in vivo* effectiveness of nanoparticle vaccination and shows that PLGA-SLP is a promising delivery vehicle for clinical application as a cancer immunotherapy.

Introduction

Cancer immunotherapy is a promising treatment modality to enhance the tumor associated antigen (Ag) specific T cell responses in cancer patients. Efficient MHC class I Ag presentation and subsequent CD8⁺ T cell priming are pre-requisites for optimal clinical efficacy of a cancer immunotherapy vaccine^{1,2}. We recently reported that synthetic long peptides (SLP) considerably facilitate MHC class I presentation in comparison to protein, which was related to faster uptake and processing of SLP by dendritic cells (DC) compared to that of protein Ag³.

SLP-vaccines emulsified in Montanide(-ISA51) water-in-oil-in-water emulsion have been studied in the clinic against various forms of cancer^{4,5} and other immunological diseases^{6,7}. However, the use of Montanide is associated with considerable adverse effects⁸⁻¹¹. In addition, montanide has poorly defined adjuvant properties and the release kinetics of the emulsified vaccine-Ag cannot be controlled. Alternative vaccine delivery systems and adjuvants for SLP, being at least as efficient as but having less side effects than Montanide, are therefore highly required like well-defined Toll like receptor ligands (TLRL). In light of this we have previously reported the successful application of nanoparticles (NP) formulated with the fully biocompatible polymer, poly-(lactic-co-glycolic-acid) (PLGA) as delivery vehicle for SLP vaccines. Encapsulating SLP in PLGA led to a significant enhancement of MHC class I Ag presentation and CD8⁺ T cell activation compared to soluble SLP¹⁰. However, PLGA-NP have low immunostimulatory properties by itself but allows controlled co-encapsulation and release of TLRL^{12,13}.

The aim of the present paper was to study 1) how PLGA-NP encapsulated SLP is routed and processed into MHC class I molecules and 2) how a defined adjuvant co-encapsulated in NP affects the efficiency and duration of CD8⁺ T cell activation by DC. For this purpose, NP were formulated together with a TLR2L (Pam3CSK4) as adjuvant, which effectively boosted vaccine-Ag specific immune responses when covalently conjugated to SLP^{14,15}.

We show here that co-encapsulating TLR2L with SLP in PLGA-NP further enhances the efficiency of MHC class I cross-presentation of SLP by DC compared to plain PLGA-SLP. In addition, loading of DC using PLGA-NP results in sustained MHC class I presentation of SLP compared to soluble SLP. However, the effect of sustained MHC class I presentation was not related to TLR2L-mediated DC maturation but likely because of the prolonged presence of PLGA-NP encapsulated SLP inside endo-lysosomal compartments upon uptake by DC. These organelles are similar to the storage compartments in DC we have described for other antigen targeting system like FcR-mediated uptake¹⁶.

Finally, we show that adoptive transfer of DC loaded with PLGA-SLP/TLR2L stimulated CD8⁺ T cells over a sustained period of time whereas soluble SLP loaded DC failed to do so. Therefore, this study presents additional evidence for the use of PLGA-NP as a clinically suitable vaccine delivery systems to enhance direct MHC class I Ag presentation and T cell activation but also maintain CD8⁺ T cell responses over a prolonged time period.

Material and methods

Mice

WT C57BL/6 (CD45.2/Thy1.2; H2-K^b) mice were obtained from Charles River Laboratories (France). TAP1 KO mice (C57BL/6 CD45.2/Thy1.2; H2-K^b) were purchased from the Jackson laboratory (Bar Harbor, ME). All mice were used at 8–12 weeks of age in accordance with national legislation and under supervision of the animal experimental committee of the University of Leiden.

Materials

The synthetic long peptide DEVSGLEQLESIINFEKLA^{24aa}AAAK (SLP-OVA_{24aa})¹⁷, covering the H2-K^b restricted CD8⁺ T cell epitope SIINFEKL of ovalbumin (OVA) and SLP-OVA_{24aa}-Bodipy-FL (Bp) were synthesized at the interdepartmental GMP facility of the Department of Clinical Pharmacy and Toxicology of Leiden University Medical Center as described previously¹⁰. Poly(D,L-lactic-co-glycolic acid) [PLGA], Resomer® RG 502H was purchased from Boehringer Ingelheim (Ingelheim, Germany). 4-(2-hydroxyethyl)-1-piperazine-ethanesulfonic acid (HEPES), dichloromethane (DCM), dimethyl sulfoxide (DMSO), and trifluoroacetic acid (TFA) were purchased from Sigma-Aldrich (Steinheim, Germany). Acetonitrile (ACN) and methanol (MeOH) were obtained from Biosolve BV (Valkenswaard, the Netherlands), Polyvinyl alcohol (PVA) 4-88 (31 kDa) was purchased from Fluka (Steinheim, Germany). Reversed phase HPLC column ReproSil-Pur C18-AQ 3 μm (150x4 mm) was purchased from Dr. Maisch HPLC GmbH (Ammerbuch-Entringen, Germany). Pam3CSK4 and Pam3CSK4-Rhodamine were purchased from Invivogen (San Diego, USA). Iscove's Modified Dulbecco's Medium (IMDM) was purchased from Lonza (Walkersville, USA). All other chemicals were of analytical grade and all aqueous solutions were prepared with milli Q water.

Nanoparticle preparation and characterization

Nanoparticles loaded with SLP-OVA_{24aa} were prepared using a double emulsion with solvent evaporation method as previously described¹⁰. In brief, 1.4 mg SLP-OVA_{24aa} were dissolved in 100 μ L 50% ACN in 0.25 mM NaOH and then added to 400 μ L 50 mM Hepes, pH 8.0. This solution was then added to 50 mg of PLGA in 1 ml of dichloromethane and the mixture was emulsified under sonication (30 s, 20 W). To this first emulsion (w1/o), 2 ml of an aqueous surfactant solution (for surfactant types, see results) were added immediately, and the mixture was emulsified again by sonication (30 s, 20 W), creating a double emulsion (w1/o/w2). The emulsion was then added drop-wise to 25 ml of extraction medium (0.3% w/v surfactant) previously heated to 40°C under agitation, to allow quick solvent evaporation, and left stirring for 1 h. The particles were then collected by centrifugation for 15 min at 15000 *g* at 10°C, washed, resuspended in Milli Q water, aliquoted and freeze-dried at -55°C in a Christ Alpha 1-2 freeze-drier (Osterode am Harz, Germany) overnight. For particles co-encapsulating SLP-OVA_{24aa} and Pam3CSK4, 250 μ g of Pam3CSK4 were dissolved in DCM together with PLGA, and for particles containing SLP-OVA_{24aa}-Bp-FL, circa 10% labeled peptide was added to the peptide solution.

Particle characterization was performed as described¹⁰. NP were diluted to 2.5 mg/ml in 1 mM Hepes pH 7.4. Size and polydispersity index (PDI) of NP were measured by dynamic light scattering, and zeta-potential was measured by laser Doppler electrophoresis, using a Zetasizer (Nano ZS, Malvern Ltd., United Kingdom).

The encapsulation efficiency (EE) was calculated according to equation 4.1 and drug loading (DL) by equation 4.2. EE of OVA₂₄ was determined by measuring the peptide content of digested particles by reversed phase HPLC as described¹⁰.

EE of Pam3CSK4-Rhodamine was determined by measuring fluorescence detected in the supernatant against a calibration curve and expressed as percentage of the total amount added.

$$\% \text{ EE} = \frac{\text{SLP/TLR2L mass in NP}}{\text{initial SLP/TLR2L mass}} \times 100 \quad (4.1)$$

$$\% \text{ DL} = \frac{\text{encapsulated SLP/TLR2L mass}}{\text{total polymer} + \text{SLP/TLR2L mass}} \times 100 \quad (4.2)$$

Cells

Freshly isolated murine DCs were cultured from mouse bone marrow (BM) cells, as described before¹⁸. The D1 cell line, an immature primary splenic DC line (C57BL/6-derived), was cultured as described elsewhere¹⁹. B3Z CD8⁺ T cells (H2-k^b/SIINFEKL) are hybridoma cell lines expressing a β -galactosidase construct which upon T-cell activation can be measured by a colorimetric assay²⁰.

Murine MHC class I Ag presentation assays

C57BL/6 BMDCs or D1 cells (1×10^5 cells/well) were plated out in triplicate using 96-well plates (Greiner #655101) and incubated for 2.5 hr with the Ag at the indicated concentrations. Cells were washed 3x with complete medium to remove excess Ag before the B3Z CD8⁺ T cells were added to assess MHC class I cross-presentation. T cells were cultured in the presence of Ag-loaded DC for 2.5 at 37°C. In some experiments, BMDC or D1 cells were pre-incubated with *epoxomicin* (324800, Merck) or *bafilomycin A1* (196000, Merck) followed by Ag-incubation as described above in the presence of the compounds. D1 cells were pre-incubated with bafilomycin A1 (196000, Merck) and MHC class I Ag presentation determined as described above. To study sustained MHC class I Ag presentation, 2×10^6 immature D1 cells were incubated for 2.5 hr with 4 μ M SLP in different formulations. After incubation, cells were harvested and transferred to 50 ml Falcon tubes, resuspended in complete medium and centrifuged. This procedure was performed 3x to wash away unbound Ag. Cells were either used directly as Ag presenting cells (APC) ("direct condition") or plated out again in petri dishes and further cultured for 96 hr ("chase condition"). Ag loaded D1 cells were then harvested and plated out in 96-wells plates (5×10^4 cells/well) and used as APC in co-culture with B3Z CD8⁺ T cells to detect capacity to cross-present SLP in MHC class I molecules using a colorimetric assay as described before²⁰.

Adoptive transfer of Ag loaded DC

C57BL/6 BMDC cells (10×10^6 cells/petri dish, Corning # 430589) were loaded with 4 μ M PLGA-SLP, PLGA-SLP/TLR2L and sSLP on $t = -96$ hr and $t = -2.5$ hr. Cells were washed to remove unbound Ag and either used directly or further cultures in the absence of Ag. On $t = -1$ day, splenocytes from Thy1.1⁺ OT-I mice were harvested and transferred i.v. to recipient animals (10×10^6 splenocytes/mouse). On $t = 0$, OVA-specific T cells enriched mice

received i.v. 1×10^6 DC loaded with PLGA-SLP, PLGA-SLP/TLR2L. Tail vein blood samples were collected on $t = \text{day } 3$ post-transfer of DC and analyzed for the percentages of $\text{Thy1.1}^+ \text{CD8}^+$ T cells using rat anti-mouse CD90.1-APC, CD3-AF800 and CD8-FITC antibodies (Biolegend). Samples were measured using an LSRII flow cytometer (BD) and analyzed with FlowJo software (Treestar).

Confocal microscopy

DCs were incubated for 24 hr with $10 \mu\text{M}$ SLP-OVA_{24aa}-Bodipy-FL in different formulations at 37°C . Specific murine DC used is described in the figure legends. After incubation cells were washed 3 times to remove excess and unbound Ag, resuspended at a concentration of 2×10^5 cells in $200 \mu\text{l}$ complete medium and plated into poly-*d*-lysine coated glass-bottom dishes (MatTek) followed by mild centrifugation to allow the cells to adhere. Adhered cells were then fixed with 0.2% paraformaldehyde. All imaging experiments were carried out on a Leica TCS SP5 confocal microscope (HCX PL APO $63\times/1.4$ NA oil-immersion objective, 12 bit resolution, 1024×1024 pixels, pinhole 2.1 Airy discs, zoom factor 1 or 7). Imaging was performed using the 488 nm line from an Argon laser collecting emission between 500 and 600 nm. Dual color images were acquired by sequential scanning, with only one laser per scan to avoid cross talk. The images were analyzed using the Leica software program (LAS AF).

Analysis of cytokine production by DC using Enzyme-linked Immunosorbent Assay (ELISA)

*BMDC were incubated for 24 hr with NP. Supernatants were harvested and tested for IL-12 p70 (BD OptEIA™ MOUSE IL-12 Cat. Nr 555256) following manufacturer's instructions.

Statistics

Graphpad prism was used as the main statistical software. Statistical analyses applied to determine the significance of differences are described in the figure legends.

RESULTS

Characterization of formulated PLGA-SLP and PLGA-SLP/TLR2L NP

PLGA-NP were formulated using a modified double emulsion method and solvent evaporation technique with SLP-OVA_{24aa} as described before, PLGA-SLP¹⁰. This formulation was adapted by adding the TLR2 ligand (TLR2L) Pam3CSK4 in the organic phase to yield PLGA-NP co-encapsulating SLP and adjuvant, PLGA-SLP/TLR2L. For visualization purposes selected batches were formulated with 10 % SLP-OVA_{24aa}-Bodipy-FL (SLP-Bp). Fluorescent SLP was added during formulation. Particle characteristics are described in Table 4.1.

Co-encapsulation of TLR2L and/or SLP-Bp did not affect the physical properties of the formulated NP, with several batches showing very similar characteristics (Table 4.1).

Enhanced cross-presentation of PLGA-NP encapsulated SLP in the presence of TLR2L

DC loaded with PLGA-SLP cross-presented SLP in the context of MHC class I molecules with higher efficiency compared to sSLP, as published previously¹⁰. TLR-stimulation is known to improve proteasome activity and thus enhance MHC class I Ag cross-presentation. Indeed, the presence of TLR2L during Ag-loading enhanced MHC class I cross-presentation

Table 4.1 Characterization of PLGA-SLP/TLR2L NP

Formulation	%DL SLP ^o	%EE SLP ^o	%DL Pam3CSK4	%EE Pam3CSK4	Size (nm)	PDI	ZP (mV)
PLGA-SLP*	1.06 ± 0.15	39 ± 6	n/a	n/a	322 ± 44	0.19 ± 0.04	-12 ± 1
PLGA-SLP/TLR2L*	1.02 ± 0.17	38 ± 6	0.32 ± 0.05	67 ± 10	293 ± 19	0.18 ± 0.04	-13 ± 1
PLGA-SLP-Bp**	1.01	37	n/a	n/a	312	0.23	-16
PLGA-SLP/TLR2L-BP**	0.95	35	0.16	33	304	0.20	-13

^oSLP-OVA_{24aa} (DEVSGLEQLESIIINFEKLAATAAAK).

*Values represent average ± SD of > 4 independently prepared batches.

**Values obtained from 1 batch.

DL = drug loading; EE = encapsulation efficiency; PDI = poly dispersity index; variance, an arbitrary measure for the degree of dispersity in particle size within one batch of particles suspension, PDI values below 0.3 was considered monodisperse and accepted for follow up studies²¹; ZP = zeta potential; The magnitude of the zeta potential is predictive of the colloidal stability. Nanoparticles with Zeta Potential values greater than +25 mV or less than -25 mV typically have high degrees of stability. Dispersions with a low zeta potential value will eventually aggregate due to Van Der Waal inter-particle attractions.

of all SLP-formulations tested compared to DC loaded in the absence of TLR2L (Figure 4.1A). PLGA-SLP/TLR2L resulted in better CD8⁺ T cell activation than PLGA-SLP. However, co-encapsulation of TLR2L was dispensable to enhance MHC class I presentation of PLGA-encapsulated SLP *in vitro* as mixtures of PLGA-SLP + soluble TLR2L (sTLR2L) showed similar potency to PLGA-SLP/TLR2L.

TLR2 stimulation failed to improve the cross-presentation of sSLP to comparable levels as observed with PLGA-encapsulated SLP (Figure 4.1A). This observation stresses the importance of an optimal delivery method to achieve high levels of Ag intracellularly and to improve MHC class I Ag processing.

In summary, combining TLR2L stimulation with PLGA-NP delivery of SLP significantly improves MHC class I presentation compared to Ag loading in the absence of TLR2L. The positive effect of TLR2L was irrespective of co-encapsulation in PLGA-NP.

Ag-delivery via PLGA-NP results in prolonged MHC class I Ag cross-presentation

The duration of MHC class I presentation and TCR recognition/binding is an important factor determining CD8⁺ T cell priming. Short TCR-stimulation leads to sub-optimal T cell priming which is associated in impaired effector functions anergy^{21,22}. The long term effects on MHC class I cross-presentation of SLP was studied by stimulating B3Z CD8⁺ T cells with 96 hr rested Ag-loaded DC. DC were incubated for 2.5 hr in the presence of 4 μM SLP in either soluble or particulate form with or without TLR2L. As a positive control, DC were incubated with SLP-TLR2L conjugates which induce the formation of Ag-storage compartments upon internalization. These compartments facilitate prolonged MHC class I presentation and sustained CD8⁺ T cell priming as we have previously reported^{14,18}. DC loaded with sSLP failed to activate CD8⁺ T cells 96 hr post Ag-incubation (Figure 4.1B). Only DC incubated with PLGA-encapsulated Ag and the SLP-TLR2L conjugate were capable of MHC class I SLP cross-presentation after 96 hr (Figure 4.1B).

TLR-stimulation has been shown to slow down the decay of MHC class I molecules thereby prolonging cell-surface expression of MHC class I molecule/peptide complexes²³. In our system however, prolonged presence of MHC class I molecules/peptide complexes is unlikely to be the main mechanism facilitating sustained CD8⁺ T cell activation by PLGA-SLP as plain particles in the absence of additional adjuvants poorly matured DC. PLGA-SLP had no phenotypical (Figure 4.2A) nor functional DC maturing effects (Figure 4.2B) on

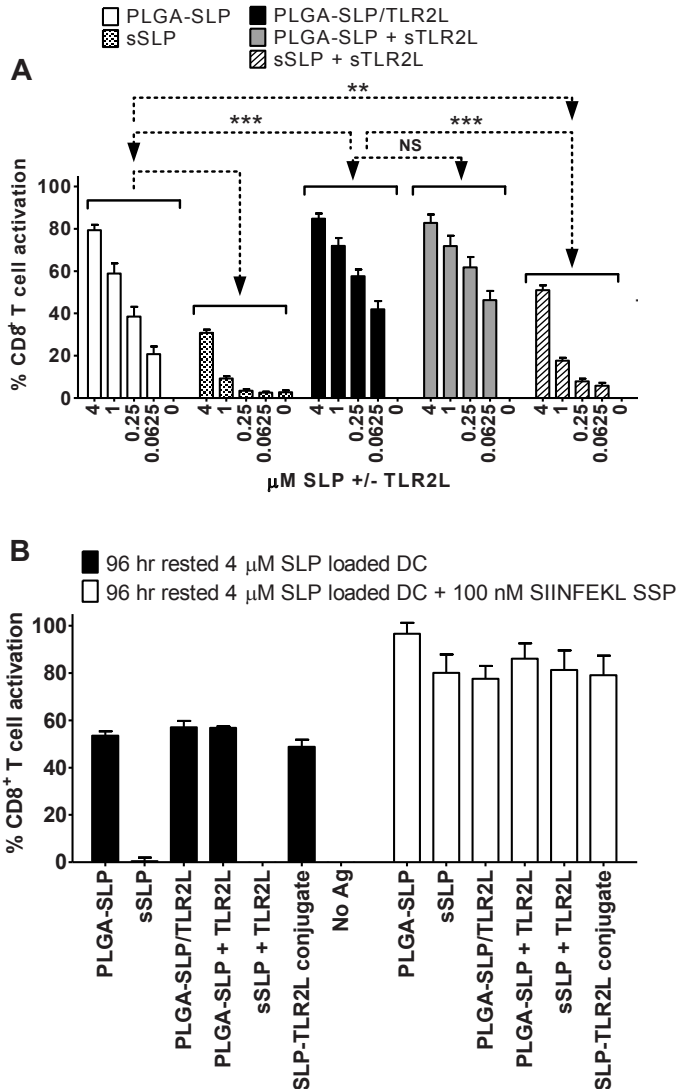


Figure 4.1 TLR2 stimulation improves MHC class I cross-presentation of PLGA-NP encapsulated SLP.

D1 cells were incubated for 2.5 h with titrated amounts of SLP-OVA_{24aa} in different formulations with or without Pam3CSK4 (TLR2L) and co-cultured overnight in the presence of (A) B3Z CD8⁺ T cells. T-cell activation was determined as described in *Materials and methods*. (B) D1 cells were incubated with 4 μM Ag for 2.5 hr on t = -96 hr (chase) and on t = -2.5 hr (direct). “Chase” and “direct” Ag loaded DC were harvested at t = 0 hr and their APC capacity to activate B3Z CD8⁺ T cells compared. Data are shown as mean + SD of three samples from one representative experiment representative of four (A) and three (B) experiments performed. *** P < 0.001 using a two-way ANOVA and Bonferroni posttests.

DC. Addition of Pam3CSK4 to PLGA-SLP formulations, to obtain PLGA-SLP/TLR2L, very efficiently matured DC (Figure 4.2). However, TLR2L stimulation did not further MHC class I Ag cross-presentation by DC loaded with PLGA-SLP or sSLP loaded DC and then rested for 96 hr in culture in the absence of Ag. Therefore, TLR2-stimulation by itself cannot explain our observations of prolonged Ag presentation by DC pulsed by PLGA-SLP.

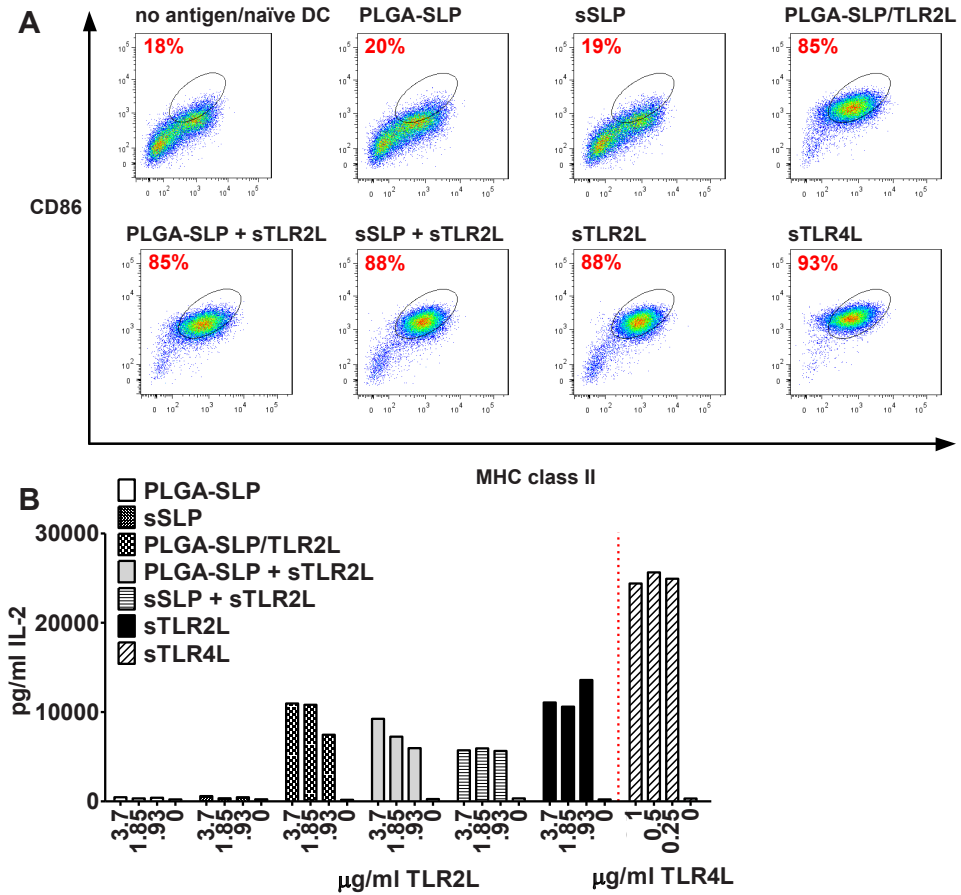


Figure 4.2 Addition of TLR2L to plain PLGA-SLP and sSLP improves adjuvanticity and results in DC maturation.

D1 cells were incubated in the presence of titrated amounts of SLP formulations with or without Pam3CSK4 (Invivogen, tlr1-pms), and soluble LPS (TLR4L) (Sigma L4130, Escherichia coli 0111:B4). After 24 hr supernatants were collected, DC harvested and stained for MHC class II and CD86 and their expression analyzed by FACS (A). Percentages indicate the numbers of double positive cells. Supernatants were analyzed via ELISA for IL-2 levels (B). Data shown are representative of three independent experiments.

In conclusion, Ag delivery via PLGA-NP results in prolonged MHC class I presentation *in vitro* and sustained CD8⁺ T cell activation. Prolonged MHC class I presentation of SLP was not dependent on DC maturation.

DC loaded with SLP encapsulated in NP are capable of sustained *in vivo* priming after adoptive transfer

The *in vitro* observations were confirmed *in vivo* by transferring DC which were loaded with Ag on t = -96 hr into recipient mice enriched with OT-I CD8⁺ T cells on day before adoptive transfer. The extent of CD8⁺ T cell expansion was compared to mice receiving DC loaded with Ag (-2.5 hr, "direct").

Only DC which were loaded with PLGA-SLP or PLGA-SLP/TLR2L induced significant OT-I CD8⁺ T expansion using freshly Ag-loaded DC (Figure 4.3). DC loaded with sSLP performed

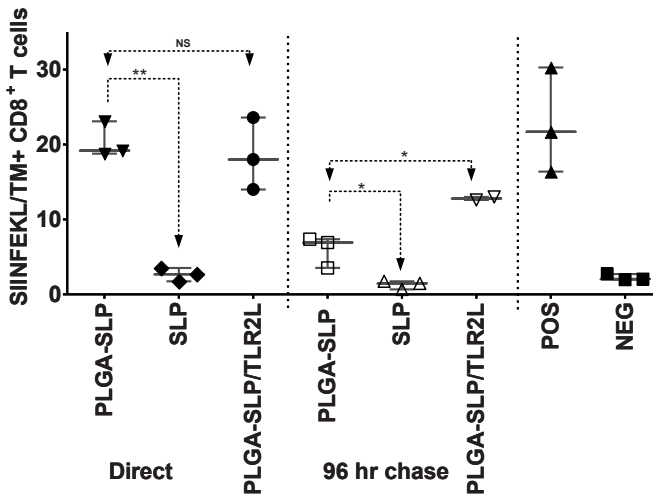


Figure 4.3 PLGA-SLP loaded DC possesses APC capacity and stimulated CD8⁺ T cells 96 hr after Ag-loading.

Ag loaded BMDC (C57BL/6) were tested for their capacity to expand specific CD8⁺ T cells *in vivo*. WT C57BL/6 animals received 10⁶ OVA-specific Thy1.1⁺ OT-I splenocytes i.v. on t = day -1. On t = 0, OVA-specific T cell enriched mice received i.v. 1*10⁶ DC loaded with PLGA-SLP, PLGA-SLP/TLR2L and sSLP on t = -96 hr and t = -2.5 hr. Blood samples were taken on t = day 3 post-transfer of DC and analyzed for the percentages of Thy1.1⁺CD8⁺ T cells. DC loaded with SIINFEKL and 10 µg/ml LPS and antigen naïve DC were used as positive (pos) and negative (neg) control. Percentages determined for each individual mice are displayed and data shown are representative of one independent experiments. * P < 0.05 using a unpaired student t-test.

poorly as APC at the concentrations of sSLP tested. Poor priming of OT-I CD8⁺ T cells can be related to the lower MHC class I presentation of sSLP compared to PLGA-SLP but is most likely a result of sub-optimal activation of naive OT-I CD8⁺ T cells, which are co-stimulation dependent, by sSLP loaded DC which have a immature phenotype (Figure 4.2). PLGA-SLP and even PLGA-NP in general, do not mature DC. However NP-based Ag delivery is very efficient leading to high density of Ag-epitope loaded MHC class I molecules on the cell-surface leading to sufficient triggering of OT-I CD8⁺ T cells for them to proliferate *in vivo*. PLGA-SLP with co-encapsulated TLR2L results in significant OT-I expansion even after 96 hrs incubation indicating sustained antigen storage of the particle-delivered antigen by DC.

Re-routing and prolonged presence of SLP into the endosomes by encapsulation in PLGA-NP

We analyzed if the intracellular localisation of PLGA-SLP after uptake by DC might play a role in the observed MHC class I presentation. For this purpose DC were incubated with sSLP, PLGA-SLP and PLGA-SLP/TLR2L and analyzed directly by confocal microscope. D1 dendritic cells and BMDC were highly capable to internalizing Bp-labeled SLP in the tested formulations (green fluorescence, Figures 4.4 & 4.5). sSLP internalized by DC was present for a large part outside the endo-lysosomes as we showed before³ whereas PLGA-encapsulated SLP showed high co-localization, with endo-lysosomes, suggested by the formation of bright yellow spots, marked in the Figures 4.4 & 4.5 by the arrows. DC which took up NP tend to have larger endo-lysosomal compartments (bright red spots, Figures 4.4 & 4.5) compared to DC which internalized sSLP which might suggest formation of phagolysosomes. The results indicate that encapsulation of SLP inside PLGA-SLP modulates intracellular trafficking of SLP by keeping the Ag inside endosomal compartments, thereby directing it away from the cytosol.

Brighter yellow spots were observed when BMDC internalized PLGA-SLP in comparison to sSLP. This suggest that DC take up much higher amounts of SLP on a single cell basis when it is encapsulated in PLGA-NP, pointing to the more efficient uptake by DC of SLP when encapsulated (Figure 4.4). Interestingly, encapsulation of TLR2L in PLGA-NP (PLGA-SLP/TLR2L) even further enhanced the efficiency (Figure 4.4B) and rapidity of NP internalization (Figure 4.4C) by BMDC suggesting an additional role for TLR2 in the internalization of NP.

DC are known to preserve internalized PLGA-(micro)spheres inside endo-lysosomal compartments for up to 48 hr which suggests that intracellular hydrolysis of PLGA particles

to be a slow process. In our study, sustained MHC class I cross-presentation of PLGA-encapsulated SLP could be detected even after 96 hr. We therefore analyzed D1 cells loaded with sSLP, PLGA-SLP, PLGA-SLP/TLR2L directly after loading (Figure 4.5A) or after 96 hr rest (Figure 4.5B). sSLP-loaded D1 cells analyzed after 96 hr rest showed clear differences with DC analyzed directly after Ag-loading. Fluorescent signal of SLP was largely undetectable in DC cultured with sSLP whereas labeled SLP originated from the PLGA-SLP or PLGA-SLP/TLR2L could be clearly detected still inside endosomal compartments (Figure 4.5).

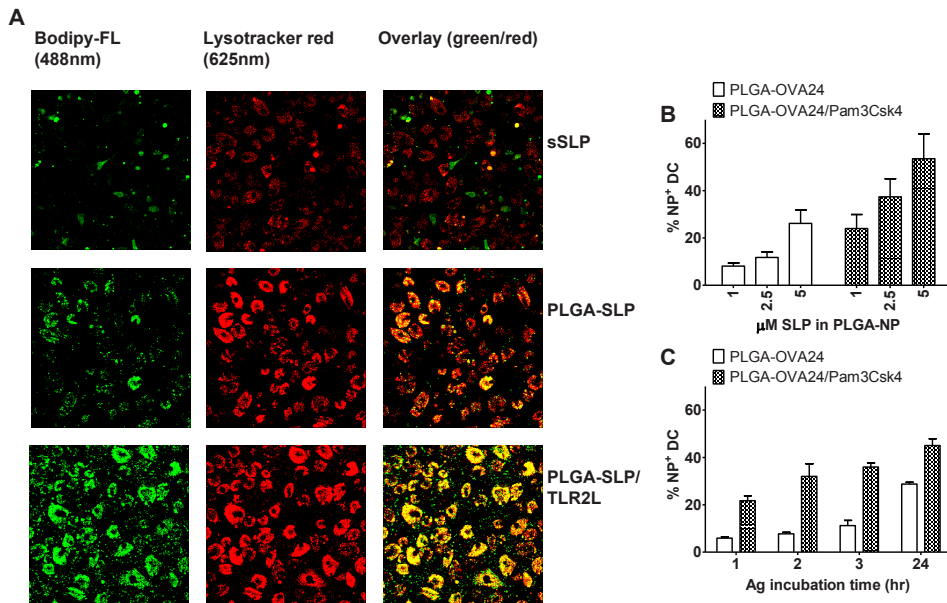


Figure 4.4 Retrouting of SLP into endo-lysosomal compartments upon encapsulation of in PLGA-NP.

BMDC were incubated with 20 μ M sSLP-Bp, 20 μ M PLGA-SLP-Bp (10% SLP-Bodipy-FL) or 20 μ M PLGA-SLP-Bp/TLR2L (10% SLP-Bodipy-FL) (excitation- 488nm, visualized as the green signal) for 2.5 hr and co-stained with Lysotracker red for visualization of the endo-lysosomes (red signal) and visualized by confocal microscopy. **(A)** 1st column shows images depicting green signal as the fluorescence of Bodipy-FL (488nm). 2nd column shows images depicting red signal as the fluorescence of the lysotracker red/endo-lysosomes (625nm). 3rd column depicts overlay images of red/green. Yellow-overlay signal marks co-localization. Images were analyzed using Leica software. BMDC were incubated at 4°C and 37°C with **(B)** titrated amounts of PLGA-SLP, PLGA-SLP/TLR2L and PLGA-SLP + sTLR2L (10% SLP-Bodipy-FL). **(C)** Alternatively, DC were incubated with with 2.5 μ M of PLGA-SLP and PLGA-SLP/TLR2L (10% SLP-Bodipy-FL). Ag uptake was quantified by flow cytometry and data shown are absolute values (% NP⁺ DC at 37°C - % NP⁺ DC at 4°C) and represent Avg + SEM of 3 independent experiments **(A)** and Avg + SD of 2 independent experiments.

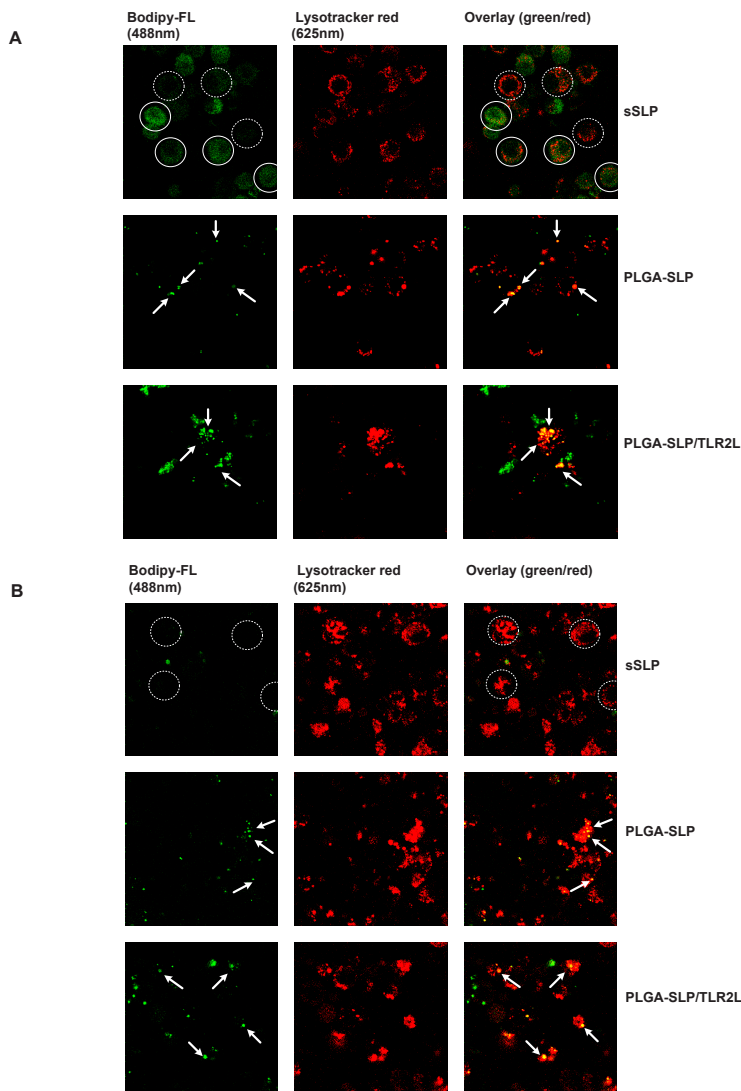


Figure 4.5 Sustained presence of PLGA-NP encapsulated SLP in endo-lysosomes.

D1 cells were incubated with 20 μ M sSLP-Bp, 20 μ M PLGA-SLP-Bp (10% SLP-Bodipy-FL) or 20 μ M PLGA-SLP-Bp/TLR2L (10% SLP-Bodipy-FL) (488nm) for 2.5 hr on $t = -2.5$ hr (A) and $t = -96$ hr (B) and co-stained with Lysotracker red for visualization of the endo-lysosomes on $t = -15$ min. Live cell imaging were performed at $t = 0$. 1st column shows images depicting green signal as the fluorescence of Bodipy-FL (488nm). 2nd column shows images depicting red signal as the fluorescence of the lysotracker red/endo-lysosomes (625nm). 3rd column depicts overlay images of red/green. White arrow indicates hotspots (yellow) within a cell where green and red co-localize. Closed circles show cells containing green-flourescent signal (and red fluorescent signal). Dashed circles depict cells containing only red fluorescent signals. Images were analyzed using Leica software.

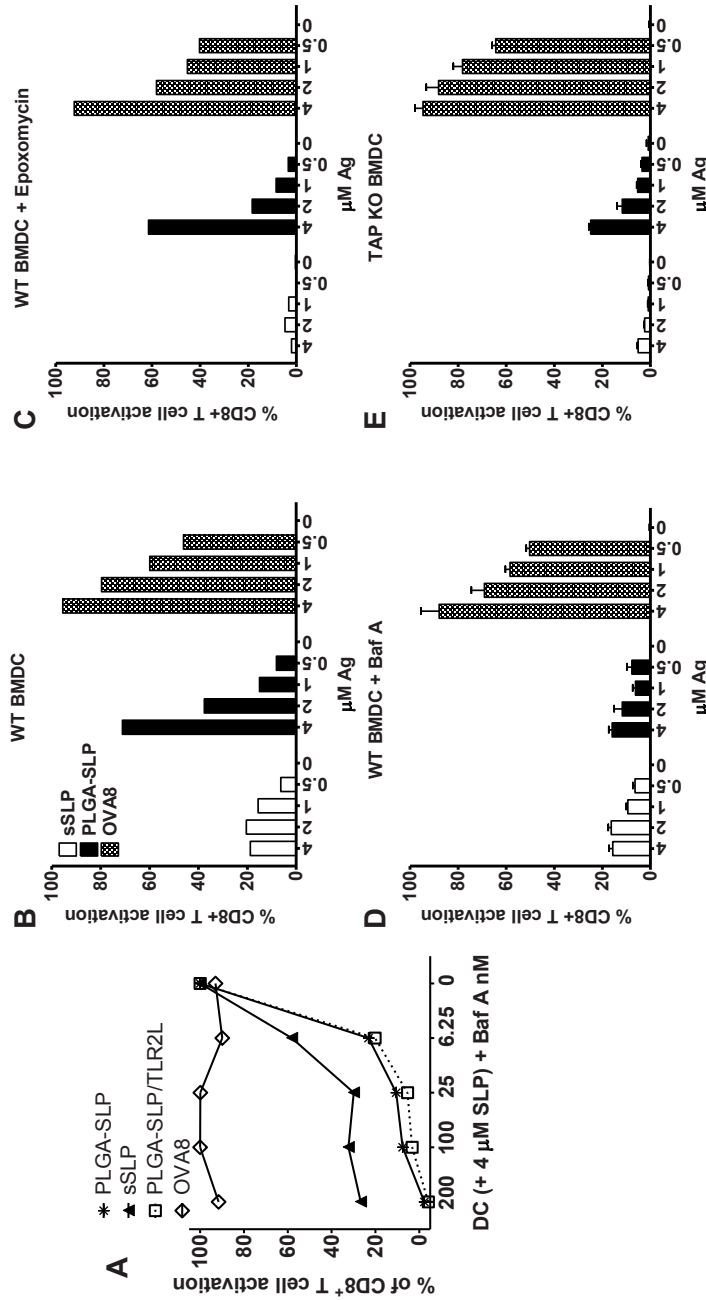


Figure 4.6 MHC class I cross-presentation PLGA-SLP and PLGA-SLP/TLR2L is impaired in the absence of functional proteasome, TAP and when endo-lysosomal acidification is inhibited by Bafilomycin A.

(A) D1 cells were pre-incubated with indicated titrated concentrations of bafilomycin A1 (196000, Merck) followed by culture in the presence of 4 μM sSLP, PLGA-SLP, PLGA-SLP/TLR2L and 5 nM SSP-OVA_{38aa} (SIINFEKL). Cells were washed 3x times with complete medium before the B3Z CD8+ T-cells were added followed by O/N incubation at 37°C. (B) WT BMDC were incubated with titrated amounts of sSLP or PLGA-SLP without additional treatments or in the presence of (C) epoxomycin or (E) Bafilomycin A. (D) TAP KO BMDC were incubated with titrated amounts of sSLP or PLGA-SLP.

It is known that internalized soluble proteins are also routed into endosomal compartments²⁴⁻²⁶. However, endosomal presence of an Ag does not guarantee preservation as soluble protein was not detected inside DC after 96 hr (Supporting Information Figure S4.1). This observation fits with our previous reports showing that soluble proteins do not lead to sustained Ag presentation¹⁸.

Processing of PLGA-NP encapsulated SLP can be blocked by inhibitors of endo-lysosomal acidification, proteasome and TAP

Exogenous Ag routed towards the MHC class I cross-presentation pathway can follow two pathways I) the classical cytosolic pathway or II) the endosomal pathway²⁷⁻²⁹. The endosomal pathway is dependent on the pH inside the endo-lysosomes but the cytosolic pathway is (mostly) independent of the pH gradient inside endo-lysosomes²⁹. We observed that CD8⁺ T cell activation by DC loaded with PLGA-SLP and PLGA-SLP/TLR2L can be completely blocked (Figure 4.6) in a dose dependent manner using the lysotropic agent, bafilomycin A (Baf A). MHC class I cross-presentation of sSLP was slightly decreased as observed before³ but CD8⁺ T cell activation could still be detected at the highest concentration of the compound tested in this study. The presentation of the minimal MHC class I binding peptide (OVA_g) was unaffected over the whole range of concentrations used. PLGA-SLP MHC class I cross-presentation was reduced in the presence of a proteasome inhibitor (Figure 4.6B & C). MHC class I processing of PLGA-SLP was significantly impaired in the absence of functional TAP (Figure 4.6B & E) or when when endo-lysosomal acidification is blocked (Figure 4.6B & D).

Discussion

In this study, we analyzed the effects on MHC class I presentation of co-encapsulating a TLR2L with SLP in PLGA-NP. SLP and PLGA-NP are inert synthetic materials with poor immunostimulating properties. The therapeutic effectivity of cancer vaccines is largely based on its potency to activate DCs, which have superior capacity to induce robust anti-tumor T cell responses.

We previously reported the successful formulation of PLGA-SLP using a novel double emulsion and solvent-evaporation technique. Applying PLGA-NP as a vaccine delivery system, the efficacy of MHC class I Ag presentation and subsequent CD8⁺ T cell activation

by DCs was significantly enhanced ¹⁰ compared to sSLP. We have also shown recently that plain PLGA-NP have poor DC activating properties compared to TLRL ¹². With the purpose of further increasing the vaccine potency of PLGA-SLP, we have included a TLR2L, Pam3CSK4; an adjuvant which has led to promising pre-clinical results when covalently coupled to SLP. To this end, TLR2L was co-encapsulated in PLGA-NP with the goal to achieve a substantial DC activation leading to better CD8⁺ T cell activation in comparison to particles which are not adjuvanted.

In light of our recent findings showing that sSLP are efficiently cross-presented because of a rapid translocation into the cytosol facilitating proteasome dependent processing; the intracellular location of PLGA-SLP was studied to elucidate if PLGA-NP further enhances translocation of SLP, after release from the NP, to the cytosol or if different mechanisms are involved in the handling of PLGA-encapsulated SLP in comparison to the sSLP.

We show here that the addition of Pam3CSK4 to PLGA-NP encapsulating SLP strongly promotes DC maturation and CD8⁺ T cell activation. The difference on Ag uptake and MHC class I cross-presentation of PLGA-SLP versus PLGA-SLP/TLR2L was max 3-fold. Lower than we expected given our previous studies using SLP-TLR2L ¹⁴.

This moderate enhancement can be explained considering the already very efficient uptake, processing and presentation of plain PLGA-SLP (NP) by DC which perhaps is already close to maximum levels.

Moreover, Pam3CSK4 was not required to be encapsulated inside particles for it to exert its positive effects on MHC class I presentation of SLP. Mixing sTLR2L with plain PLGA-SLP led to similar results as using PLGA-SLP/TLR2L. Thus Pam3CSK4 has a different effect on the potency of SLP when co-encapsulated in NP compared to covalently coupling the compound to a peptide, which results in very strong enhancement of CD8⁺ T cell activation compared to mixtures of SLP and Pam3CSK4 ¹⁴.

Pam3CSK4 has a lipidic nature and contains positively charged lysine residues which direct adsorption to the negatively charged PLGA-NP surface due to hydrophobic and (or) electrostatic interactions ³. The adsorption of Pam3CSK4 to PLGA-SLP when mixed might lead to similar NP-characteristics as PLGA-SLP/TLR2L. This effect could explain why both the mixing or co-encapsulation will result in a similar participation of Pam3CSK4 in MHC class I presentation.

In conclusion, we show that addition of a Pam3CSK4, whether co-encapsulated or not, further improves MHC class I cross-presentation of SLP and improves CD8⁺ T cell activation compared to plain PLGA-SLP.

sSLP present in the cytosol are degraded via ubiquitin proteasome system (UPS)³⁰, whereas the Ag present inside endo-lysosomal compartments can be protected from rapid degradation by the UPS. Upon internalization of PLGA-NP by DC, a majority of the Ag could be detected inside the endo-lysosomes where hydrolysis of the polymer takes place releasing the encapsulated SLP³¹. Thus, the PLGA-NP encapsulated Ag inside endo-lysosomal compartments (Figure 4.4) serves as an intracellular reservoir which gradually releases the SLP for processing via the classical proteasome-TAP dependent MHC class I processing pathways. Baf A clearly interferes with MHC class I Ag presentation of PLGA-SLP. One possibility is that the compound blocks the transportation of SLP from the endo-lysosomes to the cytosol³². Another possibility is that Baf A modulates the activity of endo-lysosomal cathepsins³¹. Cathepsin S has been shown to have a role in MHC class I cross-presentation²⁷. Using BMDC generated from Cathepsin S KO mice, we did not observe differences in MHC class I cross-presentation of PLGA-SLP compared to WT BMDC (data not shown). Taken our results using proteasome inhibitors and TAP-deficient BMDC we show that SLP encapsulated in PLGA-NP is cross-presented via the classical MHC class I processing pathway but we cannot exclude that the endo-lysosomal environment and other pH dependent proteases still play a role in the observed MHC class I Ag cross-presentation^{28,29}.

The most important observation of this study was that encapsulation of sSLP in PLGA-NP results in sustained presence of the Ag inside DC upon internalization. More over, DC loaded with PLGA-SLP or PLGA-SLP/TLR2L showed prolonged MHC class I presentation in comparison to DC loaded with sSLP. Prolonged Ag presentation was not dependent on TLR2L stimulation but the addition of Pam3CSK4 does improve and sustain CD8⁺ T cell activation over a longer time period *in vivo*. Others observed similar results using PLGA-particles encapsulating proteins³³. However, in contrast to our results, it has been reported that PLGA-particles induce membrane rupture and rapid endo-lysosomal³⁴ followed by “leakage” of the PLGA-encapsulated Ag inside the cytosol; so called endosomal escape³³. Membrane rupture by particulate Ag is associated with inflammasome activation and secretion of IL-1 β by APC³⁵. In our system, however we could not detect IL-1 β in culture supernatants using ELISA after 24 hr incubations of DC with PLGA-SLP nor PLGA-SLP/TLR2L (data not shown). As mentioned before, we could detect green-fluorescent signal

of the SLP-OVA_{24aa}-Bodipy-FL and CD8⁺ T cell activation even after 96 hr indicating that in our study the majority of PLGA-encapsulated SLP was not directly transported to the cytosol after DC internalized the NP. Thus, internalized PLGA-NP show functional similarities with intracellular storage compartments as reported for other targeted vaccine delivery systems^{14,18}.

Therefore, we postulate that the efficient and prolonged MHC class I presentation observed using PLGA-SLP and PLGA-SLP/TLR2L is related to preservation of the Ag inside intact intracellular compartments. We show here based on the intracellular localization of internalized PLGA-NP and functional studies that these particles also end up in Ag storage compartments¹⁸.

Finally, direct s.c. vaccinations with PLGA-SLP/TLR2L but not PLGA-SLP induces endogenous Ag-specific CD8⁺ T cells capable of target cell lysis (Supporting Information Figure S4.2). In conclusion, the study reported here supports a mechanism that CD8⁺ T cell responses is enhanced when the Ag is cross-presented in MHC class I molecules in a sustained manner. We show that the co-encapsulation of a TLR2L further boosts these effects and thus supports the use of PLGA-NP co-encapsulating long peptide vaccines and adjuvants as an anti-cancer vaccine. Cancer cells are notorious for providing very few “danger signals”, which is one of the causes why the immune system sometimes fails to clear cancers. However, if one vaccinates with PLGA-SLP/TLR2L, encoding tumor associated Ag (TAA), for example the sustained release of Ag and adjuvant will lead to strong DC maturation, enhanced and prolonged MHC class I presentation and efficient priming of cytotoxic CD8⁺ T cells. Indeed, vaccination with PLGA-NP based vaccines results in robust anti-tumor responses with the capacity to significantly control tumor out growth³⁶⁻³⁹.

References

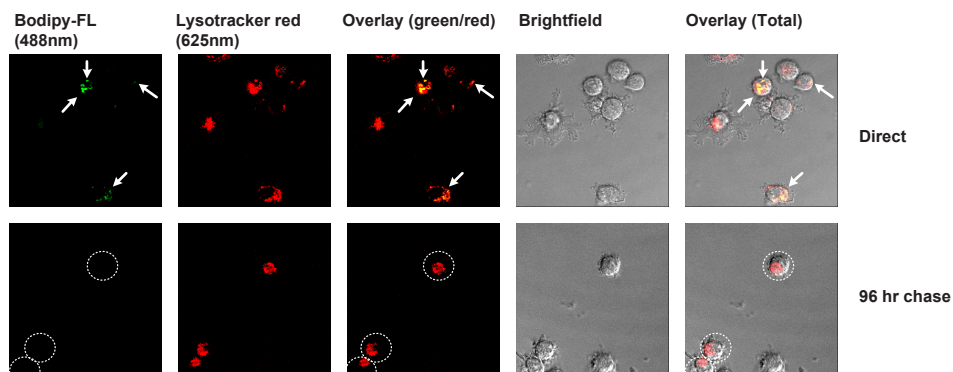
1. Flinsenbergh TW, Compeer EB, Boelens JJ, Boes M 2011. Antigen cross-presentation: extending recent laboratory findings to therapeutic intervention. *Clinical and Experimental Immunology* 165(1):8-18.
2. Melief CJ 2008. Cancer immunotherapy by dendritic cells. *Immunity* 29(3):372-383.
3. Rosalia RA, Quakkelaar ED, Redeker A, Khan S, Camps M, Drijfhout JW, Silva AL, Jiskoot W, van Hall T, van Veelen PA, Janssen G, Franken K, Cruz LJ, Tromp A, Oostendorp J, van der Burg SH, Ossendorp F, Melief CJ 2013. Dendritic cells process synthetic long peptides better than whole protein, improving antigen presentation and T-cell activation. *European Journal of Immunology* 43(10):2554-2565.
4. Sabbatini P, Tsuji T, Ferran L, Ritter E, Sedrak C, Tuballes K, Jungbluth AA, Ritter G, Aghajanian C, Bell-McGuinn K, Hensley ML, Konner J, Tew W, Spriggs DR, Hoffman EW, Venhaus R, Pan L, Salazar AM, Diefenbach CM, Old LJ, Gnjatich S 2012. Phase I trial of overlapping long peptides from a tumor self-antigen and poly-ICLC shows rapid induction of integrated immune response in ovarian cancer patients. *Clinical Cancer Research* 18(23):6497-6508.
5. Kenter GG, Welters MJ, Valentijn AR, Lowik MJ, Berends-van der Meer DM, Vloon AP, Essahsah F, Fathers LM, Offringa R, Drijfhout JW, Wafelman AR, Oostendorp J, Fleuren GJ, van der Burg SH, Melief CJ 2009. Vaccination against HPV-16 oncoproteins for vulvar intraepithelial neoplasia. *The New England Journal of Medicine* 361(19):1838-1847.
6. Park H, Adamson L, Ha T, Mullen K, Hagen SI, Nogueron A, Sylwester AW, Axthelm MK, Legasse A, Piatak M, Jr., Lifson JD, McElrath JM, Picker LJ, Seder RA 2013. Polyinosinic-polycytidylic acid is the most effective TLR adjuvant for SIV Gag protein-induced T cell responses in nonhuman primates. *J Immunol* 190(8):4103-4115.
7. Jarvi SI, Hu D, Misajon K, Collier BA, Wong T, Lieberman MM 2013. Vaccination of captive nene (*Branta sandvicensis*) against West Nile virus using a protein-based vaccine (WN-80E). *Journal of Wildlife Diseases* 49(1):152-156.
8. Leenaars PP, Koedam MA, Wester PW, Baumans V, Claassen E, Hendriksen CF 1998. Assessment of side effects induced by injection of different adjuvant/antigen combinations in rabbits and mice. *Laboratory Animals* 32(4):387-406.
9. Aucouturier J, Dupuis L, Deville S, Ascarateil S, Ganne V 2002. Montanide ISA 720 and 51: a new generation of water in oil emulsions as adjuvants for human vaccines. *Expert Review of Vaccines* 1(1):111-118.
10. Silva AL, Rosalia RA, Sazak A, Carstens MG, Ossendorp F, Oostendorp J, Jiskoot W 2013. Optimization of encapsulation of a synthetic long peptide in PLGA nanoparticles: low-burst release is crucial for efficient CD8(+) T cell activation. *European Journal of Pharmaceutics and Biopharmaceutics* 83(3):338-345.
11. Aucouturier J, Ascarateil S, Dupuis L 2006. The use of oil adjuvants in therapeutic vaccines. *Vaccine* 24 Suppl 2:S2-44-45.

12. Rosalia RA, Silva AL, Camps M, Allam A, Jiskoot W, van der Burg SH, Ossendorp F, Oostendorp J 2013. Efficient ex vivo induction of T cells with potent anti-tumor activity by protein antigen encapsulated in nanoparticles. *Cancer Immunology, Immunotherapy*: CII 62(7):1161-1173.
13. Yoshida M, Mata J, Babensee JE 2007. Effect of poly(lactic-co-glycolic acid) contact on maturation of murine bone marrow-derived dendritic cells. *Journal of Biomedical Materials Research Part A* 80(1):7-12.
14. Khan S, Bijker MS, Weterings JJ, Tanke HJ, Adema GJ, van Hall T, Drijfhout JW, Melief CJ, Overkleef HS, van der Marel GA, Filippov DV, van der Burg SH, Ossendorp F 2007. Distinct uptake mechanisms but similar intracellular processing of two different toll-like receptor ligand-peptide conjugates in dendritic cells. *The Journal of Biological Chemistry* 282(29):21145-21159.
15. Zom GG, Khan S, Filippov DV, Ossendorp F 2012. TLR ligand-peptide conjugate vaccines: toward clinical application. *Adv Immunol* 114:177-201.
16. van Montfoort N, t Hoen PA, Mangsbo SM, Camps MG, Boross P, Melief CJ, Ossendorp F, Verbeek JS 2012. Fcγ receptor IIb strongly regulates Fcγ receptor-facilitated T cell activation by dendritic cells. *J Immunol* 189(1):92-101.
17. Feltkamp MC, Vreugdenhil GR, Vierboom MP, Ras E, van der Burg SH, ter Schegget J, Melief CJ, Kast WM 1995. Cytotoxic T lymphocytes raised against a subdominant epitope offered as a synthetic peptide eradicate human papillomavirus type 16-induced tumors. *European Journal of Immunology* 25(9):2638-2642.
18. van Montfoort N, Camps MG, Khan S, Filippov DV, Weterings JJ, Griffith JM, Geuze HJ, van Hall T, Verbeek JS, Melief CJ, Ossendorp F 2009. Antigen storage compartments in mature dendritic cells facilitate prolonged cytotoxic T lymphocyte cross-priming capacity. *Proc Natl Acad Sci U S A* 106(16):6730-6735.
19. Schuurhuis DH, Ioan-Facsinay A, Nagelkerken B, van Schip JJ, Sedlik C, Melief CJ, Verbeek JS, Ossendorp F 2002. Antigen-antibody immune complexes empower dendritic cells to efficiently prime specific CD8+ CTL responses in vivo. *J Immunol* 168(5):2240-2246.
20. Rogošić M, Mencer HJ, Gomzi Z 1996. Polydispersity index and molecular weight distributions of polymers. *European Polymer Journal* 32(11):1337-1344.
21. King CG, Koehli S, Hausmann B, Schmalzer M, Zehn D, Palmer E 2012. T cell affinity regulates asymmetric division, effector cell differentiation, and tissue pathology. *Immunity* 37(4):709-720.
22. Zehn D, King C, Bevan MJ, Palmer E 2012. TCR signaling requirements for activating T cells and for generating memory. *Cellular and Molecular Life Sciences: CMLS* 69(10):1565-1575.
23. Rudd BD, Brien JD, Davenport MP, Nikolich-Zugich J 2008. Cutting edge: TLR ligands increase TCR triggering by slowing peptide-MHC class I decay rates. *J Immunol* 181(8):5199-5203.
24. Chen L, Jondal M 2004. Alternative processing for MHC class I presentation by immature and CpG-activated dendritic cells. *European Journal of Immunology* 34(4):952-960.
25. Chen L, Jondal M 2008. Brefeldin A inhibits vesicular MHC class I processing in resting but not in CpG- and disruption-activated DC. *Molecular Immunology* 46(1):158-165.

26. Chen L, Jondal M 2004. Endolysosomal processing of exogenous antigen into major histocompatibility complex class I-binding peptides. *Scandinavian Journal of Immunology* 59(6):545-552.
27. Rock KL, Farfan-Arribas DJ, Shen L 2010. Proteases in MHC class I presentation and cross-presentation. *J Immunol* 184(1):9-15.
28. Joffre OP, Segura E, Savina A, Amigorena S 2012. Cross-presentation by dendritic cells. *Nature Reviews Immunology* 12(8):557-569.
29. Compeer EB, Flinsenbergh TW, van der Grein SG, Boes M 2012. Antigen processing and remodeling of the endosomal pathway: requirements for antigen cross-presentation. *Frontiers in Immunology* 3:37.
30. Sijts EJ, Kloetzel PM 2011. The role of the proteasome in the generation of MHC class I ligands and immune responses. *Cellular and Molecular Life Sciences: CMLS* 68(9):1491-1502.
31. Baltazar GC, Guha S, Lu W, Lim J, Boesze-Battaglia K, Laties AM, Tyagi P, Kompella UB, Mitchell CH 2012. Acidic nanoparticles are trafficked to lysosomes and restore an acidic lysosomal pH and degradative function to compromised ARPE-19 cells. *PLoS one* 7(12):e49635.
32. Horiguchi M, Arita M, Kaempf-Rotzoll DE, Tsujimoto M, Inoue K, Arai H 2003. pH-dependent translocation of alpha-tocopherol transfer protein (alpha-TTP) between hepatic cytosol and late endosomes. *Genes to Cells: Devoted to Molecular & Cellular Mechanisms* 8(10):789-800.
33. Shen H, Ackerman AL, Cody V, Giodini A, Hinson ER, Cresswell P, Edelson RL, Saltzman WM, Hanlon DJ 2006. Enhanced and prolonged cross-presentation following endosomal escape of exogenous antigens encapsulated in biodegradable nanoparticles. *Immunology* 117(1):78-88.
34. Demento SL, Eisenbarth SC, Foellmer HG, Platt C, Caplan MJ, Mark Saltzman W, Mellman I, Ledizet M, Fikrig E, Flavell RA, Fahmy TM 2009. Inflammasome-activating nanoparticles as modular systems for optimizing vaccine efficacy. *Vaccine* 27(23):3013-3021.
35. Panyam J, Zhou WZ, Prabha S, Sahoo SK, Labhasetwar V 2002. Rapid endo-lysosomal escape of poly(DL-lactide-co-glycolide) nanoparticles: implications for drug and gene delivery. *FASEB Journal* 16(10):1217-1226.
36. Hamdy S, Molavi O, Ma Z, Haddadi A, Alshamsan A, Gobti Z, Elhasi S, Samuel J, Lavasanifar A 2008. Co-delivery of cancer-associated antigen and Toll-like receptor 4 ligand in PLGA nanoparticles induces potent CD8+ T cell-mediated anti-tumor immunity. *Vaccine* 26(39):5046-5057.
37. Mueller M, Reichardt W, Koerner J, Groettrup M 2012. Coencapsulation of tumor lysate and CpG-ODN in PLGA-microspheres enables successful immunotherapy of prostate carcinoma in TRAMP mice. *Journal of Controlled Release* 162(1):159-166.
38. Mueller M, Schlosser E, Gander B, Groettrup M 2011. Tumor eradication by immunotherapy with biodegradable PLGA microspheres--an alternative to incomplete Freund's adjuvant. *International Journal of Cancer / Journal International du Cancer* 129(2):407-416.

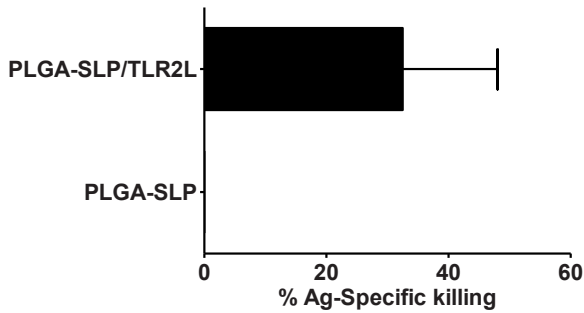
39. Zhang Z, Tongchusak S, Mizukami Y, Kang YJ, Ito T, Touma M, Reinhold B, Keskin DB, Reinherz EL, Sasada T 2011. Induction of anti-tumor cytotoxic T cell responses through PLGA-nanoparticle mediated antigen delivery. *Biomaterials* 32(14):3666-3678.

Supporting Information



Supporting Information Figure S4.1 Endosomal localisation of whole protein after internalization does not lead to prolonged Ag presence.

D1 cells were incubated with 20 μ M ovalbumin-Alexa488 (excitation- 488nm, visualized as the green signal) for 2.5 hr and either directly analyzed (upper panels) or further cultured in the absence of additional Ag or stimuli for 96 hr (lower panels). Co-staining with LysoTracker red was performed for visualization of the endo-lysosomes (red signal) and visualized by confocal microscopy. 1st column shows images depicting green signal as the fluorescence of the dye (488nm). 2nd column shows images depicting red signal as the fluorescence of the lysoTracker red/endo-lysosomes (625nm). 3rd column depicts overlay images of red/green. Yellow-overlay signal marks co-localization. Images were analyzed using Leica software.



Supporting Information Figure S4.2 Vaccinations with PLGA-SLP/TLR2L but not PLGA-SLP induces CD8⁺ T cells with *in vivo* cytotoxic capacity.

Priming efficacy of endogenous cytotoxic CD8⁺ T cells by PLGA-SLP formulations, mice were vaccinated with 20 nmol SLP encapsulated in PLGA with or without Pam3CSK4 co-encapsulated. On day 7 post-vaccination, SIINFEKL-loaded (OVA-specific) target and control-target cells were injected. To obtain OVA-specific target cells, splenocytes from naïve congenic C57BL/6 Ly5.1 mice were pulsed for 1 h with 1 μ M of SIINFEKL-peptide and co-stained with 10 μ M CFSE (CFSE-high) (Molecular Probes, Eugene, OR). As a negative control, 1 μ M of the immunodominant ASNENMETM-peptide derived from the influenza virus nucleoprotein co-stained with 0.5 μ M CFSE (CFSE-low) was used. Specific and non-specific target cells were mixed 1:1 and injected intravenously (i.v.; 10×10^6 cells of each population). 18 hr after cells were transferred, mice were sacrificed and spleen cells were harvested to prepare single cell suspensions that were then subjected to flow cytometric analysis. Injected cells were distinguished by APC-conjugated rat anti-mouse CD45.1 mAb. The percentage specific killing was calculated as follow: $100 - \left(\frac{(\% \text{ SIINFEKL-peptide pulsed in treated} / \% \text{ ASNENMETM-peptide pulsed in treated})}{(\% \text{ SIINFEKL-peptide pulsed in non-treated} / \% \text{ ASNENMETM-peptide pulsed in non-treated})} \right) \times 100$.



Chapter 5

Efficient *ex vivo* induction of T cells with potent anti-tumor activity by protein antigen encapsulated in nanoparticles

Rodney A. Rosalia, Ana Luisa Silva, Marcel Camps, Ahmed Allam,
Wim Jiskoot, Sjoerd H. van der Burg, Ferry Ossendorp & Jaap Oostendorp

Cancer Immunology, Immunotherapy 62 (7), 1161-1173

Abstract

Protein antigen (Ag)-based immunotherapies have the advantage to induce T cells with a potentially broad repertoire of specificities. However, soluble protein Ag is generally poorly cross-presented in MHC class I molecules and not efficient in inducing robust cytotoxic CD8⁺ T cell responses. In the present study, we have applied poly(lactic-co-glycolic acid) (PLGA) nanoparticles (NP) which strongly improve protein Ag presentation by dendritic cells (DC) in the absence of additional TLR ligands or targeting devices. Protein Ag loaded DC were used as antigen presenting cells (APC) to stimulate T cells *in vitro* and subsequently analyzed *in vivo* for their anti-tumor effect via adoptive transfer, a treatment strategy widely studied in clinical trials as a therapy against various malignancies. In a direct comparison with soluble protein Ag, we show that DC presentation of protein encapsulated in plain PLGA-NP results in efficient activation of CD4⁺ and CD8⁺ T cells as reflected by high numbers of activated CD69⁺ and CD25⁺ interferon (IFN)- γ and interleukin (IL)-2-producing T cells. Adoptive transfer of PLGA-NP-activated CD8⁺ T cells in tumor-bearing mice displayed good *in vivo* expansion capacity, potent Ag-specific cytotoxicity and IFN- γ cytokine production, resulting in curing mice with established tumors. We conclude that delivery of protein Ag through encapsulation in plain PLGA-NP is a very efficient and simple procedure to stimulate potent anti-tumor T cells.

Précis

This paper shows that DC loaded with protein encapsulated in biodegradable and clinically applied polymer particles efficiently activate CD8⁺ T cells *in vitro* which upon adoptive transfer *in vivo* show potent anti-tumor immune responses.

Introduction

The adaptive immune system plays a major role in anti-tumor control. Induction of a specific immune response against tumor-associated antigen (Ag) is a potential approach for targeted immunotherapy of cancer. The first step in the initiation of an effective anti-tumor response is the uptake of tumor-associated Ag by dendritic cells (DC) and their subsequent presentation to naïve T cells¹⁻³. DC are highly efficient antigen presenting cells (APC) and play a central role in initiating and regulating adaptive immunity. DC internalize and process exogenous protein Ag and present processed peptide epitopes in the grooves of MHC class I and II molecules to prime CD8⁺ cytotoxic T cells (CTL) and CD4⁺ helper T (Th) cells, respectively⁴. CTL are capable of direct clearance of malignant cells⁵. Th cells have shown to be vital in CTL priming through CD40-CD40L interactions with DC^{6,7}. In addition, activated Th cells secrete cytokines like IL-2 important for CTL proliferation^{8,9}.

Full-length protein Ag comprise all potential naturally occurring Th and CTL epitopes and can be clinically applied irrespective of the patient's HLA haplotype. For that reason, protein-based tumor-associated Ag is currently being applied in a variety of immunotherapeutic approaches against cancer^{10,11}. However, recent studies have indicated that cross-presentation of protein Ag is an inefficient process leading to poor CTL responses^{12,13}. Therefore, improving cross-presentation of protein Ag by DC is essential to further exploit cancer immunotherapy.

Nanoparticles (NP) prepared from the polymer poly(lactic-co-glycolic acid) (PLGA) are promising clinical grade carriers for improving Ag delivery to DC¹⁴⁻¹⁶. PLGA polymers were originally reported for their use as sutures and implants for surgery¹⁷ and since then they have been applied for the preparation of particles for drug delivery purposes, including the delivery of anti-cancer agents¹⁸⁻²⁰. Internalization of protein Ag-loaded PLGA particles by DC is very efficient, resulting in adequate MHC class I cross-presentation and CTL proliferation *in vitro*²¹. Despite highly efficient DC uptake and cross-presentation *in vitro*, experimental tumor models have shown that the therapeutic effect of PLGA particle-based protein vaccination *in vivo* is strictly dependent on co-encapsulation of Toll like receptor ligands (TLRL)²². The necessity for the addition of TLRL for *in vivo* responses is most likely related to observations showing that PLGA-polymers on their own exhibit poor DC or macrophage stimulatory capacity in comparison to TLR4L^{23,24}. However TLRL are dispensable for T cell activation *in vitro*, as reported by two previous studies using biodegradable polymer based artificial APC as a method to stimulate T cells *in vitro*. Applying an elegant method to

formulate artificial APC using PLGA, T cells were stimulated *in vitro* with efficient proliferative and cytokine producing capacity^{25,26}. However, the *in vivo* effector functions of the *in vitro* stimulated T cells were not studied in those reports.

In the present study, the intrinsic capacity of plain protein Ag-loaded PLGA-NP to induce anti-tumor effector T cells with potent functionality *in vivo* is reported. DC, the immune system's natural and most potent APC, express known and yet unknown co-stimulatory molecules and produce various cytokines vital for optimal T cell priming^{27,28}. Using murine DC, we performed a detailed analysis of the ability of protein Ag-loaded PLGA-NP, lacking any additional TLRL or targeting moiety, to induce potent tumor-specific effector T cells. For this analysis, we have used a murine model for adoptive T cell transfer therapy, a treatment modality that has been successfully tested in various (pre-)clinical studies against various types of cancer^{29,30}. In this murine adoptive T cell transfer therapy model, we show that protein Ag encapsulated in PLGA efficiently and rapidly induces highly activated specific effector CD8⁺ T cells with a type I cytokine profile that vigorously expand *in vivo* in tumor-bearing mice and have the potency to eradicate established aggressive tumors.

Material and methods

Cells

D1 cells, a GM-CSF dependent immature dendritic cell line derived from spleen of WT C57BL/6 (H-2^b) mice, were cultured as described previously³¹. Freshly isolated DC (BMDC) were cultured from mouse bone marrow (BM) cells by collecting femurs from WT C57BL/6 strain and cultured as published previously by our group³². After 10 days of culture, large numbers of typical DC were obtained which were at least 90% positive for murine DC marker CD11c (data not shown). B3Z CD8⁺ T cell hybridoma cell line, specific for the H-2K^b-restricted OVA₂₅₇₋₂₆₄ CTL epitope SIINFEKL, expressing a β -galactosidase construct under the regulation of the NF-AT element from the IL-2 promoter, was cultured as described before³³ OT-IIZ, a CD4⁺ T cell hybridoma cell line, specific for the I-A^b-restricted OVA₃₂₃₋₃₃₉ Th epitope, expressing the same β -galactosidase construct, was produced in house. The weakly immunogenic and highly aggressive OVA-transfected B16 tumor cell line (B16-OVA), syngeneic to the C57BL/6 strain, was cultured as described³⁴.

Preparation and characterization of protein Ag-loaded PLGA-NP

PLGA-NP were prepared using 7-17 kDa PLGA 50:50 (Resomer RG502H, Boehringer Ingelheim, Ingelheim, Germany) by applying a modified “water-in-oil-in-water” solvent evaporation method as described³⁵. In brief, 50 µl of 20 mg/ml pure, endotoxin-free ovalbumin (OVA, Worthington LS003048) dissolved in 25 mM Hepes buffer (pH 7.4) was emulsified with 1 ml of dichloromethane (DCM) containing 25 mg of PLGA with an ultrasonic processor for 15 s at 70 W (Branson Instruments, CT, USA). The secondary emulsion was prepared with 2 ml of 1% (w/v) polyvinyl alcohol (PVA) in water. The double emulsion was then transferred into 25 ml of a 0.3% (w/v) PVA solution, and stirred at 37°C for 1 h, and the resulting NP were harvested and washed twice with Milli-Q water by centrifugation at 8000 *g* for 10 min. The NP suspension was aliquoted in cryovials and lyophilized for 24 h. Prior to use, lyophilized NP particle size distribution was determined by means of dynamic light scattering (DLS) using a NanoSizer ZS (Malvern Instruments, Malvern UK) after resuspension of the particles in Milli-Q water. The zeta potential of the particles was also measured with the NanoSizer ZS by laser Doppler velocimetry. The OVA content of the particles was determined with a BCA protein assay (Pierce, Rockford, IL, USA) according to the manufacturer’s instructions, and encapsulation efficiency (%EE) was determined according to equation 5.1. 500 µg lyophilized PLGA-OVA were resuspended in 350 µl sterile MQ water and endotoxin content were determined with Bacterial endotoxins methode D. Chromogenic kinetic method’ an assay according to European Pharmacopeia 2.6.14 seventh edition.

$$\%EE = \frac{\text{protein mass in NP}}{\text{total protein mass}} \times 100 \quad (5.1)$$

In vitro release study of PLGA-encapsulated protein

For release studies, protein-loaded PLGA NP were prepared as described, but with the addition of 1% (w/w total OVA) of Ovalbumin-Alexa Fluor® 488 (PLGA-OVA-Alexa488) (Invitrogen). Encapsulation of OVA-Alexa488 proceeds with similar efficiency as the regular OVA with no dye conjugated (See Table 5.1). PLGA-OVA-Alexa488 were resuspended in 1x PBS pH 7.4 at a concentration of 10 mg PLGA/ml and maintained at 37°C in a water bath under constant tangential shaking at 100 rpm in a GFL 1086 shaking water bath (Burgwedel, Germany). At regular time intervals, 250 µl samples of the suspension were taken, centrifuged for 20 min at 18,000×*g* and supernatants were stored at 4°C until fluorescence intensity, was determined by fluorescence spectrometry (Tecan, Infinite M

Table 5.1 PLGA-NP characteristics

Formulation	Size (nm)	PDI	ZP (mV)	Protein loading (μg OVA/mg PLGA)	OVA encapsulation efficiency (%)	Endotoxin level (IU/ml)
PLGA-OVA	274 \pm 19	0.18 \pm 0.02	-27 \pm 1	25 \pm 1	62 \pm 2	0.03 \pm 0.00
PLGA-OVA Alexa	338 \pm 12	0.22 \pm 0.10	-27 \pm 5	20 \pm 1	49 \pm 4	0.03 \pm 0.03
PLGA empty	311 \pm 52	0.14 \pm 0.06	-30 \pm 7	n/a	n/a	n/a

1000). Concentration of OVA-Alexa488 in the supernatant was assessed against a calibration curve containing known concentrations of OVA-Alexa488. Protein release profiles were generated for each NP formulation in terms of cumulative antigen release (%) over time. Release was determined according to equation 5.2.

$$\% R = \frac{\text{protein mass in supernatant}}{\text{protein mass in supernatant} + \text{protein mass in NP}} \times 100 \quad (5.2)$$

Enzyme-linked Immunosorbent Assay (ELISA)

DC (100,000/well) were plated into a 96-well round bottom plate and incubated for 24 hr with titrated amounts of Ag. Supernatants were harvested and tested for IL-12 p40 using an ELISA assay kit (BD OptEIA™ MOUSE IL-12 Cat. Nr 555165) following manufacturer's instructions.

MHC class I or class II-restricted Ag presentation and T cell proliferation

DC were incubated for 24 h with soluble OVA (sOVA) or OVA encapsulated in PLGA-NP (PLGA-OVA) at the indicated concentrations. Cells were washed followed by overnight incubation at 37°C in the presence of either B3Z - to measure MHC class I Ag presentation of SIINFEKL (OVA₂₅₇₋₂₆₄) in H-2K^b - or OT-II cells - to assess MHC class II Ag presentation of ISQAVHAAHAEINEAGR (OVA₃₂₃₋₃₃₉) in I-A^b. A colorimetric assay using chlorophenol red- β -D-galactopyranoside (CPRG) as substrate was used to detect IL-2 induced lacZ activity. OVA-specific proliferation of naïve CD8⁺ and CD4⁺T cells was performed by culturing OT-I or OT-II splenocytes in the presence of DC loaded with titrated amounts of PLGA-OVA or sOVA. After 24 h incubated cells were pulsed with [³H]-thymidine and cultured further overnight. Samples were then counted on a TopCount™ microplate scintillation counter (Packard Instrument Co., Meridan, CT, USA).

Analysis of T cell phenotype and T cell cytokine profile

DC were loaded for 24 h with 0.25 μM OVA in PLGA (PLGA-OVA) or soluble OVA (sOVA), washed extensively and used as APC to stimulate spleen suspensions from OT-I and OT-II mice. DC and splenocytes were co-cultured for 24 h in the presence of 7.5 $\mu\text{g}/\text{ml}$ Brefeldin A. Total cells were harvested, washed twice with PBA buffer (0.01 M sodium phosphate, 0.15 M NaCl, 1% (w/v) BSA, and 0.01% (w/v) sodium azide) followed by staining with PerCP rat anti-mouse CD8 α monoclonal antibodies (mAb) and AF-conjugated rat anti-mouse CD3 mAb. To assess T cell activation, cells were stained with FITC-conjugated rat anti-mouse CD69 mAb or PeCy7-conjugated rat anti-mouse CD25 mAb. To study the T cell cytokine profile, CD8 $^+$ T cells were stained as above and subjected to intracellular cytokine staining using the Cytofix/Cytoperm kit according to the manufacturer's instructions (BD Pharmingen). Intracellular IFN- γ in the T cells was stained with APC-conjugated rat anti-mouse IFN- γ . Similarly, IL-2 and IL-4 were stained using PE-conjugated rat anti-mouse IL-2, IL-4 respectively. TNF- α was stained with FITC-conjugated rat anti-mouse TNF- α mAb. All antibodies were purchased from BD Pharmingen. Flow cytometry analysis was performed using a LSRII flow cytometer (BD Pharmingen) and analyzed with FlowJo software (Treestar).

In vivo cytotoxicity

To obtain OVA-specific effector CD8 $^+$ T cells, single cell suspensions were prepared from spleen and lymph nodes of OT-I mice, washed twice and resuspended in IMDM supplemented with 10% (v/v) FCS. Whole single cell suspensions were cultured in 6-wells plates with Ag (0.25 μM) loaded DC for 24 h at a ratio of 25:1. DC and splenocyte cultures were incubated for 24 hr at 37°C. Purified CD8 $^+$ T cells were obtained by a negative selection protocol using the Mouse CD8 T Cell Lymphocyte Enrichment Set - DM (BD Biosciences) according to the manufacturer's instructions. This protocol yielded CD8 $^+$ T cell purities of at least 90% (data not shown). 2.5×10^6 Purified CD8 $^+$ T cells were transferred to syngeneic WT C57BL/6 animals that were rested for 24 h after adoptive cell transfer. To obtain OVA-specific target cells, splenocytes from naïve congenic C57BL/6 Ly5.1 mice were pulsed for 1 h with 1 μM of SIINFEKL-peptide and co-stained with 10 μM CFSE (CFSE-high) (Molecular Probes, Eugene, OR). As a negative control, 1 μM of the immunodominant ASNENMETM-peptide derived from the influenza virus nucleoprotein co-stained with 0.5 μM CFSE (CFSE-low) was used. Specific and non-specific target cells

were mixed 1:1 and injected intravenously (i.v.; 10×10^6 cells of each population). Eighteen hours after cells were transferred, mice were sacrificed and spleen cells were harvested to prepare single cell suspensions that were then subjected to flow cytometric analysis. Injected cells were distinguished by APC-conjugated rat anti-mouse CD45.1 mAb. The percentage specific killing was calculated as follow: $100 - \left(\frac{(\% \text{ SIINFEKL-peptide pulsed in treated} / \% \text{ ASNENMETM-pulsed in treated})}{(\% \text{ SIINFEKL-peptide pulsed in non-treated} / \% \text{ ASNENMETM-pulsed in non-treated})} \right) \times 100$.

Adoptive transfer OVA-specific T cells in B16-OVA tumor bearing and naïve mice

WT C57BL/6 mice were injected subcutaneously (s.c.) in the right flank with 2×10^5 B16-OVA melanoma cells. Seven days after tumor injection, when tumors were palpable, mice were treated by intravenous infusion of 2.5×10^6 purified effector CD8⁺ T cells derived from OT-I mice, *ex vivo* stimulated for 24 h in the presence of DC loaded with either PLGA-OVA or sOVA. Tumor growth was measured 1–3 times a week and survival was monitored daily. Tumor size (mm²) was calculated by (length) \times (width). Mice with tumor sizes that equaled or exceeded 140 mm² were sacrificed. Tail vein blood samples were collected on day 10, 17 and 31 after CD8⁺ T cell transfer. Blood samples were prepared by erythrocyte lysis, followed by 2 washing steps with PBA buffer. Transferred CD8⁺ T cells were analyzed by co-staining with APC-conjugated rat anti-mouse Thy1.1 mAb, FITC-conjugated anti-mouse CD8 α mAb and AF-conjugated rat anti-mouse CD3 mAb in combination with APC-Cy7-conjugated anti-mouse CD44 antibody and PB-conjugated anti-mouse CD62L antibody. OVA-specific CD8⁺ T cell mediated cytokine production was detected by overnight stimulation of peripheral blood cells with SIINFEKL-peptide in the presence of 7.5 μ g/ml Brefeldin A. Medium was used as a negative control to correct for baseline cytokine production. Cytokine profile was analyzed by intracellular cytokine staining as described above.

Statistical analysis

Graph Pad Prism software was used for statistical analysis. Values and percentages of specific CD8⁺ T cells and secreted cytokine production were analyzed by two-tailed unpaired Student t test. Differences in animal survival between the different groups were calculated using Log-rank (Mantel-Cox) test.

RESULTS

Nanoparticle characterization and protein antigen load and release

We prepared several batches of PLGA-OVA NP with similar characteristics. Particles used in our study had an average size of 327 ± 65 nm (mean \pm SD; $n = 7$) and a polydispersity index (PDI) of 0.19 ± 0.07 . Encapsulation efficiency of OVA in NP was determined to be $59 \pm 5\%$. Empty particles used as control particles in this study had a comparable size (311 ± 52 nm) and PDI (0.15 ± 0.05). The endotoxin levels were determined for the prepared batches and was shown to be below 0.04 IU/ml in particle suspensions prepared as described in material and methods (see Table 5.1). Release kinetics of OVA from the PLGA-OVA particles were analyzed over a period of 35 days. The validity of using OVA-Alexa 488 fluorescence as a measure of (unlabeled) OVA release was confirmed by measuring the OVA content of the nanoparticles and the total amount released at the end of the release study by BCA assay, which gave very similar values as the fluorescence method (results not shown).

The NP had a burst release of the encapsulated OVA of $28.1 \pm 0.2\%$. At the end of the analysis, we could detect $80.4 \pm 2.2\%$ of released OVA in suspension indicating that after 35 days about 20% of the originally encapsulated OVA was still associated with NP showing the slow release character of these NP (see Supporting Information Figure S5.1).

Efficient protein MHC class I and class II Ag presentation by DC loaded with protein encapsulated in PLGA-NP

The efficiency of Ag (cross)-presentation of encapsulated protein Ag in comparison to soluble protein Ag was studied *in vitro*. DC were incubated for 24 h with titrated amounts of Ag, as indicated in μM , either encapsulated in PLGA-NP (PLGA-OVA) or in soluble form (sOVA). Ag presentation by MHC class I or II was assessed using the CD8⁺ (B3Z) and CD4⁺ (OT-IIZ) T cell hybridomas. DC loaded with PLGA-OVA very efficiently triggered B3Z T cells (Figure 5.1a). In contrast, DC pulsed with sOVA poorly stimulated B3Z CD8⁺ T cells unless very high concentrations ($\geq 64 \mu\text{M}$) of sOVA were used (data not shown). MHC class I cross-presentation of protein Ag was strictly dependent on encapsulation in PLGA-NP, as a mixture of the sOVA with empty PLGA-NP did not induce CD8⁺ T cell activation (Figure 5.1b). In addition, DC loaded with PLGA-OVA resulted in at least 100-fold enhanced activation of OT-IIZ CD4⁺ T cells in comparison to DC loaded with sOVA, indicating that also MHC class II presentation was dramatically improved by encapsulation (Figure 5.1c). Next to

Ag presentation, we analyzed proliferation of naïve CD8⁺ (OT-I) and CD4⁺ (OT-II) T cells induced by DC loaded with PLGA-OVA or sOVA. Co-culture of Ag pulsed DC with either OT-I or OT-II T cells for 72 h, including overnight incubation in the presence of [³H]-thymidine for the last 18 h showed that PLGA-OVA was at least 1000-fold more efficient than sOVA in inducing OT-I T cell proliferation (Figure 5.1d) and 100-fold better than sOVA in inducing

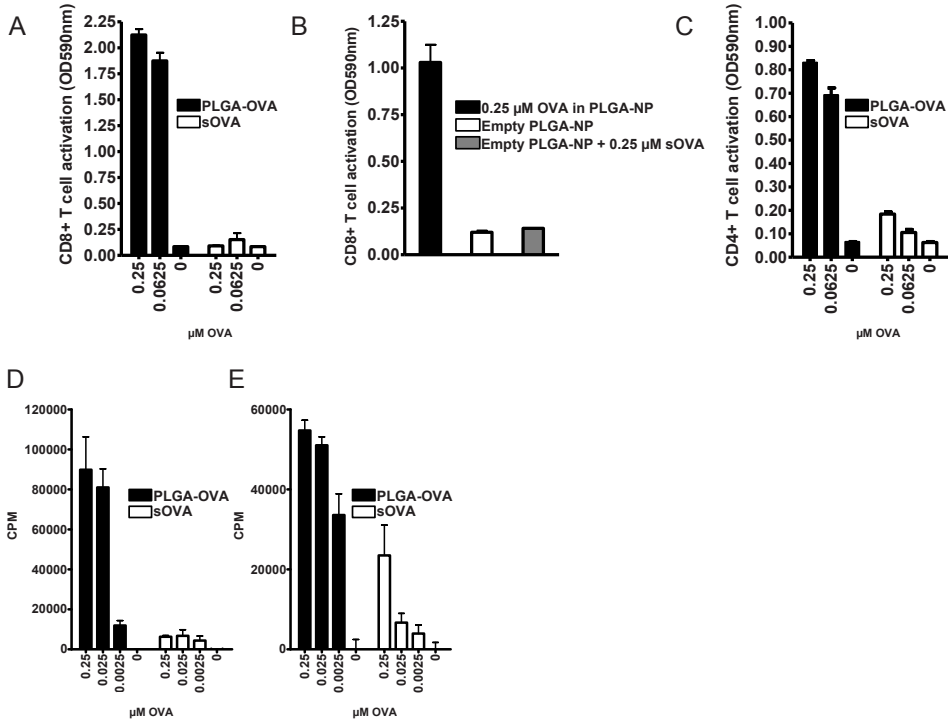


Figure 5.1 Efficient MHC class I and class II presentation of OVA Ag incorporated in PLGA-NP.

(A) D1 cells were pulsed for 24 h with titrated amounts (μM) of OVA, either in soluble form sOVA or encapsulated in PLGA-NP (PLGA-OVA). MHC class I presentation was detected by co-culture with H-2K^b/SIINFEKL-specific B3Z CD8⁺ T cells; (B) D1 cells were pulsed for 24 h with 0.25 μM OVA in PLGA-OVA, empty PLGA-NP, or a mixture of empty PLGA-NP with 0.25 μM sOVA, washed and co-cultured with B3Z CD8⁺ T cells to assess MHC class I Ag presentation; (C) D1 cells were pulsed for 24 h with titrated amounts of PLGA-OVA or sOVA, washed, and co-cultured with I-A^b/ISQAVHAAHAEINEAGR-specific OT-II Z CD4⁺ T cells to assess MHC class II Ag presentation. BMDC were loaded with titrated amounts of PLGA-OVA or sOVA. Ag loaded DC were subsequently used to activate naïve OT-I (D) or OT-II (E) cells for 72 h. T cell proliferation was measured in triplicate by [³H]-thymidine uptake. Data shown are means of triplicate measurements \pm SD from one representative example out of at least three independent experiments.

OT-II T cell proliferation (Figure 5.1e). Similar to the used D1 dendritic cells, freshly isolated BMDC loaded with PLGA-OVA were superior in comparison to sOVA-loaded BMDC in the stimulation of OT-I and OT-II T cells resulting in improved T cell proliferation (Supporting Information Figure S5.2). In addition, we analyzed DC maturation by surface expression of CD86 and determining the amount of IL-12 in culture supernatants after incubation with the NP after 24 hr incubation. Our data show that the empty or OVA-loaded PLGA NP do not detectably activate and mature DC (Supporting Information Figure S5.3) in contrast to LPS (TLR4L) or PolyI:C (TLR3L). This indicates that encapsulation of soluble protein antigen in plain PLGA NP strongly enhances antigen presentation by DC irrespective of DC maturation.

Activation of T cells by DC loaded with PLGA-NP-encapsulated protein Ag

We analyzed whether PLGA-NP based delivery of protein Ag could induce T cell activation and production of pro-inflammatory cytokines. Naïve OVA-specific CD8⁺ (OT-I) and CD4⁺ (OT-II) T cells were stimulated for 24 h in the presence of PLGA-OVA- or sOVA-loaded DC and analyzed for cells expressing the early activation marker CD69. Both CD8⁺ (Figure 5.2a) and CD4⁺ (Figure 5.2b) T cells showed strongly enhanced percentages of CD69⁺ cells upon stimulation by PLGA-OVA pulsed DC in a dose-dependent manner. By contrast, and in line with poor Ag presentation, stimulation with sOVA pulsed DC resulted in low expression of CD69 on T cells. The majority of CD8⁺ T cells stimulated with PLGA-OVA pulsed DC also expressed the interleukin-2 receptor-alpha chain (CD25) after 24 h, whereas only a small population of sOVA induced CD8⁺ T cells showed expression of CD25 (Figure 5.2c). Furthermore, we analyzed the capacity of activated CD8⁺ and CD4⁺ T cells to produce IL-2, IFN- γ , TNF- α and IL-4 by intracellular cytokine analysis of the T cells. Whereas hardly any cytokine-producing CD8⁺ and CD4⁺ T cells were observed after stimulation with sOVA pulsed DC, high numbers of IFN- γ - and IL-2-producing CD8⁺ T cells (Figure 5.2d) and CD4⁺ T cells (Figure 5.2e) were detected after stimulation with PLGA-OVA-loaded DC. The majority of cytokine-producing CD4⁺ T cells were single producers of IL-2, whereas cytokine producing CD8⁺ T cells consisted of a population of IL-2 and IFN- γ double producers, single IFN- γ producers and a relatively smaller population of IL-2 single producers. The cytokines IL-4 and TNF- α could not be detected after *in vitro* stimulation of either CD8⁺ or CD4⁺ T cells with PLGA-OVA pulsed DC (data not shown).

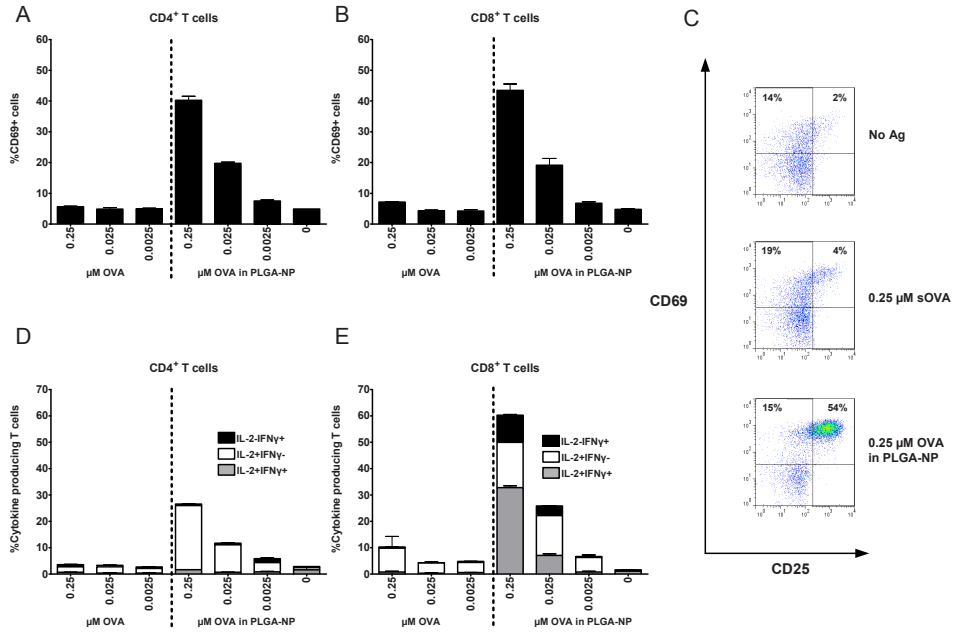


Figure 5.2 DC pulsed with PLGA-OVA, but not sOVA, induce strong activation of T cells.

D1 cells were pulsed for 24 h with titrated amounts of sOVA or PLGA-OVA. Ag loaded DC were washed to remove excess Ag, and co-cultured for an additional 24 h with OT-I or OT-II splenocytes. Cells were harvested and analyzed by flow cytometry for the cell surface expression of CD69 on CD8⁺ T (A) cells and CD4⁺ T cells (B); (C) Expression of CD25 and CD69 was analyzed on CD8⁺ T cells which were stimulated for 24 h with DC which were loaded with either PLGA-OVA or sOVA. Immature DC without Ag served as negative control. Intracellular production of IL-2 and IFN-γ by CD8⁺ T cells (D); and CD4⁺ T cells (E) was analyzed by flow cytometry after 24 hr stimulation with DC pulsed with titrated amounts of PLGA-OVA or sOVA. One representative experiment out of three independent experiments is shown. Data shown are means of triplicate measurements ± SD.

DC loaded PLGA-NP-encapsulated protein Ag induces CD8⁺ T cells with *in vivo* cytotoxic capacity

To assess their cytotoxic capacity, CD8⁺ T cells stimulated *in vitro* by PLGA-OVA-loaded DC were studied for their ability to lyse Ag-pulsed target cells *in vivo*. Following stimulation, the purified CD8⁺ T cells were transferred into recipient mice. After 24 h SIINFEKL-loaded target and control-target cells were injected and 18 h later mice were sacrificed and spleen single cell suspensions were analyzed by flow cytometry. In line with the observed activation status and cytokine profile, CD8⁺ T cells stimulated with PLGA-OVA-loaded DC

demonstrated cytotoxicity against SIINFEKL-loaded target cells. In contrast, CD8⁺ T cells co-cultured in the presence of sOVA-loaded DC were not capable of killing target cells (Figure 5.3a and b).

PLGA-NP-encapsulated protein Ag induces CD8⁺ T cells with potent anti-tumor activity

To investigate the therapeutic potential of CD8⁺ T cells induced by DC loaded with PLGA-NP-encapsulated protein antigen against established tumors, mice were inoculated s.c. with OVA-expressing B16 melanoma tumor cells. After 7 days, animals were treated by adoptive T cell transfer therapy by a single i.v. injection of 2.5×10^6 purified OVA-specific CD8⁺ T cells stimulated for 24 h *in vitro* in the presence of DC loaded with either PLGA-OVA or sOVA. Tumor growth and animal survival in CD8⁺ T cell transferred mice were compared to those in non-treated animals. Animals were developing palpable tumors within 10 days

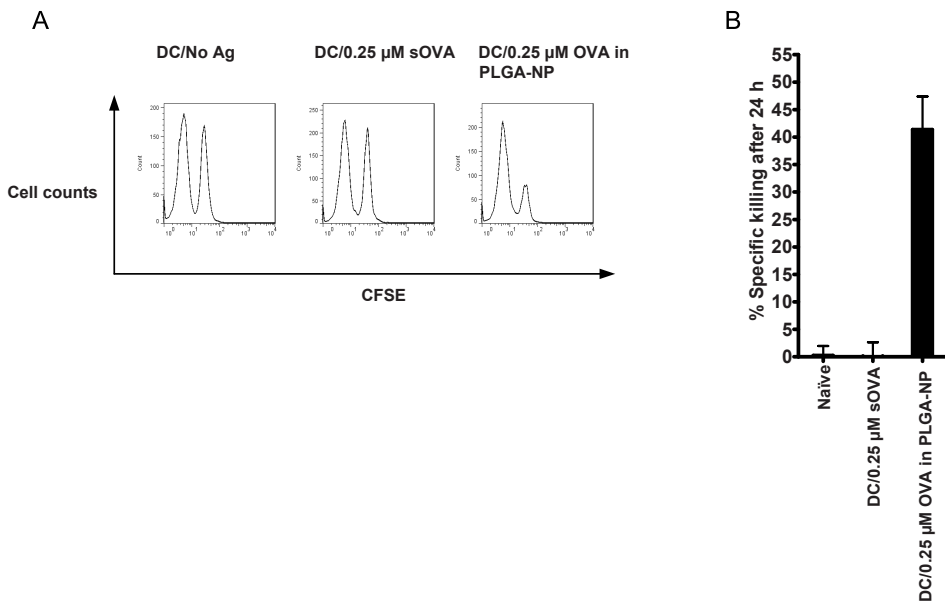


Figure 5.3 Enhanced *in vivo* cytotoxicity of *ex vivo* PLGA-OVA-stimulated CD8⁺ T cells.

(A) Mice were transferred with purified CD8⁺ OT-IT cells which were *in vitro* stimulated with D1 cells loaded with PLGA-OVA and sOVA. Differentially CFSE-labeled SIINFEKL-peptide loaded and control target cells were i.v. administered. After 18 h the spleens from recipient animals were harvested and analyzed by flow cytometry for percentage of specific killing of target cells; (B) Experiment was performed twice and averages \pm SEM of $n = 7$ mice for each condition are shown in bar graphs.

after s.c. tumor inoculation. In tumor-bearing mice that were treated by adoptive transfer with OVA-specific CD8⁺ T cells stimulated in the presence of PLGA-OVA-loaded DC, we observed a clear therapeutic effect which resulted in delayed tumor growth in comparison to non-treated animals and animals treated with CD8⁺ T cells stimulated with sOVA loaded DC. We observed regression of tumors in the range of 2–4 mm² in some animals by day 14, which were undetectable on day 18 after tumor challenge (insert in Figure 5.4a). By day 22, four animals within this group had tumor recurrences which eventually grew out. Nevertheless, 8 out of 12 tumor-challenged mice treated with PLGA-OVA induced CD8⁺ T cells remained tumor free for the duration of the experiment (Figure 5.4a). By contrast, in tumor challenged animals that received sOVA induced CD8⁺ T cells, tumors reappeared in 11 out of 12 mice and grew out, albeit at a decreased rate when compared to non-treated animals (Figure 5.4b). In all non-treated animals, tumors grew out fast and all mice were sacrificed by day 24, because of maximum allowed tumor burden (Figure 5.4c). Tumors that did grow in animals that received PLGA-OVA induced CD8⁺ T cells had a significantly slower average growth rate when compared to tumors from mice that received sOVA induced CD8⁺ T cells. Consequently, the survival of mice treated with PLGA-OVA induced CD8⁺ T cells was significantly higher when compared to mice treated with CD8⁺ T cells stimulated in the presence of sOVA-loaded DC (Figure 5.4d).

CD8⁺ T cells stimulated with PLGA-NP-encapsulated protein Ag efficiently expand and produce type I cytokines *in vivo*

We measured by flow cytometry the actual numbers of OVA-specific CD8⁺ T cells (CD8⁺Thy1.1⁺ OT-I cells) in peripheral blood of tumor challenged mice up to a month after adoptive transfer. Ten days after adoptive transfer of equal amounts of purified OVA-specific CD8⁺ T cells, mice that had received PLGA-OVA induced cells showed 5-fold higher levels of CD8⁺ T cells than animals that had received sOVA stimulated CD8⁺ T -cells (Figure 5.5a). The percentage of PLGA-OVA induced CD8⁺ T cells remained significantly higher at day 17 and 31 after transfer (Figure 5.5b). A similar *in vivo* expansion capacity of PLGA-OVA induced CD8⁺ T cells was observed upon transfer in naïve mice, i.e. not challenged with tumors (data not shown). Furthermore, we analyzed the production of cytokines by CD8⁺ T cells in peripheral blood by intracellular staining. To this end, peripheral blood mononuclear cells were harvested from mice at day 10, 17 and 31 after adoptive transfer and stimulated overnight in the presence of SIINFEKL-peptide. IFN- γ -, IL-2- and TNF- α -producing CD8⁺ T cells were detectable by flow cytometry. On day 10 after adoptive transfer, we observed

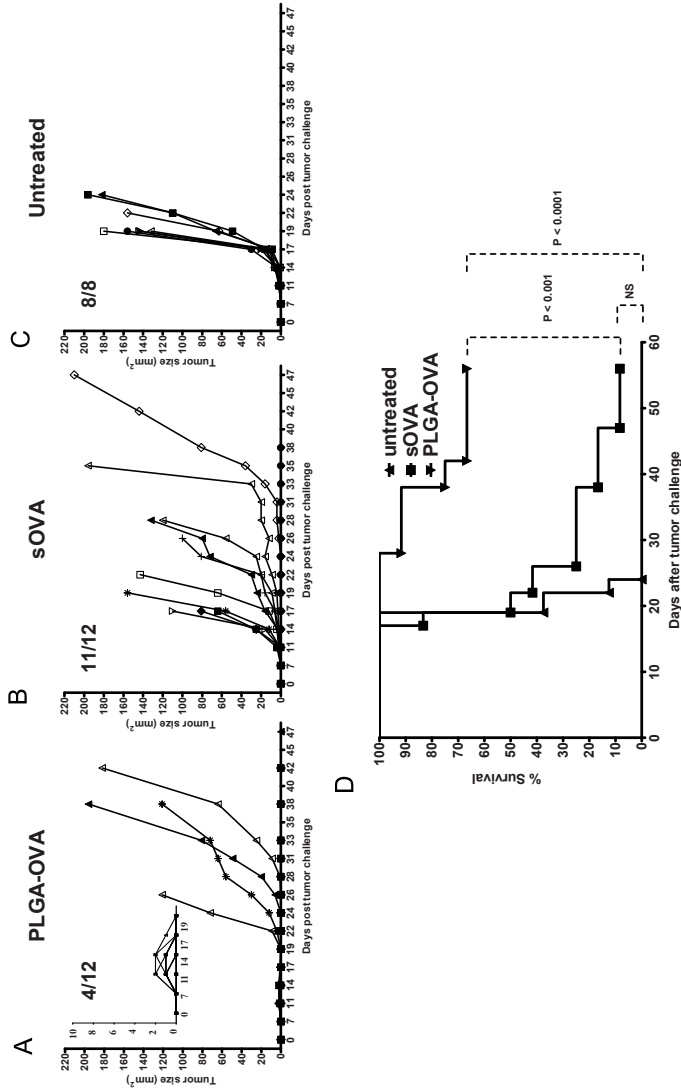


Figure 5.4 CD8⁺ T cells primed by PLGA-OVA loaded DC eradicate established tumors.

Animals were inoculated s.c. on the right flank with 2×10^5 B16-OVA tumor cells and rested for 1 week followed by a single i.v. injection of 2.5×10^6 purified CD8⁺ T cells which were *ex vivo* stimulated with Ag loaded DC as described above. Tumor growth was monitored in individual animals treated with DC/PLGA-OVA induced CD8⁺ T cells (A; n = 12 animals), DC/sOVA induced CD8⁺ T cells (B; n = 12 animals) or in untreated animals (C; n = 8 animals). Insert in (A) represents tumor growth curves in the initial 19 days after tumor challenge; (D) Animal survival per group was assessed and differences between the different groups were calculated using Log-rank (Mantel-Cox) test. P < 0.0001 for animals treated with DC/PLGA-OVA compared to DC/sOVA induced CD8⁺ T cells. P < 0.0001 for animals treated with DC/PLGA-OVA compared to untreated animals. NS = P > 0.05 for animals treated with DC/sOVA compared to untreated animals.

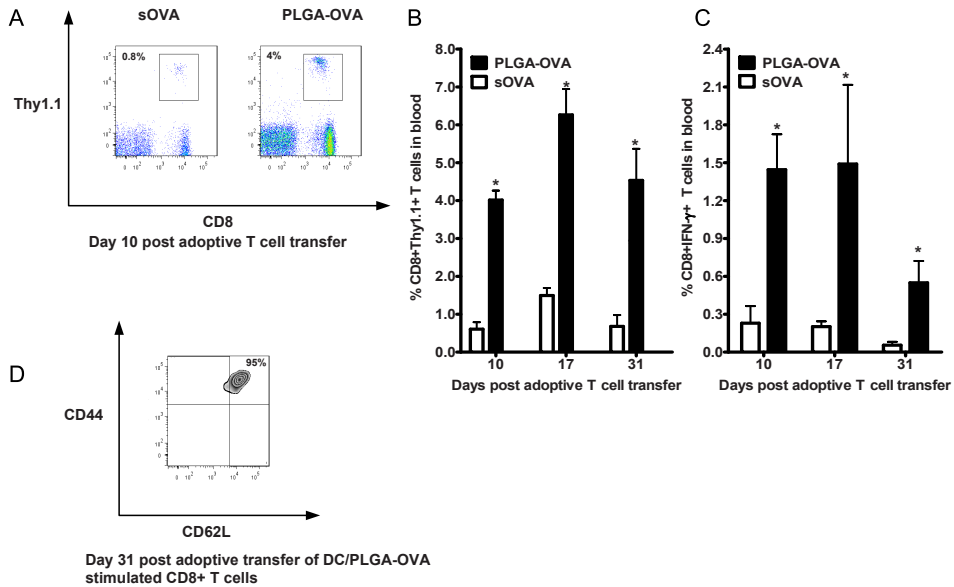


Figure 5.5 PLGA-OVA stimulated CD8⁺ T cells expand and persist in the peripheral blood and have higher capacity to produce IFN-γ.

(A) Tumor bearing animals received a single i.v. injection of CD8⁺ T cells stimulated with PLGA-OVA-loaded DC. Tail vein blood samples were taken on day 10 after adoptive transfer of the CD8⁺ T cells and numbers of CD8⁺Thy1.1⁺ T cells were measured by flow cytometry; (B) *In vivo* persistence of i.v. transferred CD8⁺Thy1.1⁺ T cells in tumor bearing animals was monitored for 4 weeks in blood on day 17 and 31; (C) Intracellular IFN-γ production by CD8⁺ T cells was analyzed on day 10, 17 and 31 after adoptive transfer; (D) Memory phenotype of transferred DC/PLGA-OVA *in vitro* stimulated CD8⁺Thy1.1⁺ T cells was determined by analysis of CD44 and CD62L surface expression. Results shown are averages ± SEM from n = 3–12 mice per group, dependent on the number of animals alive at each time-point post tumor challenge. * = P < 0.05 for animals treated with DC/PLGA-OVA compared to DC/sOVA induced CD8⁺ T cells using a un-paired student t test.

significantly higher percentages of IFN-γ-producing CD8⁺ T cells in mice that had received PLGA-OVA induced CD8⁺ T cells when compared to mice that had received sOVA induced CD8⁺ T cells. We were unable to detect IFN-γ-producing CD8⁺ T cells in tumor-bearing animals which were not treated using adoptive T cell transfer therapy (data not shown). Although, the percentage of IFN-γ producing CD8⁺ T cells declined at day 17 and 31 after adoptive transfer, the IFN-γ-producing CD8⁺ T cells remained significantly higher throughout the analysis period (Figure 5.5c). A trend in increased levels of IL-2- and TNF-α-producing CD8⁺ T cells could be observed in mice transferred with PLGA-OVA but not

with sOVA induced CD8⁺T cells (data not shown). In addition, the phenotype of peripheral blood OVA-specific T cells at day 17 and 31 after adoptive transfer of PLGA-OVA induced CD8⁺T cells was analyzed. The majority of the cells possessed a central memory phenotype based on high expression of CD62L (L-selectin) and CD44 (Figure 5.5d) showing the superior functionality of the T cells expanded with this simple expansion protocol with NP encapsulated protein antigen.

Discussion

In this study we analyzed the phenotype and *in vivo* functionality of T cells stimulated *in vitro* by DC loaded with plain PLGA-NP encapsulated protein Ag with no additional immune stimulatory agent or targeting moiety. We showed that encapsulation of protein Ag in plain PLGA-NP not only enhanced Ag (cross-)presentation by DC but also improved the functionality of the induced T cells to cure animals from tumors upon adoptive T cell transfer. OVA antigen in PLGA-NP was more efficiently processed and presented in MHC class I and II by DC and resulted in potent activation and proliferation of OVA-specific CD8⁺ and CD4⁺ T cells, high production of type I cytokines and tumor control resulting in an overall survival of 75% of tumor-bearing animals.

PLGA-based particles as vaccine delivery systems were pioneered already more than 30 years ago¹⁴. Several studies have shown that efficient anti-tumor immune responses *in vivo* by PLGA-particles require not only encapsulated Ag, but also a co-encapsulated adjuvant such as a TLR, surface coating of particles with mannan or protamine to stimulate immunity or DC targeting moieties, for example anti-DEC205 antibodies^{22,36-38}.

CD8⁺ T cells induced in our study were applied for adoptive T cell transfer purposes. Adoptive T cell transfer therapy potency in (pre)clinical setting is enhanced upon efficient *ex vivo/in vitro* stimulation/manipulation of donor T cells^{30,39,40}. Using a similar murine model, efficient stimulation of T cells with potent effector functions was reported using artificial APC systems²⁶. They constructed PLGA-based artificial APC expressing MHC class I molecules containing a specific CTL short-peptide epitope, which also provides T cell co-stimulation in the form of CD28 and CD3 triggering and releases IL-2^{41,42}. We propose that our simple approach with natural APC is equally efficient and has the advantage that our method is not restricted to the known MHC class I and II-presented T cells epitopes. In addition, the use of natural DC as APC might facilitate priming of T cells via more co-stimulatory pathways⁴³⁻⁴⁵ and additional DC-mediated cytokines required for optimal

type I pro-inflammatory T cell activation, for example IL-12⁴⁶, and avoids sub-optimal formation of the immunological synapse as has been described for other bead-based artificial APC systems⁴⁷.

Adoptive T cell therapy has yielded promising results as a cancer immunotherapy in the last decade^{30,48}. Standard adoptive transfer protocols mandate that T cells are cultured for 2–14 days in the presence of specific Ag and exogenous cytokines^{39,49-51} for optimal stimulation and expansion. In contrast, we opted for a short 24 h stimulation of T cells without addition of any exogenous cytokines. We favor short incubation with DC loaded with PLGA-OVA, which potently activates T cells, because longer incubation periods might tip the balance to activation induced cell death (AICD)^{52,53}. In addition, our protocol allowed us to transfer T cells that were not skewed based on the cytokines added to the cultures^{54,55} nor negatively affected by the added cytokines^{42,56,57}.

In our culture systems we used two types of DC: D1 cells, a well characterized murine splenic DC cell line, originally isolated from WT C57BL/6 animals⁵⁸ and bone marrow derived DC. Both CD11c⁺ myeloid types of DC were cultured as immature cells in GM-CSF containing media. D1 DC do not exhibit substantial functional differences with BMDC, they possess equal capacity to prime T cells and upon transfer to recipient animals show similar efficiency to induce protective anti-tumor immunity³². We compared CD4⁺ and CD8⁺ T cell proliferation by PLGA-NP encapsulated protein Ag and we observed similar observations using either D1 cells or WT BMDC as APC. Therefore, easily cultured myeloid types of DC are well suited for the T cell activation protocol with NP encapsulated Ag we describe here.

In this study splenocytes from OT-I mice, which contain high numbers of OVA-specific T cells, were used to activate and adoptively transfer into recipient animals. We are aware that in clinical settings, majority of patients which were treated with adoptive T cell transfer therapy exhibit lower precursor frequencies of TAA-specific T cells that require stimulation and expansion to yield sufficient numbers for adoptive transfer. Our system still works by DC/PLGA-OVA stimulation of cell cultures containing lower amounts (between 1–10%) of OVA-specific T cells regarding T cell activation and cytokine production (data not shown). On the other hand, higher precursor frequencies of both CD4⁺ and CD8⁺ Ag-specific T cells have been observed in draining lymph nodes of cervical cancer patients^{59,60}. These cells were able to produce type I pro-inflammatory cytokines and proliferate upon specific stimulation suggesting that these cells might be suitable for future adoptive T cell transfer protocols. Indeed, in a melanoma patient case report, it was shown that CD4⁺ T cells isolated

in relatively higher precursor frequencies could be successfully stimulated and transferred to the recipient back to the patient resulting in a clinical response ⁶¹.

The PLGA-OVA particles used in our study are devoid of any additional TLR or immunostimulatory agents. We observed no differences in T cell proliferation by MyD88 KO BMDC loaded with PLGA-OVA (data not shown), it is therefore unlikely that any unanticipated TLR-stimulation plays a role in our system. The enhanced T cell proliferation and activation is most likely the result of enhanced uptake of Ag available for efficient processing and MHC presentation. Uptake of particulate matter proceeds via phagocytosis ^{62,63} of protein Ag-loaded PLGA particles by DC resulting in adequate MHC class I cross-presentation to CTL ⁶⁴. DC internalize particles and maintain these intracellularly for up to 72 hr ⁶⁵. Prolonged presence of Ag inside cells has been shown to result in sustained MHC class I Ag presentation and efficient priming of CD8⁺ T cells ⁶⁶.

Transferred DC/PLGA-OVA stimulated CD8⁺ T cells were still detectable 31 days post adoptive transfer and the majority of these cells possessed a central memory phenotype correlating with tumor control. Numbers of specific T cells *in vivo* have been shown to directly correlate with tumor-regression ⁶⁷. Efficient tumor killing is achieved upon efficient CD8⁺ T cell activation accompanied with high production of type I pro-inflammatory associated cytokines which is dependent on the method of *in vitro* activation ^{68,69}. Our data are in line with these reports as peripheral CD8⁺ T cells from mice which received DC/PLGA-OVA stimulated CD8⁺ T cells were capable of producing type I pro-inflammatory cytokines upon specific peptide stimulation. Indeed, expansion of IFN- γ producing T cells correlates with clinical effect in patients with human papillomavirus type 16 induced vulvar intraepithelial neoplasia ⁷⁰.

Numbers of cytokine-producing cells decreased with time in all treated animal groups. The decrease in numbers of cytokine-producing OVA-specific CD8⁺ T cells in time might be related to lack of sufficient OVA-specific CD4⁺ T cells. Co-transfer of DC/PLGA-OVA *in vitro* stimulated CD4⁺ T cells may prolong and sustain higher numbers of cytokine producing effector CD8⁺ T cells ⁷¹.

We conclude that protein Ag delivery by PLGA-NP might be an attractive and simple strategy to improve *ex vivo* tumor-specific T cell stimulation for clinical adoptive T transfer therapy. Apparently, the intrinsic characteristics of PLGA-Ag NP to be efficiently internalized and processed by DC is sufficient to induce effector T cells *in vitro* with expansion capacity *in vivo*, and with strong therapeutic effectiveness. So, encapsulation of tumor associated

protein Ag in PLGA-NP may serve as a clinically feasible strategy to generate T cells with optimal effector quality for adoptive transfer-based immunotherapy of cancer.

Acknowledgements

This study was supported by grants from Immune System Activation (ISA) Pharmaceuticals, University of Leiden and the Leiden University Medical Center. We thank Ing. S. Marlina Sibuea for the studies performed to determine the release kinetics of the protein from the PLGA-NP and Ing. W.M.Ramp-Koopmanschap for the analysis of endotoxin levels of the formulated PLGA-OVA batches.

References

1. Banchereau J, Steinman RM 1998. Dendritic cells and the control of immunity. *Nature* 392:245-252.
2. Melief CJ 2008. Cancer immunotherapy by dendritic cells. *Immunity* 29:372-383.
3. Steinman RM, Hemmi H 2006. Dendritic cells: translating innate to adaptive immunity. *Curr Top Microbiol Immunol* 311:17-58.
4. Petersen TR, Dickgreber N, Hermans IF 2010. Tumor antigen presentation by dendritic cells. *Crit Rev Immunol* 30:345-386.
5. Kawakami Y, Eliyahu S, Delgado CH, Robbins PF, Sakaguchi K, Appella E, Yannelli JR, Adema GJ, Miki T, Rosenberg SA 1994. Identification of a human melanoma antigen recognized by tumor-infiltrating lymphocytes associated with in vivo tumor rejection. *Proc Natl Acad Sci U S A* 91:6458-6462.
6. Ossendorp F, Mengede E, Camps M, Filius R, Melief CJ 1998. Specific T helper cell requirement for optimal induction of cytotoxic T lymphocytes against major histocompatibility complex class II negative tumors. *J Exp Med* 187:693-702.
7. Schoenberger SP, Toes RE, van der Voort EI, Offringa R, Melief CJ 1998. T-cell help for cytotoxic T lymphocytes is mediated by CD40-CD40L interactions. *Nature* 393:480-483.
8. Blachere NE, Morris HK, Braun D, Saklani H, Di Santo JP, Darnell RB, Albert ML 2006. IL-2 is required for the activation of memory CD8+ T cells via antigen cross-presentation. *J Immunol* 176:7288-7300.
9. Keene JA, Forman J 1982. Helper activity is required for the in vivo generation of cytotoxic T lymphocytes. *J Exp Med* 155:768-782.
10. Mischo A, Bubel N, Cebon JS, Samaras P, Petrusch U, Stenner-Liewen F, Schaefer NG, Kubuschok B, Renner C, Wadle A 2011. Recombinant NY-ESO-1 protein with ISCOMATRIX adjuvant induces broad antibody responses in humans, a RAYS-based analysis. *Int J Oncol* 39:287-294.
11. Sang M, Lian Y, Zhou X, Shan B 2011. MAGE-A family: attractive targets for cancer immunotherapy. *Vaccine* 29:8496-8500.
12. Zandvliet ML, van LE, Jedema I, Veltrop-Duits LA, Willemze R, Guchelaar HJ, Falkenburg JH, Meij P 2010. Co-ordinated isolation of CD8(+) and CD4(+) T cells recognizing a broad repertoire of cytomegalovirus pp65 and IE1 epitopes for highly specific adoptive immunotherapy. *Cytotherapy* 12:933-944.
13. Zhang H, Hong H, Li D, Ma S, Di Y, Stoten A, Haig N, Di GK, Yu Z, Xu XN, McMichael A, Jiang S 2009. Comparing pooled peptides with intact protein for accessing cross-presentation pathways for protective CD8+ and CD4+ T cells. *J Biol Chem* 284:9184-9191.
14. Newman KD, Samuel J, Kwon G 1998. Ovalbumin peptide encapsulated in poly(D, L lactic-co-glycolic acid) microspheres is capable of inducing a T helper type 1 immune response. *J Control Release* 54:49-59.

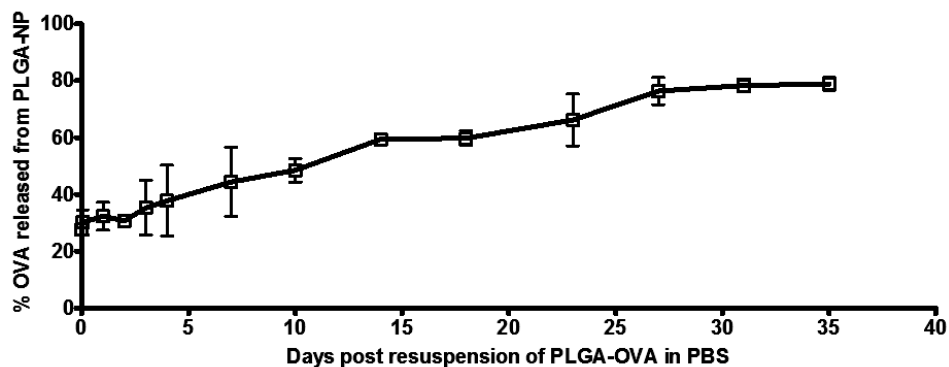
15. Waeckerle-Men Y, Gander B, Groettrup M 2005. Delivery of tumor antigens to dendritic cells using biodegradable microspheres. *Methods Mol Med* 109:35-46.
16. Zhang Z, Tongchusak S, Mizukami Y, Kang YJ, Ioji T, Touma M, Reinhold B, Keskin DB, Reinherz EL, Sasada T 2011. Induction of anti-tumor cytotoxic T cell responses through PLGA-nanoparticle mediated antigen delivery. *Biomaterials* 32:3666-3678.
17. Gilding DK, Reed AM 1979. Biodegradable polymers for use in surgery. *J Polym Sci Polym Chem Ed* 17:1459-1464.
18. Mahapatro A, Singh DK 2011. Biodegradable nanoparticles are excellent vehicle for site directed in-vivo delivery of drugs and vaccines. *J Nanobiotechnology* 9:55.
19. Jain AK, Das M, Swarnakar NK, Jain S 2011. Engineered PLGA nanoparticles: an emerging delivery tool in cancer therapeutics. *Crit Rev Ther Drug Carrier Syst* 28:1-45.
20. Hamdy S, Haddadi A, Hung RW, Lavasanifar A 2011. Targeting dendritic cells with nanoparticulate PLGA cancer vaccine formulations. *Adv Drug Deliv Rev* 63:943-955.
21. Shen H, Ackerman AL, Cody V, Giodini A, Hinson ER, Cresswell P, Edelson RL, Saltzman WM, Hanlon DJ 2006. Enhanced and prolonged cross-presentation following endosomal escape of exogenous antigens encapsulated in biodegradable nanoparticles. *Immunology* 117:78-88.
22. Schlosser E, Mueller M, Fischer S, Basta S, Busch DH, Gander B, Groettrup M 2008. TLR ligands and antigen need to be coencapsulated into the same biodegradable microsphere for the generation of potent cytotoxic T lymphocyte responses. *Vaccine* 26:1626-1637.
23. Demento SL, Eisenbarth SC, Foellmer HG, Platt C, Caplan MJ, Mark SW, Mellman I, Ledizet M, Fikrig E, Flavell RA, Fahmy TM 2009. Inflammasome-activating nanoparticles as modular systems for optimizing vaccine efficacy. *Vaccine* 27:3013-3021.
24. Yoshida M, Mata J, Babensee JE 2007. Effect of poly(lactic-co-glycolic acid) contact on maturation of murine bone marrow-derived dendritic cells. *J Biomed Mater Res A* 80:7-12.
25. Han H, Peng JR, Chen PC, Gong L, Qiao SS, Wang WZ, Cui ZQ, Yu X, Wei YH, Leng XS 2011. A novel system of artificial antigen-presenting cells efficiently stimulates Flu peptide-specific cytotoxic T cells in vitro. *Biochem Biophys Res Commun* 411:530-535.
26. Steenblock ER, Fahmy TM 2008. A comprehensive platform for ex vivo T-cell expansion based on biodegradable polymeric artificial antigen-presenting cells. *Mol Ther* 16:765-772.
27. Palucka K, Banchereau J 2012. Cancer immunotherapy via dendritic cells. *Nat Rev Cancer* 12:265-277.
28. Steinman RM 2012. Decisions about dendritic cells: past, present, and future. *Annu Rev Immunol* 30:1-22.
29. Rosenberg SA, Dudley ME 2009. Adoptive cell therapy for the treatment of patients with metastatic melanoma. *Curr Opin Immunol* 21:233-240.
30. Restifo NP, Dudley ME, Rosenberg SA 2012. Adoptive immunotherapy for cancer: harnessing the T cell response. *Nat Rev Immunol* 12:269-281.

31. Winzler C, Rovere P, Rescigno M, Granucci F, Penna G, Adorini L, Zimmermann VS, Davoust J, Ricciardi-Castagnoli P 1997. Maturation stages of mouse dendritic cells in growth factor-dependent long-term cultures. *J Exp Med* 185:317-328.
32. Schuurhuis DH, Ioan-Facsinay A, Nagelkerken B, van Schip JJ, Sedlik C, Melief CJ, Verbeek JS, Ossendorp F 2002. Antigen-antibody immune complexes empower dendritic cells to efficiently prime specific CD8+ CTL responses in vivo. *J Immunol* 168:2240-2246.
33. Sanderson S, Shastri N 1994. LacZ inducible, antigen/MHC-specific T cell hybrids. *Int Immunol* 6:369-376.
34. Moore MW, Carbone FR, Bevan MJ 1988. Introduction of soluble protein into the class I pathway of antigen processing and presentation. *Cell* 54:777-785.
35. Slutter B, Bal S, Keijzer C, Mallants R, Hagenaars N, Que I, Kaijzel E, van EW, Augustijns P, Lowik C, Bouwstra J, Broere F, Jiskoot W 2010. Nasal vaccination with N-trimethyl chitosan and PLGA based nanoparticles: nanoparticle characteristics determine quality and strength of the antibody response in mice against the encapsulated antigen. *Vaccine* 28:6282-6291.
36. Hamdy S, Haddadi A, Shayeganpour A, Samuel J, Lavasanifar A 2011. Activation of antigen-specific T cell-responses by mannan-decorated PLGA nanoparticles. *Pharm Res* 28:2288-2301.
37. Mueller M, Schlosser E, Gander B, Groettrup M 2011. Tumor eradication by immunotherapy with biodegradable PLGA microspheres--an alternative to incomplete Freund's adjuvant. *Int J Cancer* 129:407-416.
38. Tacke PJ, Zeelenberg IS, Cruz LJ, van Hout-Kuijter MA, van de Glind G, Fokkink RG, Lambeck AJ, Figdor CG 2011. Targeted delivery of TLR ligands to human and mouse dendritic cells strongly enhances adjuvanticity. *Blood* 118:6836-6844.
39. Klebanoff CA, Gattinoni L, Palmer DC, Muranski P, Ji Y, Hinrichs CS, Borman ZA, Kerker SP, Scott CD, Finkelstein SE, Rosenberg SA, Restifo NP 2011. Determinants of successful CD8+ T-cell adoptive immunotherapy for large established tumors in mice. *Clin Cancer Res* 17:5343-5352.
40. Montagna D, Turin I, Schiavo R, Montini E, Zaffaroni N, Villa R, Secondino S, Schiavetto I, Caliogna L, Locatelli F, Libri V, Pession A, Tonelli R, Maccario R, Siena S, Pedrazzoli P 2012. Feasibility and safety of adoptive immunotherapy with ex vivo-generated autologous, cytotoxic T lymphocytes in patients with solid tumor. *Cytotherapy* 14:80-90.
41. Boyman O, Sprent J 2012. The role of interleukin-2 during homeostasis and activation of the immune system. *Nat Rev Immunol* 12:180-190.
42. Boyman O, Purton JF, Surh CD, Sprent J 2007. Cytokines and T-cell homeostasis. *Curr Opin Immunol* 19:320-326.
43. Denoed J, Moser M 2011. Role of CD27/CD70 pathway of activation in immunity and tolerance. *J Leukoc Biol* 89:195-203.
44. Gerdes N, Zirlik A 2011. Co-stimulatory molecules in and beyond co-stimulation - tipping the balance in atherosclerosis? *Thromb Haemost* 106:804-813.

45. Schreiber TH, Wolf D, Boder M, Gonzalez L, Podack ER 2012. T Cell Costimulation by TNFR Superfamily (TNFRSF)4 and TNFRSF25 in the Context of Vaccination. *J Immunol*.
46. Trinchieri G 2003. Interleukin-12 and the regulation of innate resistance and adaptive immunity. *Nat Rev Immunol* 3:133-146.
47. Turtle CJ, Riddell SR 2010. Artificial antigen-presenting cells for use in adoptive immunotherapy. *Cancer J* 16:374-381.
48. Gattinoni L, Powell DJ, Jr., Rosenberg SA, Restifo NP 2006. Adoptive immunotherapy for cancer: building on success. *Nat Rev Immunol* 6:383-393.
49. Dudley ME, Wunderlich JR, Shelton TE, Even J, Rosenberg SA 2003. Generation of tumor-infiltrating lymphocyte cultures for use in adoptive transfer therapy for melanoma patients. *J Immunother* 26:332-342.
50. Ho WY, Nguyen HN, Wolf M, Kuball J, Greenberg PD 2006. In vitro methods for generating CD8+ T-cell clones for immunotherapy from the naive repertoire. *J Immunol Methods* 310:40-52.
51. Le HK, Graham L, Miller CH, Kmiecik M, Manjili MH, Bear HD 2009. Incubation of antigen-sensitized T lymphocytes activated with bryostatin 1 + ionomycin in IL-7 + IL-15 increases yield of cells capable of inducing regression of melanoma metastases compared to culture in IL-2. *Cancer Immunol Immunother* 58:1565-1576.
52. Budd RC 2001. Activation-induced cell death. *Curr Opin Immunol* 13:356-362.
53. Green DR, Droin N, Pinkoski M 2003. Activation-induced cell death in T cells. *Immunol Rev* 193:70-81.
54. Dobrzanski MJ, Reome JB, Hollenbaugh JA, Dutton RW 2004. Tc1 and Tc2 effector cell therapy elicit long-term tumor immunity by contrasting mechanisms that result in complementary endogenous type 1 antitumor responses. *J Immunol* 172:1380-1390.
55. Garcia-Hernandez ML, Hamada H, Reome JB, Misra SK, Tighe MP, Dutton RW 2010. Adoptive transfer of tumor-specific Tc17 effector T cells controls the growth of B16 melanoma in mice. *J Immunol* 184:4215-4227.
56. Hinrichs CS, Spolski R, Paulos CM, Gattinoni L, Kerstann KW, Palmer DC, Klebanoff CA, Rosenberg SA, Leonard WJ, Restifo NP 2008. IL-2 and IL-21 confer opposing differentiation programs to CD8+ T cells for adoptive immunotherapy. *Blood* 111:5326-5333.
57. Waldmann TA 2006. The biology of interleukin-2 and interleukin-15: implications for cancer therapy and vaccine design. *Nat Rev Immunol* 6:595-601.
58. Winzler C, Rovere P, Rescigno M, Granucci F, Penna G, Adorini L, Zimmermann VS, Davoust J, Ricciardi-Castagnoli P 1997. Maturation stages of mouse dendritic cells in growth factor-dependent long-term cultures. *J Exp Med* 185:317-328.
59. de Vos van Steenwijk PJ, Heusinkveld M, Ramwadhoebe TH, Lowik MJ, van der Hulst JM, Goedemans R, Piersma SJ, Kenter GG, van der Burg SH 2010. An unexpectedly large polyclonal repertoire of HPV-specific T cells is poised for action in patients with cervical cancer. *Cancer Res* 70:2707-2717.

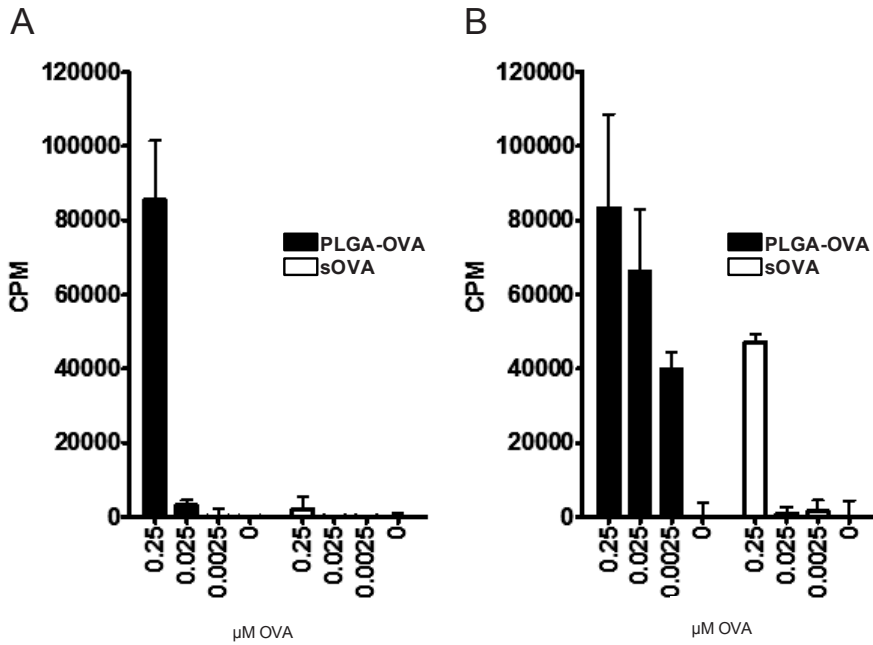
60. Piersma SJ, Welters MJ, van der Hulst JM, Kloth JN, Kwappenberg KM, Trimbos BJ, Melief CJ, Hellebrekers BW, Fleuren GJ, Kenter GG, Offringa R, van der Burg SH 2008. Human papilloma virus specific T cells infiltrating cervical cancer and draining lymph nodes show remarkably frequent use of HLA-DQ and -DP as a restriction element. *Int J Cancer* 122:486-494.
61. Hunder NN, Wallen H, Cao J, Hendricks DW, Reilly JZ, Rodmyre R, Jungbluth A, Gnjatich S, Thompson JA, Yee C 2008. Treatment of metastatic melanoma with autologous CD4+ T cells against NY-ESO-1. *N Engl J Med* 358:2698-2703.
62. Prior S, Gander B, Blarer N, Merkle HP, Subira ML, Irache JM, Gamazo C 2002. In vitro phagocytosis and monocyte-macrophage activation with poly(lactide) and poly(lactide-co-glycolide) microspheres. *Eur J Pharm Sci* 15:197-207.
63. Yoshida M, Babensee JE 2006. Differential effects of agarose and poly(lactic-co-glycolic acid) on dendritic cell maturation. *J Biomed Mater Res A* 79:393-408.
64. Shen H, Ackerman AL, Cody V, Giodini A, Hinson ER, Cresswell P, Edelson RL, Saltzman WM, Hanlon DJ 2006. Enhanced and prolonged cross-presentation following endosomal escape of exogenous antigens encapsulated in biodegradable nanoparticles. *Immunology* 117:78-88.
65. Schliehe C, Schliehe C, Thiry M, Tromsdorf UI, Hentschel J, Weller H, Groettrup M 2011. Microencapsulation of inorganic nanocrystals into PLGA microsphere vaccines enables their intracellular localization in dendritic cells by electron and fluorescence microscopy. *J Control Release* 151:278-285.
66. van MN, Camps MG, Khan S, Filippov DV, Weterings JJ, Griffith JM, Geuze HJ, van HT, Verbeek JS, Melief CJ, Ossendorp F 2009. Antigen storage compartments in mature dendritic cells facilitate prolonged cytotoxic T lymphocyte cross-priming capacity. *Proc Natl Acad Sci U S A* 106:6730-6735.
67. Coulie PG, Connerotte T 2005. Human tumor-specific T lymphocytes: does function matter more than number? *Curr Opin Immunol* 17:320-325.
68. Dobrzanski MJ, Reome JB, Hollenbaugh JA, Dutton RW 2004. Tc1 and Tc2 effector cell therapy elicit long-term tumor immunity by contrasting mechanisms that result in complementary endogenous type 1 antitumor responses. *J Immunol* 172:1380-1390.
69. Garcia-Hernandez ML, Hamada H, Reome JB, Misra SK, Tighe MP, Dutton RW 2010. Adoptive transfer of tumor-specific Tc17 effector T cells controls the growth of B16 melanoma in mice. *J Immunol* 184:4215-4227.
70. Welters MJ, Kenter GG, de Vos van Steenwijk PJ, Lowik MJ, Berends-van der Meer DM, Essahsah F, Stynenbosch LF, Vloon AP, Ramwadhoebe TH, Piersma SJ, van der Hulst JM, Valentijn AR, Fathers LM, Drijfhout JW, Franken KL, Oostendorp J, Fleuren GJ, Melief CJ, van der Burg SH 2010. Success or failure of vaccination for HPV16-positive vulvar lesions correlates with kinetics and phenotype of induced T-cell responses. *Proc Natl Acad Sci U S A* 107:11895-11899.
71. Bos R, Sherman LA 2010. CD4+ T-cell help in the tumor milieu is required for recruitment and cytolytic function of CD8+ T lymphocytes. *Cancer Res* 70:8368-8377.

Supporting Information



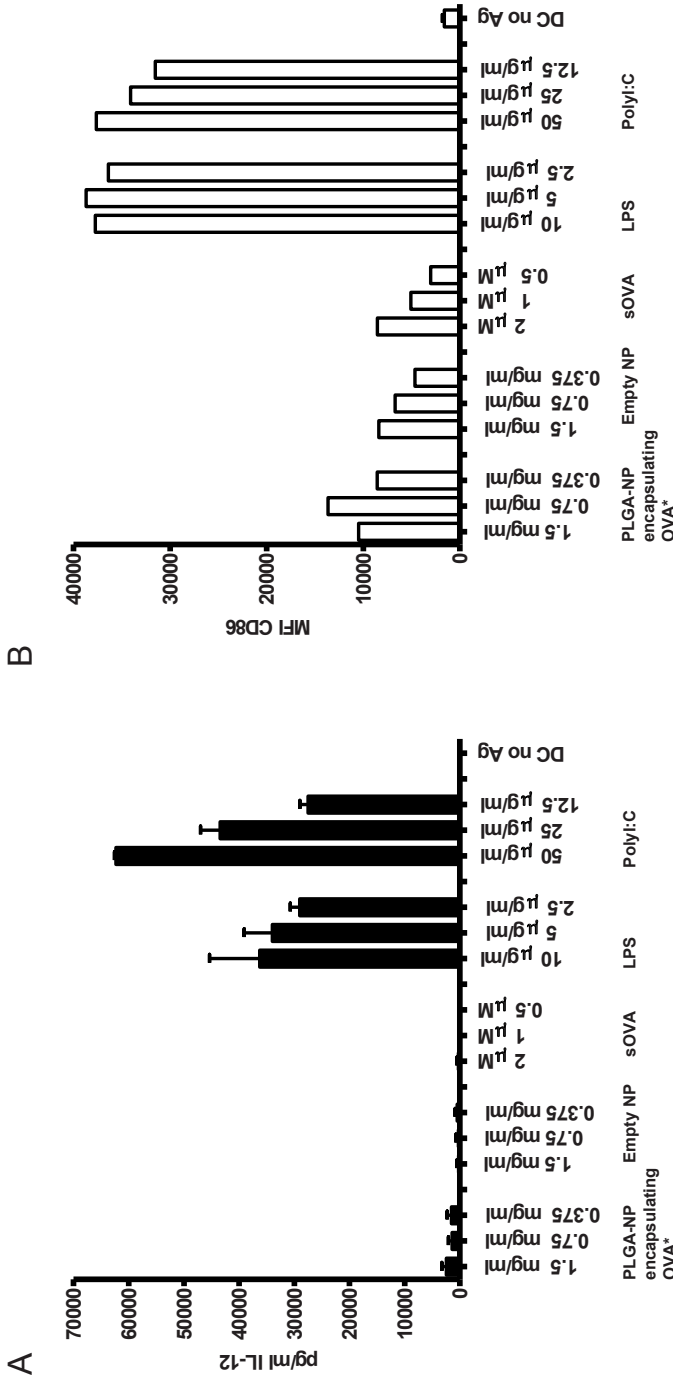
Supporting Information Figure S5.1 Encapsulated OVA is released gradually from PLGA-NP.

PLGA-OVA-Alexa488 with an average OVA content of $14.11 \pm 2.89 \mu\text{g OVA/mg PLGA}$ were resuspended at a concentration of 10 mg/mL of PBS and incubated at 37°C under constant shaking. At indicated time points 250 μL samples were collected, centrifuged for 20 min at 18,000 $\times g$ and the amount of OVA-Alexa488 in the supernatant determined by fluorescence, as described in the material and methods. Average results of two independent release studies with four different batches of PLGA-OVA are shown, mean \pm SD.



Supporting Information Figure S5.2 Improved CD4⁺ and CD8⁺ T cell proliferation by BMDC loaded with PLGA-OVA in comparison to sOVA-loaded BMDC.

WT C57BL/6 BMDC were incubated with titrated amounts of PLGA-OVA or sOVA. Ag loaded BMDC were subsequently used as APC in a co-culture with naïve OT-I (A) or OT-II (B) cells for 72 h. T cell proliferation was measured in triplicate by ³[H]-thymidine uptake. Data shown are representative of two independent experiments.



Supporting Information Figure S5.3 PLGA-OVA do not mature DC in comparison to TLRL.

DC were incubated in the presence of titrated amounts of PLGA-OVA, empty PLGA-NP, sOVA, a mixture of sOVA and empty PLGA-NP, LPS (Sigma L4130, Escherichia coli 0111:B4) and Poly:I:C (Invivogen, tlr-picw). After 24 hr supernatants were collected and analyzed via ELISA for IL-12 levels (A). DC were harvested and analyzed by flow cytometry for the expression of CD86 (B). Data shown are representative of three independent experiments. *1.5 mg/ml of PLGA-NP encapsulating OVA (PLGA-OVA) is required to obtain of 0.25 μM OVA.



Chapter 6

Poly-(lactic-co-glycolic-acid)-based particulate vaccines: nano-size is a key parameter for dendritic cell uptake and immune activation

Ana Luisa Silva*, Rodney A. Rosalia*, Eleni Varypataki,
Shanti Sibuea, Ferry Ossendorp & Wim Jiskoot

* Contributed equally to this study

Manuscript in preparation for publication

Abstract

Poly(lactide-co-glycolide) (PLGA) particulate vaccines have been extensively studied as delivery systems to improve the potency of protein based vaccines. In this study we analyzed how the size of PLGA particles, and hence their ability to be engulfed by dendritic cells, affects the type and magnitude of the immune response. PLGA microparticles (MP, volume mean diameter $\approx 112 \mu\text{m}$) and nanoparticles (NP, Z-average diameter $\approx 350 \text{ nm}$) co-encapsulating ovalbumin (OVA) and poly(I:C), with comparable antigen (Ag) release characteristics, were prepared and characterized. NP were efficiently taken up by dendritic cells and induced MHC I Ag presentation *in vitro*, whereas MP failed to do so. Vaccination with NP resulted in significantly higher numbers of Ag-specific CD8+ T cells compared to MP and OVA emulsified with incomplete Freund's adjuvant (IFA). In addition, NP induced a balanced T_H1/T_H2 -type antibody response, whereas MP failed to increase antibody titers and vaccinations with IFA led to a predominant T_H2 -type response. In conclusion, we postulate that particulate vaccines should be formulated in the nano- but not micro-size range to achieve efficient uptake, significant MHC class I cross-presentation and improved T and B cell responses.

Introduction

In the past few years, extensive efforts in the field of cancer immunotherapy have led to the development of several therapeutic vaccine strategies currently being studied in clinical trials against various immunological diseases¹⁻³. Protein- and peptide-based vaccines are popular forms of therapeutic vaccines³⁻⁵ which have been tested successfully in (pre-)clinical studies against various forms of cancer⁶⁻⁸. However, clinical benefits can still be significantly improved. Different methods can be applied to improve the efficacy of protein- or peptide-based vaccines, such as the combination with adjuvants, for example toll-like receptor ligands (TLRL), to enhance the otherwise poor immunogenicity of synthetic proteins and peptides^{9,10}. In addition, optimizing the delivery of vaccines through the usage of biodegradable particles as vaccine carriers has resulted in promising results and significantly improved vaccine efficacy. Usage of biodegradable particles facilitates the co-delivery of a vaccine antigen (Ag) and TLR as one entity to dendritic cells (DC)^{11,12}.

DC are the most important and potent Ag-presenting cells (APC) of the immune system, scavenging the environment for potential pathogens^{13,14}. DC have superior capacity to cross-present exogenous Ag in MHC I molecules and activate CD8⁺ T cell responses. TLR-stimulation leads to DC maturation. Mature DC possess improved capacity to prime robust T cell response, essential for eradication of established tumors or clearance of pathogens. Therefore DC are considered the major target for cancer vaccines¹⁵⁻¹⁷.

Montanide-based water-in-oil (w/o) emulsions are currently the main vaccine delivery systems used in the clinic. Montanide is a GMP-grade version of incomplete Freund's adjuvant (IFA). The Ag is dispersed in the emulsion which is injected subcutaneously (s.c.) or intradermal (i.d.) forming a local depot which slowly releases the emulsified Ag. Montanide (and) IFA have poorly defined adjuvant properties, but it is known to trigger inflammation at the injection site and immune cell infiltration^{18,19}. However, the use of Montanide is associated with significant local adverse effects⁶. For these reasons, there is an urgent need for an alternative Ag delivery system²⁰.

Biodegradable particulate delivery systems are promising alternatives for Montanide²¹. Nanoparticles (NP) and microparticles (MP) prepared from poly(L-lactic-co-glycolic acid) (PLGA) have been studied extensively for the sustained delivery of proteins and therapeutic agents²²⁻²⁴. Plain PLGA particles have sub-optimal adjuvant properties^{10,25} but PLGA-particulate vaccines have shown potent anti-tumor effects by co-encapsulating tumor-associated Ag (TAA) and TH1-immunity promoting Toll like Receptor ligands (TLRL)^{11,26,27}.

Generally, particulate Ag (Ag) are better routed into MHC class I cross-presentation pathways, compared to soluble Ag, and therefore facilitate the priming of strong CD8⁺ T cell responses.

It is generally assumed that NP, compared to MP, are ideal for (targeted) drug delivery due to better bio-distribution^{28,29} and ability to cross biological barriers³⁰. However, there is little agreement when it comes to vaccines for immunotherapy^{31,32}. This may be related to different parameters that can direct the type and potency of the immune response, the target APC which the vaccine should be delivered to^{33,34}, efficiency of vaccine uptake by APC, Ag release kinetics and route of administration upon vaccination³⁵⁻³⁸. We have recently shown that low-burst release of the encapsulated Ag is critical for efficient MHC class I Ag presentation and CD8⁺ T cell activation³⁹. Accession of the MHC class I cross-presentation pathways was also shown to be dependent on particle size⁴⁰, however which size leads to the most efficient Ag cross-presentation remains debatable.

In this study, to compare the importance of particle uptake for the induction of an immune response, we developed NP and MP, formulated using PLGA, co-encapsulating the model Ag ovalbumin (OVA) and the TLR3L poly(I:C). NP can be internalized by DC⁴⁰, releasing the Ag inside endo-lysosomal compartments or directly inside the cytosol after uptake⁴¹, versus MP which are poorly taken up by DC. MP most likely releases the encapsulated Ag in the extracellular matrix at the site of injection, similarly to Montanide. Formulated NP and MP contained equivalent amounts of Ag and TLR and had comparable long-term Ag release profiles. We report here that NP are more efficiently internalized by DC *in vitro* and resulting in efficacious MHC class I cross-presentation and subsequent CD8⁺ T cell activation *in vitro*. *In vivo*, NP showed superior vaccine potency compared to MP to stimulate cellular immune responses. In addition, NP out-performed water-in-mineral oil emulsion IFA as a vaccine carrier, more efficiently boosting CD8⁺ T cell activation and (IgG2a) antibody production.

Materials and methods

Animals

WT C57BL/6 (CD45.2/Thy1.2; H-2^b) were obtained from Charles River Laboratories. Ly5.1/CD45.1 (C57BL/6 background) were bred in the specific pathogen-free animal facility of the Leiden University Medical Center. All animal experiments were approved by the animal experimental committee of Leiden University.

Reagents

PLGA Resomer RG 502H (50:50 MW 5,000–15,000 Da) was purchased from Boehringer Ingelheim (Ingelheim am Rhein, Germany) and PLGA Resomer RG 752H (75:25 MW 4,000–15,000 Da) was purchased from Sigma-Aldrich (Steinheim, Germany). Ovalbumin (OVA) grade V, 44 kDa was purchased from Worthington (LS003048) (New Jersey, USA). Alexa Fluor 488 labeled OVA was obtained from Invitrogen (Merelbeke, Belgium). Dichloromethane (DCM), dimethyl sulfoxide (DMSO), Hepes were purchased from Sigma–Aldrich (Steinheim, Germany). Tween 20 was purchased from Merck Schuchardt (Hohenbrunn, Germany) and polyvinyl alcohol (PVA) 4–88 (31 kDa) was purchased from Fluka (Steinheim, Germany). Poly(l:C) LMW and rhodamine labeled poly(l:C) were purchased from InvivoGen (San Diego, USA). Incomplete Freund adjuvant (IFA) was purchased from Difco Laboratories (Detroit, USA) Phosphate-buffered saline (NaCl 8.2 g/L; Na₂HPO₄·12 H₂O 3.1 g/L; NaH₂PO₄·2H₂O 0.3 g/L) (PBS) was purchased from B. Braun (Melsungen, Germany). All fluorescently labeled antibodies used for staining were purchased from BD Pharmingen (San Diego, USA) and the APC-SIINFEKL/H2-K^b tetramers were produced in house. All other chemicals were of analytical grade and all aqueous solutions were prepared with milli Q water.

IFA vaccine formulations were prepared by vortexing for 30 min a 1:1 IFA:PBS mixture. The vaccine-Ag was suspended in the PBS prior to addition to the IFA.

Cells

D1 cells, a GM-CSF dependent immature dendritic cell line derived from spleen of WT C57BL/6 (H-2^b) mice, were cultured as described previously⁴². Bone-marrow derived DC (BMDC) were freshly isolated from femurs from WT C57BL/6 strain and cultured as published previously⁴³. After 10 days of culture, large numbers of cells were obtained which were at least 90% positive for murine DC marker CD11c (data not shown). B3Z CD8⁺ T cell hybridoma cell line, specific for the H-2K^b-restricted OVA_{257–264} CTL epitope SIINFEKL, expressing a β-galactosidase construct under the regulation of the NF-AT element from the IL-2 promoter, was cultured as described before⁴⁴. OT-IIZ, a CD4⁺ T-cell hybridoma cell line, specific for the I-A^b-restricted OVA_{323–339} Th epitope, expressing the same β-galactosidase construct, was produced in house. The weakly immunogenic and highly aggressive OVA-transfected B16 tumor cell line (B16-OVA), syngeneic to the C57BL/6 strain, was cultured as described⁴⁵.

Preparation and characterization of OVA- and poly(I:C)-loaded PLGA particles

In this study, NP and MP were prepared containing the model Ag OVA and the TLR3 ligand poly(I:C). Plain PLGA-NP particles exhibit low immune activating properties²⁵ and are therefore poor vaccine-candidates. For this reason, all experiments were performed with particles co-encapsulating PolyI:C.

PLGA 50:50 and PLGA 75:25 NP were prepared by a water-in-oil-in-water (w/o/w) double emulsion with the solvent evaporation method as previously described [24]. The two types of PLGA, with different lactic acid:glycolic acid ratios (50:50 or 75:25 PLGA), influences hydrophobicity, polymer degradation rate and the release kinetics of OVA and poly(I:C).

In brief, 1 mg OVA (Worthington LS003048), 0.25 mg poly(I:C), were dissolved in 85 μ l of 25 mM Hepes pH 7.4 and emulsified in 1 ml dichloromethane (DCM) containing 25 mg PLGA with an ultrasonic processor for 15 s at 20 W (Branson Instruments, CT, USA). A second emulsion was obtained by addition of 2 ml of 1% (w/v) PVA followed by sonication as described above. The double emulsion was added drop wise to 25 ml of an aqueous 0.3% PVA (w/v) solution at 40°C and the resulting mixture was stirred for 1 h. The resulting particles were harvested and washed twice with water by centrifugation (8000 g, 10 min).

PLGA 50:50 MP were prepared by adding 1 mg OVA, 0.25 mg poly(I:C) dissolved in 500 μ l of 25 mM Hepes pH 7.4 to 1 ml DCM containing 125 mg PLGA 50:50. The mixture was emulsified with a homogenizer (30 sec) (max speed = 25,000 rpm) (Heidolph Ultrax 900, Sigma, Germany). The resulting emulsion was transferred to 10 ml of 2% (w/v) PVA and the 2nd emulsion was obtained by magnetic stirring (10 min, 750 rpm) at RT. Stirring was continued for 1 hr (500 rpm) (40°C) to allow evaporation of DCM. MP were harvested and washed with water twice by centrifugation (2000 g, 2 min). Particles $\geq 20 \mu$ m were separated via dia-filtration with 3 L water under continuous stirring in a Solvent Resistant Stirred Cell (Milipore, USA) filtration system with a 20 μ m stainless steel metal sieve (Advantech, USA). The retentate was collected and MP recovered by centrifugation (2000 g, 2 min). MP larger than 200 μ m were eliminated by using a 200 μ m stainless steel metal sieve (Advantech, USA). The intactness of MP before and after filtration, were visualized with an Axioskop microscope (50 μ l samples), equipped with an Axiocam ICc 5 (Carl Zeiss, Munich, Germany), using a 20x amplification objective. Images were collected using the ProgRes CapturePro v2.8.8 software (Jenoptik AG, Jena, Germany). Both NP and MP suspensions were aliquoted in cryovials and freeze-dried.

Alternatively, some particles were formulated with and 10 µg (10% w/w) OVA-Alexa488 and 1 µg (0.4%) poly(I:C)-rhodamine which were added to the inner emulsion for the preparation of NP and MP. This allowed quantification based on fluorescence and visualization by flow cytometry.

Mean size, size distribution and polydispersity index (PDI), obtained by dynamic light scattering (DLS) and Zeta potential (ZP) (applying laser Doppler velocimetry) of NP were using a NanoSizer ZS (Malvern Instruments, Malvern, UK) at room temperature (RT) in 5 mM Hepes pH 7.4. The size distribution of MP was determined by light obscuration (LO) using a PAMAS SVSS system (PAMAS GmbH, Rutesheim, Germany) equipped with an HCB-LD-25/25 sensor and a 1-ml syringe. Results are averages of triplicate measurements, using runs, each of 0.2 ml (flow rate of 10 ml/min).

BCA assay (Pierce, Rockford, IL, USA) was used to determine OVA concentration in particles (before and after filtration) according to the manufacturer's instructions, after dissolving the particles in DMSO and 0.5 M NaOH + 0.5% SDS⁴⁶. Encapsulation efficiency (EE) (see equation 6.1) of the protein was based on the OVA-Alexa-488 fluorescence (excitation 495 nm, emission 520 nm) and of TLR3L based on poly(I:C)-rhodamine (excitation 546 nm, emission 576 nm) detected in the supernatant using an Infinite® M 1000 Pro (Tecan, Switzerland) microplate reader. The drug loading (DL) was calculated according to equation 6.2. ("compound" stands for OVA or poly(I:C)):

$$\% \text{ EE} = \frac{\text{encapsulated compound mass}}{\text{initial compound mass}} \times 100 \quad (6.1)$$

$$\% \text{ DL} = \frac{\text{encapsulated compound mass}}{\text{polymer mass} + \text{encapsulated compound mass}} \times 100 \quad (6.2)$$

Microscopic analysis showed the quality and intactness of MP before filtration (BF) and after filtration (AF) (Figure 6.1). Physicochemical characterization of NP and MP is summarized in Table 6.1. NP were fairly monodisperse (PDI < 0.25), with NP 50:50 being 357 ± 25 nm and NP 75:25 being 400 ± 16 nm. The two different NP-formulations were produced with the aim to obtain NP of similar size but with varying release characteristics of the encapsulated protein. In addition, it was of importance to obtain NP with comparable Ag (and adjuvant)-release characteristics as MP for the purpose of studying the importance of size, while excluding other factors.

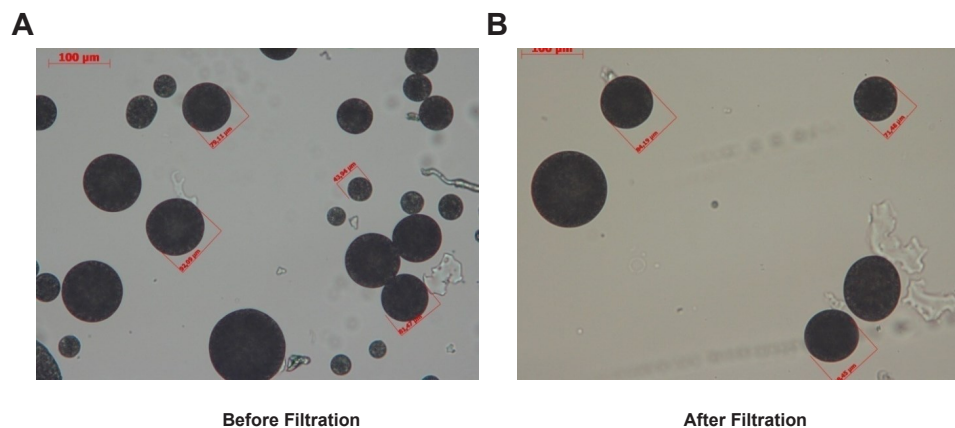


Figure 6.1 Representative images of MP preparations analyzed by optical microscopy (20x magnification) before and after stirred-cell filtration.

Table 6.1 Physical characteristics of OVA/poly(I:C)-loaded PLGA NP and MP*

Formulation	Size	PDI	ZP (mV)	OVA		Poly I:C	
				EE	DL	EE	DL
PLGA 50: 50 [#] NP	357 ± 25 nm	0.16 ± 0.03	-41 ± 7	52 ± 7	2.01 ± 0.27	66 ± 8	0.63 ± 0.07
PLGA 75: 25 [#] NP	400 ± 16 nm	0.25 ± 0.02	-25 ± 3	75 ± 1	2.87 ± 0.03	59 ± 7	0.56 ± 0.07
PLGA 50: 50 [#] MP	17 ± 5 µm (n) 112 ± 26 µm (v)	n/a	-14 ± 3	86 ± 2	0.68 ± 0.01	81 ± 2	0.16 ± 0.00

*Values represent mean +/- standard deviation of 3 independently prepared batches .

[#]The two types of PLGA, with different lactic acid:glycolic acid ratios (50:50 or 75:25 PLGA), influences hydrophobicity, polymer degradation rate and the release kinetics of OVA and poly(I:C).

DL = drug loading; is a quantitative value for the ratio of protein:polymer; EE = encapsulation efficiency; is a qualitative value to define the efficiency of the formulation process to entrap the protein in the PLGA-polymer matrix = particles; PDI = poly dispersity index; variance, an arbitrary measure for the degree of dispersity in particle size within one batch of particles suspension, PDI values below 0.3 was considered monodisperse and accepted for follow up studies ⁴⁷; ZP = zeta potential; The magnitude of the zeta potential is predictive of the colloidal stability. Nanoparticles with Zeta Potential values greater than +25 mV or less than -25 mV typically have high degrees of stability. Dispersions with a low zeta potential value will eventually aggregate due to Van Der Waal inter-particle attractions.

For MP, size distribution, the average mean diameter based on volume Supporting Information Figure S6.1A and number Supporting Information Figure 6.1B before- and after filtration was determined.

The particle number-based mean diameter of MP, which is the average when considering the number distribution, increased from 5 ± 1 µm before filtration to 17 ± 5 µm after

filtration, showing that the filtration step effectively decreased the number of particles smaller than 20 μm , though not totally. However, the particle volume-based mean diameter was similar BF and AF (114 ± 16 vs 112 ± 26 μm) showing the relative minor contribution of small particles to the total particle volume. During the double-emulsion and solvent evaporation process, the OVA-protein added is equally distributed through the PLGA-polymer matrix and resulting particles. Thus the volume-based mean diameter results indicate that less than 1% of the total volume, and consequently the amount of the OVA added during formulation, corresponded to particles with diameters smaller than 20 μm after filtration (Supporting Information Table S6.1). Therefore, it is unlikely that residual NP after filtration would have a significant effect on Ag uptake, MHC class I Ag presentation and CD8⁺ T cell activation, making them insignificant in terms of final immune response. Encapsulation efficiency of OVA (EE) was above 50% for all particle batches formulated with MP generally having higher EE% compared to NP. As explained above, the higher EE of OVA corresponds to the higher amount of PLGA content of MP compared to NP, which is reflected by the lower drug loading DL (Table 6.1). The use of different ratio of PLGA-polymer to formulate NP did not affect the EE of the protein nor the poly(I:C).

***In vitro* release studies**

For release studies, PLGA particles (encapsulating 1% (w/w) of OVA-Alexa-488 and Poly(I:C)-rhodamine were resuspended in PBS/0.01% Tween-20/0.01% NaN_3 (pH 7.4) (10 mg PLGA/ml) at continuous tangential shaking (100 rpm) at 37°C in a GFL 1086 water bath (Burgwedel, Germany) for 30 days. At indicated time points, 250 μl samples of the suspension were taken, and centrifuged (18000 $\times g$) for 20 min and stored at 4°C until fluorescence intensity was determined as described above. Concentrations of OVA-Alexa-488 and poly(I:C)-rhodamine was assessed against a calibration curve. Release kinetics were based on fluorescence intensity because of the higher sensitivity achieved in comparison to the BCA assay. OVA content in the remaining supernatant (SN) on the last day of the release study were also analyzed using a BCA assay to compare to the results obtained using fluorescence measurements. The BCA assay and fluorescence assay showed comparable results (Supporting Information Table S6.2), justifying the use of fluorescence to assess OVA release from PLGA particles.

Release (R) profiles were generated in terms of cumulative release (%), as determined by equation 6.3, where “compound” is OVA or poly(I:C).

$$\% R = \frac{\text{compound mass in supernatant}}{\text{compound mass in supernatant} + \text{compound mass in particles}} \times 100 \quad (6.3)$$

The OVA and poly(I:C) release kinetics were followed for 30 days. Release studies showed sustained release of OVA and poly(I:C) from PLGA 50:50 NP over this period (Figure 6.2A). Ag-release properties of MP were matched to those of NP by modifying the inner volume and salt content of the first emulsion during preparation of the MP (see Supporting Information Figure S6.2 for inner phase compositions).

OVA dissolved in 500 μ l of 25 mM HEPES resulted in the fastest OVA release from MP (circa 40% OVA released after 15 days) comparable to that from NP (Figure 6.2C). The burst release of MP was decreased after filtration (AF) in comparison to MP analyzed before filtration (BF), most likely due to the elimination of the smaller MP (Supporting Information Figure S6.1 & Table 6.1). PLGA 75:25 NP (Figure 6.2B) showed release profiles resembling those of the MP. Thus, we formulated NP and MP using PLGA 50:50 with a similar composition but different Ag release properties; and NP using PLGA 75:25 with similar Ag-release profiles as PLGA 50:50 MP.

Ag release from particles appears to consist of an initial burst, followed by sustained release. After 30 days we observed a total release of $66 \pm 6\%$ OVA and 94 ± 7 poly(I:C) for NP 50:50, $51 \pm 6\%$ OVA and 64 ± 3 poly(I:C) for NP 75:25, and $44 \pm 5\%$ OVA and 54 ± 3 poly(I:C) for MP 50:50 (Figure 6.2).

In summary, we prepared NP and MP with similar long-term release characteristics, which will allow us to fairly compare the effects of particle size on *in vitro* DC uptake, MHC class I presentation and resulting *in vivo* immune activating properties.

Analysis of particle uptake by DC

Particle uptake by DC was determined by plating out D1 cells in 96-wells plate (10^5 cells/well) and pre-cooling the cells on ice (10 min). Pre-cooled cells were then further cultured for 1 h at 4°C (on ice) or at 37°C in the presence of PLGA particles (PLGA-OVA/poly(I:C) NP/MP containing OVA-Alexa488) at the indicated concentrations. After incubation, cultured cells were washed and centrifuged twice with cold saline buffer to remove unbound particles and cells fixed with 4% paraformaldehyde (100 μ l/well). Fixation was blocked by the addition of 100 μ l/well fetal calf serum (FCS) and washing with cold PBS. From this point on cells were kept at RT and stained with rat anti-mouse CD45.2-APC fluorescent

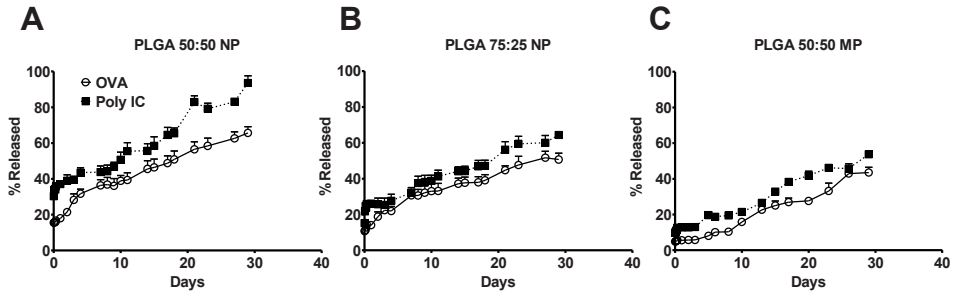


Figure 6.2 *In vitro* release kinetics of OVA and poly(I:C) from NP and MP.

OVA and poly(I:C) release in PBS/0.01% Tween-20/0.01% NaN₃ (pH 7.4) of (A) NP PLGA 50:50, (B) NP PLGA 75:25, and (C) MP PLGA 50:50 were monitored for 30 days at 37°C. Data are presented as average \pm SD of 3 independent batches.

antibodies to allow detection of cells which were positive for particle association, based on OVA-Alexa488 fluorescence as analyzed using a BD LSRII flow cytometer. Samples were acquired using the BD FACS DIVA software and analyzed with Flow Jo software (treestar).

MHC class I Ag presentation

DC were incubated for 2 hr with PLGA-OVA formulations at the indicated concentrations, washed and followed by an overnight incubation (37°C) in the presence of B3Z CD8⁺ T cell hybridoma's to measure MHC class I presentation. A colorimetric assay using chlorophenol red- β -D-galactopyranoside as substrate was used to detect IL-2 induced *lacZ* activity after recognition of SIINFEKL (OVA₂₅₇₋₂₆₄) in H-2K^b by B3Z T cells⁴⁸. To determine the relative maximum B3Z T cell activation DC were loaded with the minimal epitope SIINFEKL and the extinction value set as 100% ($OD_{590nm} = 2.53 = 100\% = \text{maximal CD8}^+ \text{T cell activation}$).

Vaccination studies

Animals were vaccinated with the various PLGA-OVA/poly(I:C) formulations, soluble OVA/poly(I:C) in PBS, or OVA/poly(I:C) emulsified in IFA by s.c. injection into the right flank. Animals were vaccinated again on day 28 (boost). Priming of *in vivo* cytotoxic CD8⁺ T cells was assessed seven days after the 1st vaccination or 14 days after the 2nd vaccination by transferring splenocytes prepared from congenic Ly5.1 C57BL/6 animals which were pulsed with the SIINFEKL short peptide (OVA₈, vaccine specific target cells) or ASNENMETM

short peptide (FLU9, vaccine non-specific control target cells). The target cells were labeled with either 10 μ M (OVA) or 0.5 μ M (Flu) CFSE. The cells were mixed 1:1 and 10^7 total cells were injected intravenously (i.v.) into the vaccinated animals. 18 hr post transfer of target cells, animals were sacrificed and single cell suspensions were prepared from isolated spleens. Injected target cells were distinguished by APC-conjugated rat anti-mouse CD45.1 mAb (BD Pharmingen, San Diego, USA). *In vivo* cytotoxicity was determined by flow cytometry as described above after 18 hr using equation 6.4:

$$\% \text{ OVA - specific killing} = \left(1 - \left[\left(\frac{\text{CFSE} - \text{peak area OVA}}{\text{CFSE} - \text{peak area FLU}} \right)^{\text{vaccinated animals}} \right] \right) \times \left(\frac{\text{CFSE} - \text{peak area OVA}}{\text{CFSE} - \text{peak area FLU}} \right)^{\text{non-vaccinated animals}} \times 100 \quad (6.4)$$

OVA-specific CD8⁺ T cells present in the spleens were analyzed by co-staining with APC-conjugated SIINFEKL/H2-K^b tetramers, AF-conjugated anti-mouse CD8 α mAb and V500-conjugated rat anti-mouse CD3 mAb. Flow cytometry analysis was performed as described above.

Detection of antibody responses

Antibody responses were determined by collecting serum samples on day 21 after initial vaccination (1 week before 2nd vaccination) and on day 35 (1 week after 2nd vaccination). IgG1, IgG2a and IgG2b titers against OVA were determined by ELISA. In brief, high absorbent 96-wells (Nunc immunoplates) plates were coated with 5 μ g/ml OVA in PBS and incubated with titrated serum samples in 10% FCS in PBS. The specific antibodies were detected using streptavidine conjugated rabbit anti-murine IgG1, IgG2a and IgG2b mAb, followed by addition of horse-radish-peroxidase conjugated biotin. 3,3',5,5'-Tetramethylbenzidine (TMB) was used as a substrate and the color conversion was stopped after 10 min with 0.16 M H₂SO₄, which was then measured on a spectrophotometer by absorbance at 450 nm (OD_{450_{nm}}). To determine immune polarization the IgG2a/IgG1 ratios were determined using OD_{450_{nm}} values determined at 1:100 dilution given that values applied were \geq 2-fold OD_{450_{nm}} of the negative control (sera from non-immunized mice).

RESULTS

PLGA-particles in the nano-size range facilitate efficient internalization by DC compared to MP

Efficiency of particle association with DC was studied by culturing DC in the presence of the 3 different particle formulations at 4°C (binding) and 37°C (binding & internalization). DC showed very high capacity to bind and internalize NP compared to MP (Figure 6.3A). DC were incubated with various concentrations of protein Ag encapsulated in both sizes of particles and we observed consistently that both 50:50 and 75:25 PLGA-NP showed similar effects and were engulfed with higher efficacy than (PLGA 50:50) MP (Figure 6.3B & C).

Efficient MHC class I Ag presentation by DC incubated with NP

MHC class I Ag cross-presentation of encapsulated protein Ag in NP compared to MP by dendritic cells was studied *in vitro*. DC were incubated with titrated amounts of Ag formulations and specific antigen presentation was analyzed by OVA epitope (SIINFEKL)-specific T cells. DC loaded with NP 50:50 and 75:25 efficiently activated B3Z CD8⁺ T cells (Figure 6.4). Normalized values in panel A were calculated based on the OD590_{nm} values obtained using DC loaded with SIINFEKL cultured together with B3Z CD8⁺ T cells (OD590_{nm} = 2.53 = 100% = maximal CD8⁺ T cell activation). In contrast, DC pulsed with MP 50:50 poorly stimulated B3Z CD8⁺ T cells.

Effective *in vivo* priming of Ag-specific CD8⁺ T cells by NP-encapsulated protein

The *in vitro* experiments showed that NP, in contrast to MP, are efficiently internalized by DC followed by processing of encapsulated protein Ag into the MHC class I processing pathways, resulting in strong activation of B3Z CD8⁺ T cells. NP 50:50 and NP 75:25 showed similar effects. Moreover, NP 50:50 showed similar or CD8⁺ T cell priming *in vivo* as NP 75:25 (data not shown). Therefore, NP 50:50 were used for comparative *in vivo* studies with MP 50:50 and classical IFA emulsions.

The *in vivo* vaccine potency of NP and MP formulations was analyzed in comparison to protein Ag and poly(I:C) solution emulsified in IFA. Animals were vaccinated and 7 days

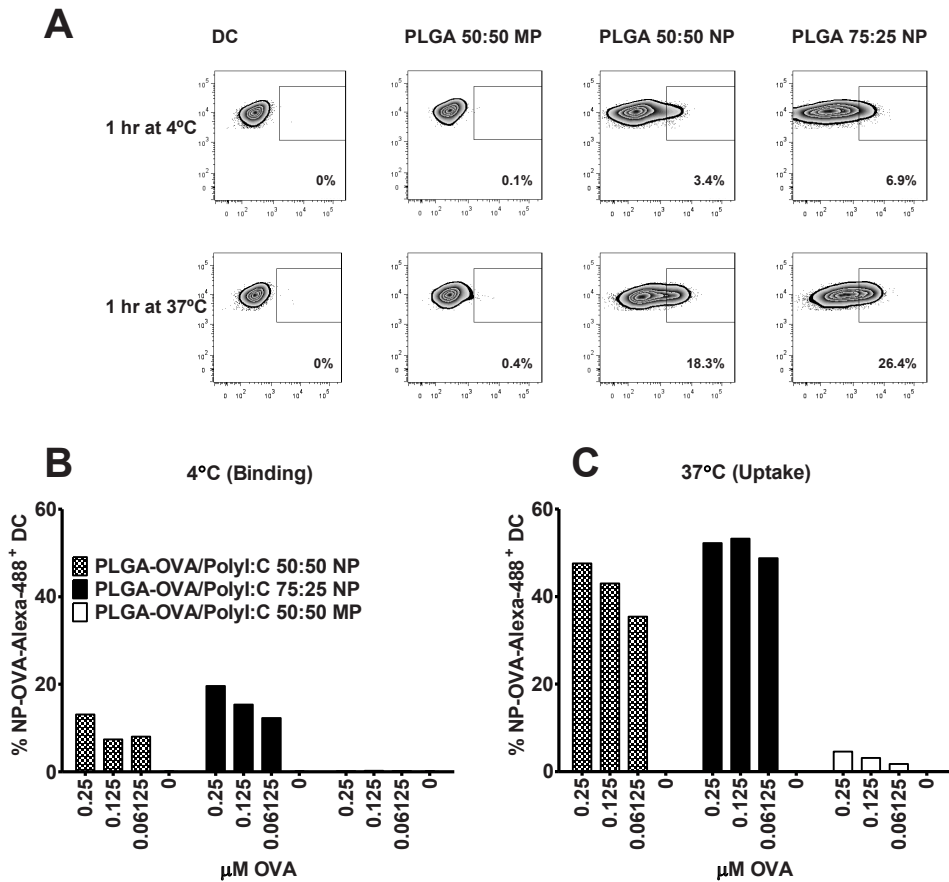


Figure 6.3 Binding and uptake of NP-encapsulated protein Ag by dendritic cells compared to MP-encapsulated Ag.

(A) D1 dendritic cells were incubated for 1 h with titrated amounts (μM) of OVA encapsulated in PLGA-NP (PLGA-OVA/poly(I:C) NP 50:50 or PLGA-OVA/poly(I:C) NP 75:25, or PLGA-MP PLGA-OVA/poly(I:C) MP 50:50 containing OVA-Alexa488 dye. Ag incubation with DC was performed in parallel at (B) 4°C (binding) and (C) 37°C (binding & internalization), followed by extensive washing to remove unbound Ag and cell fixation with 4% PFA. Cells were analyzed by flow cytometry to determine green fluorescence. Percentages of DC positive for OVA-Alexa-488 were quantified at different Ag concentrations. Data shown are measurements from one experiment.

later sacrificed to determine the number of primed endogenous Ag-specific CD8⁺T cells in the spleen (Figure 6.5). Vaccinations with NP 50:50 resulted in significantly higher numbers of SIINFEKL-TM⁺ CD8⁺T cells compared to MP 50:50 ($P = 0.01$) and IFA ($P = 0.04$).

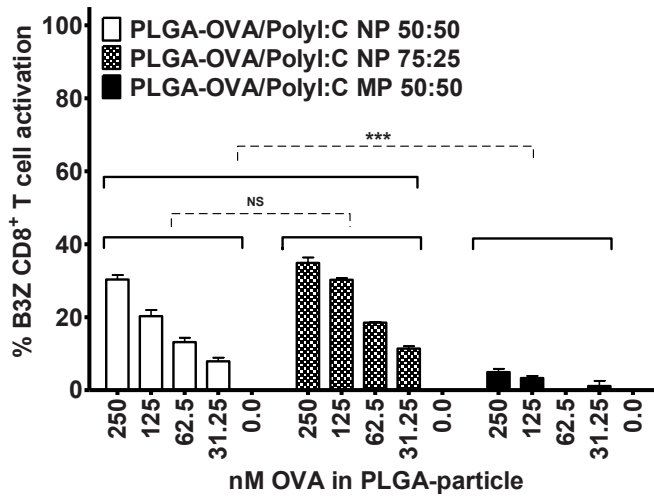


Figure 6.4 Efficient MHC class I cross-presentation of protein Ag incorporated in PLGA-NP but not PLGA-MP.

D1 cells were pulsed for 2 h with titrated amounts (μM) of OVA (and Poly(l:C) encapsulated in 50:50 PLGA-NP or 75:25 PLGA-NP or 50:50 PLGA-MP. MHC class I presentation of processed OVA protein antigen was detected by co-culture with H-2K^b/SIINFEKL-specific B3Z CD8⁺ T cells. Data shown are means of triplicate measurements \pm SD as % from one representative example out of at least three independent experiments.

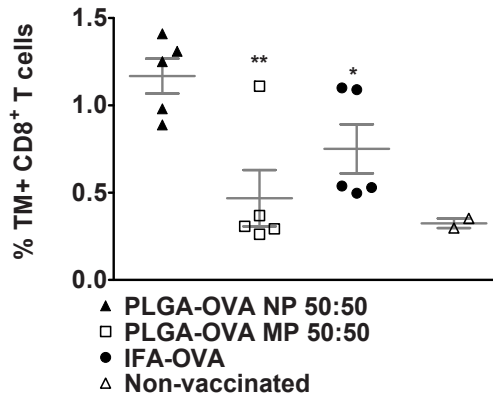


Figure 6.5 PLGA-OVA/poly(l:C) NP vaccine shows effective CD8⁺ T cell priming potency.

Naïve animals received a single s.c. vaccination with the 50 μg OVA and 20 μg poly(l:C) formulated in particles or in IFA. Mice were sacrificed on day 7 after vaccination and the % of SIINFEKL-TM⁺ CD8⁺ T cells were measured by flow cytometry. Results shown are representative of one experiment out of two and present averages \pm SEM from $n = 3-5$ mice per group, * = $P < 0.05$ & ** = $P < 0.01$ using an unpaired student t test. Each symbol represents the specific T cell response in an individual mouse.

PLGA NP efficiently prime CD8⁺ cytotoxic T cells which produce IFN- γ

Splenocytes of vaccinated mice were re-stimulated *ex vivo* with the minimal CD8⁺ T cell OVA epitope SIINFEKL. The cytokines IL-2 and IFN- γ were analyzed in the culture supernatants after 72 h (Figure 6.6). Significant amounts of IFN- γ were detected with the highest amounts produced by spleen cultures from animals vaccinated with NP 50:50 (Figure 6.6A) compared to the other vaccinated groups. However after one single vaccination, IL-2 production was barely above background levels (Figure 6.6B). Under these conditions we also analyzed the CD8⁺ T cell *in vivo* cytotoxicity induced by vaccination with NP 50:50 compared to IFA-OVA/poly(I:C). In line with the relative higher number of specific CD8⁺ T cells induced with NP, we observed that animals vaccinated with NP 50:50 showed effective OVA-specific cytotoxicity to injected target cells *in vivo* (Supporting Information Figure S6.3).

Long term immune responses after a boost vaccination on day 28 were studied by analyzing *ex vivo* cytokine production on day 42. Using OVA-protein based vaccine formulations, poor overall production of IFN- γ was detected at this time point (Figure 6.6C). Notably, the 2nd

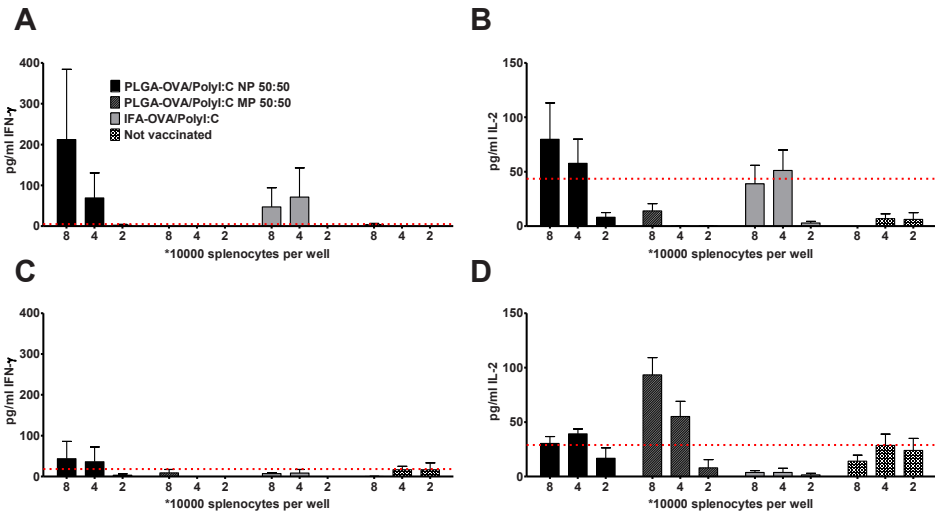


Figure 6.6 IFN- γ and IL-2 production after vaccination with PLGA-OVA/poly(I:C) NP.

Animals were vaccinated with 50 μ g OVA and 20 μ g poly(I:C) formulated in particles or in IFA. Mice were sacrificed on day 7 post-vaccination, spleens harvested and single cell suspensions re-stimulated with 1 μ M SSP-OVA_{8aa} (SIINFEKL). 72 h later the amount of Ag-specific (A) IFN- γ and (B) IL-2 produced determined by ELISA. Animals vaccinated twice (day 0 and 28) were sacrificed on day 42 and the *ex vivo* (C) IFN- γ and (D) IL-2 cytokine production analyzed 72 h later. Red dotted lines indicate average background production of cytokines in the absence of specific stimulation.

vaccination on day 28 resulted in higher levels of specific Ag-specific IL-2 production by splenocytes especially with MP 50:50 rather than the other groups (Figure 6.6D).

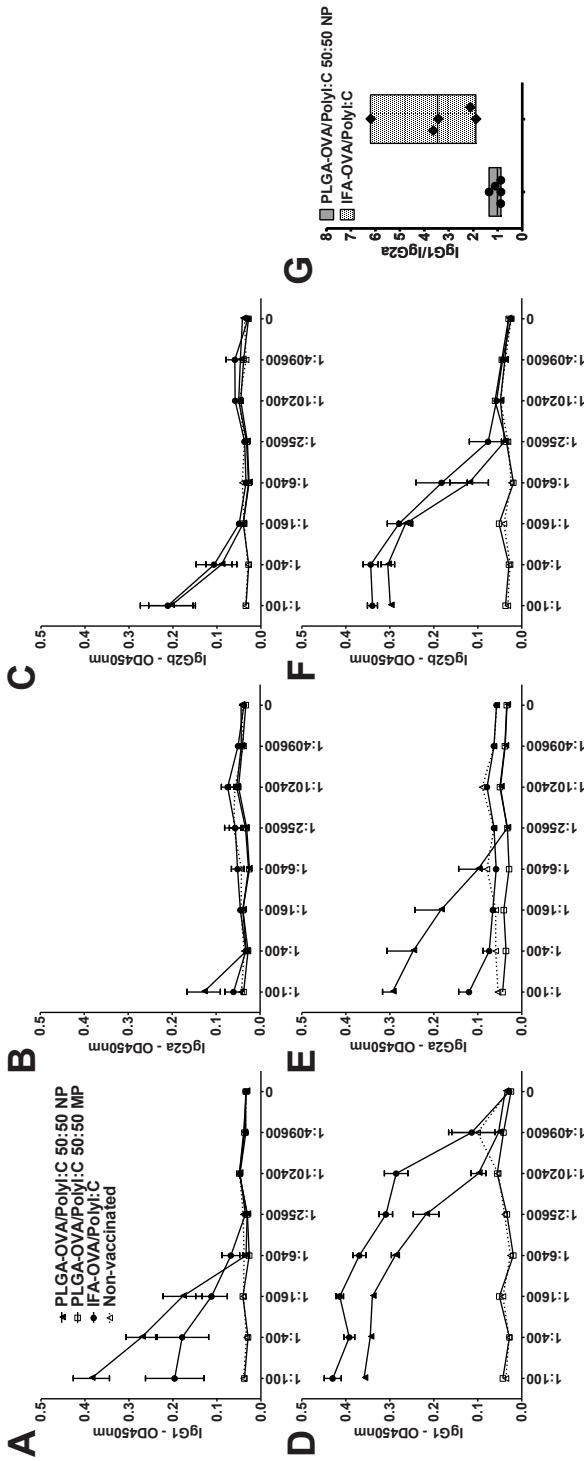
In conclusion, vaccination with NP resulted in the strongest production of IFN- γ compared to IFA or MP based vaccine formulations. NP did not induce strong production of IL-2 after a single vaccination nor double vaccinations. In contrast, MP were capable of inducing IL-2 production, but not IFN- γ , and only after the boost.

Ag-specific TH1 type humoral responses induced by vaccinations with PLGA-NP in contrast to IFA based vaccine

Blood samples were collected on day 21 or 35 after vaccinations. The titers of IgG1, IgG2a and IgG2b antibodies were determined as described in the section “materials & methods”. NP 50:50 and IFA, but not MP, induced IgG1 production after one single vaccination (prime) (Figure 6.7A). Low titers of IgG2a and IgG2b were detected after NP and IFA vaccinations (Figure 6.7B & C). A second vaccination (boost) considerably enhanced the antibody titers. IFA and NP 50:50 led to the highest titers of IgG1, with MP formulations again failing to induce IgG1 titers (Figure 6.7D). Significant IgG2a titers were induced after a 2nd vaccination with NP 50:50 but poorly by the other vaccines (Figure 6.7E). IgG2b titers were induced to a similar level by vaccinations with IFA and NP 50:50 (Figure 6.7F). IgG2a is the IgG-subtype associated with T_H1 responses in mice. Analysis of the IgG1/IgG2a ratio allows one to determine the immune-polarization. Vaccinations with NP 50:50 resulted in a more balanced T_H1/T_H2 antibody response characterized by similar titers of IgG1 and IgG2a (IgG1/IgG2a \approx 1). In contrast, vaccinations with IFA led to a predominant T_H2 response (IgG1/IgG2a > 2) (Figure 6.7G).

Discussion

Particulate vaccines are promising vaccine modalities to enhance immune activation. The immune system reacts more vigorously to vaccines presented in a particulate form compared to soluble ones^{20,49,50}. However, the exact parameters needed to achieve robust immune responses using particulate vaccines are a matter of debate. Using PLGA particles co-encapsulating protein Ag and a TLR3L, we compared NP versus MP and studied the advantages of internalization of particles by DC to induce MHC class I cross-presentation *in vitro* and improve immune responses *in vivo*. We report here the importance to formulate



nano-sized particles, to enhance MHC class I Ag-cross presentation and to improve both cellular and humoral immune responses.

Our observations are most probably associated with the fact that MP are poorly internalized as an whole entity cause of their large size. MP release the encapsulated via an initial burst followed by a more gradual escape of the Ag (Figure 6.2) due to the hydrolysis of the polymer. Therefore, MP basically deliver soluble Ag to DC. We and others have previously shown that DC poorly cross-present protein Ag when it's delivered in plain soluble form. Therefore, if the aim is to induce a robust CD8⁺ T cell response through vaccination, MP might not be the right candidates for this purpose. Indeed, we observed very poor immune activation using MP as a vaccine carrier.

Our results argue against the application of MP as T cell vaccine carrier, however there exists some controversy in the literature regarding particle size and its importance for the formulation of efficient vaccine delivery systems and its effect on the activation of an immune response^{37,38,51,52}. APC may take up and process Ag with similar dimensions to pathogens, from viruses, to bacteria, with the size influencing the mechanisms of uptake and processing by APC⁵³. It has been reported that particles in the range of 20–200 nm are efficiently taken up by DC and facilitate the induction of cellular immune responses, whereas particles of 0.5–5 µm mainly generates humoral responses. There was limited uptake of 10 µm or larger particles leading to defective immune activation^{32,36}. In contrast, others have reported that vaccinations with MP to also induce CTL responses, comparable to IFA or Montanide based delivery systems^{20,54}.

To study the effect of particle uptake on the subsequent immune response, NP and MP co-encapsulating OVA and poly(I:C) were required with similar Ag-release properties. Using the well-described double emulsion and solvent evaporation MP formulation technique⁵⁵, we at first obtained MP with very slow Ag-release properties (data not shown). Hence, the formulation process was modified and MP were engineered to accelerate release and to match the release properties of NP. For this purpose the inner emulsion volume and composition were modified to create a more porous matrix by adding salt to the inner water phase. Increasing the porosity accelerates drug diffusion and release from particles⁵⁶⁻⁵⁹. Replacing water with 25 mM Hepes pH 7.4 resulted in an increased Ag release rate from MP comparable to NP 75:25, respectively. TLRL always shows higher release rate than Ag, most likely due to its smaller size and more hydrophilic nature. NP are internalized by DC, whereas MP are not. We hypothesize that when administered *in vivo*, NP we formulated to

be taken up by APC as shown by others (Groettrup et al., *Jl* 2012, Zhang et al., *Biomaterials* 2011), leading to sustained intracellular release^{41,60}.

MP were inferior to NP in facilitating MHC class I cross-presentation of encapsulated Ag with both NP 50:50 and NP 75:25 performing similarly, irrespective of release kinetics. Our observations are strengthened by the report of Joshi et al., who observed that efficiency of particle uptake and up regulation of MHC class I and CD86 expression on BMDC was dependent on particle size. However, considering the big differences in release kinetics observed, caution should be taken to conclude if these observations are indeed only dependent on the size and not caused by the considerable difference in Ag and TLRL release properties of the particles, since the initial (burst) release accounted for nearly all of the total Ag and or TLRL release.

Vaccinations with NP led to considerably higher numbers of Ag-specific CD8⁺T cells compared to MP ($P = 0.01$) and IFA ($P = 0.04$), with almost no difference being observed between vaccination with MP and non-vaccinated mice (Figure 6.5). NP also performed better than IFA, suggesting that internalization of the particles may be of importance in inducing a stronger cellular immune response in comparison to sustained release from a local Ag depot.

Though observing a substantial difference in burst release, the initial difference between NP and MP eventually attenuates over time, as MP slowly release Ag and TLRL into the extracellular matrix. Co-encapsulation of OVA and TLRL has previously shown to induce anti-OVA (IgG) humoral responses, as well as polarization of the immune response^{36,61-63}. Vaccinations with NP 50:50 resulted in a more balanced T_H1/T_H2 antibody response characterized by similar titers of IgG1 and IgG2a (IgG1/IgG2a ≈ 1). In contrast, vaccinations with IFA led to a predominant T_H2 response (IgG1/IgG2a > 2), which might contribute to the differences in CD8⁺T cell responses detected after vaccinations. A predominant humoral TH2 response will likely be accompanied by a weak CD8⁺T cell response. A balance between type 1 and type 2 responses is accompanied by robust CD8⁺T cell response induction in our NP system. The higher production of IgG2a after particle vaccination is linked to the increased uptake by DC of particles encapsulating the protein and adjuvant⁶⁴, compared to soluble protein and (most likely also) Poly(I:C). In addition, direct stimulation of B cells by the particles compared might also promote better IgG2a responses compared to IFA-based vaccine formulations^{65,66}.

In conclusion, our results show that the ability of a DC to internalize PLGA-particles is a crucial factor when aiming to achieve effective MHC class I presentation and to elicit an

immune response against encapsulated and processed Ag. Furthermore, because of the superior responses induced in comparison to IFA, our data support the application of biodegradable PLGA-NP delivery systems as a substitute for mineral oil emulsions for the delivery of protein vaccines for cancer immunotherapy.

Acknowledgements

The authors thank Ahmed Allam for the contribution to particle formulation studies. This study was supported by grants from Immune System Activation (ISA) Pharmaceuticals and the Leiden University Medical Center.

References

1. Ada G 2005. Overview of vaccines and vaccination. *Mol Biotechnol* 29:255-272.
2. Arens R, van HT, van der Burg SH, Ossendorp F, Melief CJ 2013. Prospects of combinatorial synthetic peptide vaccine-based immunotherapy against cancer. *Semin Immunol*.
3. Melief CJM 2008. Cancer Immunotherapy by Dendritic Cells. *Immunity* 29:372-383.
4. Waeckerle-Men Y, Allmen EU, Gander B, Scandella E, Schlosser E, Schmidtke G, Merkle HP, Groettrup M Encapsulation of proteins and peptides into biodegradable poly(D,L-lactide-co-glycolide) microspheres prolongs and enhances antigen presentation by human dendritic cells.
5. Zhang H, Hong H, Li D, Ma S, Di Y, Stoten A, Haig N, Di GK, Yu Z, Xu XN, McMichael A, Jiang S 2009. Comparing pooled peptides with intact protein for accessing cross-presentation pathways for protective CD8+ and CD4+ T cells. *J Biol Chem* 284:9184-9191.
6. Kenter GG, Welters MJ, Valentijn AR, Lowik MJ, Berends-van der Meer DM, Vloon AP, Essahsah F, Fathers LM, Offringa R, Drijfhout JW, Wafelman AR, Oostendorp J, Fleuren GJ, van der Burg SH, Melief CJ 2009. Vaccination against HPV-16 oncoproteins for vulvar intraepithelial neoplasia. *N Engl J Med* 361:1838-1847.
7. Atanackovic D, Altorki NK, Stockert E, Williamson B, Jungbluth AA, Ritter E, Santiago D, Ferrara CA, Matsuo M, Selvakumar A, Dupont B, Chen YT, Hoffman EW, Ritter G, Old LJ, Gnjatic S 2004. Vaccine-induced CD4+ T cell responses to MAGE-3 protein in lung cancer patients. *J Immunol* 172:3289-3296.
8. Sabbatini P, Tsuji T, Ferran L, Ritter E, Sedrak C, Tuballes K, Jungbluth AA, Ritter G, Aghajanian C, Bell-McGuinn K, Hensley ML, Konner J, Tew W, Spriggs DR, Hoffman EW, Venhaus R, Pan L, Salazar AM, Diefenbach CM, Old LJ, Gnjatic S 2012. Phase I trial of overlapping long peptides from a tumor self-antigen and poly-ICLC shows rapid induction of integrated immune response in ovarian cancer patients. *Clin Cancer Res* 18:6497-6508.
9. Celis E 2007. Toll-like Receptor Ligands Energize Peptide Vaccines through Multiple Paths. *Cancer Research* 67:7945-7947.
10. Kasturi SP, Skountzou I, Albrecht RA, Koutsonanos D, Hua T, Nakaya HI, Ravindran R, Stewart S, Alam M, Kwissa M, Villinger F, Murthy N, Steel J, Jacob J, Hogan RJ, Garcia-Sastre A, Compans R, Pulendran B 2011. Programming the magnitude and persistence of antibody responses with innate immunity. *Nature* 470:543-547.
11. Heit A, Schmitz F, Haas T, Busch DH, Wagner H Antigen co-encapsulated with adjuvants efficiently drive protective T cell immunity.
12. Schlosser E, Mueller M, Fischer S, Basta S, Busch DH, Gander B, Groettrup M 2008. TLR ligands and antigen need to be coencapsulated into the same biodegradable microsphere for the generation of potent cytotoxic T lymphocyte responses. *Vaccine* 26:1626-1637.
13. Banchereau J, Steinman RM 1998. Dendritic cells and the control of immunity. *Nature* 392:245-252.

14. Steinman RM 2001. Dendritic cells and the control of immunity: enhancing the efficiency of antigen presentation. *Mt Sinai J Med* 68:160-166.
15. Melief CJ 2008. Cancer immunotherapy by dendritic cells. *Immunity* 29:372-383.
16. Steinman RM 2012. Decisions about dendritic cells: past, present, and future. *Annu Rev Immunol* 30:1-22.
17. Tacken PJ, de Vries IJ, Torensma R, Figdor CG 2007. Dendritic-cell immunotherapy: from ex vivo loading to in vivo targeting. *Nat Rev Immunol* 7:790-802.
18. Vitoriano-Souza J, Moreira N, Teixeira-Carvalho A, Carneiro CM, Siqueira FA, Vieira PM, Giunchetti RC, Moura SA, Fujiwara RT, Melo MN, Reis AB 2012. Cell recruitment and cytokines in skin mice sensitized with the vaccine adjuvants: saponin, incomplete Freund's adjuvant, and monophosphoryl lipid A. *PLoS One* 7:e40745.
19. Harris RC, Chianese-Bullock KA, Petroni GR, Schaefer JT, Brill LB, Molhoek KR, Deacon DH, Patterson JW, Slingluff CL, Jr. 2012. The vaccine-site microenvironment induced by injection of incomplete Freund's adjuvant, with or without melanoma peptides. *J Immunother* 35:78-88.
20. Mueller M, Schlosser E, Gander B, Groettrup M 2011. Tumor eradication by immunotherapy with biodegradable PLGA microspheres--an alternative to incomplete Freund's adjuvant. *Int J Cancer* 129:407-416.
21. Silva JM, Videira M, Gaspar R, Preat V, Florindo HF Immune system targeting by biodegradable nanoparticles for cancer vaccines.
22. Mundargi RC, Babu VR, Rangaswamy V, Patel P, Aminabhavi TM Nano/micro technologies for delivering macromolecular therapeutics using poly(D,L-lactide-co-glycolide) and its derivatives.
23. Newman KD, Elamanchili P, Kwon GS, Samuel J 2002. Uptake of poly(D,L-lactic-co-glycolic acid) microspheres by antigen-presenting cells in vivo. *J Biomed Mater Res* 60:480-486.
24. Putney SD, Burke PA Improving protein therapeutics with sustained-release formulations.
25. Rosalia RA, Silva AL, Camps M, Allam A, Jiskoot W, van der Burg SH, Ossendorp F, Oostendorp J 2013. Efficient ex vivo induction of T cells with potent anti-tumor activity by protein antigen encapsulated in nanoparticles. *Cancer Immunol Immunother*.
26. Badiie A, Davies N, McDonald K, Radford K, Michiue H, Hart D, Kato M 2007. Enhanced delivery of immunoliposomes to human dendritic cells by targeting the multilectin receptor DEC-205. *Vaccine* 25:4757-4766.
27. Zhang XQ, Dahle CE, Baman NK, Rich N, Weiner GJ, Salem AK Potent antigen-specific immune responses stimulated by codelivery of CpG ODN and antigens in degradable microparticles.
28. Link A, Zabel F, Schnetzler Y, Titz A, Brombacher F, Bachmann MF 2012. Innate immunity mediates follicular transport of particulate but not soluble protein antigen. *J Immunol* 188:3724-3733.
29. Manolova V, Flace A, Bauer M, Schwarz K, Saudan P, Bachmann MF 2008. Nanoparticles target distinct dendritic cell populations according to their size. *Eur J Immunol* 38:1404-1413.

30. Simon LC, Sabliov CM 2013. The effect of nanoparticle properties, detection method, delivery route and animal model on poly(lactic-co-glycolic) acid nanoparticles biodistribution in mice and rats. *Drug Metab Rev*.
31. Jain S, O'Hagan DT, Singh M The long-term potential of biodegradable poly(lactide-co-glycolide) microparticles as the next-generation vaccine adjuvant.
32. Oyewumi MO, Kumar A, Cui Z Nano-microparticles as immune adjuvants: correlating particle sizes and the resultant immune responses.
33. Kreutz M, Tacke PJ, Figdor CG 2013. Targeting dendritic cells: why bother? *Blood*.
34. Schliehe C, Redaelli C, Engelhardt S, Fehlings M, Mueller M, van RN, Thiry M, Hildner K, Weller H, Groettrup M 2011. CD8- dendritic cells and macrophages cross-present poly(D,L-lactate-co-glycolate) acid microsphere-encapsulated antigen in vivo. *J Immunol* 187:2112-2121.
35. Johansen P, Storni T, Rettig L, Qiu Z, Der-Sarkissian A, Smith KA, Manolova V, Lang KS, Senti G, Mullhaupt B, Gerlach T, Speck RF, Bot A, Kundig TM 2008. Antigen kinetics determines immune reactivity. *Proc Natl Acad Sci U S A* 105:5189-5194.
36. Joshi VB, Geary SM, Salem AK 2013. Biodegradable particles as vaccine delivery systems: size matters. *AAPS J* 15:85-94.
37. Fifis T, Gamvrellis A, Crimeen-Irwin B, Pietersz GA, Li J, Mottram PL, McKenzie IF, Plebanski M 2004. Size-dependent immunogenicity: therapeutic and protective properties of nano-vaccines against tumors. *J Immunol* 173:3148-3154.
38. Gutierrez I, Hernandez RM, Igartua M, Gascon AR, Pedraz JL 2002. Size dependent immune response after subcutaneous, oral and intranasal administration of BSA loaded nanospheres. *Vaccine* 21:67-77.
39. Silva AL, Rosalia RA, Sazak A, Carstens MG, Ossendorp F, Oostendorp J, Jiskoot W 2013. Optimization of encapsulation of a synthetic long peptide in PLGA nanoparticles: low-burst release is crucial for efficient CD8(+) T cell activation. *Eur J Pharm Biopharm* 83:338-345.
40. Tran KK, Shen H 2009. The role of phagosomal pH on the size-dependent efficiency of cross-presentation by dendritic cells. *Biomaterials* 30:1356-1362.
41. Shen H, Ackerman AL, Cody V, Giodini A, Hinson ER, Cresswell P, Edelson RL, Saltzman WM, Hanlon DJ 2006. Enhanced and prolonged cross-presentation following endosomal escape of exogenous antigens encapsulated in biodegradable nanoparticles. *Immunology* 117:78-88.
42. Winzler C, Rovere P, Rescigno M, Granucci F, Penna G, Adorini L, Zimmermann VS, Davoust J, Ricciardi-Castagnoli P 1997. Maturation stages of mouse dendritic cells in growth factor-dependent long-term cultures. *J Exp Med* 185:317-328.
43. Schuurhuis DH, Ioan-Facsinay A, Nagelkerken B, van Schip JJ, Sedlik C, Melief CJ, Verbeek JS, Ossendorp F 2002. Antigen-antibody immune complexes empower dendritic cells to efficiently prime specific CD8+ CTL responses in vivo. *J Immunol* 168:2240-2246.
44. Sanderson S, Shastri N 1994. LacZ inducible, antigen/MHC-specific T cell hybrids. *Int Immunol* 6:369-376.

45. Moore MW, Carbone FR, Bevan MJ 1988. Introduction of soluble protein into the class I pathway of antigen processing and presentation. *Cell* 54:777-785.
46. Sah H 1997. A new strategy to determine the actual protein content of poly(lactide-co-glycolide) microspheres. *J Pharm Sci* 86:1315-1318.
47. Rogo+ii-ç M, Mencer HJ, Gomzi Z 1996. Polydispersity index and molecular weight distributions of polymers. *European Polymer Journal* 32:1337-1344.
48. Khan S, Bijker MS, Weterings JJ, Tanke HJ, Adema GJ, van HT, Drijfhout JW, Melief CJ, Overkleef HS, van der Marel GA, Filippov DV, van der Burg SH, Ossendorp F 2007. Distinct uptake mechanisms but similar intracellular processing of two different toll-like receptor ligand-peptide conjugates in dendritic cells. *J Biol Chem* 282:21145-21159.
49. Braun M, Jandus C, Maurer P, Hammann-Haenni A, Schwarz K, Bachmann MF, Speiser DE, Romero P 2012. Virus-like particles induce robust human T-helper cell responses. *Eur J Immunol* 42:330-340.
50. Tacke PJ, Zeelenberg IS, Cruz LJ, van Hout-Kuijter MA, van de Glind G, Fokkink RG, Lambeck AJ, Figdor CG 2011. Targeted delivery of TLR ligands to human and mouse dendritic cells strongly enhances adjuvanticity. *Blood* 118:6836-6844.
51. O'Hagan DT, Singh M Microparticles as vaccine adjuvants and delivery systems.
52. Mottram PL, Leong D, Crimeen-Irwin B, Gloster S, Xiang SD, Meanger J, Ghildyal R, Vardaxis N, Plebanski M Type 1 and 2 immunity following vaccination is influenced by nanoparticle size: formulation of a model vaccine for respiratory syncytial virus.
53. Xiang SD, Scholzen A, Minigo G, David C, Apostolopoulos V, Mottram PL, Plebanski M Pathogen recognition and development of particulate vaccines: does size matter?
54. Mata E, Igartua M, Hernandez RM, Rosas JE, Patarroyo ME, Pedraz JL Comparison of the adjuvanticity of two different delivery systems on the induction of humoral and cellular responses to synthetic peptides.
55. van de Weert M, van 't Hof R, van der Weerd J, Heeren RM, Posthuma G, Hennink WE, Crommelin DJ Lysozyme distribution and conformation in a biodegradable polymer matrix as determined by FTIR techniques.
56. Yeo Y, Park K Control of encapsulation efficiency and initial burst in polymeric microparticle systems.
57. Zhang Y, Zale S, Sawyer L, Bernstein H Effects of metal salts on poly(DL-lactide-co-glycolide) polymer hydrolysis.
58. Leelarasamee N, Howard SA, Malanga CJ, Luzzi LA, Hogan TF, Kandzari SJ, Ma JK Kinetics of drug release from polylactic acid-hydrocortisone microcapsules.
59. Mansour HM, Sohn M, Al-Ghananeem A, Deluca PP Materials for pharmaceutical dosage forms: molecular pharmaceuticals and controlled release drug delivery aspects.

60. Cruz LJ, Tacke PJ, Fokkink R, Joosten B, Stuart MC, Albericio F, Torensma R, Figdor CG 2010. Targeted PLGA nano- but not microparticles specifically deliver antigen to human dendritic cells via DC-SIGN in vitro. *J Control Release* 144:118-126.
61. Pulendran B, Ahmed R 2011. Immunological mechanisms of vaccination. *Nat Immunol* 12:509-517.
62. Krishnamachari Y, Salem AK Innovative strategies for co-delivering antigens and CpG oligonucleotides.
63. Slutter B, Plapied L, Fievez V, Sande MA, des Rieux A, Schneider YJ, Van Riet E, Jiskoot W, Preat V Mechanistic study of the adjuvant effect of biodegradable nanoparticles in mucosal vaccination.
64. Joshi VB, Geary SM, Salem AK 2013. Biodegradable particles as vaccine delivery systems: size matters. *AAPS J* 15:85-94.
65. Kasturi SP, Skountzou I, Albrecht RA, Koutsonanos D, Hua T, Nakaya HI, Ravindran R, Stewart S, Alam M, Kwissa M, Villinger F, Murthy N, Steel J, Jacob J, Hogan RJ, Garcia-Sastre A, Compans R, Pulendran B 2011. Programming the magnitude and persistence of antibody responses with innate immunity. *Nature* 470:543-547.
66. Eckl-Dorna J, Batista FD 2009. BCR-mediated uptake of antigen linked to TLR9 ligand stimulates B-cell proliferation and antigen-specific plasma cell formation. *Blood* 113:3969-3977.

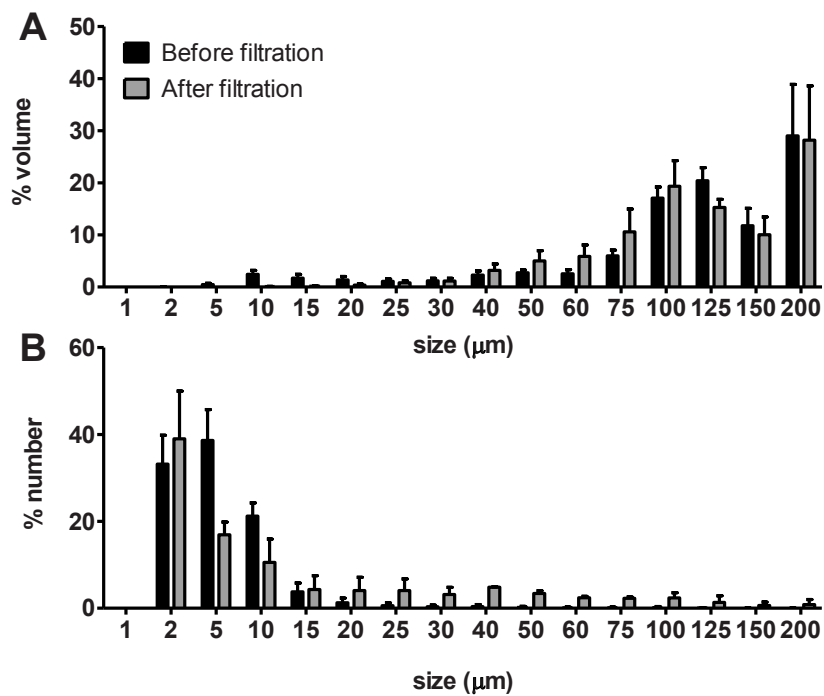
Supporting Information

Supporting Information Table S6.1 Distribution of MP diameters (μm) determined before (BF) and after filtration (AF) in terms of % of total particle numbers and of total particle volume. Mean diameter values calculated using the PAMAS PMA software are presented in the last row

Diameter (μm)	% Number		% Volume	
	BF	AF	BF	AF
1–2	33.2 \pm 6.7	39.0 \pm 11.0	0.0 \pm 0.0	0.0 \pm 0.0
2–5	38.6 \pm 7.1	16.9 \pm 2.9	0.5 \pm 0.3	0.0 \pm 0.0
5–10	21.2 \pm 3.0	10.5 \pm 5.4	2.4 \pm 1.4	0.1 \pm 0.1
10–15	3.7 \pm 2.1	4.3 \pm 3.2	1.7 \pm 1.2	0.1 \pm 0.1
15–20	1.3 \pm 1.0	4.0 \pm 3.1	1.4 \pm 1.1	0.4 \pm 0.3
20–25	0.6 \pm 0.6	4.1 \pm 2.7	1.1 \pm 0.8	0.8 \pm 0.7
25–30	0.3 \pm 0.4	3.2 \pm 1.7	1.2 \pm 0.9	1.2 \pm 0.9
30–40	0.4 \pm 0.5	4.8 \pm 0.1	2.3 \pm 1.4	3.2 \pm 2.1
40–50	0.2 \pm 0.2	3.4 \pm 0.6	2.7 \pm 0.9	5.0 \pm 3.5
50–60	0.1 \pm 0.1	2.4 \pm 0.3	2.5 \pm 1.4	5.9 \pm 3.8
60–75	0.1 \pm 0.1	2.2 \pm 0.3	6.0 \pm 1.9	10.6 \pm 7.6
75–100	0.2 \pm 0.2	2.4 \pm 1.2	17.1 \pm 3.7	19.3 \pm 8.5
100–125	0.1 \pm 0.1	1.4 \pm 1.5	20.4 \pm 4.3	15.3 \pm 2.7
125–150	0.0 \pm 0.0	0.6 \pm 0.8	11.8 \pm 5.7	10.0 \pm 5.9
150–200	0.0 \pm 0.0	0.8 \pm 1.1	29.0 \pm 17.1	28.2 \pm 18.1
Mean diameter	5 \pm 1.0	17 \pm 5.0	114 \pm 16.0	112 \pm 26.0

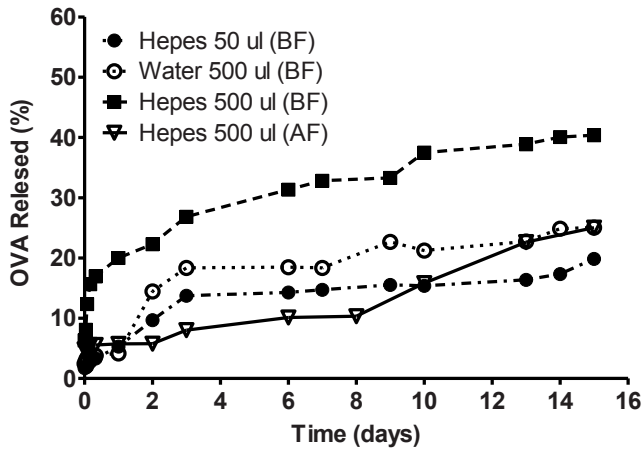
Supporting Information Table S6.2 OVA concentration sampled on the last day (day 30) of the release study. OVA concentration in supernatant (SN) was quantified by BCA assay and by fluorescence expressed as % of total encapsulated OV

Particles	BCA Assay (% in SN)	Fluorescence (% in SN)
PLGA 50:50 NP	82 \pm 14	85 \pm 14
PLGA 75:25 NP	53 \pm 10	52 \pm 9
PLGA 50:50 MP	48 \pm 10	40 \pm 3



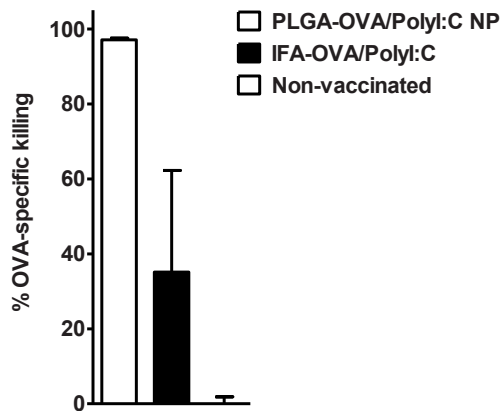
Supporting Information Figure S6.1 Size distribution of MP before filtration (BF) and after filtration (AF) determined by LO.

(A) Number distribution. (B) Volume distribution. Data are presented as average \pm standard deviation of $n = 3$ independent batches.



Supporting Information Figure S6.2 OVA release after filtration (AF) and before filtration (BF) of MP with different inner phase composition using PLGA 50:50 observed for 15 days.

Hepes 50 μ l (BF) (open diamonds) corresponds to an inner phase of 50 μ l of 20 mg/ml OVA solution in 25 mM Hepes pH 7.4; and Water 500 μ l (BF) (open triangles) to an inner phase of 500 μ l of 2 mg/ml OVA in water. Hepes 500 μ l (BF) (closed squares) and Hepes 500 μ l (AF) (closed circles) correspond to an inner phase of 500 μ l of 2 mg/ml OVA in 25 mM Hepes pH 7.4, before and after stirred-cell filtration, respectively.



Supporting Information Figure S6.3 PLGA-OVA/poly(I:C) NP induce cytotoxic CD8⁺ T cells *in vivo*.

In vivo cytotoxic capacity of primed OVA-specific T cells were determined in animals which received a single s.c. vaccinations with the 50 μ g OVA and 20 μ g poly(I:C) formulated in 50:50 PLGA-NP 50:50 or IFA. Vaccinated mice received CFSE-labeled SIINFEKL (specific) or ASNENMETM (control) short peptide loaded target cells (Ly5.1. splenocytes) 7 days after vaccination. Animals were sacrificed 18 hr later and the % target cells determined flow cytometry and calculated as described in M&M. Results shown are from one experiment and present averages \pm SEM from n = 5 mice per group.



Chapter 7

CD40-targeted dendritic cell delivery of PLGA-nanoparticle vaccine induce potent anti-tumor responses

Rodney A. Rosalia*, Luis Javier Cruz*, Suzanne van Duikeren, Angelino Tromp, Ana Luisa Silva, Wim Jiskoot, Tanja de Gruijl, Clemens Löwik, Jaap Oostendorp, Sjoerd H. van der Burg, Ferry Ossendorp

* Contributed equally to this study

Submitted for publication

Abstract

Dendritic cells (DC) play a prominent role in the priming of CD8⁺T cells. Vaccination is a promising treatment to boost tumor-specific CD8⁺T cells which is crucially dependent on adequate delivery of the vaccine to DC. Upon subcutaneous (s.c.) injection, only a small fraction of the vaccine is delivered to DC whereas the majority is cleared by the body or engulfed by other immune cells.

To overcome this, we studied vaccine delivery to DC via CD40-targeting using a multi-compound particulate vaccine with the aim to induce potent CD8⁺T cell responses. To this end, biodegradable poly(lactic-co-glycolic acid) nanoparticles (NP) were formulated encapsulating a protein Ag, Pam3CSK4 and Poly(I:C) and coated with an agonistic α CD40-mAb (*NP-CD40*). Targeting NP to CD40 led to very efficient and selective delivery to DC *in vivo* upon s.c. injection and improved priming of CD8⁺T cells against two independent tumor associated Ag. Therapeutic application of *NP-CD40* enhanced tumor control and prolonged survival of tumor-bearing mice.

We conclude that CD40-mediated delivery to DC of NP-vaccines, co-encapsulating Ag and adjuvants, efficiently drives specific T cell responses, and therefore, is an attractive method to improve the efficacy of protein based cancer vaccines undergoing clinical testing in the clinic.

Introduction

Dendritic Cells (DC) are the main antigen (Ag) presenting cells (APC) of the immune system ^{1,2} and their ability to orchestrate innate and adaptive immunity is widely being exploited to develop cancer immunotherapies ³. Immature DC have high endocytic capacity, express various intra- and extracellular pathogen recognition receptors, such as toll-like receptors (TLR), and continuously sample their surroundings for danger signals. TLR-triggering results in phenotypical changes, facilitated Ag processing, MHC presentation and increased cytokine production, a process termed DC maturation ⁴.

Therapeutic vaccinations against cancer are centered on the delivery of tumor associated Ag (TAA) to DC which then initiate Ag-specific T cell responses ^{5,6}. However, *in vivo* generation of robust anti-tumor cytotoxic CD8⁺ T cells (CTL) remains a major challenge. Targeted delivery of TAA to DC using nanoparticle (NP) vaccine carriers formulated with poly(lactic-co-glycolic acid) (PLGA) is an attractive approach to enhance specific T cell responses. PLGA NP can be formulated to encapsulate protein ⁷ or short- ⁸ and long-peptide ⁹ Ag encoding TAA and TLR ligands (TLRL) ¹⁰. Encapsulation of Ag in NP facilitates MHC Ag presentation ⁸ and *in vivo* anti-tumor T cell responses compared to soluble Ag ¹¹. Encapsulation of Ag in NP facilitates MHC Ag presentation and *in vivo* anti-tumor T cell responses compared to soluble Ag.

Due to their physical characteristics, NP are prone to be internalized by scavenger cells, such as macrophages (M ϕ), which offer poor T cell priming capacity compared to DC. Protection from nonspecific uptake is achieved by pegylation of NP which also prolongs the *in vivo* half-life ¹². Pegylated NP can be specifically (re-)targeted to DC by additional surface modifications which is suggested to enhance *in vivo* T cell responses. Indeed, C-type lectin specific antibodies coated to PLGA-PEG NP ^{13,14} but also compounds such as protamine and mannose coated to the PLGA-NP surface core ^{15,16} have been shown to improve *in vitro* binding and internalization by DC and promote better T cell responses. However, no direct evidence was provided in these studies for selective DC-targeting and improved delivery of the vaccine to DC *in vivo*.

Facilitating *in vivo* delivery of PLGA-NP-vaccines to DC via CD40 and the resulting vaccine induced T cell responses is the subject of this study. CD40 is a tumor necrosis factor-receptor family cell surface receptor highly expressed on DC. CD40/CD40L ligation plays a crucial role in the maturation of DC into fully competent APC and is a key signal for CD4⁺ T helper dependent CD8⁺ T cell priming ^{17,18}. Moreover, targeting soluble Ag via CD40 using antibody

constructs was shown to facilitate the internalization of Ag into early-endosomes¹⁹, intracellular compartments associated with efficient MHC class I Ag cross-presentation, and promotes tumor-specific T cell responses²⁰.

In this study, we evaluated CD40-targeting of a particulate Ag, by formulating PLGA-NP co-encapsulating ovalbumin protein, the adjuvants Pam3Csk4 (TLR2L) and Poly(I:C) (TLR3L), as well as the murine α CD40-mAb FGK45¹⁷ coupled to the NP-surface, PLGA(-Ag/TLR2+3L)- α CD40 (*NP-CD40*).

We report here, that *NP-CD40* administered as a vaccine displays selective and improved capacity to deliver Ag to DC *in vivo*, over other APC, and better DC maturation in comparison to non-targeted NP-vaccines. Vaccinations with *NP-CD40* resulted in the priming of robust Ag-specific CD8⁺ T cells with the capacity to control tumor growth and prolong survival of tumor-bearing animals.

Material and methods

Animals

C57BL/6 (CD45.2/Thy1.2; H-2^b) mice were obtained from Charles River Laboratories. Ly5.1/CD45.1 (C57BL/6 background), CD40 KO (C57BL/6 background), transgenic OT-I/Thy1.1/CD45.2 (specific for the OVA₂₅₇₋₂₆₄ CTL epitope presented by H2-K^b) and transgenic OT-II/Ly5.1/CD45.1 mice (specific for the OVA₃₂₃₋₃₃₉ Th epitope presented by I-A^b) were bred in the specific pathogen-free animal facility of the Leiden University Medical Center. All animal experiments were approved by the animal experimental committee of Leiden University.

DC and cell lines

Mouse BMDC were cultured published previously¹⁸. In brief, Freshly isolated mouse bone marrow (BM) cells from WT C57BL/6 mice or CD40 KO femurs were and cultured for 10 days in medium supplemented with GM-CSF (50 ng/ml). After 10 days of culture, large numbers of typical DC were obtained which were at least 90% positive for murine DC marker CD11c (data not shown). D1 cells, a GM-CSF dependent immature dendritic cell line were cultured as described before²¹. OVA-transfected B16 tumor cell line (B16-OVA), syngeneic to the C57BL/6 strain, was cultured as described previously²².

Preparation and characterization of targeted PLGA-NP

PLGA-NP (Ag/TLRL)-mAb were formulated encapsulating a model protein Ag and in combination with TLR2L (Pam3Csk4) and/or TLR3L (Poly(I:C)) using double-emulsion and solvent evaporation technique as previously described²⁰. PLGA-NP was coated with mAbs, murine agonistic α CD40 mAb, FGK45 and mouse IgG2a Isotype control respectively, essentially as described before²³. In brief, 100 mg of PLGA in 2 mL of ethyl acetate containing OVA antigen free from endotoxin (10 mg) and/or Poly(I:C) (InvivoGen) (4 mg) and/or Pam3CSK4 (InvivoGen) (1 mg) were emulsified under sonification (Branson, sonifier 250) during 60 seconds. This first emulsion was rapidly added to 1 mL of 1% polyvinyl alcohol/7% ethyl acetate in distilled water during 15 second. A combination of pegylated lipids (DSPE-PEG(2000) succinic acid (6 mg) and mPEG 2000 PE (6 mg)) were dissolved in chloroform and added to the vial. The chloroform was removed by a stream of nitrogen gas. Subsequently, the emulsion was rapidly added to the vial containing the lipids and the solution was homogenized during 30 seconds using a sonicator. This solution was added to 100 mL of 0.3% PVA/7% of ethyl acetate in distilled water and stirred overnight to evaporate ethyl acetate. The PLGA-NP were collected by centrifugation at 12000 x g for 10 min, washed four times with distilled water and lyophilized. Next, mAbs was covalently coupled to 10 mg of PLGA-NP by activating surface carboxyl groups in isotonic 0.1 M MES buffer pH 5.5 containing 1-ethyl-3-[3-dimethylaminopropyl] carbodiimide hydrochloride (10 equiv.) and N-hydroxysuccinimide (10 equiv.) for 1 h. Mouse IgG2a Isotype control (Clone:C1.18.4 Catalog #:BE0085) was purchased from Bio X Cell Antibody Production and Purification. The activated carboxyl-PLGA-NP was washed one time with MES buffer by centrifugation. Subsequently, mAbs (200 μ g per mg NP) were added and the suspension was stirred during 3 h at room temperature and later overnight at 4°C. Unbound antibodies were removed by centrifugation (12000 x g, during 10 min) and the PLGA-NPs-mAbs was washed four times with PBS. The presence of Abs on the particle surface was determined by Coomassie dye protein assay. Physicochemical characteristics of formulated NP are summarized in Table 7.1.

Dynamic light scattering and zeta-potential measurements

Dynamic light scattering (DLS) measurements were taken on different PLGA-NP using an ALV light-scattering instrument equipped with an ALV5000/60X0 Multiple Tau Correlator and an Oxixus SLIM-532 150 mW DPSS laser operating at a wavelength of 532 nm. A

Table 7.1 Physicochemical characteristics of formulated PLGA-NP

Samples	Poly(I:C) Pam3Csk4 ($\mu\text{g}/\text{mg NP}$) (w/w)	Ag ($\mu\text{g}/\text{mg NP}$) (w/w)	Nanoparticles dm \pm S.D. (nm)	Polydispersity index \pm S.D.	Zeta potential \pm S.D. (mV)	Coated mAb ($\mu\text{g}/\text{mg PLGA-NP}$)
PLGA-(OVA)-IgG2a	---	40.0	240.6 \pm 13.5	0.136 \pm 0.053	-35.4 \pm 6.2	23.0 \pm 2.9
PLGA-(OVA)- α CD40	---	40.0	233.7 \pm 8.3	0.139 \pm 0.045	-31.2 \pm 5.2	29.1 \pm 3.1
PLGA-(OVA/TLR3L)-Ig2a	15.0	55.1	198.2 \pm 12.9	0.085 \pm 0.016	-33.6 \pm 5.5	32.0 \pm 3.2
PLGA-(OVA/TLR3L)- α CD40	15.0	55.1	194.7 \pm 11.6	0.148 \pm 0.068	-30.0 \pm 4.6	25.0 \pm 3.7
PLGA-(OVA/TLR2L)-Ig2a	4	64	192.1 \pm 11.3	0.097 \pm 0.046	-32.2 \pm 2.5	34.0 \pm 2.4
PLGA-(OVA/TLR2L)- α CD40	4	64	195.4 \pm 14.3	0.122 \pm 0.049	-31.0 \pm 4.6	29.0 \pm 3.2
PLGA-(OVA/TLR2+3L)-Ig2a	45 4	60	241.4 \pm 16.7	0.159 \pm 0.033	-36.3 \pm 1.6	35.0 \pm 3.1
PLGA-(OVA/TLR2+3L)- α CD40	45 4	60	242.3 \pm 25.0	0.167 \pm 0.031	-38.5 \pm 1.7	32.0 \pm 2.2
PLGA-(OVA-Alexa647/TLR2+3L)-Ig2a	16 4	12	212.2 \pm 10.4	0.121 \pm 0.027	-31.4 \pm 2.3	34.5 \pm 3.2
PLGA-(OVA-Alexa647/TLR2+3L)- α CD40	16 4	12	209.8 \pm 11.1	0.114 \pm 0.022	-32.2 \pm 2.8	31.3 \pm 1.8
PLGA-(HPV-E7/TLR2+3L)-Ig2a	15 4	12	239 \pm 13.6	0.234 \pm 0.072	-29.6 \pm 1.8	34.4 \pm 1.4
PLGA-(HPV-E7/TLR2+3L)- α CD40	15 4	12	246 \pm 16.1	0.204 \pm 0.062	-28.5 \pm 2.1	29.0 \pm 1.9

refractive index matching bath of filtered cis-decalin surrounded the cylindrical scattering cell, and the temperature was controlled at 21.5 ± 0.3 °C using a Haake F3-K thermostat. In each sample, the $g_2(\tau)$ auto-correlation function was recorded ten times at a detection angle of 90°. For each measurement, the diffusion coefficient (D) was determined by using the second-order cumulant, and the corresponding PLGA-NP diameter was calculated assuming that the PLGA-NP were spherical in shape. Zeta potential measurements were performed on PLGA-NP using a Malvern ZetaSizer 2000 (UK).

Quantifying encapsulated OVA in NPs

OVA-protein encapsulating efficiency was determined after hydrolyzing 5 mg PLGA-NPs in 0.5 mL 0.8 M NaOH overnight at 37°C. The OVA-protein content was then measured using Coomassie Plus Protein Assay Reagent (Pierce) according to the manufacturer's protocol. OVA encapsulation efficiency was calculated by dividing the measured amount of encapsulated Ag by the theoretical amount assuming all was encapsulated.

Quantifying encapsulated TLR ligands

Biodegradable PLGA-NP was hydrolyzed with 0.8 M NaOH overnight at 37°C. The encapsulation efficiency of Poly(I:C) was determined by reversed-phase high-performance liquid chromatography (RP_HPLC) and was also determined by UV spectrometry using a Nanodrop system (Thermo Scientific). Poly(I:C) was assayed by RP-HPLC at room temperature using a Shimadzu system (Shimadzu Corporation, Kyoto, Japan) equipped with a reversed-phase Symmetric C18 column (250 mm x 4.6 mm). The flow rate was fixed at 1 mL/min and detection was obtained by UV detection at 254 nm. A linear gradient of 0% to 80% of acetonitrile (containing 0.036% trifluoroacetic acid) in water (containing 0.045% trifluoroacetic acid) was used for Poly(I:C). The retention time of the Poly(I:C) was approximately 20 min. The regression analysis was constructed by plotting the peak–area ratio of Poly(I:C) versus concentration. The calibration curves were linear within the range of 2.5 µg to 150 µg for Poly(I:C). The correlation coefficient (R^2) was greater than 0.99.

Analysis of *in vitro* NP-association with DC

WT C57BL/6 or CD40 KO BMDC (100,000/well) were plated into a 96-well flat bottom plate and incubated for 1 hr at either 4°C (binding analysis) or 37°C (uptake analysis) with titrated

amounts of CD40-targeted or non-targeted (PLGA-Ag/TLR2+3L)-PEG-mAb formulations labeled with the near infrared dye (near-IR dyes, CW800). Cells were washed twice to remove residual non-bound NP. Binding and uptake of PLGA-NP by DC was determined based on near-IR fluorescence using odyssey equipment (LI-COR) at 800 nm. Data analyses were corrected for the number of amount cells per measurement via co-staining with TO-PRO® (Invitrogen) at 700 nm.

Analysis of *in vivo* NP-uptake by immune cells

Animals were vaccinated with the CD40-targeted or non-targeted (PLGA-Ag/TLR2+3L)-PEG-mAb formulations containing OVA-Alexa647 (Invitrogen) by subcutaneous (s.c.) injection into the right flank. *In vivo* NP-uptake by cells was analyzed 24 or 48 hr after vaccination by sacrificing the animals and isolating the inguinal lymph nodes. Single cell suspensions were prepared and flow cytometry was used to determine the fluorescence intensity of OVA-Alexa647 in F4/80-CD11b⁺CD11c⁺ DC and CD19⁺B220⁺ B cells as a measure for NP-uptake. All fluorescent-mAb used for staining were purchased from BD Pharmingen. Flow cytometry was performed using a LSRII (BD Pharmingen) and data analyzed with FlowJo software (Treestar).

***In vitro* MHC class II-restricted Ag presentation and T cell priming**

DC were incubated for 5 hr with the various (PLGA-Ag/TLRL)-mAb formulations at the indicated OVA concentrations. After incubation, supernatants were harvested and cells were then further co-cultured for 72 hr in the presence of OT-II splenocytes to assess OVA-specific MHC class II-restricted proliferation of naïve CD4⁺ T cells. Cells were pulsed with [³H]-thymidine for the last 16 hours of culture. Samples were then counted on a TopCount™ microplate scintillation counter (Packard Instrument Co., Meridan, CT, USA). Stimulation index was used as a measure for proliferation and was calculated as the fold increase of [³H]-thymidine CPM over the CPM counts obtained with medium as negative control.

Analysis of cytokine production by DC or T cells using Enzyme-linked Immunosorbent Assay (ELISA)

DC (100,000/well) were plated into a 96-well round bottom plate and incubated for 24 hr with titrated amounts of Ag. Supernatants were harvested and tested for IL-12 p70 by ELISA (BD OptEIA™ MOUSE IL-12 Cat. Nr 555256) following the manufacturer's instructions.

Vaccination and immunization schemes

Animals were vaccinated with the various targeted or non-targeted NP formulations (Table 7.1) by s.c. injection into the right flank. *In vivo* priming of cytotoxic CD8⁺ T cells was studied 1 week post-vaccination by transferring splenocytes prepared from congenic Ly5.1 C57BL/6 animals which were pulsed with the SIINFEKL (OVA₈/specific target cells) or ASNENMETM (FLU9/non-specific target cells) short peptide. The target cells were labeled with either 10 μM (OVA) or 0.5 μM (Flu) CFSE mixed 1:1 and 10⁷ total cells were injected intravenously (i.v.) into vaccinated animals. 18 hr post transfer of target cells, animals were sacrificed and single cell suspensions were prepared from isolated spleens. Injected target cells were distinguished by APC-conjugated rat anti-mouse CD45.1 mAb (BD Pharmingen). *In vivo* cytotoxicity was determined by flow cytometry using the following formula: $(1 - [(CFSE\text{-peak OVA}/CFSE\text{-peak FLU})^{\text{vaccinated animals}} \times (CFSE\text{-peak OVA}/CFSE\text{-peak FLU})^{\text{non-vaccinated animals}}]) \times 100\%$. Vaccine efficacy against the HPV-E7 oncoprotein was determined in blood of TC-1 tumor bearing mice (60000/TC-1 cells per mice inoculated s.c. in the left flank). Mice were vaccinated on day 7 with 15 μg HPV-E7 protein encapsulated in CD40-targeted NP, control formulations or in soluble form and HPV-E7 -specific CD8⁺ T cell responses were measured by quantification via flow cytometry of RAHYNIVTF/H2-D^b-TM (APC-labeled) positive CD8⁺ T cells co-stained with AF-conjugated anti-mouse CD8α mAb and V500-conjugated rat anti-mouse CD3 mAb.

Tumor challenge

Therapeutic and prophylactic vaccine capacity of CD40-targeted NP and relevant controls were studied by analyzing their efficiency to induce anti-tumor immune responses. For prophylactic tumor challenges mice were vaccinated s.c. in the right flank and seven days later OVA-expressing melanoma cells (B16-OVA) were inoculated s.c. on the opposite flank. Tumor size (mm³) was calculated by $(\text{length}) \times (\text{width}) \times (\text{length} + \text{width}/2)$. Animal survival was then followed and mice were sacrificed when humane end-points were met as described in Code of practice for animal experiments in oncological related research (*Code of practice dierproeven in het kankeronderzoek*).

To assess the therapeutic capacity of CD40-targeted NP we inoculated 2×10^5 B16-OVA melanoma cells s.c. in the right flank of WT C57BL/6 mice. On day 7 and day 17 post tumor inoculation, mice were s.c. vaccinated with 10 μg of OVA encapsulated in PLGA-(OVA/TLR2+3L)-αCD40 and PLGA-(OVA/TLR2+3L)-IgG2a NP (12 mice per group) on the opposite

flank. Tumor growth was measured 1–3 times a week and survival was monitored daily. Tail vein blood samples were collected on day 14 after tumor challenge. Blood samples were prepared by erythrocyte lysis, followed by 2 washing steps with PBA buffer. OVA-specific CD8⁺ T cells were analyzed by co-staining with APC-conjugated SIINFEKL/H2-K^b tetramers (TM), AF-conjugated anti-mouse CD8 α mAb and V500-conjugated rat anti-mouse CD3 mAb. All fluorescent-antibodies used for staining were purchased from BD Pharmingen and the APC-SIINFEKL/H2-Kb tetramers were produced in house. Flow cytometry analysis was performed as described above.

Statistical analysis

Graph Pad Prism software version 5 was used for statistical analysis. Two-way analysis of variance (ANOVA) tests were used to evaluate cytokine production by DC or T cells across different concentrations of PLGA-(OVA/TLR)-mAb and to analyze differences in *in vitro* binding/uptake studies. The differences in OVA-Alexa647 fluorescence upon *in vivo* uptake by immune cells were analyzed using the two-tailed unpaired Students t test or Mann Whitney test. Dose-response *in vitro* studies were analyzed using two-way ANOVA with Bonferroni posttests. Differences in animal survival were calculated using Log-rank (Mantel-Cox) test. Statistical significance was considered when $P < 0.05$.

RESULTS

Coupling of α CD40-mAb to NP improves binding and internalization by DC *in vitro* and *in vivo*

The efficiency of targeting via CD40 was analyzed by determining the efficacy of binding and internalization of NP by DC. Two types of formulations were compared and unless otherwise stated PLGA-(Ag/TLR2+3L)- α CD40 NP are referred to as *NP-CD40* and PLGA-(Ag/TLR2+3L)-IgG2a (NP) as *NP-Iso* (IgG2a-isotype control mAb coated NP). DC were incubated for 1 hr with fluorescently labeled NP at 4°C (binding) and 37°C (internalization). Coupling of the α CD40-mAb significantly improved the association of NP with DC compared to isotype control mAb (Figure 7.1). The effect of CD40-targeting was also observed in a mixed cell culture. *NP-CD40* added to spleen single cell suspensions *in vitro* were internalized better by DC than B cells (Supporting Information Figure S7.1). But F4/80⁺CD11b⁺CD11c⁻ M ϕ showed poor capacity to take up NP, irrespective of targeting (data not shown).

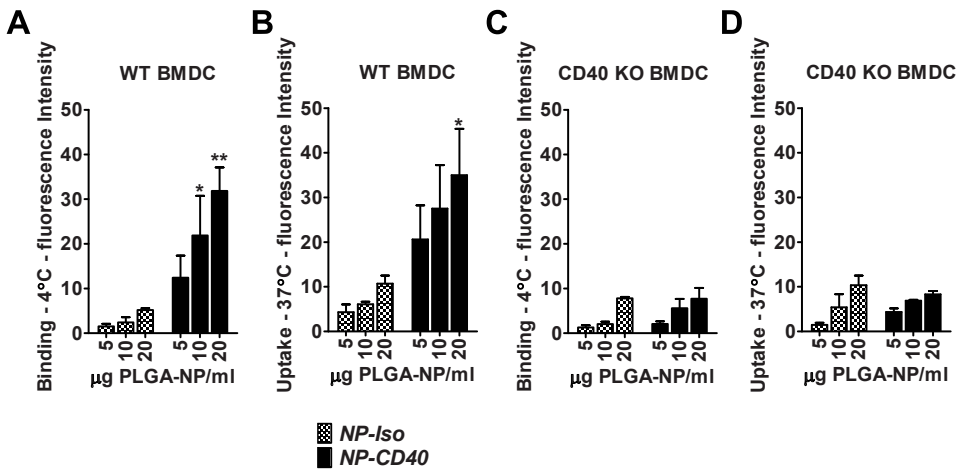


Figure 7.1 DC more efficiently binds and internalizes NP-CD40 compared to NP-Iso.

WT BMDC were incubated with titrated amounts of NP-CD40 or NP-Iso for 1 hr at 4°C to study binding (A) or 37°C for uptake (B) followed by extensive washing with medium to remove unbound NP. CD40-mediated binding and uptake of NP was tested CD40 KO BMDC (C & D). Fluorescence intensity was measured by scanning on the Odyssey® and results shown are mean fluorescence intensities of a duplicate analysis + deviation. Data are from one out of two independent experiments performed with two different batches of NP. Differences in NP-binding and uptake were analyzed applying two-way ANOVA with Bonferroni posttests, * = $P < 0.05$ or *** = $P < 0.0001$.

The *in vivo* uptake was examined by injecting mice s.c. in the flank with NP-CD40 or NP-Iso and the draining inguinal lymph node (LN) excised 48 hr later. Higher amounts of NP-CD40 were taken up by CD11c⁺CD11b⁺F4/80⁻ DC than NP-Iso (Figure 7.2A). In addition, the LN contained significantly higher numbers of NP⁺ DC when NP-CD40 were injected (Figure 7.2B). CD19⁺B220⁺ B cells also internalized NP-CD40 although to a lesser extent than DC (Figure 7.2C and 7.2D). Control injections of NP-Iso mixed with same amount of soluble anti-CD40 showed the necessity of coating the αCD40-mAb to the NP surface. In summary, CD40-targeting of NP improves binding and uptake and facilitates efficient *in vivo* delivery of NP to DC.

Enhanced maturation of DC via CD40-targeted delivery of TLR2 and TLR3 ligands encapsulated in PLGA-NP

The potency of various NP formulations (Table 7.1) to activate DC was studied *in vitro* by analyzing the cell-surface expression of the T cell co-stimulatory molecules CD86 and

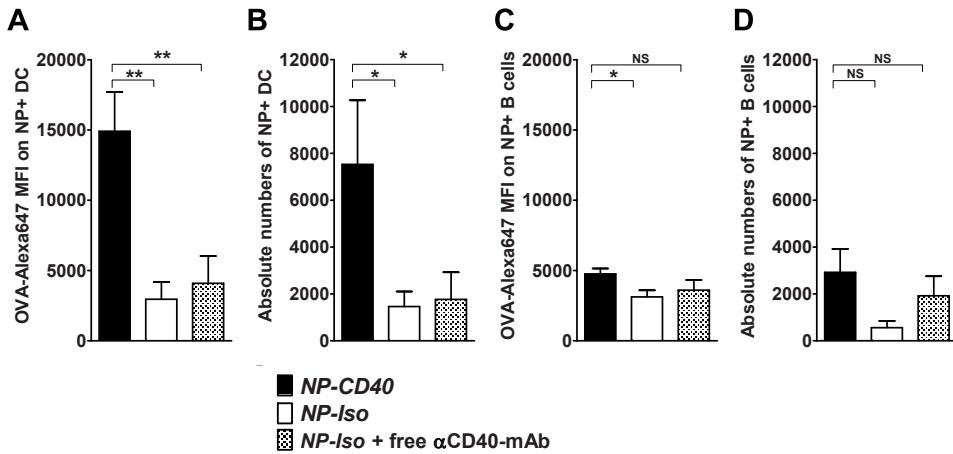


Figure 7.2 NP-CD40 are better targeted *in vivo* to and internalized by DC upon s.c. injection.

WT mice were injected s.c. in the right flank with *NP-CD40* or *NP-Iso* encapsulating 10 μ g OVA-Alexa647 or NP-Iso mixed with soluble α CD40. After 48 hr mice were sacrificed and single-cell suspensions prepared from the inguinal LN and stained with fluorescent DC-specific mAb. The different immune cell populations positive for Alexa-647 fluorescence were distinguished by flow cytometry. The absolute numbers of NP⁺ CD11c⁺CD11b⁺F4/80⁺ DC were calculated and the results shown are averages \pm SEM of two independent experiments using 3–5 mice per group (A). Relative amount of particles internalized per cell was based on the Alexa-647 MFI on the NP⁺ DC and values depicted as mean \pm SEM (B). NP⁺ CD19⁺B220⁺ B cells (C) and MFI on the NP⁺ B cells (D) were quantified. The Mann Whitney or the unpaired student's test was used to compare the absolute numbers of NP⁺ cells after vaccinations with *NP-CD40* and *NP-Iso* and the resulting MFI on NP⁺ cells, * = $P < 0.05$ & ** = $P < 0.01$.

CD40 on DC and the capacity of these cells to produce IL-12. The strongest DC maturation resulted from incubation with *NP-CD40* as reflected by the highest production of IL-12, (Figure 7.3A), but also by IL-6 and IL-2 production (data not shown) and the enhanced surface expression of CD86 and CD40 (Figure 7.3B & C). At the concentrations tested, single formulations of (PLGA-Ag/TLRL)-mAb NP containing either Pam3Csk4, Poly(I:C) or FGK45 showed poor (FGK45 & TLR2L), or low (Poly(I:C)) capacity to activate DC compared to NP formulations co-encapsulating Pam3Csk4 and Poly(I:C) (Supporting Information Figure S7.2). Coupling of the α CD40-mAb to NP encapsulating TLRL appeared to be essential to achieve the synergistic activation of DC as *NP-Iso* mixed with soluble (free) α CD40-mAb showed lower potency compared to *NP-CD40* (Figure 7.3D). Furthermore, DC incubated

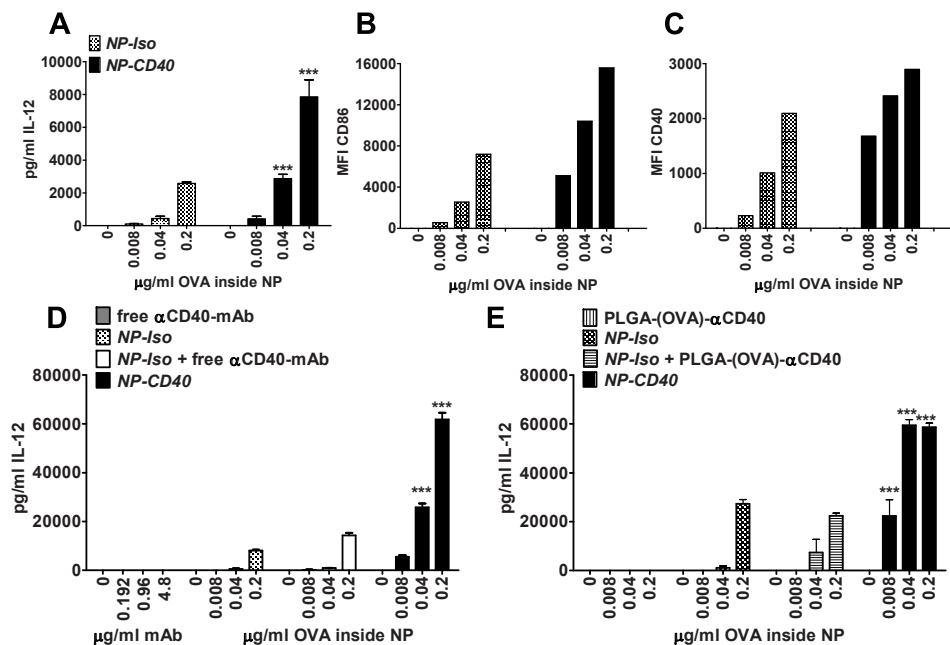


Figure 7.3 CD40-targeted PLGA-(Ag/TLR2+3L) NP show superior capacity to mature DC compared to non-targeted NP.

WT BMDC (100,000 cells/well) were incubated with titrated amounts of *NP-CD40* or *NP-Iso* for 24 hr at 37°C. Culture supernatants were harvested and the amount of IL-12 determined by ELISA (A). Post-incubation, DC were stained with fluorescent antibodies against CD86 (B) and CD40 (C) followed by Flow Cytometry analysis. IL-12 was determined in culture supernatants after 24 hr incubation of DC with *NP-CD40*, *NP-Iso* and control formulations of *NP-Iso* mixed with soluble αCD40 mAb (D) or PLGA-(OVA)-αCD40 NP (E). Differences in cytokine production were analyzed applying two way ANOVA with Bonferroni posttests, *** = $P < 0.001$.

with mixtures of *NP-Iso* with PLGA-(Ag)-αCD40 NP (lacking both TLR ligands) did not induce DC maturation to a similar extent as *NP-CD40* (Figure 7.3E). No DC maturation was induced by NP formulations encapsulating just OVA, independent of CD40-targeting (data not shown). We tested up to 25-fold higher amounts of soluble OVA compared to the amount encapsulated in NP, either alone or in combination with TLR and αCD40-mAb but observed no additive stimulatory effect on DC maturation (data not shown). In summary, we show that CD40-targeted delivery of NP, co-encapsulating Poly(I:C) and Pam3Csk4, synergistically enhances DC maturation in contrast to non-targeted NP containing the same Ag/TLRL cargo.

Improved CD4⁺ T cell proliferation and IFN- γ production by NP-CD40

We studied if DC loaded with NP-CD40 resulted in efficient MHC class II Ag processing and activation of naïve CD4⁺ T cells *in vitro*. In line with the previous results, OVA-specific CD4⁺ T cells proliferated better but especially produced significantly higher amounts of IFN- γ when primed by DC loaded with NP-CD40 compared to stimulation by NP-Iso loaded DC (Figure 7.4). In conclusion, CD40-targeted delivery to DC of Pam3Csk4 and Poly(I:C) co-encapsulated with protein Ag in NP, also facilitates MHC class II presentation and enhances effector CD4⁺ T cell functionality. DC loaded with NP-CD40 and NP-Iso both had potent APC capacity resulting in similar proliferation and IFN- γ production by naïve CD8⁺ T cells *in vitro* (data not shown).

Vaccination with NP-CD40 improves CD8⁺ T cell responses

The quantity and quality of TAA-specific CD8⁺ T cells are important determinants for a robust anti-tumor immune response. Enhancing CD8⁺ T cell responses in the presence

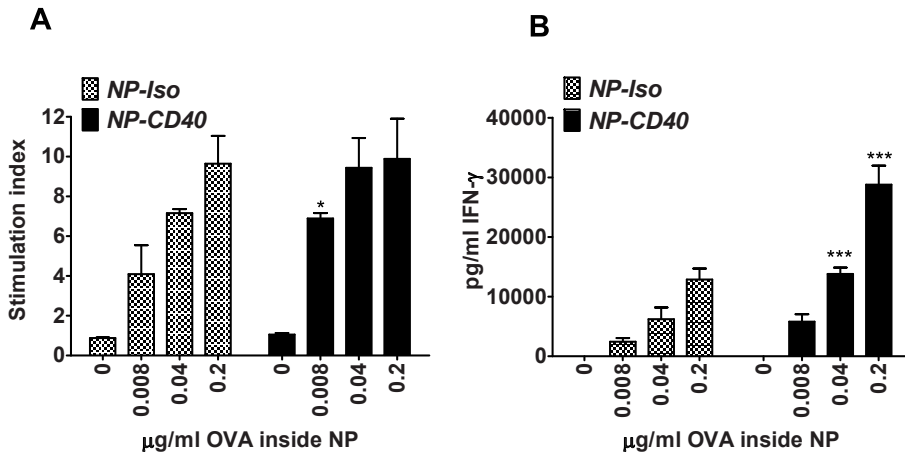


Figure 7.4 DC loaded with NP-CD40 have improved APC-capacity to stimulate CD4⁺ T cell proliferation and IFN- γ production.

BMDC from C57BL/6 were incubated with titrated amounts of NP-CD40 or NP-Iso for 5 hr at 37°C. After incubation with Ag, 75% of the culture medium was removed and splenocytes from OT-II mice added (200000 splenocytes/200 μ l/well). OVA-specific CD4⁺ T cell proliferation was analyzed 72 hr later by analysis of [³H]-thymidine incorporation which was added in the final 16 hours of culture (A). Samples were taken after 48 hr of co-culture between Ag-loaded DC and OT-II splenocytes and analyzed for IFN- γ levels (B). Differences in CD4⁺ T cell proliferation and cytokine production were analyzed using the two way ANOVA with Bonferroni posttests, * = P < 0.5 and *** = P < 0.0001.

of a tumor is a crucial merit of therapeutic vaccines. Therefore, to study how *NP-CD40* modulate an ongoing anti-tumor CD8⁺ T cell response we collected blood samples of tumor-bearing animals 7 days after vaccination. *NP-CD40* significantly boosted the %

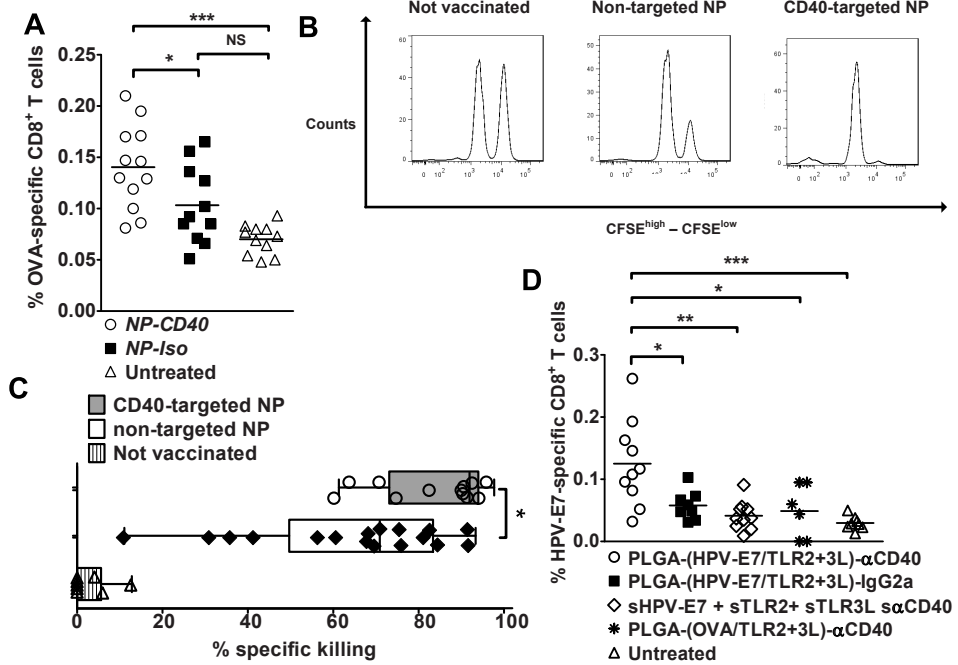


Figure 7.5 Vaccinations with *NP-CD40* prime CD8⁺ T cells with improved cytotoxic capacity compared to *NP-Iso*.

Tail vein blood samples were taken on day 14 post-tumor inoculation from tumor bearing mice which received vaccinations with either *NP-CD40* or *NP-Iso*. Blood samples were prepared as stated in M&M and stained with SIINFEKL-Tetramers to determine OVA-specific CD8⁺ T cells by FACS (**A**) WT mice were vaccinated s.c. with 10 μg OVA encapsulated in CD40-targeted PLGA-(Ag/TLR2+3L) NP or non-targeted PLGA-(Ag/TLR2+3L) control NP in the right flank. On day 7 day post vaccination, SIINFEKL-loaded CFSE^{high} OVA-specific target cells and ASNENMETM-loaded CFSE^{low} INFLUENZA-specific target cells (negative controls) were injected i.v. in a 1:1 ratio and mice sacrificed 18 hr later to determine the degree of OVA-specific lysis of the target cells (**B**). The average % OVA-specific target cell killing, of 3 independent experiments, was quantified as described in M&M (**C**). TC-1 tumor-bearing mice were vaccinated on day 7 with NP-formulations encapsulating 15 μg HPV-E7 protein and TLR or soluble protein/TLR mixture. On day 15, tail vein blood samples were collected and the % of RAHYNIVTF/H2-D^b specific CD8⁺ T cells determined (**D**). Differences in % of Ag specific CD8⁺ T cells and *in vivo* killing or target cells were analyzed applying the Mann Whitney tests, * = P < 0.05.

of TAA-specific CD8⁺ T cells compared to *NP-Iso* vaccinated and untreated mice (Figure 7.5A). Ag-specific CD8⁺ T cells after vaccination of naïve animals with *NP-CD40* showed strong *in vivo* cytotoxic capacity (Figure 7.5B), which resulted in efficient killing of target cells (Figure 7.5C). Similarly, CD40-targeted NP encapsulating HPV-E7 protein significantly enhanced RAHYNIVTF-specific CD8⁺ T cells in blood after a single vaccination compared to non-targeted NP formulations or a mixture of soluble HPV-E7-protein and adjuvants. Encapsulation of specific Ag in CD40-targeted NP was required for the observed T cell priming as TLR and an irrelevant protein targeted to CD40 failed to boost HPV-E7 specific responses (Figure 7.5D). NP formulations with no or only one TLR were inferior vaccines as compared to *NP-CD40* (Supporting Information Figure S7.3). These observations show significant improvement of CD8⁺ T cell quantity and functional quality via CD40-targeted NP-vaccines.

CD40-targeting of NP improves anti-tumor vaccine potency

The prophylactic vaccine potency of NP-vaccines was studied in a murine melanoma-OVA model. Mice were vaccinated or left un-treated and 7 days later challenged with B16-OVA tumors. But both NP-vaccines inhibited tumor growth (Figure 7.6A) and exhibited similar efficacy ($P < 0.001$) in prolonging animal survival compared to un-treated mice (Figure 7.6B). Single TLR NP-vaccines also induced partial protection against tumor challenge, however; *NP-CD40* inhibited tumor out growth in 50% of tumor bearing animals resulting in the longest median survival time compared to animals vaccinated with the other NP-vaccines (Supporting Information Figure S7.4).

The therapeutic vaccine potency of *NP-CD40* and *NP-Iso* was assessed by vaccinating tumor-bearing mice on day 7 and 17 post tumor inoculation. Comparison based on average tumor size per group could be determined until day 22; hereafter the first animals were sacrificed because of tumor burden. *NP-CD40* vaccinated animals displayed statistically smaller tumors compared to non-treated ($P < 0.01$) and *NP-Iso* treated animals ($P < 0.05$) (Figure 7.6D). Furthermore, *NP-CD40* vaccinated animals displayed a better prolonged survival compared to the control groups ($P < 0.02$) (Figure 7.6D). Collectively, the results indicate that CD40-targeting of PLGA-(Ag/TLR2+3L)-NP potentiates vaccine efficacy and induces (or boosts) anti-tumor responses inhibiting tumor growth and prolonging survival of animals.

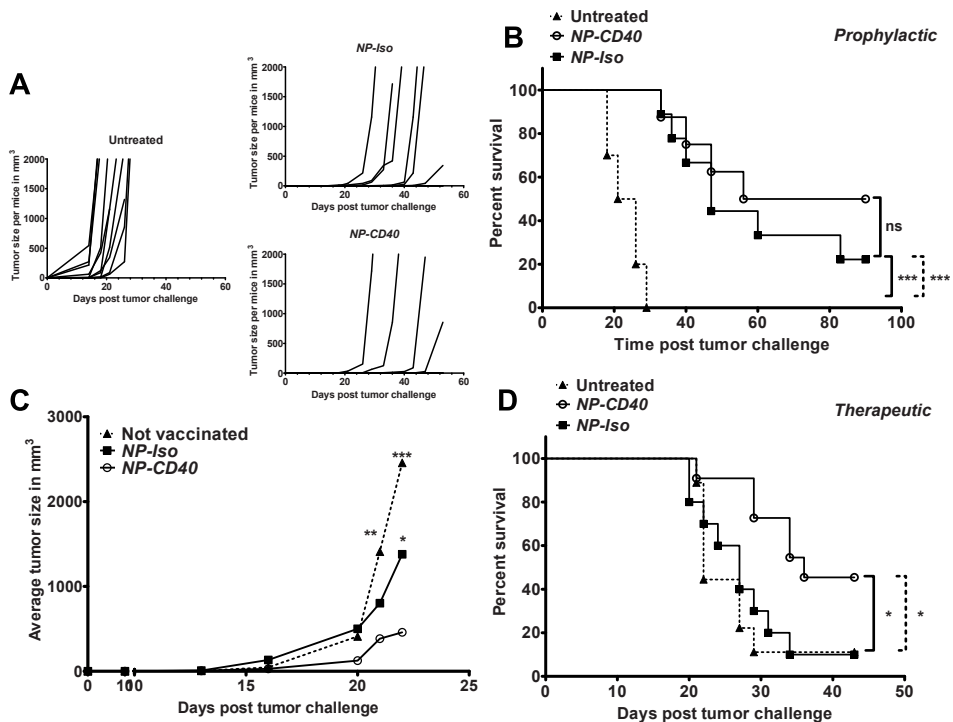


Figure 7.6 Vaccinations with PLGA-(Ag/TLR2+3L)- α CD40 NP induce potent anti-tumor responses.

WT mice were vaccinated in the right flank with 10 μ g OVA encapsulated in NP-CD40 and NP-Iso on day 0 or left untreated. On day 7 post-vaccination 2×10^5 B16-OVA tumor cells were inoculated s.c. on the opposite flank. Tumor growth (A) and animal survival (B) were monitored. Untreated animals were all required to be sacrificed because of tumor burden by day 29. 2×10^5 B16-OVA tumor cells were inoculated s.c. in the left flank of WT mice and these rested for 1 week followed by vaccinations on day 7 and 17 with 10 μ g OVA encapsulated in NP. Average tumor size per group was followed in time until day 22, the final time point when all animals were still alive (C), and survival monitored (D). Differences in tumor sizes per group were determined by regular two-way ANOVA with Bonferroni posttests to calculate the difference in mean values at each time point. Animal survival per group was assessed using Log-rank (Mantel-Cox) test, *** = $P < 0.001$, ** = $P < 0.01$ and * = $P < 0.05$.

Discussion

In this study we formulated a PLGA-NP based multi-compound particulate vaccine which target DC and deliver protein Ag and adjuvants via the cell-surface molecule CD40 with

the aim to activate efficient cytotoxic CD8⁺ T cell responses. The effects of CD40-targeting on vaccine potency were evaluated using a murine melanoma tumor model.

The results described here indicate that the selective and efficient *in vivo* delivery of particulate NP-vaccines to DC via CD40 is feasible and results in efficacious T cell responses. Combined CD40-targeting with TLR2- and TLR3-triggering synergistically enhanced IL-12 production by DC and IFN- γ production by CD4⁺ T cells *in vitro*, suggesting that NP-CD40 facilitates a TH1-mediated pro-inflammatory immune response. TH1 immune polarization by vaccines is essential to sustain robust anti-tumor CD8⁺ T cell responses *in vivo*²⁴. In line with this direct vaccinations with NP-CD40 improved the induction of Ag-specific cytotoxic CD8⁺ T cells and tumor-control.

The covalent coupling of the α CD40-mAb to the NP (NP-CD40) greatly enhanced the maturation effect of the NP-vaccine on DC (Figure 7.3). The better capacity of NP-CD40 to mature DC is possibly a consequence of triggering distinct adapter proteins involved in signaling pathways upstream of NF- κ B transcription regulation of DC maturation; TRAF (CD40)²⁵, MyD88 (TLR2) and TRIF (TLR3)²⁶. Another possibility is that receptor-mediated internalization via CD40 leads to higher quantities of Poly(I:C) and Pam3Csk4 inside intracellular compartments of DC compared to non-targeted NP¹³ inducing stronger TLR-stimulation. Additional experiments are ongoing to elucidate the mechanisms responsible for the enhanced DC maturation by NP-CD40.

Enhanced vaccine-delivery to DC can also be achieved via passive targeting by modifying the size of the vaccine which influences lymph node drainage of the vaccine²⁷. Alternatively, active vaccine-targeting strategies via CD40, as shown in this study, or through C-type lectins such as DEC-205, DC-SIGN and Glec9a greatly improves Ag delivery, processing and T cell priming by DC over non-targeted controls^{14,16,23,28,29}.

It is clear that DC express many cell-surface molecules which can function as potential targets for vaccine-delivery resulting in improved binding and internalization of the vaccine. The cell-surface molecule chosen is based on the DC-subtype possessing the optimal APC-properties for the desired type of immune response³⁰ one aims to activate. Figdor and colleagues have recently questioned the necessity to target vaccines to specific DC-subsets³¹, even though some DC-subtypes can possess a specialized role in peripheral tolerance^{32,33} or in the activation of CD8⁺ T cell mediated immune responses³⁴. However, owing to the plasticity in function of several DC-subtypes^{35,36} and on the results described here and published previously by our group³⁷ we hypothesize that the success

of therapeutic vaccinations is not critically dependent on the DC-subtype targeted but rather on the efficient delivery of the vaccine and importantly the adjuvants in sufficient amounts to activate CD11c⁺ DC instead of non-professional APC.

We recently performed a study using PLGA-(Ag/TLR3+7L)-NP and compared the delivery to DC via the targeting of CD40, CD11c or DEC-205. Our results indicate that the binding and internalization of the NP via these molecules similarly facilitate DC maturation *in vitro* but that CD40-targeting leads to slightly better CD8⁺ T cell responses *in vivo* (L.Cruz & R.Rosalia et al., manuscript in press 10.1016/j.jconrel.2014.07.040).

The surface expression of most targeting molecules is promiscuous on several immune cells. CD40 expression is not restricted to DC. For example, B cells also express CD40 and therefore might contribute to the anti-tumor responses observed after vaccinations with NP-CD40. A small percentage of B cells bind NP *in vivo*, however due to their inferior endocytic capacity³⁸ and T cell activating capacity³⁹ compared to DC it is likely that T cell stimulation by B cells *in vivo* played a minor role in this study.

PLGA-particles were shown to be internalized by M ϕ *in vivo* leading to cross-presentation of particle-encapsulated protein and priming of CD8⁺ T cells⁴⁰. We observed that M ϕ poorly internalized NP-CD40 and NP-Iso compared to DC (data not shown) likely because of the PEG-layer on the NP which blocks non-specific phagocytosis⁴¹. Targeting to CD40 did not lead to better *in vivo* internalization of NP-CD40 by M ϕ and we observed that CD11c⁺CD11b⁺F4/80⁻ DC have higher cell-surface expression of CD40 compared to CD19⁺B220⁺ B cells and CD11c⁺CD11b⁺F4/80⁺ M ϕ (data not shown). The higher CD4-expression on DC may form a mechanistic basis for the improved *in vivo* delivery of NP-CD40 compared to other APC.

Lymphoid organ resident CD8 α ⁺ DC are considered the main Ag cross-presenting and CD8⁺ T cell priming DC in the mouse⁴². We observed a trend that CD8 α ⁺ DC more efficiently internalized NP (Supporting Information Figure S7.1) than CD8 α ⁻ DC. A surprising finding as CD8⁺ and CD8⁻ CD11c⁺ DC were shown to possess similar phagocytic capacity⁴³, but differed in the mechanisms and efficiency of Ag-presentation⁴⁴. Cell-surface expression of CD40 was reported to be higher on CD8 α ⁺ DC in mice⁴⁵ which could explain why more CD8 α ⁺ DC internalize higher numbers of NP-CD40 via receptor mediated endocytosis.

CD40 seems to be a suitable target to deliver other types of particulate vaccines. Similar *ex vivo* and *in vivo* DC-specific delivery of a CD40-targeted adenoviral tumor vaccine was previously reported⁴⁶ inducing stronger anti-tumor responses than the non-targeted

vectors, which supports CD40 on DC to be a suitable target to deliver not only PLGA-NP based vaccines but also other types of particulate vaccines.

DC were poorly matured by (PLGA-Ag)- α CD40 NP or soluble α CD40-mAb in the absence of TLRL. This was surprising as α CD40-mAb bound to polystyrene⁴⁷, poly(γ -glutamic acid)⁴⁸ and porous silicon NP⁴⁹ resulted in DC maturation. FGK45 is a relatively weaker DC activating adjuvant compared to most TLRL⁵⁰ and we hypothesized that coupling of α CD40-mAb to PLGA-NP would improve the cross-linking of CD40 on DC and enhance the stimulatory effect of FGK45. But, our data suggests that the stimulating properties of FGK45 coupled to PLGA-NP at the quantities tested were insufficient to strongly activate DC as a single adjuvant. Higher concentrations of FGK45, than reported in our study, coupled to NP could not be achieved due to already saturating amounts of the mAb coupled to the NP-surface. Of course, increasing the size (Table 7.1) of the NP would allow the coupling of more antibodies, but we opted not to as the amounts of α CD40-mAb coupled to the NP were already sufficient to significantly boost the immune activating properties of TLRL encapsulated in NP. And importantly, higher dosages of systemic α CD40-mAb after injection might lead to liver toxicity as reported recently by Fransen et al.⁵¹. Vaccinations using NP-CD40 resulted in the most efficient T cell responses *in vitro* and *in vivo*. Multi-adjuvant vaccines are known to improve immune responses compared to single adjuvant based vaccines⁵² and Berzofsky et al. recently showed that this effect is related to a qualitative differences of the primed effector T cells⁵³. Our observations support this report as the strongest CD8⁺ T cell cytotoxicity was achieved with vaccines combining TLR2L, TLR3L and α CD40-mAb.

Efficient and potent therapies against infectious diseases and cancer are highly necessary in the clinic. With recent exciting developments in immunotherapy, active vaccinations are close to being implemented as an accepted anti-cancer therapy but also against infectious diseases, for example Influenza⁵⁴. However, fine-tuning is required to achieve maximum vaccine potency via DC-controlled anti-tumor immune responses. We show here that CD40-targeting is an attractive strategy to deliver PLGA-NP-based well-defined vaccines to CD11c⁺ DC resulting in significant tumor control. Using the TC-1 tumor model, we showed in a clinically-relevant Ag model that CD40-targeting enhances HPV-E7 specific CD8⁺ T cell responses (Figure 7.5D) suggesting broad applicability of CD40-targeted NP-vaccines to boost immune responses against other TAA. But possibly also as therapy for other diseases caused by microorganisms with known Ag-specificity, for example the parasite *Plasmodium vivax* which causes malaria.

In conclusion, significant boosting of effector T cells is achieved by improving the delivery of PLGA-(Ag/TLR2+3L) NP to DC via CD40 targeting. DC efficiently internalized the vaccine leading to full blown maturation and efficient priming of CD8⁺ T cells which led to prolonged survival of tumor-bearing animals.

Acknowledgements

Financial support for this study was provided by the clinical pharmacy and toxicology department of the Leiden University Medical Center

References

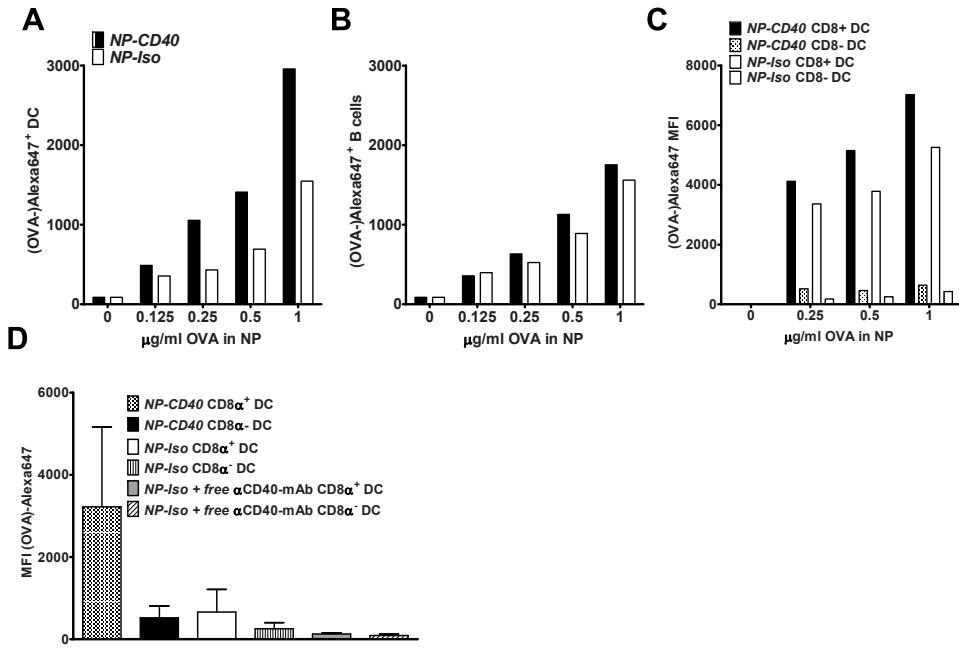
1. Palucka K, Ueno H, Fay J, Banchereau J 2011. Dendritic cells and immunity against cancer. *Journal of Internal Medicine* 269(1):64-73.
2. Banchereau J, Steinman RM 1998. Dendritic cells and the control of immunity. *Nature* 392(6673):245-252.
3. Palucka K, Banchereau J 2012. Cancer immunotherapy via dendritic cells. *Nature Reviews Cancer* 12(4):265-277.
4. Pasare C, Medzhitov R 2005. Toll-like receptors: linking innate and adaptive immunity. *Adv Exp Med Biol* 560:11-18.
5. Tacke PJ, de Vries IJ, Torensma R, Figdor CG 2007. Dendritic-cell immunotherapy: from ex vivo loading to in vivo targeting. *Nature Reviews Immunology* 7(10):790-802.
6. Melief CJ 2008. Cancer immunotherapy by dendritic cells. *Immunity* 29(3):372-383.
7. Shen H, Ackerman AL, Cody V, Giodini A, Hinson ER, Cresswell P, Edelson RL, Saltzman WM, Hanlon DJ 2006. Enhanced and prolonged cross-presentation following endosomal escape of exogenous antigens encapsulated in biodegradable nanoparticles. *Immunology* 117(1):78-88.
8. Fischer S, Schlosser E, Mueller M, Csaba N, Merkle HP, Groettrup M, Gander B 2009. Concomitant delivery of a CTL-restricted peptide antigen and CpG ODN by PLGA microparticles induces cellular immune response. *Journal of Drug Targeting* 17(8):652-661.
9. Silva AL, Rosalia RA, Sazak A, Carstens MG, Ossendorp F, Oostendorp J, Jiskoot W 2013. Optimization of encapsulation of a synthetic long peptide in PLGA nanoparticles: low-burst release is crucial for efficient CD8(+) T cell activation. *European Journal of Pharmaceutics and Biopharmaceutics* 83(3):338-345.
10. Silva JM, Videira M, Gaspar R, Preat V, Florindo HF 2013. Immune system targeting by biodegradable nanoparticles for cancer vaccines. *Journal of Controlled Release* 168(2):179-199.
11. Mueller M, Schlosser E, Gander B, Groettrup M 2011. Tumor eradication by immunotherapy with biodegradable PLGA microspheres--an alternative to incomplete Freund's adjuvant. *Int J Cancer* 129(2):407-416. doi: 410.1002/ijc.25914. Epub 22011 Mar 25928.
12. Bazile D, Prud'homme C, Bassoullet MT, Marlard M, Spenlehauer G, Veillard M 1995. Stealth Me.PEG-PLA nanoparticles avoid uptake by the mononuclear phagocytes system. *Journal of Pharmaceutical Sciences* 84(4):493-498.
13. Tacke PJ, Zeelenberg IS, Cruz LJ, van Hout-Kuijter MA, van de Glind G, Fokkink RG, Lambeck AJ, Figdor CG 2011. Targeted delivery of TLR ligands to human and mouse dendritic cells strongly enhances adjuvanticity. *Blood* 118(26):6836-6844. doi: 6810.1182/blood-2011-6807-367615. Epub 362011 Oct 367613.
14. Macho-Fernandez E, Cruz LJ, Ghinnagow R, Fontaine J, Bialecki E, Frisch B, Trottein F, Faveeuw C 2014. Targeted Delivery of alpha-Galactosylceramide to CD8alpha+ Dendritic Cells Optimizes Type I NKT Cell-Based Antitumor Responses. *Journal of Immunology* 193(2):961-969.

15. Hamdy S, Haddadi A, Shayeganpour A, Samuel J, Lavasanifar A 2011. Activation of antigen-specific T cell-responses by mannan-decorated PLGA nanoparticles. *Pharm Res* 28(9):2288-2301. doi: 2210.1007/s11095-11011-10459-11099. Epub 12011 May 11011.
16. Han R, Zhu J, Yang X, Xu H 2011. Surface modification of poly(D,L-lactic-co-glycolic acid) nanoparticles with protamine enhanced cross-presentation of encapsulated ovalbumin by bone marrow-derived dendritic cells. *Journal of Biomedical Materials Research Part A* 96(1):142-149.
17. Schoenberger SP, Toes RE, van der Voort EI, Offringa R, Melief CJ 1998. T-cell help for cytotoxic T lymphocytes is mediated by CD40-CD40L interactions. *Nature* 393(6684):480-483.
18. Schuurhuis DH, Laban S, Toes RE, Ricciardi-Castagnoli P, Kleijmeer MJ, van der Voort EI, Rea D, Offringa R, Geuze HJ, Melief CJ, Ossendorp F 2000. Immature dendritic cells acquire CD8(+) cytotoxic T lymphocyte priming capacity upon activation by T helper cell-independent or -dependent stimuli. *The Journal of Experimental Medicine* 192(1):145-150.
19. Cohn L, Chatterjee B, Esselborn F, Smed-Sorensen A, Nakamura N, Chalouni C, Lee BC, Vandlen R, Keler T, Lauer P, Brockstedt D, Mellman I, Delamarre L 2013. Antigen delivery to early endosomes eliminates the superiority of human blood BDCA3+ dendritic cells at cross presentation. *The Journal of Experimental Medicine* 210(5):1049-1063.
20. Schjetne KW, Fredriksen AB, Bogen B 2007. Delivery of antigen to CD40 induces protective immune responses against tumors. *Journal of Immunology* 178(7):4169-4176.
21. Schuurhuis DH, van Montfoort N, Ioan-Facsinay A, Jiawan R, Camps M, Nouta J, Melief CJ, Verbeek JS, Ossendorp F 2006. Immune complex-loaded dendritic cells are superior to soluble immune complexes as antitumor vaccine. *Journal of Immunology* 176(8):4573-4580.
22. Moore MW, Carbone FR, Bevan MJ 1988. Introduction of soluble protein into the class I pathway of antigen processing and presentation. *Cell* 54(6):777-785.
23. Cruz LJ, Tacke PJ, Fokkink R, Joosten B, Stuart MC, Albericio F, Torensma R, Figdor CG 2010. Targeted PLGA nano- but not microparticles specifically deliver antigen to human dendritic cells via DC-SIGN in vitro. *J Control Release* 144(2):118-126. doi: 110.1016/j.jconrel.2010.1002.1013. Epub 2010 Feb 1013.
24. Ossendorp F, Mengede E, Camps M, Filius R, Melief CJ 1998. Specific T helper cell requirement for optimal induction of cytotoxic T lymphocytes against major histocompatibility complex class II negative tumors. *The Journal of Experimental Medicine* 187(5):693-702.
25. Mackey MF, Wang Z, Eichelberg K, Germain RN 2003. Distinct contributions of different CD40 TRAF binding sites to CD154-induced dendritic cell maturation and IL-12 secretion. *European Journal of Immunology* 33(3):779-789.
26. Brown J, Wang H, Hajishengallis GN, Martin M 2011. TLR-signaling networks: an integration of adaptor molecules, kinases, and cross-talk. *Journal of Dental Research* 90(4):417-427.
27. Manolova V, Flace A, Bauer M, Schwarz K, Saudan P, Bachmann MF 2008. Nanoparticles target distinct dendritic cell populations according to their size. *Eur J Immunol* 38(5):1404-1413. doi: 1410.1002/eji.200737984.

28. Raghuwanshi D, Mishra V, Suresh MR, Kaur K 2012. A simple approach for enhanced immune response using engineered dendritic cell targeted nanoparticles. *Vaccine* 30(50):7292-7299.
29. Schreibelt G, Klinkenberg LJ, Cruz LJ, Tacken PJ, Tel J, Kreutz M, Adema GJ, Brown GD, Figdor CG, de Vries IJ 2012. The C-type lectin receptor CLEC9A mediates antigen uptake and (cross-) presentation by human blood BDCA3+ myeloid dendritic cells. *Blood* 119(10):2284-2292.
30. Merad M, Sathe P, Helft J, Miller J, Mortha A 2013. The dendritic cell lineage: ontogeny and function of dendritic cells and their subsets in the steady state and the inflamed setting. *Annu Rev Immunol* 31:563-604.
31. Kreutz M, Tacken PJ, Figdor CG 2013. Targeting dendritic cells--why bother? *Blood* 121(15):2836-2844. doi: 2810.1182/blood-2012-2809-452078. Epub 452013 Feb 452076.
32. Idoyaga J, Fiorese C, Zbytnuik L, Lubkin A, Miller J, Malissen B, Mucida D, Merad M, Steinman RM 2013. Specialized role of migratory dendritic cells in peripheral tolerance induction. *J Clin Invest* 123(2):844-854. doi: 810.1172/JCI65260. Epub 62013 Jan 65269.
33. Gottschalk C, Damuzzo V, Gotot J, Kroczeck RA, Yagita H, Murphy KM, Knolle PA, Ludwig-Portugall I, Kurts C 2013. Batf3-dependent dendritic cells in the renal lymph node induce tolerance against circulating antigens. *Journal of the American Society of Nephrology* 24(4):543-549.
34. Kroczeck RA, Henn V 2012. The Role of XCR1 and its Ligand XCL1 in Antigen Cross-Presentation by Murine and Human Dendritic Cells. *Frontiers in Immunology* 3:14.
35. Dresch C, Leverrier Y, Marvel J, Shortman K 2012. Development of antigen cross-presentation capacity in dendritic cells. *Trends in Immunology* 33(8):381-388.
36. Shortman K, Liu YJ 2002. Mouse and human dendritic cell subtypes. *Nature Reviews Immunology* 2(3):151-161.
37. van Montfoort N, Mangsbo SM, Camps MG, van Maren WW, Verhaart IE, Waisman A, Drijfhout JW, Melief CJ, Verbeek JS, Ossendorp F 2012. Circulating specific antibodies enhance systemic cross-priming by delivery of complexed antigen to dendritic cells in vivo. *European Journal of Immunology* 42(3):598-606.
38. Rabinovitch M 1995. Professional and non-professional phagocytes: an introduction. *Trends in Cell Biology* 5(3):85-87.
39. Lim TS, Goh JK, Mortellaro A, Lim CT, Hammerling GJ, Ricciardi-Castagnoli P 2012. CD80 and CD86 differentially regulate mechanical interactions of T-cells with antigen-presenting dendritic cells and B-cells. *PLoS One* 7(9):e45185.
40. Schliehe C, Redaelli C, Engelhardt S, Fehlings M, Mueller M, van Rooijen N, Thiry M, Hildner K, Weller H, Groettrup M 2011. CD8- dendritic cells and macrophages cross-present poly(D,L-lactate-co-glycolate) acid microsphere-encapsulated antigen in vivo. *Journal of Immunology* 187(5):2112-2121.
41. Gref R, Luck M, Quelled P, Marchand M, Dellacherie E, Harnisch S, Blunk T, Muller RH 2000. 'Stealth' corona-core nanoparticles surface modified by polyethylene glycol (PEG): influences of the corona (PEG chain length and surface density) and of the core composition on phagocytic uptake and plasma protein adsorption. *Colloids and Surfaces B, Biointerfaces* 18(3-4):301-313.

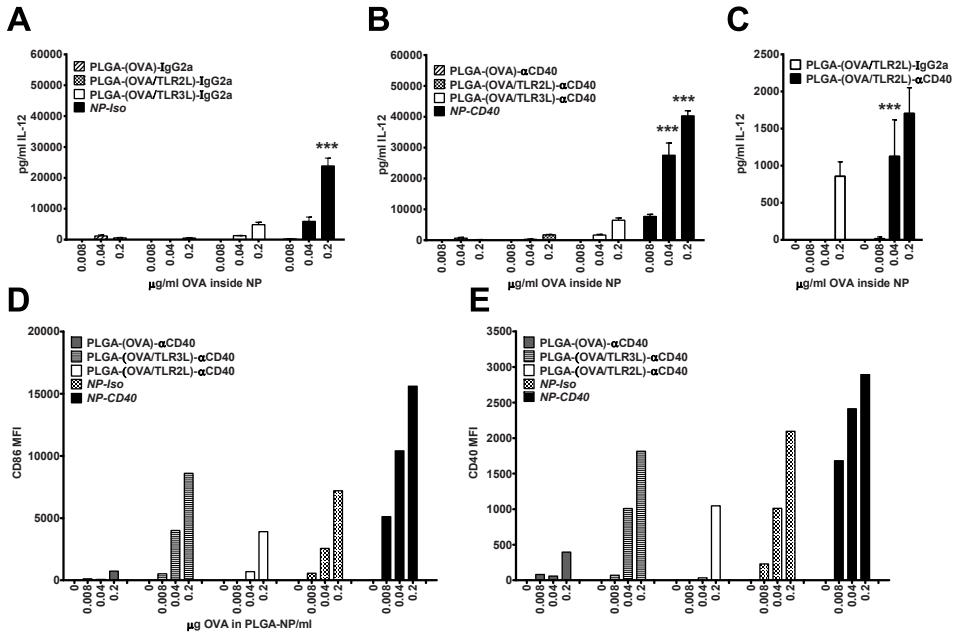
42. Shortman K, Heath WR 2010. The CD8⁺ dendritic cell subset. *Immunological Reviews* 234(1):18-31.
43. Schnorrer P, Behrens GM, Wilson NS, Pooley JL, Smith CM, El-Sukkari D, Davey G, Kupresanin F, Li M, Maraskovsky E, Belz GT, Carbone FR, Shortman K, Heath WR, Villadangos JA 2006. The dominant role of CD8⁺ dendritic cells in cross-presentation is not dictated by antigen capture. *Proceedings of the National Academy of Sciences of the United States of America* 103(28):10729-10734.
44. Kamphorst AO, Guermonprez P, Dudziak D, Nussenzweig MC 2010. Route of antigen uptake differentially impacts presentation by dendritic cells and activated monocytes. *Journal of Immunology* 185(6):3426-3435.
45. Gao X, Wang S, Fan Y, Bai H, Yang J, Yang X 2010. CD8⁺ DC, but Not CD8⁻DC, isolated from BCG-infected mice reduces pathological reactions induced by mycobacterial challenge infection. *PLoS One* 5(2):e9281.
46. Hangalapura BN, Oosterhoff D, de Groot J, Boon L, Tuting T, van den Eertwegh AJ, Gerritsen WR, van Beusechem VW, Pereboev A, Curiel DT, Scheper RJ, de Gruijl TD 2011. Potent antitumor immunity generated by a CD40-targeted adenoviral vaccine. *Cancer Research* 71(17):5827-5837.
47. Kempf M, Mandal B, Jilek S, Thiele L, Voros J, Textor M, Merkle HP, Walter E 2003. Improved stimulation of human dendritic cells by receptor engagement with surface-modified microparticles. *Journal of Drug Targeting* 11(1):11-18.
48. Broos S, Sandin LC, Apel J, Totterman TH, Akagi T, Akashi M, Borrebaeck CA, Ellmark P, Lindstedt M 2012. Synergistic augmentation of CD40-mediated activation of antigen-presenting cells by amphiphilic poly(γ -glutamic acid) nanoparticles. *Biomaterials* 33(26):6230-6239.
49. Gu L, Ruff LE, Qin Z, Corr M, Hedrick SM, Sailor MJ 2012. Multivalent porous silicon nanoparticles enhance the immune activation potency of agonistic CD40 antibody. *Advanced Materials (Deerfield Beach, Fla)* 24(29):3981-3987.
50. Welters MJ, Bijker MS, van den Eeden SJ, Franken KL, Melief CJ, Offringa R, van der Burg SH 2007. Multiple CD4 and CD8 T-cell activation parameters predict vaccine efficacy in vivo mediated by individual DC-activating agonists. *Vaccine* 25(8):1379-1389.
51. Fransen MF, Sluijter M, Morreau H, Arens R, Melief CJ 2011. Local activation of CD8 T cells and systemic tumor eradication without toxicity via slow release and local delivery of agonistic CD40 antibody. *Clinical Cancer Research* 17(8):2270-2280.
52. Kasturi SP, Skountzou I, Albrecht RA, Koutsonanos D, Hua T, Nakaya HI, Ravindran R, Stewart S, Alam M, Kwissa M, Villinger F, Murthy N, Steel J, Jacob J, Hogan RJ, Garcia-Sastre A, Compans R, Pulendran B 2011. Programming the magnitude and persistence of antibody responses with innate immunity. *Nature* 470(7335):543-547.
53. Zhu Q, Egelston C, Gagnon S, Sui Y, Belyakov IM, Klinman DM, Berzofsky JA 2010. Using 3 TLR ligands as a combination adjuvant induces qualitative changes in T cell responses needed for antiviral protection in mice. *The Journal of clinical investigation* 120(2):607-616.
54. Slutter B, Pewe LL, Lauer P, Harty JT 2013. Cutting edge: rapid boosting of cross-reactive memory CD8 T cells broadens the protective capacity of the Flumist vaccine. *Journal of immunology* 190(8):3854-3858.

Supporting Information



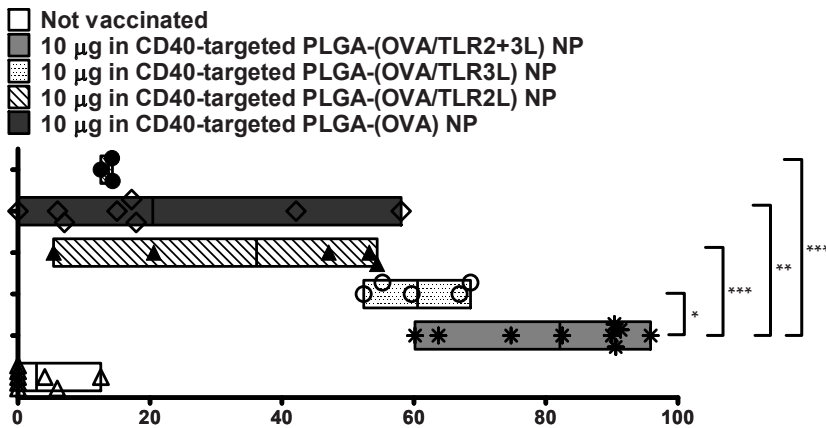
Supporting Information Figure S7.1 DC and B Cells internalize NP-CD40 and NP-Iso in vitro and NP-CD40 are preferentially internalized by CD8⁺CD11⁺ DC.

Splenocytes were for 1 hr with (200,000 cells/well of a 96-wells plate) with titrated (2-step dilutions based on encapsulated OVA-protein in NP) amounts of PLGA-(OVA/TLR2+3L)- α CD40 or PLGA-(OVA/TLR2+3L)-IgG2a NP containing OVA-Alexa647. Cells were kept cold after incubation, washed 3x with PBS to remove unbound NP. Cells were then stained with antibodies against various cell surface molecules and analyzed by flow cytometry DC were designated as CD3⁺F4/80⁻CD11b⁺CD11c⁺ (**A**) or divided into CD8⁺ or CD8⁻ cells (**C**). B cells were gated as CD3⁺CD19⁺B220⁺ cells (**B**). NP encapsulated was determined based on the OVA-Alexa647 fluorescence intensity. C57BL/6 animals were vaccinated s.c. in the right flank with 10 μ g OVA-Alexa647 encapsulated in NP and sacrificed 48 hr post-vaccination and the inguinal LN harvested and single-cell suspensions, stained with various fluorescent antibodies to distinguish the different immune cell populations which are positive for Alexa-647 fluorescence by Flow Cytometry (**D**).



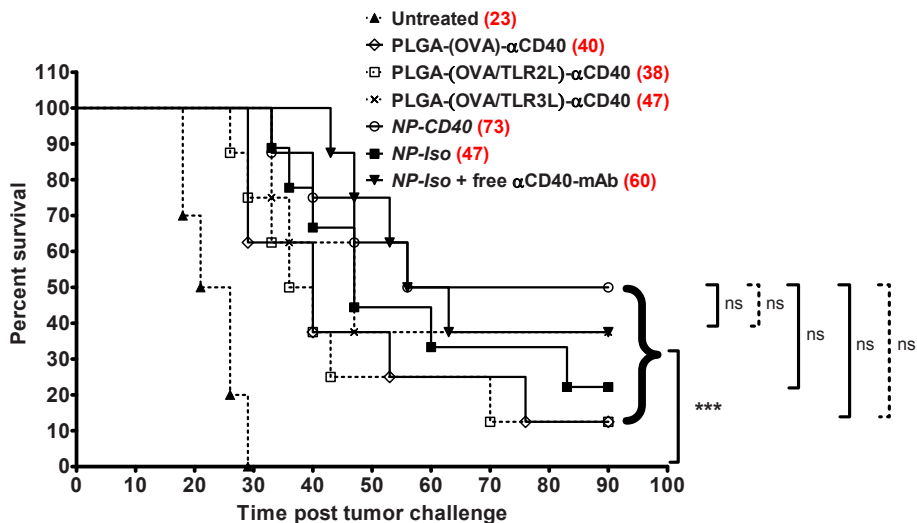
Supporting Information Figure S7.2 Combining triplicate adjuvants (TLR2L, TL3L and $\alpha\text{CD40-mAb}$) leads to strong synergistic activation of DC compared to singlet or doublet adjuvant combinations.

WT BMDC (100,000 cells/well) were incubated with titrated amounts of various PLGA-NP formulations encapsulating TLR2L, TLR3L or $\alpha\text{CD40-mAb}$. Culture supernatants were harvested and the amount of IL-12 determined by ELISA (**A**, **B** and **C**). Post-incubation, DC were stained with fluorescent antibodies against CD86 (**D**) and CD40 (**E**) followed by Flow Cytometry analysis. Differences in cytokine production were analyzed applying two way ANOVA with Bonferroni posttests, *** = $P < 0.001$.



Supporting Information Figure S7.3 CD40-targeted delivery of two TLR co-encapsulated with protein Ag in NP results in superior priming of effector CD8⁺ T cells.

C57BL/6 were vaccinated s.c. in the right flank with 10 µg OVA encapsulated in various CD40-targeted PLGA-(Ag/TLRL) NP formulations. On day 7 day post vaccination, SIINFEKL-loaded CFSE^{high} OVA-specific target cells and ASNENMETM-loaded CFSE^{low} INFLUENZA-specific target cells (negative controls) were injected i.v. in a 1:1 ratio. Mice were sacrificed 18 hr later and the degree of OVA-specific lysis of the target cells determined by FACS and the % killing of OVA-specific target cells quantified as described in M&M. Differences in *in vivo* cytotoxicity of primed CD8⁺ T cells were analyzed applying the Mann Whitney tests, *** = P < 0.001, ** = P < 0.01 & * = P < 0.05.



Supporting Information Figure S7.4 Vaccinations with PLGA-(Ag/TLRL)-mAb NP prolong survival of tumor challenged animals.

C57BL/6 were vaccinated on the right flank with 10 µg OVA encapsulated in different PLGA-(Ag/TLRL)-mAb NP formulations (Table 7.1 manuscript). On day 7 post-vaccination 2×10^5 B16-OVA tumor cells were inoculated s.c. on the opposite flank. Tumor growth was followed and animal survival in the treatment groups were assessed and compared to untreated animals. Untreated animals were all required to be sacrificed because of tumor burden by day 29. Animal survival per group was assessed and differences between the different groups were calculated using Log-rank (Mantel-Cox) test. *** = $P < 0.0001$ for animals treated with the different PLGA-(Ag/TLRL)-mAb NP formulations vs untreated. Numbers in red indicate median survival in days.



Chapter 8

**Targeting nanoparticles to CD40,
DEC-205 or CD11c molecules on DC
for efficient CD8⁺ T cell responses;
a comparative study**

Luis J. Cruz*, Rodney A. Rosalia*, Jan Willem Kleinovink,
Felix Rueda, Clemens W.G.M. Löwik, Ferry Ossendorp

* Contributed equally to this study

Accepted for publication, in press in Journal of controlled release
DOI: 10.1016/j.jconrel.2014.07.040

Abstract

Here we demonstrate the importance of targeting antigens (Ags) to dendritic cell (DC) receptors to achieve an efficient cytotoxic T cell response which was associated with a strong activation of DC. Pegylated poly(lactic-co-glycolic acid) (PLGA) nanoparticles (NP), encapsulating Ovalbumin (OVA) as a model protein Ag and Toll like receptor (TLR) 3 and 7 ligands were targeted to distinct DC cell-surface molecules; CD40, a TNF- α family receptor, DEC205, a C-type lectin receptor or CD11c, an integrin receptor, by means of specific monoclonal antibodies (mAb) coupled to the NP. The efficiency of these different targeting strategies to activate DC and elicit a potent CD8⁺ T cell response was studied. PLGA-(Ag/TLR3+7L) NP were more efficiently targeted to and internalized by DC *in vitro* compared to the control non-targeted NP. We observed a small but significantly improved internalization of CD40-targeted NP compared to DEC-205 or CD11c targeted NP. In contrast to non-targeted NP, all targeted NP equally stimulated IL-12 production and expression of co-stimulatory molecules by DC, inducing strong proliferation and IFN- γ production by T cells *in vitro*. Upon subcutaneous (s.c.) vaccination CD40, DEC-205 and CD11c targeted NP consistently showed higher efficacy than non-targeted NP to stimulate CD8⁺ T cell responses. However, all targeted NP vaccines showed equal capacity to prime CD8⁺ T cells capable of target cell lysis *in vivo*. In conclusion, delivery of NP-vaccines to DC by targeting via cell-surface molecules leads to strong enhancement of vaccine potency and induction of T cell responses compared to non-specific delivery of NP to DC.

Introduction

The specificity, strength, and persistence of the immune response have led many research teams to focus their efforts on producing vaccines against various immunological diseases. It is well described that the immune system has the potential to recognize and eliminate cancerous cells¹⁻³. The primary goal of cancer vaccination is the generation of robust and specific T cell responses with the capacity to inhibit tumor growth⁴⁻⁶ in cancer patients with otherwise poor natural tumor specific immunity. In this respect, dendritic cells (DCs) have a crucial role as these cells are considered the most efficient and specialized Ag-presenting cells (APCs) with the capacity stimulate strong cytotoxic T cell responses by cross-presenting tumor-derived protein antigens. Vaccination strategies involving DCs have been studied owing to their function in coordinating innate and adaptive immune responses *in vivo*⁷⁻⁹, and given that DCs are stimulated appropriately they initiate and direct robust antitumor immune responses. DC-based therapies have shown some clinical benefits; however their use is hampered by laborious vaccine preparations requiring multiple and complex steps to adhere to good manufacturing practices (GMP)-regulations and donor variabilities.

The drawbacks of DC-based therapies can be circumvented by delivery of specific protein antigens (Ags) to DCs directly *in vivo* via specific surface receptors using for example poly-(lactic-co-glycolic-acid) (PLGA) particulate delivery systems. One of the greatest benefits of particle-based Ag delivery systems resides in their capacity to carry polypeptide Ags and adjuvants concomitantly to the same APC, which was shown to efficiently induce T cell responses¹⁰⁻¹³. Furthermore, the targeted delivery of Ags to DC surface receptors enhances presentation to T cells¹⁴. However, it is not fully clear, which cell surface molecule or receptor expressed by DC should targeted for optimal T cell activation.

To address this issue, three distinct cell-surface receptors will be analyzed for the targeting and delivery of NP-based vaccines to DC: CD40, a TNF- α family receptor with known DC activating properties after binding of its specific ligand, DEC-205, a C-type lectin receptor, and integrin receptor CD11c which does not induce DC activation after binding of their respective ligands. In this work, Ovalbumin protein Ag will be encapsulated together with the Toll-like Receptor (TLR) ligands (TLRLs) polyinosinic:polycytidylic acid (poly I:C) (TLR3) and resiquimod (R848) (TLR7), two potent immunostimulatory agents that mimic pathogen-derived material and function by triggering endosomal TLRs.

NP delivery to DC by targeting the appropriate cell-surface receptor might further enhance the activation of DC by TLRLs, either via enhanced internalization of the TLRLs into the

endosomes or through triggering of cell-surface molecules with separate downstream DC-activating signaling pathways which possibly synergizes with TLR-stimulation.

Herein a comparative study of the responses induced by targeting these different DC receptors is presented. We show here the strong requirement for cell surface molecule targeting on DC to enhance internalization of NP by DC and enhance immune activation compared to non-targeted controls. However in our model, targeting CD40, DEC-205 or CD11c resulted in comparable immune responses. This is highlighted by observing similar rates of diffusion of all targeted NP out of the injection site, whereas non-targeted NP were significantly slower in this process. In addition, vaccination with the different targeted NP led to CD8⁺ T cell responses with similar proliferative potential, IFN- γ production and *in vivo* cytotoxicity against specific target cells.

Material and methods

Materials and reagents

PLGA (Resomer RG 502 H, lactide:glycolide molar ratio 48:52 to 52:48); MW: 7000-17000 Da was purchased from Boehringer Ingelheim, Germany. Solvents for peptide synthesis and PLGA preparation (dichloromethane (DCM), N,N'-dimethylformamide (DMF) and ethyl acetate) were obtained from Sigma-Adrich (The Netherlands). Lipids purchased from Avanti Polar Lipids (USA) include 1,2-distearoyl-sn-glycero-3-phosphoethanolamine-N-[succinic acid(polyethylene glycol)2000] (ammonium salt) and 1,2-distearoyl-sn-glycero-3-phosphoethanolamine-N-[methoxy(polyethylene glycol)-2000] (ammonium salt) (mPEG 2000 PE). R848 was from Axorra, poly I:C from Sigma and endotoxin free OVA from Hyglos GmbH.

Anti-CD40 mAb (clone FGK45, IgG2a) was produced in house after obtaining the hybridoma from A. Rolink (Basel Institute for Immunology, Basel, Switzerland)¹⁵. Mouse anti-CD11c and the murine anti-DEC205 (CD205) Abs were from BIO-X-CELL (West Lebanon, NH). Mouse IgG2a Isotype control (Clone:C1.18.4 Catalog #:BE0085) and mouse IgG2b Isotype control (Clone:MPC-11Catalog #:BE0086) were also purchased from Bio X Cell Antibody Production and Purification.

Preparation and characterization of PLGA NP

PLGA-NP coated with Abs was generated using the copolymer PLGA essentially as described before^{16,17}. In brief, 100 mg of PLGA in 2 mL of ethyl acetate containing OVA Ag free endotoxin (10 mg) and/or poly I:C (4 mg) and/or R848 (1 mg) were emulsified under sonification (Branson, sonifier 250) during 60 seconds. This first emulsion was rapidly added to 1 mL of 1% polyvinylalcohol(PVA)/7% ethyl acetate in distilled water during 15 second. A combination of lipids (DSPE-PEG(2000) succinic acid (8 mg) and mPEG 2000 PE (8 mg)) were dissolved in chloroform and added to the vial. The chloroform was removed by a stream of nitrogen gas. Subsequently, the emulsion was rapidly added to the vial containing the lipids and the solution was homogenized during 30 seconds using a sonicator. This solution was added to 100 mL of 0.3% PVA 7% of ethyl acetate in distilled water and stirred overnight to evaporate ethyl acetate. The PLGA-NP were collected by centrifugation at 12000 x g for 10 min, washed four times with distilled water and lyophilized. Next, abs was covalently coupled to 10 mg of PLGA NP by activating surface carboxyl groups in isotonic 0.1 M MES buffer pH 5.5 containing 1-ethyl-3-[3-dimethylaminopropyl] carbodiimide hydrochloride (10 equiv.) and N-hydroxysuccinimide (10 equiv.) for 1 h. The activated carboxyl-PLGA NP was washed one time with MES buffer by centrifugation. Subsequently, abs (α CD40, α CD11c, α DEC-205 and isotype controls respectively (200 μ g per mg NP) were added and the solution was stirred during 3 h at room temperature and later overnight at 4°C. Unbound antibodies were removed by centrifugation (12000 x g, during 10 min) and the PLGA NPs-Abs was washed four times with PBS. The presence of Abs on the particle surface was determined by Coomassie dye protein assay (Table 8.1).

Dynamic light scattering and zeta-potential measurements

Dynamic light scattering (DLS) measurements were taken on different PLGA-NP using an ALV light-scattering instrument equipped with an ALV5000/60X0 Multiple Tau Correlator and an Oxixus SLIM-532 150 mW DPSS laser operating at a wavelength of 532 nm. A refractive index matching bath of filtered cis-decalin surrounded the cylindrical scattering cell, and the temperature was controlled at 21.5 ± 0.3 °C using a Haake F3-K thermostat. In each sample, the $g_2(\tau)$ auto-correlation function was recorded ten times at a detection angle of 90°. For each measurement, the diffusion coefficient (D) was determined by using the second-order cumulant, and the corresponding PLGA NP diameter was calculated

assuming that the PLGA NP were spherical in shape. Zeta potential measurements were performed on PLGA NP using a Malvern ZetaSizer 2000 (UK).

Quantifying encapsulated OVA in NP

OVA-protein encapsulating efficiency was determined after hydrolyzing 5 mg PLGA NP in 0.5 mL 0.8 M NaOH overnight at 37°C. The OVA-protein content was then measured using Coomassie Plus Protein Assay Reagent (Pierce) according to the manufacturer's protocol. OVA encapsulation efficiency was calculated by dividing the measured amount of encapsulated Ag by the theoretical amount assuming all was encapsulated.

Quantifying encapsulated TLR ligands

Biodegradable PLGA NP was hydrolyzed with 0.8 M NaOH overnight at 37°C. The encapsulation efficiency of TLR ligands was determined by high-performance liquid chromatograph (HPLC). HPLC analysis was performed at room temperature using a Shimadzu system (Shimadzu Corporation, Kyoto, Japan) equipped with a RP-C18 symmetry column (250 mm x 4.6 mm). The flow rate was fixed at 1 mL/min and detection was obtained by UV detection at 220 nm. A linear gradient of 0% to 100% of acetonitrile (0.036% TFA) in water containing (0.045% TFA) was used for the separation of R848 and Poly I:C. The peak of R848 was well separated from that of the Poly I:C in the established chromatographic condition. The retention times of the Poly I:C and R848 were approximately 20 and 26 min, respectively. The regression analysis was constructed by plotting the peak-area ratio of R848 or Poly I:C versus concentration (ug/mL). The calibration curves were linear within the range of 1 ug/mL to 10 ug/mL for R848 and 2.5 ug/mL to 100 ug/mL for Poly I:C. The correlation coefficient (R^2) were always greater than 0.99, indicating a good linearity.

Animals

WT C57BL/6 mice (CD45.2/Thy1.2; H-2^b) were obtained from Charles River Laboratories. Albino B6 (B6(Cg)-Tyrc-2J/J), Ly5.1/CD45.1 (C57BL/6 background), transgenic OT-I/Thy1.1/CD45.2 (specific for the OVA₂₅₇₋₂₆₄ CTL epitope presented by H2-K^b), and transgenic OT-II/Ly5.1/CD45.1 mice (specific for the OVA₃₂₃₋₃₃₉ Th epitope presented by I-A^b) were bred in the specific pathogen-free animal facility of the Leiden University Medical Center. All animal experiments were approved by the animal experimental committee of Leiden University.

Cell lines

D1 cells, a GM-CSF dependent immature dendritic cell line derived from spleen of WT C57BL/6 (H-2b) mice were cultured as described previously¹⁸. Freshly isolated DC (BMDC) were cultured from mouse bone marrow (BM) cells by collecting femurs from WT C57BL/6 mice or CD40 KO mice and cultured as published previously by our group¹⁸. After 10 days of culture, large numbers of typical DC were obtained which were at least 90% positive for murine DC marker CD11c (data not shown). The weakly immunogenic and highly aggressive OVA-transfected B16 tumor cell line (B16-OVA), syngeneic to the C57BL/6 strain, was cultured as described¹⁹.

Analysis of *in vitro* NP-association with DC

WT C57BL/6 or CD40 KO BMDC (100,000/well) were plated into a 96-well flat bottom plate and incubated for 1 h at either 4°C (binding analysis) or 37°C (uptake analysis and kinetic uptake) with titrated amounts of targeted or non-targeted (PLGA-CW800-Ag/TLR3+7L)-PEG-mAbs (DC40, DEC-205, CD11c, IgG2b and IgG2a) formulations labeled with the near infrared dye (near-IR dyes, CW800). Cells were washed four times to remove residual non-bound NP. Binding, uptake and kinetic uptake of PLGA NP by DC was determined based on near-IR fluorescence using odyssey scanning (LI-COR) at 800 nm. Data analyses were corrected for the number of amount of cells per measurement via co-staining with TO-PRO® (Invitrogen) at 700 nm.

Analysis of *in vivo* NP-uptake upon vaccination

Animals were vaccinated with the CD11c, DEC-205 and CD40-targeted or non-targeted (PLGA-Ag/TLR3+7L) NP formulations containing OVA-Alexa647 (Invitrogen) by subcutaneous injection into the right flank. *In vivo* NP-uptake by cells was analyzed 48 h after vaccination by sacrificing the animals and isolating the inguinal lymph nodes and spleens. Single cell suspensions were prepared and flow cytometry was used to determine the fluorescence intensity of OVA-Alexa647 in F4/80⁺CD11b⁺CD11c⁺ DC as a measure for NP-uptake. All fluorescent-mAb used for staining were purchased from BD Pharmingen. Flow cytometry analysis was performed using a LSRII flow cytometer (BD Pharmingen) and analyzed with FlowJo software (Treestar).

***In vitro* MHC class I and II-restricted Ag presentation and T cell priming**

DC were incubated for 5 h with the various (PLGA-Ag/TLRL)-mAb formulations at the indicated concentrations of OVA-protein Ag encapsulated in NP. After Ag incubation, supernatant were harvested and cells were then further co-cultured for 72 h in the presence of OT-I and OT-II splenocytes to assess OVA-specific MHC class II and class I-restricted proliferation of naïve CD4⁺ T cells and CD8⁺ respectively. Cells were pulsed with [³H]-thymidine for the last 16 hours of culture. Samples were then counted on a TopCount™ microplate scintillation counter (Packard Instrument Co., Meridan, CT, USA). Stimulation index was used as a measure for proliferation and was calculated as the fold increase of [³H]-thymidine CPM over the CPM counts obtained with medium as negative control.

Analysis of cytokine production by DC or T cells using Enzyme-linked Immunosorbent Assay (ELISA)

DC (100,000/well) were plated into a 96-well round bottom plate and incubated for 24 h with titrated amounts of Ag. Supernatants were harvested and tested for IL-12 p70 (BD OptEIA™ MOUSE IL-12 Cat. Nr 555256), IL-2 (BD OptEIA™ MOUSE IL-2 Cat. Nr 555148), following manufacturer's instructions.

***In vivo* visualization of NP vaccines**

Nanoparticles carrying OVA labeled with the near-infrared fluorescent dye CW800 were visualized using the IVIS Spectrum preclinical *in vivo* imaging system (PerkinElmer). The fluorescent signal at the injection site was measured in time by drawing a region of interest (ROI) around the injection site and quantifying the total radiant efficiency in the 840 nm emission filter, expressed in [p/s]/ [μW/cm²]. The signal was corrected for the background signal based on an identical ROI at an irrelevant position of the mouse.

OT-I transfer and analysis of CD8⁺ T cell expansion

The spleen was taken of an OT-I mouse on a CD90.1 background, mashed on a 70 μm cell strainer to create a single-cell suspension. Then the CD8-negative cells were depleted by the CD8⁺ enrichment kit from BD. These cells were injected intravenously in the tail vein of the mice, in 200 μL PBS.

The mice were sacrificed and the inguinal LNs and the spleen were taken and mashed on a 70 µm cell strainer. The left and right inguinal LNs were pooled, as they are both vaccine-draining. The cells were then stained with 7-AAD and with fluorescently labeled antibodies against CD8b and CD90.1. The *in vivo* proliferation of the OT-I cells was analyzed by calculating the percentage of CD90.1⁺ cells within the total CD8b⁺ population, excluding all 7-AAD⁺ (dead) cells from the analysis.

Vaccination and immunization schemes

Animals were vaccinated with the various targeted or non-targeted (PLGA-Ag/TLRL) NP formulations by subcutaneous (s.c.) injection into the right flank or in the tail base region. Vaccine potency and activation of CD8⁺ T cells were studied by transferring purified CD8⁺ T cells from OT-I mice 2 days after tail-base vaccinations with different NP formulations. Priming of *in vivo* cytotoxic CD8⁺ T cells were assessed seven days after vaccination in the right-flank by transferring spleen cells prepared from congenic Ly5.1 C57BL/6 animals which were pulsed with the SIINFEKL short peptide (OVA₈/specific target cells) or ASNENMETM short peptide (FLU9/non-specific target cells). The target cells were labeled with either 10 µM (OVA) or 0.5 µM (Flu) CFSE. The cells were mixed 1:1 and 10*10⁶ total cells were injected intravenously (i.v.) into the vaccinated animals. 18 h post transfer of target cells, animals were sacrificed and single cell suspensions were prepared from isolated spleens. Injected target cells were distinguished by APC-conjugated rat anti-mouse CD45.1 mAb (BD pharmingen). *In vivo* cytotoxicity was determined by flow cytometry using the following formula: $(1 - [(CFSE\text{-peak OVA}/CFSE\text{-peak FLU})^{\text{vaccinated animals}} \times (CFSE\text{-peak OVA}/CFSE\text{-peak FLU})^{\text{non-vaccinated animals}}]) \times 100\%$.

Statistical analysis

Graph Pad Prism software version 5 was used for statistical analysis. Two-way Analysis of Variance (ANOVA) tests were used to evaluate cytokine production by DC or T cells across different concentrations of PLGA-NP containing adjuvants. Two-way ANOVA was also used to analyse differences in *in vitro* binding/uptake studies measuring NIR fluorescence. The differences in OVA-Alexa647 fluorescence upon *in vivo* uptake by immune cells were analyzed using the two-tailed unpaired Student *t* test or Mann Whitney test. Dose-response *in vitro* studies were analyzed using two-way ANOVA with Bonferroni posttests.

RESULTS

Design, preparation and characterization of PLGA NP

PLGA NP vaccines were generated using the biodegradable polymer PLGA. Figure 8.1 shows a schematic diagram of the targeted NP vaccine. The PLGA NP surface was coated with a polyethylene glycol (PEG)-lipid layer to minimize non-specific binding to cells other than DCs and to allow the incorporation of distinct DC receptors-specific Abs to effectively target mouse DCs. The morphology of PLGA NP was determined by transmission electron microscopy (TEM). Figure 8.1 shows a representative picture where the PLGA NP were uniform in size and showed spherical shape. TEM imaging clearly shows the presence of the PEG-lipid layer on the PLGA NP.

The characteristics of targeted PLGA NP containing fluorescent OVA Ag and TLR ligands (size distribution, polydispersity index, zeta potential, fluorescent Ag entrapment efficiency and amount of Abs conjugated to PLGA NP surface) are shown in Table 8.1. The encapsulation efficiency of fluorescent OVA Ag and TLRs within the PLGA NP was determined by fluorescence assay and reverse phase high performance liquid chromatography respectively (Table 8.1). Exploiting dynamic light scattering (DLS) we found that the size of PLGA NP harboring fluorescent OVA with TLR ligands varied from 192.1 ± 11.3 nm and 246.0 ± 16.1 nm. It should be noted that the conjugation of Abs to

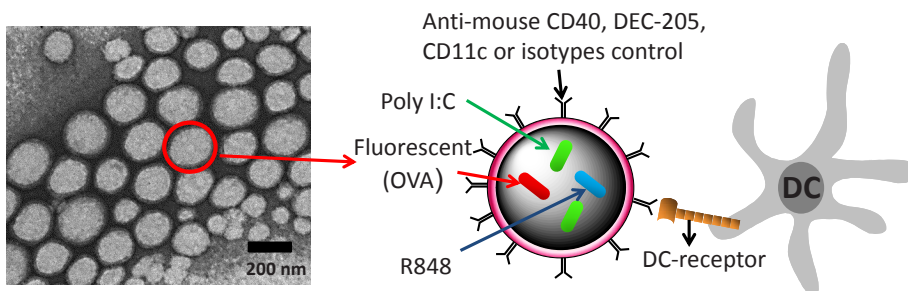


Figure 8.1 Schematic diagram of PLGA NP vaccines targeting DC-specific receptor on mouse DCs and PLGA NP analysis by TEM.

NP vaccines were generated carrying fluorescent OVA in combination with the TLR3 ligand poly I:C and the TLR7/8 ligand R848. Carriers were coated with a lipid-PEG layer to which distinct Abs (α CD40, α DEC-205, α CD11c and isotypes) were covalently attached on the PLGA NP surface. TEM image of a representative PLGA preparation. Image analysis revealed the presence of the PEG-lipid layer surrounding the NP. (Scale bar, 200 nm; magnification, 25000 x).

the PLGA NP alters the size. The hydrodynamic diameter of the PLGA NP increases when the Abs were incorporated on the PLGA NP surface. In addition, the zeta potential of Ab-coated PLGA NP was considerably less negative than the PLGA NP without Abs (Table 8.1). This reduction in the zeta potential reflects the conjugation reaction between the carboxyl group of PLGA NP and the amino groups of the Abs, providing additional evidence that the Abs were present on the PLGA NP surface. The amount of Abs present on the PLGA NP surface was in the range of $29.1 \pm 3.1 \mu\text{g}$ to $37.0 \pm 2.5 \mu\text{g}$ per mg PLGA, as determined by a Coomassie-based protein assay (see Table 8.1). All PLGA NP showed a relatively uniform size distribution, which was reflected by low polydispersity indexes (below to 0.234).

Analysis of PLGA NP binding and uptake by DC *in vitro*

DCs from wild type C57BL/6 mice were incubated with different amounts of PLGA NP (CW800-Ag/TLR3+7L)-targeted to CD40, DEC205 and CD11c receptors and isotype control (non-targeted) respectively at 4°C to determine their binding capacity towards DCs (Figure 8.2A). Fluorescence intensity was measured by Odyssey scanning as the ratio of PLGA NP containing CW800-OVA at 800 nm and the number of cell amount determined by nuclei staining at 700 nm. The ratio value indicates the level of binding of PLGA NP to the DC. A direct relation between the PLGA NP concentration and binding capacity was observed. Targeted PLGA NP showed statistically significant differences with respect to their non-targeted counterparts, being PLGA NP targeted to CD40 which presented the greatest binding capacity to the DC (Figure 8.2A).

Similar behavior was observed when the assay was performed at 37°C to analyze the uptake of PLGA NP by DCs (Figure 8.2B). Again, all the targeted PLGA NP showed statistically significant differences with respect to non-targeted NP and a direct relation among uptake and NP concentration was observed (Figure 8.2B). Additionally, when the kinetics of NP uptake by DC were studied over a 24 h period (Supporting Information Figure S8.1) a significant difference in the uptake of targeted PLGA NP was observed with respect to non-targeted PLGA NP.

Activation of DCs *in vitro* by targeted PLGA NP

The expression of CD40 and CD86, co-stimulatory molecules associated with DC-maturation, was studied by flow cytometry (Figure 8.3A). Almost the whole (> 90%) population of DCs was CD40⁺CD86⁺ double positive when PLGA NP were targeted to CD40, DEC205 and CD11c with respect to their non-targeted counterparts or soluble

Table 8.1 Physicochemical characterization of targeted and non-targeted PLGA NP, size distribution and zeta potential

Samples	Poly I:C ($\mu\text{g}/\text{mg}$ NP) (w/w) R848 ($\mu\text{g}/\text{mg}$ NP) (w/w)	Antigen ($\mu\text{g}/\text{mg}$ NP) (w/w)	PLGA NP diameter \pm S.D. (nm)	Polydispersity index \pm S.D.	Zeta potential \pm S.D. (mV)	mAbs ($\mu\text{g}/\text{mg}$ PLGA NP)
PLGA NP(OVA + Poly I:C + R848)-Non-mAbs	22 2.5	50	186.6 \pm 09.0	0.086 \pm 0.012	-34.4 \pm 6.2	---
PLGA NP(OVA + Poly I:C + R848)- α CD40	22 2.5	50	200.7 \pm 12.5	0.109 \pm 0.025	-30.8 \pm 2.3	29.1 \pm 3.1
PLGA NP(OVA + Poly I:C + R848)- α DEC-205	22 2.5	50	198.2 \pm 12.9	0.085 \pm 0.016	-28.8 \pm 2.5	32.0 \pm 3.2
PLGA NP(OVA + Poly I:C + R848)- α CD11c	22 2.5	50	194.7 \pm 11.6	0.148 \pm 0.068	-30.0 \pm 4.6	25.0 \pm 3.7
PLGA NP(OVA + Poly I:C + R848)-Isotype (IgG2a)	22 2.5	50	192.1 \pm 11.3	0.097 \pm 0.046	-26.2 \pm 2.5	34.0 \pm 2.4
PLGA NP(OVA + Poly I:C + R848)-Isotype (IgG2b)	22 2.5	50	195.4 \pm 14.3	0.122 \pm 0.049	-31.0 \pm 4.6	29.0 \pm 3.2
PLGA NP(CW800-OVA + Poly I:C + R848)-Non-mAbs	12 2	25	204.8 \pm 10.1	0.099 \pm 0.016	-36.3 \pm 1.6	---
PLGA NP(CW800-OVA + Poly I:C + R848)- α CD40	12 2	25	242.3 \pm 25.0	0.167 \pm 0.031	-30.4 \pm 2.4	32.0 \pm 2.2
PLGA NP(CW800-OVA + Poly I:C + R848)- α DEC-205	12 2	25	212.2 \pm 10.4	0.121 \pm 0.027	-31.4 \pm 2.3	28.2 \pm 3.2

PLGA NP(CW800-OVA + Poly I:C + R848)- α CD11c	12 2	25	219.8 \pm 11.1	0.114 \pm 0.022	-32.2 \pm 2.8	31.3 \pm 1.8
PLGA NP(CW800-OVA + Poly I:C + R848)-Isotype (IgG2a)	12 2	25	239.0 \pm 13.6	0.234 \pm 0.072	-29.6 \pm 1.8	30.4 \pm 1.4
PLGA NP(CW800-OVA + Poly I:C + R848)-Isotype (IgG2b)	12 2	25	232 \pm 14.2	0.194 \pm 0.058	-27.0 \pm 2.4	32.0 \pm 1.4
PLGA NP(Alexa-647-OVA + Poly I:C + R848)- Non-mAbs	20 2	15	202.5 \pm 11.4	0.094 \pm 0.042	-29.0 \pm 2.4	---
PLGA NP(Alexa-647-OVA + Poly I:C + R848)- α CD40	20 2	15	216.0 \pm 11.2	0.080 \pm 0.032	-23.2 \pm 2.9	35.0 \pm 3.1
PLGA NP(Alexa-647-OVA + Poly I:C + R848)- α DEC-205	20 2	15	218.2 \pm 13.4	0.074 \pm 0.042	-24.5 \pm 1.8	31.0 \pm 2.3
PLGA NP(Alexa-647-OVA + Poly I:C + R848)- α CD11c	20 2	15	214.6 \pm 14.1	0.064 \pm 0.032	-22.5 \pm 2.5	36.0 \pm 2.5
PLGA NP(Alexa-647-OVA + Poly I:C + R848)- Isotype (IgG2a)	20 2	15	216.8 \pm 16.1	0.074 \pm 0.022	-26.5 \pm 2.4	37.0 \pm 2.5
PLGA NP(Alexa-647-OVA + Poly I:C + R848)- Isotype (IgG2b)	20 2	15	218.6 \pm 10.1	0.084 \pm 0.024	-23.5 \pm 1.8	32.0 \pm 2.4

PLGA NPs were characterized by DLS measurements and zeta potential measurements. PLGA NPs size data represent the mean value \pm SD of ten readings from dynamic light scattering measurements. Zeta potential data represent the mean value \pm SD of five readings. The encapsulation efficiency of TLR ligands (μ g Poly I:C or R848 per mg NP) was determined by HPLC. The amount of antigens encapsulated inside of PLGA NPs (μ g antigen per mg NP) was determined by Coomassie dye protein assay. The amount of antibody introduced into the PLGA NPs was determined indirectly by Coomassie Plus Protein Assay Reagent by measuring a small aliquot from the antibody solution at the starting point and at the end of the reaction.

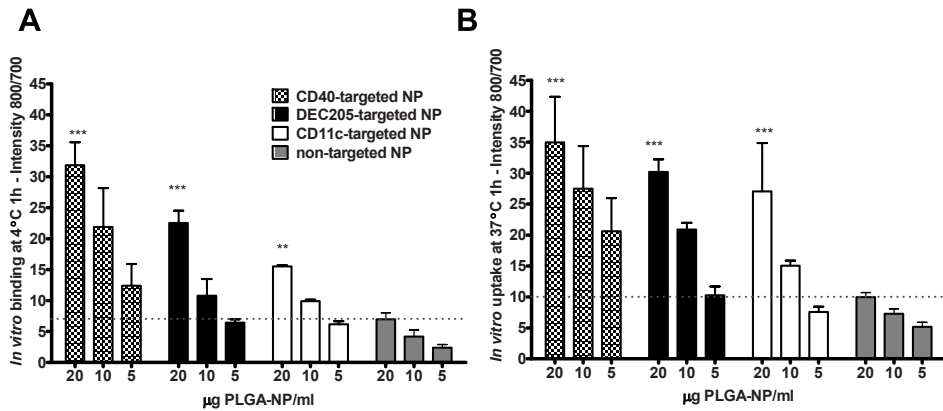
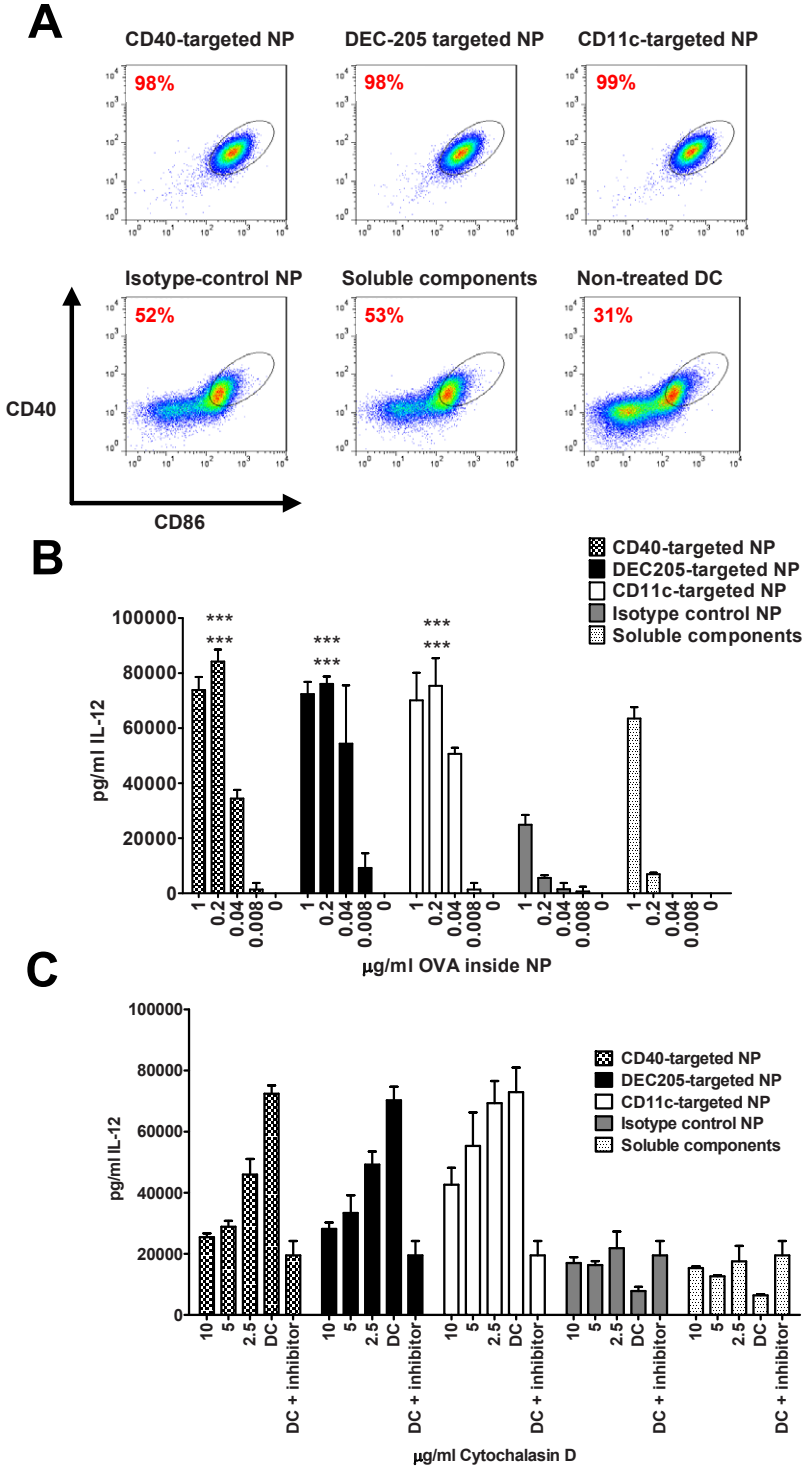


Figure 8.2 Targeting PLGA NP to DC facilitates binding and internalization compared to non-targeted NP.

WT C57BL/6 BMDC (100000 cells/well) were incubated with titrated amounts of PLGA-(Ag/TLR3+7L)- α CD40, PLGA-(Ag/TLR3+7L)- α DEC-205 and PLGA-(Ag/TLR3+7L)- α CD11c NP or isotype control (PLGA-(Ag/TLR3+7L)-non-targeted(pool of IgG2a and IgG2b bound PLGA-(Ag/TLR3+7L) NP NP-formulations for 1 h at 4°C (A) or 37°C (B). Following washing (at least four time) to remove unbound NP, cells were co-staining with DNA-binding TO-PRO[®], allowing quantification of number of cells per well and correlate with PLGA NP-binding or uptake per cells. Fluorescence intensity was measured by scanning on the Odyssey (LI-COR) and results shown the ratio of 800/700 nm fluorescence intensities of a duplicate analysis + deviation. Data are from one out of two independent experiments performed with two different batches of PLGA NP. Differences in PLGA NP-binding and uptake were analyzed applying two-way ANOVA with Bonferroni posttests, * = $P < 0.05$, ** = $P < 0.01$ and *** = $P < 0.0001$.

Figure 8.3 Improved maturation of targeted DC receptors by PLGA-(Ag/TLR3+7L) NP compared to PLGA-(Ag/TLR3+7L)-Isotype NP.

C57BL/6 BMDC (100000 cells/well) were incubated with titrated amounts of PLGA-(Ag/TLR3+7L) NP, either targeted or not, for 24 h at 37°C. Culture supernatants were harvested and the amount of IL-12 determined by ELISA (A and B). Differences in cytokine production were analyzed applying two way ANOVA with Bonferroni posttests, * = $P < 0.05$, ** = $P < 0.01$ and *** = $P < 0.0001$. Data shown are mean \pm SD from one representative experiment out of 3 independent experiments. (C) D1 dendritic cells (C57BL/6 background) were pre-incubated for 1 hr at 37°C with titrated amounts of cytochalasin D followed by a 24 h incubation with PLGA-(Ag/TLR3+7L) NP (based on 0.2 μ g/mL encapsulated OVA), either targeted to CD40, DEC-205 and CD11c or non-targeted. Indicated amounts of cytochalasin D were maintained during the 24 h incubation with NP. After incubation, culture supernatants were harvested and analyzed for IL-12 amounts by ELISA as described in *Material and methods*.



compounds which resulted in 50% or 30% CD40⁺CD86⁺ double positive cells, respectively (Figure 8.3A).

The *in vitro* production of IL-12 was also determined; DC loaded with PLGA NP targeted to the different receptors (namely CD40, DEC205 and CD11c) showed better IL-12 production with respect to the controls (Figure 8.3B). However, no activation differences were observed between the distinct formulations of targeted PLGA NP assayed for the above-mentioned receptors. Furthermore, it seems that an activation threshold exists with respect to the PLGA NP content. Thus, no differences were observed at the two highest amounts of NP used, indicated by 1 and 0.2 µg/mL of OVA, in contrast with the sharp drop observed when < 0.2 µg or lower were tested (Figure 8.3B). A lower production of IL-12 was observed using the isotype control NP and the soluble components (OVA, Poly I:C and R848 mixed) at all concentrations tested (Figure 8.3B).

Dendritic cells treated with titrated concentrations of Cytochalasin D, an inhibitor of actin polymerization which disrupts actin microfilaments associated with phagocytic uptake of exogenous material, showed a marked reduction of IL-12 production when cultured in the presence of targeted NP (Figure 8.3C). However, treatment with Cytochalasin D did not reduce the IL-12 production of DC cultured with non-targeted NP or soluble TLRs (Figure 8.3C) (not shown).

T cell activation induced *in vitro* by PLGA NP containing Ag and TLR ligands targeted to specific DCs receptors

DC treated with the different PLGA-NP vaccines were used as APCs in co-cultures with splenocytes from OT-I mice (Figure 8.4A and C) or OT-II mice (Figure 8.4B and D) to determine the CD8⁺ and CD4⁺ T cell proliferation and IFN-γ production.

T cell proliferation (expressed as T cell stimulation index) of both CD8⁺ and CD4⁺ cells were efficiently induced by DCs loaded with targeted NP but not by the non-targeted counterparts (Figure 8.4A and B). However, no significant differences in the induction of T cell proliferation were observed between DCs loaded with the different targeted NP vaccines.

Similar observations were made analyzing IFN-γ amounts in culture supernatants after 48 h of culture (Figure 8.4C and D). Noteworthy was the sharp drop in IFN-γ amounts for all targeted formulations when < 0.2 µg/mL of OVA encapsulated in NP was tested (Figure 8.4C and D).

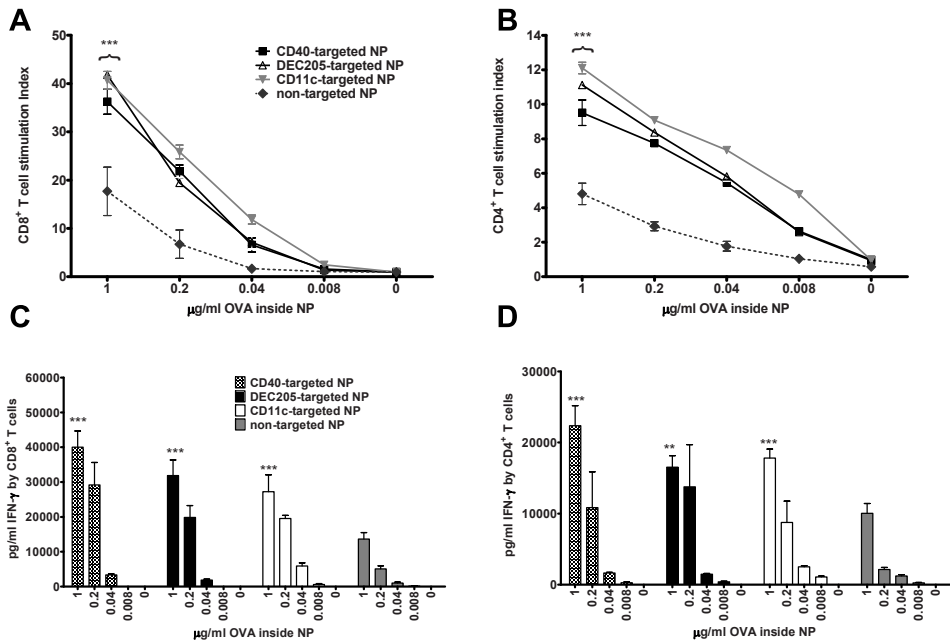


Figure 8.4 DCs loaded with CD40, DEC-205 or CD11C targeted NP containing OVA and TLR7 and 3 agonists show improved T cell stimulatory capacity compared to non-targeted controls. BMDC from C57BL/6 were incubated for 5 h at 37°C with titrated amounts of PLGA-(Ag/TLR3+7L) NP, either targeted to CD40, DEC-205 and CD11c or non-targeted. After incubation with Ag, 75% of the culture medium was removed and splenocytes (20,000 splenocytes/well in a final volume of 200 μL/well) from OT-I (A) or OT-II (B) mice were added. OVA-specific T cell proliferation was measured 72 h later by analysis of [³H]-thymidine incorporation which was added the last 16 hours of culture. Culture supernatants taken after 48 h of co-culture between Ag-loaded DC and OT-I or OT-II splenocytes were analyzed for IFN-γ levels (C and D). Differences compared to non-targeted in T cell proliferation and cytokine production at the different conditions were analyzed applying two way ANOVA with Bonferroni posttests, * = P < 0.05, ** = P < 0.01 and *** = P < 0.0001. Data shown are mean ± SEM of two independent experiments.

Vaccination of C57BL/6 mice with PLGA NP targeted to CD40, DEC-205 or CD11c receptors

Vaccination with non-targeted or CD11c, DEC-205 or CD40 targeted NP (PLGA-Ag/TLR3+7L) containing TLR3 and 7 agonists and CW800-fluorescent labeled OVA as Ag were performed by subcutaneous injection into the tail base. At the indicated time points over a period

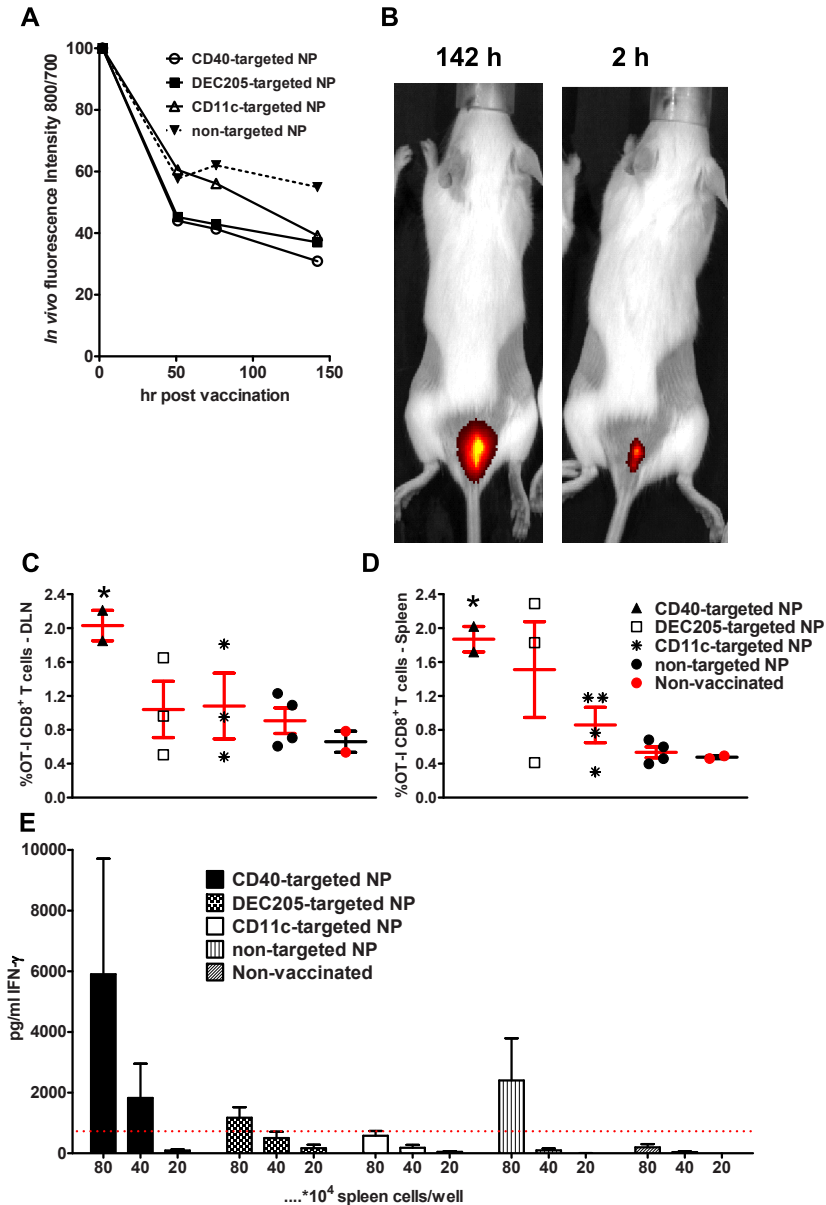


Figure 8.5 Facilitated transport out of the vaccination site results in better priming of CD8⁺ T cells by targeted PLGA NP.

Albino B6 mice were vaccinated s.c. in the tail-base region with 500 μ g of PLGA NP containing CW800 fluorescent dye labeled OVA. PLGA NP were targeted to CD40, DEC-205 and CD11c or non-targeted. At designated time points animals were anesthetized. Live imaging of the vaccination site was performed to determine the outflow of particles in time (A) and graphically quantified as fluorescence intensity (B). 48 h after vaccination, mice received $1 \cdot 10^6$ purified OT-I CD8⁺ T cells. 4 days

of 6 days (Figure 8.5A) animals were anesthetized and live imaging of the fluorescence intensity at the injection site was carried out to determine the outflow of NP in time. The fluorescent signal declined over the first 24 h to 40–60% for all the formulations, whether targeted or not. The fluorescent signal progressively decreased during the next five days by 70%, except for the non-targeted formulation which remained at 40% (Figure 8.5B).

To determine the T cell activation induced by the targeted and non-targeted PLGA NP, 48 h after vaccination, mice received 1×10^6 purified OT-I CD8⁺ T cells. Four days later mice were sacrificed and the expansion specific of CD8⁺ T cells in the draining inguinal lymph nodes (Figure 8.5C) and spleens (Figure 8.5D) was quantified by flow cytometry. CD40 targeted PLGA NP were most efficient in inducing T cell activation and expansion (Figure 8.5C and D).

Spleen cells from vaccinated animals were re-stimulated *ex vivo* with an OVA SIINFEKL-short peptide for 72 h and the production of IFN- γ was quantified in the culture supernatant (Figure 8.5E). A trend was observed that the CD40 targeted PLGA NP improved cytokine production after peptide stimulation compared to DEC205 and CD11c targeted PLGA NP but due to the high variability the differences were not statistically different (Figure 8.5E).

Vaccination of wild type mice with CD40, DEC-205 or CD11c-targeted PLGA-(Ag/TLR3+7L)-NP induces CD8⁺ T cells with potent cytotoxic capacity *in vivo*

C57BL/6 mice were vaccinated s.c. in the right flank with 10 μ g OVA encapsulated in CD40, DEC-205 or CD11c-targeted PLGA-(Ag/TLR3+7L) NP or non-targeted PLGA-(Ag/TLR3+7L) NP as a control. On day 7 post vaccination, target cells were labeled differentially with the CFSE label, pulsed with SIINFEKL short peptide (OVA_g/specific target cells) and negative control peptide as described in materials and methods. Cytotoxic activity induced by vaccination with PLGA NP targeted to DCs receptors was determined 18 h post transfer of these CFSE-Ag loaded target cells by flow cytometric analysis of single cell suspensions prepared from

later after CD8⁺ T cell transfer mice were sacrificed and the % of OT-I cells from total CD8⁺ T cells was analyzed in the DLN (C) and spleen (D). Titrated amounts of spleen cells from vaccinated animals were stimulated with SIINFEKL-peptide for 72 h and the amount of IFN- γ in culture supernatants determined by ELISA (E). Differences in fluorescence intensity were determined using student t tests (144 h post vaccination). Differences in OT-I CD8⁺ T cell priming were analyzed applying the Mann Whitney test, * = $P < 0.05$ and cytokine production by the different vaccinated groups were compared using two-way ANOVA with Bonferonni post-test, * = $P < 0.05$. Data shown are from one experiment using 2–4 mice per group.

isolated spleens of sensitized animals. Injected target cells were distinguished from host spleen cells by the congenic marker CD45.1. Flow cytometric analyses showed the nearly complete disappearance of the target cell population (Figure 8.6A), while this population remains present in the animals vaccinated with the non-targeted PLGA NP and still more clearly in non-vaccinated animals (Figure 8.6A). Vaccination with PLGA NP targeted to CD40, DEC205 or CD11c induced efficient *in vivo* cytotoxicity, about 80% specific killing, compared to 40% induced by non-targeted PLGA NP loaded with the same Ag and adjuvants, or no killing by the control non-vaccinated animals (Figure 8.6B).

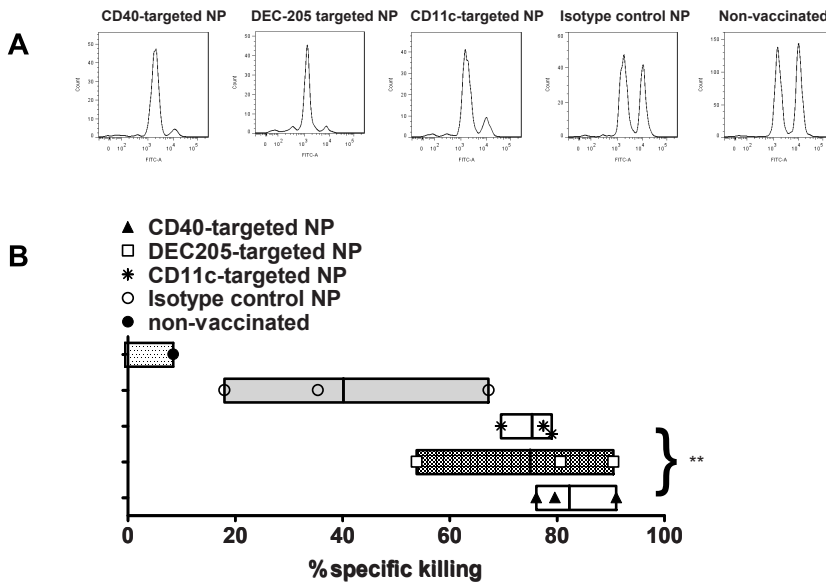


Figure 8.6 Vaccinations with PLGA-(Ag/TLR3+7L)- α CD40, DEC205 or CD11c NP induce better CD8⁺ T cells with potent *in vivo* cytotoxic capacity compared to PLGA-(Ag/TLR3+7L)-non-targeted NP.

C57BL/6 were vaccinated s.c. in the right flank with 10 μ g OVA encapsulated in CD40, DEC-205 and CD11c- targeted PLGA-(Ag/TLR3+7L) NP or non-targeted PLGA-(Ag/TLR3+7L)-non-targeted (pull of IgG2a and IgG2b) control NP. On day 7 day post vaccination, SIINFEKL-loaded CFSE^{high} OVA-specific target cells and ASNENMETM-loaded CFSE^{low} INFLUENZA-specific target cells (negative controls) were injected i.v. in a 1:1 ratio. Mice were sacrificed 18 h later and the degree of OVA-specific lysis of the target cells determined by FACS (A) and the % killing of OVA-specific target cells quantified as described in M&M. *In vivo* cytotoxicity was determined using the following formula: $(1 - [(CFSE\text{-peak OVA}/CFSE\text{-peak FLU})^{\text{vaccinated animals}} \times (CFSE\text{-peak OVA}/CFSE\text{-peak FLU})^{\text{non-vaccinated animals}}]) \times 100\%$ (B). Data shown are from one experiment consisting of 3 mice per group and differences in *in vivo* cytotoxicity of primed CD8⁺ T cells were analyzed applying an unpaired student t-test, ** = $P < 0.01$ comparing targeted NP versus non-targeted NP.

Discussion

Despite the large amount of successful protective vaccines against several infectious agents, efforts to develop effective therapeutic vaccines against cancer have been largely disappointing. However, effector mechanisms to eradicate cancer cells and pathogens are present in the immune system as has been demonstrated by the multiple examples of tumor immune surveillance^{2,3}. Therefore, cancer vaccines should potentially be able to achieve similar success as vaccines against infectious agents²⁰. However, tumors are weakly immunogenic, and therefore cancer vaccines must trigger the release of danger signals to potently activate the immune system against the tumor-associated Ags. This could be achieved by incorporating TLRs in the vaccine formulation, which induce a strong immune response²¹. In our work we have introduced Poly I:C and R848, synthetic agonists of the TLR 3 and 7 respectively, in the PLGA NP produced in the vaccine development.

Furthermore, unless DCs are cultured and loaded *in vitro*, a technically complex and costly process, cancer vaccines could be dispersed and/or degraded in body fluids (reduced half-life) and even activate inappropriate cells when administered in soluble form via injections. Therefore, in order to protect Ags from degradation and to ensure efficient delivery of the Ag to DC, we encapsulated the model protein Ag in NP coated with polyethylene glycol (PEG), which helps to avoid non-specific interactions²², and couple mAb targeted to CD40, DEC-205 or CD11c receptors expressed on the surface of DCs. Binding of these receptors can facilitate internalization, activation of signalling pathways which induce the maturation of DC and finally increase Ag presentation and enhance the induction of T cell responses²³⁻²⁵.

The mechanism of Ag internalization by DC of targeted NP was demonstrated by the strong inhibition induced by Cytochalasin D, a potent inhibitor of actin polymerization which disrupts actin microfilaments associated with phagocytosis. Therefore, internalization of NP via CD40, DEC-205 and to a lesser extent CD11c requires actin polymerization to translocate NP towards antigen processing compartments to produce peptides for presentation by MHC class I and MHC class II. Indeed, uptake of targeted NP resulted in very efficient CD8⁺ and CD4⁺ T cell priming.

Targeting strategies to improve vaccine efficacy and to achieve increased delivery to DC have been tested by passive^{26,27} and active targeting¹⁴. It was shown that DC targeting endocytic lectin receptors, such as DC-SIGN and DEC-205 with mAb coupled to PLGA NP induces strong CD8⁺ T cell responses^{28,29}, which demonstrated that exogenous Ags taken up by these receptors reach the cytoplasm by endosomal escape and are then presented to

T cells via MHC I, a process known as cross-presentation³⁰. Endocytosis via CD40 has been shown to facilitate MHC class I cross-presentation of exogenous Ag by routing internalized Ag into early endosomal compartments³¹ whereas DEC-205 targeted Ag are routed to late endosomes, compartments associated with sub-optimal MHC class I presentation, which was not confirmed in our work. CD11c is a receptor predominantly expressed on dendritic cells (DC), to which Ag targeting has been shown to induce an efficient Ag processing and presentation on MHC classes I and II products, as well as robust CD4⁺ and CD8⁺ T cell immunity³².

In this work, although CD40 showed a trend at performing slightly better in facilitating NP uptake *in vitro*, no significant differences were observed *in vivo* between the immunological responses induced by the PLGA NP targeted to different receptors (CD40, DEC-205 or CD11c). This suggests that the most important parameter in NP vaccine targeting is to facilitate and optimize endocytic capacity of the NP by DC. The inclusion of potent TLRs will subsequently lead to robust T cell responses, irrespective of the DC surface molecule targeted.

Therefore, the T cell priming capacity of the DC-targeted NP could be more related to the presence of TLR3 and 7 agonists than to the activation of targeted receptors itself, or at most they are additive. Possibly the activation by TLR ligands could be substantially higher than those induced by the receptors targeted by the PLGA NP, therefore hiding the effect of the latter. However, targeting seems essential, since non-targeted PLGA NP containing the TLR3 and 7 agonists did not show strong activation capacity both *in vitro* and *in vivo*. *In vivo* assays show that the PLGA NP dispersion is much higher in non-targeted NP, or at least targeting PLGA NP to phagocytic receptors seems to be important for uptake by DCs (Figure 8.5 and 6). Furthermore, the capacity to induce specific *in vivo* killing shows significant differences between targeted and non-targeted NP *in vivo* (Figure 8.6B) indicating that targeted NP can prime specific cytotoxic CD8⁺ T cells from the endogenous naïve T cell repertoire.

To investigate the influence of the target specificity of PLGA NP in the whole body biodistribution *in vivo*, NP were loaded with Alexa-647-OVA (fluorescent marker). 48 h post-injection mice were sacrificed and the main organs were harvested. PLGA NP can be quickly cleared from the blood by the reticulo-endothelial system or can remain in organs, such as the liver, lung and spleen, for prolonged periods of time. Design considerations, such as size, shape, surface coating and dosing, can be manipulated to prolong blood

circulation and enhance treatment efficacy, but nonspecific distribution has thus far been unavoidable. It has been described that NP remained detectable in the brain, heart, kidney, liver, lungs, and spleen after 7 days³³⁻³⁵. In our work, no obvious differences in tissue biodistribution of PLGA NP targeted to the CD11c, DEC-205 and CD40 receptors, or non-targeted (isotype control) were observed after 48 h (Supporting Information Figure S8.2). This suggests that, despite the high numbers of PLGA NP draining freely throughout the body and being available for uptake in the major organs, PLGA NP are more efficiently scavenged by DCs when carrying receptor-specific Abs. In draining lymph nodes and other lymphoid organs small differences in fluorescence intensity in favor of specific targeted NP were observed (Supporting Information Figure S8.3).

In conclusion, we present here a study using PLGA NP-vaccines containing an Ag model and TLR agonist, as adjuvants, coated with mAb targeted to specific receptors on DCs. Targeted NP have shown to be a potent system to induce strong immune responses, both CD4 and CD8 *in vitro* and *in vivo*. Due to the flexibility of the PLGA to encapsulate multiple polypeptide Ags, this is a versatile system to develop NP-vaccines tailored to different types of tumors.

Acknowledgements

The authors wish to thank the technicians of the LUMC Radiology Department for assistance. This work was financially supported by the VIDI personal grant (project number 723.012.110), BrainPath (PIAPP-GA-2013-612360) and CTMM project Cancer Vaccine Tracking (03O-302).

References

1. Dunn GP, Bruce AT, Ikeda H, Old LJ, Schreiber RD 2002. Cancer immunoediting: from immunosurveillance to tumor escape. *Nature immunology* 3(11):991-998.
2. Swann JB, Smyth MJ 2007. Immune surveillance of tumors. *The Journal of clinical investigation* 117(5):1137-1146.
3. Kim R, Emi M, Tanabe K 2007. Cancer immunoediting from immune surveillance to immune escape. *Immunology* 121(1):1-14.
4. Hutchings CL, Gilbert SC, Hill AV, Moore AC 2005. Novel protein and poxvirus-based vaccine combinations for simultaneous induction of humoral and cell-mediated immunity. *Journal of immunology* 175(1):599-606.
5. Paschen A, Eichmuller S, Schadendorf D 2004. Identification of tumor antigens and T-cell epitopes, and its clinical application. *Cancer immunology, immunotherapy : CII* 53(3):196-203.
6. Spagnoli GC, Adamina M, Bolli M, Weber WP, Zajac P, Marti W, Oertli D, Heberer M, Harder F 2005. Active antigen-specific immunotherapy of melanoma: from basic science to clinical investigation. *World journal of surgery* 29(6):692-699.
7. Banchereau J, Briere F, Caux C, Davoust J, Lebecque S, Liu YJ, Pulendran B, Palucka K 2000. Immunobiology of dendritic cells. *Annu Rev Immunol* 18:767-811.
8. Celluzzi CM, Mayordomo JI, Storkus WJ, Lotze MT, Falo LD, Jr. 1996. Peptide-pulsed dendritic cells induce antigen-specific CTL-mediated protective tumor immunity. *The Journal of experimental medicine* 183(1):283-287.
9. Steinman RM 1991. The dendritic cell system and its role in immunogenicity. *Annual review of immunology* 9:271-296.
10. Delamarre L, Mellman I 2011. Harnessing dendritic cells for immunotherapy. *Seminars in immunology* 23(1):2-11.
11. Blander JM, Medzhitov R 2006. Toll-dependent selection of microbial antigens for presentation by dendritic cells. *Nature* 440(7085):808-812.
12. Schlosser E, Mueller M, Fischer S, Basta S, Busch DH, Gander B, Groettrup M 2008. TLR ligands and antigen need to be coencapsulated into the same biodegradable microsphere for the generation of potent cytotoxic T lymphocyte responses. *Vaccine* 26(13):1626-1637.
13. Wille-Reece U, Flynn BJ, Lore K, Koup RA, Kedl RM, Mattapallil JJ, Weiss WR, Roederer M, Seder RA 2005. HIV Gag protein conjugated to a Toll-like receptor 7/8 agonist improves the magnitude and quality of Th1 and CD8+ T cell responses in nonhuman primates. *Proceedings of the National Academy of Sciences of the United States of America* 102(42):15190-15194.
14. Tacken PJ, de Vries IJ, Torensma R, Figdor CG 2007. Dendritic-cell immunotherapy: from ex vivo loading to in vivo targeting. *Nat Rev Immunol* 7(10):790-802.
15. Rolink A, Melchers F, Andersson J 1996. The SCID but not the RAG-2 gene product is required for S mu-S epsilon heavy chain class switching. *Immunity* 5(4):319-330.

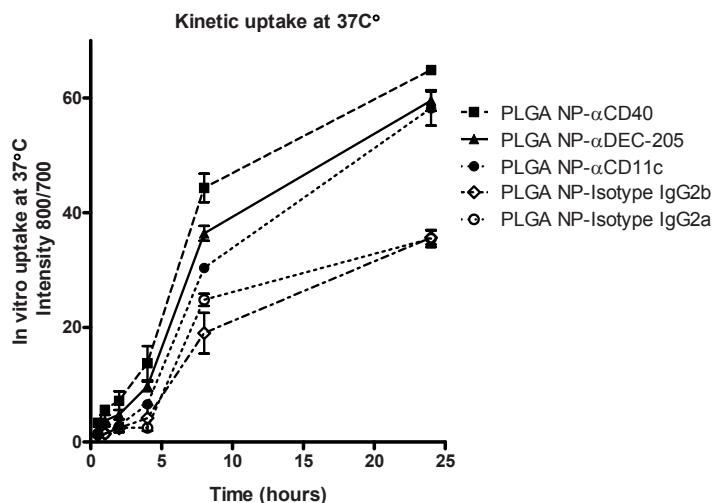
16. Cruz LJ, Tacke PJ, Rueda F, Domingo JC, Albericio F, Figdor CG 2012. Targeting nanoparticles to dendritic cells for immunotherapy. *Methods in enzymology* 509:143-163.
17. Cruz LJ, Tacke PJ, Bonetto F, Buschow SI, Croes HJ, Wijers M, de Vries IJ, Figdor CG 2011. Multimodal imaging of nanovaccine carriers targeted to human dendritic cells. *Molecular pharmaceutics* 8(2):520-531.
18. Rosalia RA, Quakkelaar ED, Redeker A, Khan S, Camps M, Drijfhout JW, Silva AL, Jiskoot W, van Hall T, van Veelen PA, Janssen G, Franken K, Cruz LJ, Tromp A, Oostendorp J, van der Burg SH, Ossendorp F, Melief CJ 2013. Dendritic cells process synthetic long peptides better than whole protein, improving antigen presentation and T-cell activation. *European journal of immunology* 43(10):2554-2565.
19. Moore MW, Carbone FR, Bevan MJ 1988. Introduction of soluble protein into the class I pathway of antigen processing and presentation. *Cell* 54(6):777-785.
20. Umar A, Dunn BK, Greenwald P 2012. Future directions in cancer prevention. *Nature reviews Cancer* 12(12):835-848.
21. Heine H, Lien E 2003. Toll-like receptors and their function in innate and adaptive immunity. *International archives of allergy and immunology* 130(3):180-192.
22. Cruz LJ, Tacke PJ, Fokkink R, Joosten B, Stuart MC, Albericio F, Torensma R, Figdor CG Targeted PLGA nano- but not microparticles specifically deliver antigen to human dendritic cells via DC-SIGN in vitro. *J Control Release* 144(2):118-126.
23. Geijtenbeek TB, Gringhuis SI 2009. Signalling through C-type lectin receptors: shaping immune responses. *Nature reviews Immunology* 9(7):465-479.
24. Elgueta R, Benson MJ, de Vries VC, Wasiuk A, Guo Y, Noelle RJ 2009. Molecular mechanism and function of CD40/CD40L engagement in the immune system. *Immunological reviews* 229(1):152-172.
25. Figdor CG, van Kooyk Y, Adema GJ 2002. C-type lectin receptors on dendritic cells and Langerhans cells. *Nature reviews Immunology* 2(2):77-84.
26. Zhang Z, Tongchusak S, Mizukami Y, Kang YJ, Ijji T, Touma M, Reinhold B, Keskin DB, Reinherz EL, Sasada T 2011. Induction of anti-tumor cytotoxic T cell responses through PLGA-nanoparticle mediated antigen delivery. *Biomaterials* 32(14):3666-3678.
27. Manolova V, Flace A, Bauer M, Schwarz K, Saudan P, Bachmann MF 2008. Nanoparticles target distinct dendritic cell populations according to their size. *European journal of immunology* 38(5):1404-1413.
28. Raghuvanshi D, Mishra V, Suresh MR, Kaur K 2012. A simple approach for enhanced immune response using engineered dendritic cell targeted nanoparticles. *Vaccine* 30(50):7292-7299.
29. Tacke PJ, Figdor CG 2011. Targeted antigen delivery and activation of dendritic cells in vivo: steps towards cost effective vaccines. *Seminars in immunology* 23(1):12-20.
30. Burgdorf S, Kurts C 2008. Endocytosis mechanisms and the cell biology of antigen presentation. *Current opinion in immunology* 20(1):89-95.

31. Chatterjee B, Smed-Sorensen A, Cohn L, Chalouni C, Vandlen R, Lee BC, Widger J, Keler T, Delamarre L, Mellman I 2012. Internalization and endosomal degradation of receptor-bound antigens regulate the efficiency of cross presentation by human dendritic cells. *Blood* 120(10):2011-2020.
32. Castro FV, Tutt AL, White AL, Teeling JL, James S, French RR, Glennie MJ 2008. CD11c provides an effective immunotarget for the generation of both CD4 and CD8 T cell responses. *European journal of immunology* 38(8):2263-2273.
33. Almeida JP, Chen AL, Foster A, Drezek R 2011. In vivo biodistribution of nanoparticles. *Nanomedicine* 6(5):815-835.
34. Sa LT, Albernaz Mde S, Patricio BF, Falcao MV, Jr., Coelho BF, Bordim A, Almeida JC, Santos-Oliveira R 2012. Biodistribution of nanoparticles: initial considerations. *Journal of pharmaceutical and biomedical analysis* 70:602-604.
35. Semete B, Booyesen L, Lemmer Y, Kalombo L, Katata L, Verschoor J, Swai HS 2010. In vivo evaluation of the biodistribution and safety of PLGA nanoparticles as drug delivery systems. *Nanomedicine* 6(5):662-671.

Supporting Information

Analysis of PLGA NP kinetic uptake by DC *in vitro*

DCs from wild type C57BL/6 mice were incubated with different PLGA NP (CW800-Ag/TLR3+7L)-targeted to CD40, DEC205 and CD11c receptors and isotype control (non-targeted) respectively at 37°C to determine their kinetic of internalization capacity towards DCs (Supporting Information Figure S8.1). Thereby, the kinetics uptake was studied during 24 h. Fluorescence intensity was measured by odyssey scanning by the ratio of PLGA NP containing CW800-OVA at 800 nm and the number of cell amount determined by nuclei staining at 700 nm. The ratio value indicates the level of uptake of PLGA NP to DC. A direct relation between the PLGA NP concentration and uptake capacity was observed. Targeted PLGA NP showed statistically significant differences with respect to their non-targeted counterparts.

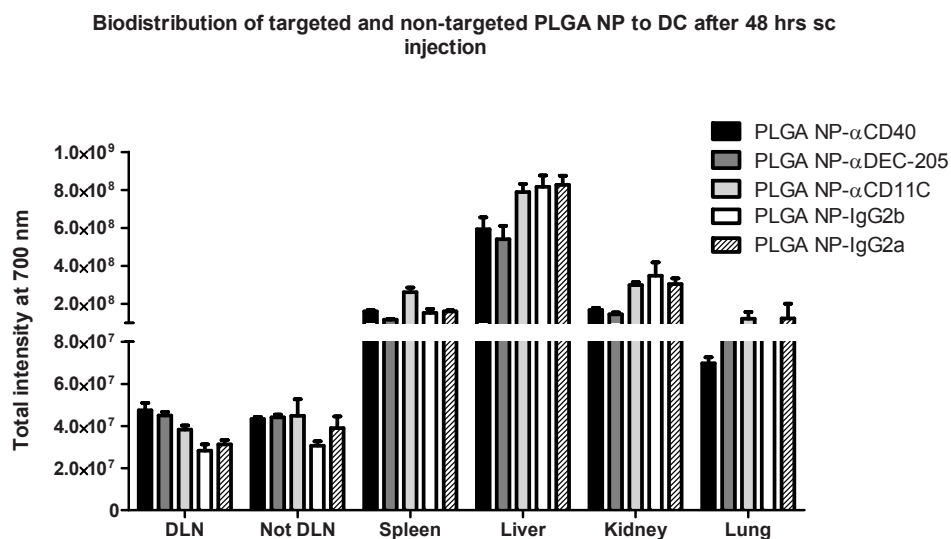


Supporting Information Figure S8.1 Kinetic uptake of targeting NP to DC improves internalization compared to non-targeted NP.

WT C57BL/6 BMDC (100000 cells/well) were incubated with fixed amounts of 5 μ g/mL PLGA-(Ag/TLR3+7L)- α CD40, PLGA-(Ag/TLR3+7L)- α DEC-205 and PLGA-(Ag/TLR3+7L)- α CD11c NP or isotype control (PLGA-(Ag/TLR3+7L)-IgG2a and PLGA-(Ag/TLR3+7L)-IgG2b) NP-formulations at distinct time points at 37°C. Following washing for the removal of unbound PLGA NP cells were co-stained with DNA-binding TO-PRO[®], allowing quantification of number of cells per well and correlation with PLGA NP-binding or uptake per cells. Fluorescence intensity was measured by scanning on the Odyssey (Li-Cor) and results show the ratio of 800/700 nm fluorescence intensities of a duplicate analysis + deviation. Data are from one out of two independent experiments performed with two different batches of PLGA NP.

Biodistribution of targeted and non-targeted PLGA NP

No obvious differences in tissue biodistribution of PLGA NPs targeted to the CD11c, DEC-205 and CD40 receptors, or non-targeted (isotype control) were observed after 48 h (Supporting Information Figure S8.2). This suggests that, despite the fact that high numbers of PLGA NPs drain freely throughout the body and are available for uptake, PLGA NP are more efficiently scavenged by DCs when carrying receptor-specific Abs. Although PLGA NP were mainly found in major organs of the body as previously described, in draining lymph nodes (DLN) and other lymphoid organs differences in fluorescence intensity in favor of specific targeted NP were observed.

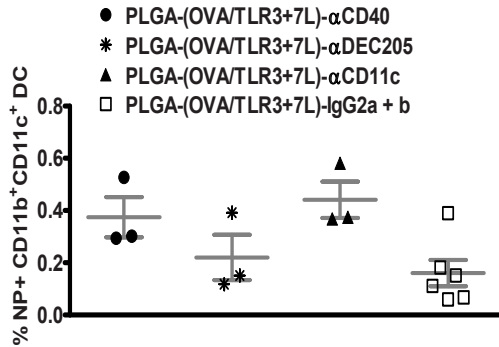


Supporting Information Figure S8.2 Biodistribution of targeting and non-targeted PLGA NP.

Mice were vaccinated s.c. with 10 μ g of Alexa-647-OVA. Mice were sacrificed 48 h post-injection and the main organs were harvested. Tissue biodistribution profile of targeted and non-targeted PLGA NPs harboring Alexa-647-OVA was determined. Relative fluorescent values were determined for each group depicted as mean \pm SEM (D).

Better *in vivo* DC-uptake of targeted PLGA-(Ag/TLR3+7L) NP compared to non-targeted PLGA NP

This suggests that high numbers of PLGA NPs are specifically taken up by DCs in the spleen. Therefore, PLGA NP are more efficiently scavenged by DCs when carrying receptor-specific Abs (Supporting Information Figure S8.3).



Supporting Information Figure S8.3 Improved *in vivo* DC-uptake by targeted PLGA-(Ag/TLR3+7L) NP compared to isotype control and non-targeted PLGA NP.

C57BL/6 animals were vaccinated s.c. in the right flank with 10 µg OVA-Alexa647 encapsulated in PLGA-(Ag/TLR3+7L)-αCD40, PLGA-(Ag/TLR3+7L)-αDEC-205 or PLGA-(Ag/TLR3+7L)-αCD11c NP, as well as with non-targeted PLGA-(Ag/TLR3+7L)-IgG2a and PLGA-(Ag/TLR3+7L)-IgG2b NP. Animals were sacrificed 48 hr post-vaccination and the Spleen harvested and single-cell suspensions prepared. Analysis by flow cytometry of the different immune cell populations which were positive for Alexa-647 fluorescence was performed by staining cells with various fluorescent antibodies. Results shown are from one experiment using 3 mice per group.



Chapter 9

Discussion



In this thesis we described our studies aimed at optimizing the efficacy of synthetic long peptide (SLP) vaccines via the encapsulation in Poly-(lactic-co-glycolic acid) (PLGA) particles. Encapsulation in biodegradable PLGA particles could serve to improve the delivery of the SLP to professional antigen presenting cells (APC), allow better control of the pharmacokinetics and biodistribution of the vaccine and finally, reduce the therapy related side effects associated with the current (pre-)clinical procedure of administering SLP vaccines delivery emulsified in water-in-oil preparations.

Immunotherapy based on SLP-vaccines has resulted in strong tumor specific immune response¹⁻⁴ and importantly, improved clinical benefit in patients with pre-malignant lesions⁵.

SLPs used as vaccines are overlapping synthetic peptides of 15–35 amino acids; thus considerably longer than the minimal CTL-epitopes of 8–9 amino acids. SLP vaccines will 1) cover the entire sequence of the native TAA-encoding protein to which an immune response is targeted. SLPs 2) require internalization and processing by DCs for optimal presentation in MHC class I and class II molecules^{3,6,7}. 3) SLP vaccines makes the necessity for HLA-typing of cancer patients obsolete because internalization of overlapping peptides by APCs allows natural epitope processing and selection in vivo based on the patient's own HLA-profile. APC-specific processing of SLPs will 4) facilitate simultaneous priming of T cells against multiple epitopes, both dominant and sub-dominant. Thus vaccinations will result in a broad T-cell response which decreases the chance of tumor escape related to loss of expression of immuno-dominant TAA-epitope⁸⁻¹¹. With each novel TAA discovered/described, SLP-vaccines targeting this TAA can be manufactured in advance, in large quantities and under the required strict GMP-quality standards making SLP-vaccines a clinically and pharmaceutically attractive therapeutic compound.

One important drawback associated with SLP-vaccines is their current form of administration in montanide, a clinical grade water-in-oil (w/o) emulsion. Montanide and Incomplete Freund's Adjuvant (IFA), the emulsion used for pre-clinical studies, consist of mineral oils with mannide monooleate as a surfactant emulsified with saline.

Aside from its slow release characteristics and protection of the antigen for degradation, w/o emulsions induce local inflammation and attraction of immune cells to the site of injection¹². Montanide however causes significant side-effects at the site of injection^{5,13}. Overwijk et al. showed that short peptide vaccines administered in w/o emulsions lead to poor tumor bed infiltration by activated CD8⁺ T cells which was a consequence of

the primed CD8⁺ T cells being “trapped” in the high inflammatory environment at the injection site containing the water-in-oil emulsion Ag depot¹⁴. Interestingly, substituting short peptide vaccines with SLP-vaccines abrogated this negative effect and resulted in superior tumor control.

The aim of this Ph.D project was to devise an alternative method of delivery which overcomes the drawbacks associated with the use of Montanide. For this purpose we explored the use of PLGA (nano)particles (NP) as a delivery vehicle for SLP. Several important aspects of SLP encapsulated in PLGA NP (PLGA-SLP) were assessed in this thesis; from the pharmaceutical formulation to the immunological characterization of different PLGA-SLP preparations.

Together, the data presented in this thesis show that PLGA-NP mediated delivery of SLP is a very efficient method to target, load and mature Dendritic cells (DCs) as immune stimulatory compounds can be co-encapsulated with the vaccine Ag.

Although the results of these studies have been discussed in detail in the separate chapters preceding this general discussion, some remaining points will be discussed below including the applicability of PLGA particles vaccines to improve SLP-based immunotherapy and the tasks which need to be overcome to successfully translate this promising therapeutic application to the clinic.

Efficient internalization and processing of vaccine Ag by DCs is an important aspect to consider when developing peptide vaccines for therapy against cancers. The use of synthetic long peptide (SLP) vaccines based on the elongation of the N- and/or C-terminus^{15,16} of the minimal cytotoxic CD8⁺ T cell or CD4⁺ T cell peptide epitopes were shown by our group^{5,17-20} and others^{2,21-23} to elicit, robust and sustained *in vivo* T cell responses with the capacity to control the growth of experimental tumors and eradicate pre-malignant lesions of the vulva. In patients with late-stage cancers, SLP-vaccines in the majority of cases failed to induce durable clinical responses even though the administration of the vaccines strongly enhanced specific immunity to tumor associated antigens (TAA)²⁴. SLP-vaccines have also been studied in combinatorial approaches with DNA-vaccines as a therapy against AIDS^{25,26}. These studies have led to encouraging observations; the vaccines elicited high frequencies of simian immunodeficiency virus-specific IFN- γ -positive T cells which could afford partial protection against a subsequent viral challenge.

To summarize, the use of SLP-vaccines leads to the potent CD4⁺ and CD8⁺ T cell responses with broad a cytokine profile and anti-tumor effector functions. Importantly, administering

cocktails of overlapping SLP covering the whole sequence of the native protein more effectively boosts the immune system when compared to vaccination with the native protein²⁷. Nevertheless, owing to the low clinical benefit in cancer patients, it is clear that therapies based on SLP-vaccines require optimization. To proceed in this process, it is vital to understand how DCs “handle” long peptide Ag.

In **chapter 2** we showed the superior capacity of both mouse and human DCs to cross-present long peptides in MHC class I molecules in contrast to whole protein Ag. Interestingly, we were able to detect SLP at early time-points outside of endo-lysosomes implying that SLP internalized from the extracellular environment are translocated to the cytosol very fast once inside the DC. We were puzzled by this observation and considered the possibility that the long peptides directly access the cytosol via passive diffusion through the cell membrane. Others have shown that facilitated Ag-delivery into the cytosol endows even non-professional APC with MHC class I cross-presentation capacity²⁸ which would suggest that all immune cells can potentially cross-present SLP. However, internalization via passive diffusion of SLP into the cytosol through the cell membrane is unlikely; *in vitro* and *ex vivo* MHC class I Ag cross-presentation was specifically detected only when DCs were used as APC (**chapter 2**, Figure 2.5) and not by other immune cells, such as B cells. The transport of SLP into the cytosol was recently described by Menager et al. who using human DCs established a role for the ER-associated degradation machinery (ERAD)-related protein p97/VCP in the transport of SLP from early endosomes to the cytosol²⁹. We also studied the method of SLP internalization using murine and human DCs. But the uptake and MHC class I cross-presentation of SLP(-OVA_{24aa}) by DC cultured in the presence of Filipin (caveolae-dependent endocytosis), dimethyl amiloride (macropinocytosis), monodansylcadavanine (inhibitor of clathrin-mediated endocytosis) or cytochalasin D (inhibitor of actin polymerization dependent phagocytosis) were inconclusive. Another group, using cytochalasin B, another inhibitor of receptor-mediated endocytosis, showed, that treatment of human DCs during SLP-Ag loading decreased, but not fully blocked, CD8⁺ T cell activation³⁰ demonstrating that DC internalize long peptides at least partially via a yet unknown endocytic receptor.

Taken the data described in **chapter 4** into consideration one can conclude that MHC class I Ag cross-presentation by DC of long peptides or protein Ag is influenced by the capacity to rapidly internalize large amounts of Ag and the localization of the Ag inside the cell post-internalization. Soluble SLP (sSLP) are taken up much faster by DC than whole protein resulting in better MHC class I and II Ag presentation. Soluble proteins in contrast are

internalized slower and collect inside endolysosomal compartments where it poorly gains entry in the cytosol resulting in poor MHC class I and II presentation. The poor translocation of proteins into the cytosol is likely related to the much larger size compared to SLP (43 kD vs 2.4 kD). Size of an Ag critically determines the extent of transport to the cytosol³¹.

Despite of the high amounts of sSLP internalized in the first hours, peptides were barely detectable inside the cytosol after 24 hr suggesting near complete degradation by ubiquitin proteasome system (UPS)^{32,33}. Interestingly, encapsulation of SLP in PLGA-NP seems to re-route or, alternatively, store the SLP inside the endo-lysosomal compartments where it can be detected up to the 72 hr post Ag loading. This observation suggests that the Ag present inside endo-lysosomal compartments is protected from the rapid degradation by the UPS as occurs with sSLP. This mechanism of sustained antigen presence in storage compartments has also been observed using immunocomplexed protein and TLR-SLP conjugates³⁴.

The prolonged CD8⁺ T cell activation observed using PLGA-SLP points to the possibility that the internalized NP gradually releases the encapsulated SLP inside the endo-lysosomal compartments, via hydrolysis of the polymer. The released SLP is then transported into the cytosol which results in the continuous proteasome processing and sustained MHC class I Ag presentation. The enhanced MHC class I presentation observed using PLGA-SLP compared to sSLP is most probably related to the sheer higher amounts of Ag taken up through phagocytosis of NP compared to sSLP. DCs loaded with PLGA-SLP showed modest capacity to sustain *in vivo* CD8⁺ T cell responses. Co-encapsulation of Pam3CSK4, a TLR2 agonist, significantly enhances the capacity for DCs to prolong MHC class I Ag presentation and CD8⁺ T cell activation *in vivo*. TLR stimulation promotes Ag processing and increases the half-life of MHC class I molecules on the cell surface³⁵⁻³⁷ which together with the prolonged presence of PLGA-SLP/TLR2L inside endolysosomal compartments can account for the sustained CD8⁺ T cell activation we described.

For successful implementation of PLGA-NP as a delivery vehicle for SLP-vaccines in the clinic, the pharmaceutical formulation should be straightforward, reproducible and meet GMP quality requirements and regulations. Of importance, PLGA-NP should be applicable to encapsulate cocktails of various SLP with different physicochemical properties, for example the overlapping long peptides encoding the HPV-16 oncoproteins. Our initial attempts to successfully encapsulate the model Ag, SLP-OVA_{24aa} using the well-known “double emulsion method with solvent evaporation” technique commonly used to encapsulate

proteins or short peptides³⁸⁻⁴² in PLGA-particles required considerable modifications, as we reported in **chapter 3**. Several formulation parameters were modified, especially the inner and outer emulsion compositions which led to successful encapsulation of SLP-OVA_{24aa}. One important advantage of PLGA-particles is the capacity to control the release kinetics of the encapsulated Ag from the particles upon s.c. administration. Ag dosing over time *in vivo* is crucial as it determines the breadth of an immune response⁴³. With our novel PLGA-NP formulation method we were able to encapsulate SLP-OVA_{24aa} with up to 40% encapsulation efficiency, exhibiting minimal burst release, and a total peptide release of circa 30% over the first 24 hr. We applied the novel formulation method to encapsulate SLP-OVA_{17aa} and two versions of gp100-SLP encoding for an immunodominant CTL-epitope present in this melanoma associated differentiation Ag⁴⁴. Thus different SLP can be successfully encapsulated inside PLGA-NP using our novel “double emulsion and evaporation” formulation technique. This PLGA-NP formulation will allow us to encapsulate the overlapping SLP encoding the HPV-E6 or HPV-E7 proteins inside PLGA-NPs and test these vaccines in pre-clinical models or on patient peripheral blood samples.

The use of particulate vaccine delivery systems is considered a promising method to achieve the desired robust and potent T cell responses that is sometimes lacking when administering vaccines in soluble form emulsified in Montanide or mixed in PBS.

The unexpected challenges at the start of the Ph.D project associated with the poor encapsulation of SLP-OVA_{24aa} and SLP-OVA_{8aa} initiated a parallel project pursuing the use of liposome based vaccine delivery strategies, which were argued to offer facilitated incorporation of SLPs compared to PLGA-NP delivery systems. Liposomes encapsulating the SLP-MUC-1_{25aa} and MPLA-4, L-BLP25, have led to significant survival benefits in stage III non-small cell lung cancer patients compared to the patients receiving the standard treatment alone⁴⁵. Despite these promising results, the authors describe that liposomal formulation includes several disadvantages that possibly limit its application in large clinical settings. Most of these disadvantages are related to the pharmaceutical formulation of the liposomes; such as laborious and expensive procedures, difficulties to scale-up the formulation process and production of sterile products. In contrast to liposomes, the formulation process of PLGA-NPs and scaling-up are easier and cost-effective⁴⁶. Of importance, the use of PLGA co-polymers provides extra advantages over liposomes related to the ability to manipulate several physicochemical properties of the particle carrier and control the degradation rate and Ag release kinetics as discussed before in more detail in **chapter 3**.

Regarding the encapsulation of protein, it was convincingly shown that PLGA-particles are superior carriers to induce T cell responses with the capacity to control a bacterial challenge. In this study, PLGA-NP and Liposome-NP induced similar antibody titers, however liposomes failed to trigger a robust T cell response, whereas PLGA-particles showed potent capacity to induce IFN- γ producing, memory phenotype, CD8⁺ T cells^{35-37,47}. However, results obtained with protein Ag do not necessarily predicts results using long peptides as vaccine-Ag. Therefore, the ongoing studies with liposomes in our group, will address which particulate carrier is the best suited for the *in vivo* delivery of SLP-vaccines.

In **chapter 6**, we studied the role of particle size to induce an immune response. Our results point towards the use of NPs instead of microparticles (MPs) for the purpose of cancer immunotherapy as the first induced much better CD8⁺ T cell responses. Other studies have led to similar conclusions^{48,49}. Taking into consideration particle size, Ag release kinetics, adjuvanticity and *in vivo* uptake we can conclude that a robust CD8⁺ T cell response is obtained by using nanoparticles, but not microparticles, co-encapsulating potent immunostimulatory agents (**chapter 4, 5 and 8**). The formulated particles should have a low burst release of the encapsulated Ag for optimal MHC class I presentation (**chapter 3**), to allow uptake of the particle co-encapsulating Ag and TLR⁵⁰ by APC. Succeeding the initial phase when the PLGA-particles comes in contact with an aqueous environment, the release of the encapsulated Ag should be gradual, in other words “slow” rather than “fast”, to induce an humoral response and most likely also efficient CD8⁺ T cell responses⁴⁷. Interestingly, we observed better CD8⁺ T cells responses using PLGA-NP in comparison to IFA as a vaccine delivery system. Thus, our data and other studies^{47,51} support the application of PLGA-NP delivery systems for vaccination purposes. Biodegradable NPs are a suitable replacement for w/o emulsions or Aluminium based adjuvants for the delivery of protein vaccines for cancer immunotherapy.

In **chapter 7** and **chapter 8** we explored novel targeting strategies to enhance the immune activating potency of PLGA-NP based vaccines. CD40, DEC-205 and CD11c molecules, which are highly expressed on the cell surface of DCs were the receptors of choice for these studies. Given the essential role that CD40 molecules have in DC activation and subsequent T cell priming, we hypothesized that delivering PLGA-NP encapsulated Ag via CD40 would convey two complementary effects; 1) enhance DC activation and 2) improve Ag uptake, MHC class I and II presentation and subsequent T cell priming.

Ag delivery via the targeting of the C-type lectin DEC-205 has been successfully used by many others and is therefore an established method to enhance T cell responses with tumor controlling properties⁵²⁻⁵⁴. Interestingly, DEC-205 has also been used a targeting molecule with the aim to facilitate the induction of immune tolerance, through the priming of Ag-specific Tregs^{36,37}. DEC-205 targeting promotes vaccine delivery to CD8 α ⁺ secondary lymphoid organ resident DCs and CD103⁺ migratory skin-resident DC. Especially the latter has been associated with strong induction of Ag-specific immune tolerization⁵⁵⁻⁵⁷. CD11c, an integrin, likewise has been studied in the murine system as a method to increase delivery of several types of vaccines to DC to potentiate tumor immunity. Indeed, targeting DC via CD11c significantly enhances anti-tumor immune responses^{58,59} or anti-viral immunity⁶⁰. We compared the efficacy to prime CD8⁺ T cells injecting particles containing TLR7 and TLR8 and protein Ag targeted to these three receptors vs the control formulation without a targeting mAb. Our results point to the importance of targeting to achieve efficient priming of T cell responses as the non-targeted NPs poorly triggered CD8⁺ T cell activation. Interestingly, we did not detect significant differences to stimulate OT-I CD8⁺ T cells or induce *in vivo* cytotoxicity by endogenous T cells using the three targeting strategies.

As we discussed in **chapter 8**, it is possible that the efficacy of cancer immunotherapy based on PLGA-NPs is not critically dependent on the DC subtype targeted as has been shown for soluble Ag⁶¹ as long as the vaccine is efficiently transferred to the early endosomes^{62,63}. Indeed, the necessity to target DC has been questioned recently by Figdor and colleagues⁶⁴. One study analysing the requirement for DC to prime cytotoxic T cells showed conclusively that CD8⁺ T cells could be primed after vaccination of PLGA-particles in the absence of CD8 α ⁺ and CD103⁺ DCs implying the *in vivo* other APC, considered to be inferior cross-presenting cells are playing a role in the priming of vaccine Ag-specific CD8⁺ T cells. In fact, the same study pointed to the priming of CD8⁺ T cells by M Φ and CD8 α ⁻ DCs. However our data in **chapter 7** show that upon injection, CD40-targeted PLGA-NP preferably bound CD11c⁺CD8 α ⁺ DCs but poorly bound M Φ or CD8 α ⁻ DCs.

In conclusion, targeting PLGA-NP to DC is essential to stimulate a robust CD8⁺ T cell mediated response. But the critical importance of targeting only one DC subtype based on the specific expression of a specific cell-surface receptor, for optimal immune activation, remains to be studied and clarified.

For the clinical application, the results described in this thesis present sufficient evidence for the use of PLGA-NP as a vaccine delivery system to target DC and being an alternative

for montanide as clinical vaccine carrier. However, the formulation, reproducibility and GMP-production of large amounts of different PLGA-NP vaccines might be a hurdle as multi-compound vaccines will probably require fine-tuning and modification of the original double-emulsion-method-with-solvent-evaporation technique to successfully encapsulate the desired SLP and/or adjuvant which each having unique physicochemical properties. Of importance, approval of multi-compound vaccines for clinical use will require that each individual compound encapsulated in the NP is tested first for toxicity and potentially also for therapeutic benefit.

From immunological perspective, however, we have strong evidence that encapsulation of SLP together with a potent immunostimulatory agent in PLGA-NP is a suitable strategy to optimize SLP-vaccines and enhance the clinical efficacy in cancer patients.

Future perspectives on the use of SLP-vaccines and particulate-based delivery methods for their delivery

The potency of SLP-vaccines to boost TAA-specific CD4⁺ and CD8⁺ T cell responses is clear as shown by our group and others. But despite the significant induction of tumor-specific immunity post-vaccination with SLP, objective and durable clinical responses have been rare.

Tumor immunity is complex phenomena consisting of pro-inflammatory anti-tumor effector mechanisms and, arguably of even more significance, anti-inflammatory, suppressive mechanisms that unfortunately turns out very hard to overcome in cancer patients. In this thesis we have described our studies how to enhance the pro-inflammatory milieu anti-tumor effector mechanisms by co-encapsulating long peptide Ag, or alternatively protein Ag, in PLGA-NP. Our results show the potency of PLGA-NP-vaccines to prime CD8⁺ T cells which could control tumor growth.

Bearing in mind the several promising cancer vaccines formulated in our research groups but also the multitude of other vaccines undergoing (pre-)clinical testing or already successfully tested in phase I and/or II trials, I believe that the main obstacle for the use of therapeutic (SLP) cancer vaccines will not lie with the incapacity to prime strong T cell responses. Instead, immunologists and clinicians should implement combinatorial treatment approaches to maintain the potency of these vaccine-induced T cell responses. It is well established that T cell exhaustion and the induction of tumor-induced immune-suppression have a detrimental effect on the clinical efficacy of cancer vaccines.

Anti-CTLA-4, anti-PD1 and anti-PDL1 mAbs are immune checkpoint blockade inhibitors which are emerging as very potent immunotherapies. Their administration has led to several cases of durable clinical benefits in end-stage cancer patients. One can envision a treatment strategy starting with a cocktail of TAA-encoding SLP-vaccines to stimulate a broad T cell response followed by the administration these modulators of anti-CTLA-4, anti-PD1 or both to sustain the potency of the ongoing anti-tumor immune response.

Another attractive strategy and the topic of my current post-doctoral research project is the combination of SLP vaccines with cytokine immunotherapy. Combining IL-2/anti-IL-2 mAb complexes (IL-2-Cx) with SLP-vaccines leads to synergistic anti-tumor responses resulting improved tumor control compared to single therapies of SLP-vaccines or IL-2-Cx.

Addition of IL-2-Cx not only boosted the effector functions also seemed to rescue tumor infiltrating lymphocytes from exhaustion, evident by decreased PD-1 expression. Therefore, the provision of IL-2-Cx post SLP-vaccines will 1) supply vaccine-activated T cells with essential growth-factors and enhance their numbers and 2) maintain their pro-inflammatory phenotype by promoting their effector functions such as IFN- γ and granzyme B production. Finally, IL-2-Cx will 3) counter T cell exhaustion.

Based on these arguments I propose combining IL-2-Cx with the “best SLP-vaccine on the market” to boost tumor specific T cell responses. I strongly support the use of DC-targeting vaccines. Following vaccination, treatment cycles with IL-2-Cx will sustain the ongoing anti-tumor responses.

This combinatorial immunotherapy approach will likely result in significantly better therapeutic benefits over the individual monotherapies, consisting of only SLP-vaccines or IL-2-Cx, and lead to improved patient treatment with manageable adverse effects.

References

1. Leffers N, Vermeij R, Hoogeboom BN, Schulze UR, Wolf R, Hamming IE, van der Zee AG, Melief KJ, van der Burg SH, Daemen T, Nijman HW 2012. Long-term clinical and immunological effects of p53-SLP(R) vaccine in patients with ovarian cancer. *Int J Cancer* 130:105-112.
2. Sabbatini P, Tsuji T, Ferran L, Ritter E, Sedrak C, Tuballes K, Jungbluth AA, Ritter G, Aghajanian C, Bell-McGuinn K, Hensley ML, Konner J, Tew W, Spriggs DR, Hoffman EW, Venhaus R, Pan L, Salazar AM, Diefenbach CM, Old LJ, Gnjjatic S 2012. Phase I trial of overlapping long peptides from a tumor self-antigen and poly-ICLC shows rapid induction of integrated immune response in ovarian cancer patients. *Clin Cancer Res* 18:6497-6508.
3. Eikawa S, Kakimi K, Isobe M, Kuzushima K, Luescher I, Ohue Y, Ikeuchi K, Uenaka A, Nishikawa H, Udono H, Oka M, Nakayama E 2013. Induction of CD8 T-cell responses restricted to multiple HLA class I alleles in a cancer patient by immunization with a 20-mer NY-ESO-1f (NY-ESO-1 91-110) peptide. *Int J Cancer* 132:345-354.
4. Wada H, Isobe M, Kakimi K, Mizote Y, Eikawa S, Sato E, Takigawa N, Kiura K, Tsuji K, Iwatsuki K, Yamasaki M, Miyata H, Matsushita H, Udono H, Seto Y, Yamada K, Nishikawa H, Pan L, Venhaus R, Oka M, Doki Y, Nakayama E 2014. Vaccination with NY-ESO-1 overlapping peptides mixed with Picibanil OK-432 and montanide ISA-51 in patients with cancers expressing the NY-ESO-1 antigen. *J Immunother* 37:84-92.
5. Kenter GG, Welters MJ, Valentijn AR, Lowik MJ, Berends-van der Meer DM, Vloon AP, Essahsah F, Fathers LM, Offringa R, Drijfhout JW, Wafelman AR, Oostendorp J, Fleuren GJ, van der Burg SH, Melief CJ 2009. Vaccination against HPV-16 oncoproteins for vulvar intraepithelial neoplasia. *N Engl J Med* 361:1838-1847.
6. Rosalia RA, Quakkelaar ED, Redeker A, Khan S, Camps M, Drijfhout JW, Silva AL, Jiskoot W, van HT, van Veelen PA, Janssen G, Franken K, Cruz LJ, Tromp A, Oostendorp J, van der Burg SH, Ossendorp F, Melief CJ 2013. Dendritic cells process synthetic long peptides better than whole protein, improving antigen presentation and T-cell activation. *Eur J Immunol* 43:2554-2565.
7. Bijker MS, van den Eeden SJ, Franken KL, Melief CJ, van der Burg SH, Offringa R 2008. Superior induction of anti-tumor CTL immunity by extended peptide vaccines involves prolonged, DC-focused antigen presentation. *Eur J Immunol* 38:1033-1042.
8. Goldberger O, Volovitz I, Machlenkin A, Vadai E, Tzehoval E, Eisenbach L 2008. Exuberated numbers of tumor-specific T cells result in tumor escape. *Cancer Res* 68:3450-3457.
9. Egorov IK 2006. Mouse models of efficient and inefficient anti-tumor immunity, with emphasis on minimal residual disease and tumor escape. *Cancer Immunol Immunother* 55:1-22.
10. Garcia-Lora A, Algarra I, Gaforio JJ, Ruiz-Cabello F, Garrido F 2001. Immunoselection by T lymphocytes generates repeated MHC class I-deficient metastatic tumor variants. *Int J Cancer* 91:109-119.
11. Garrido F, Algarra I, Garcia-Lora AM 2010. The escape of cancer from T lymphocytes: immunoselection of MHC class I loss variants harboring structural-irreversible "hard" lesions. *Cancer Immunol Immunother* 59:1601-1606.

12. Calabro S, Tortoli M, Baudner BC, Pacitto A, Cortese M, O'Hagan DT, De GE, Seubert A, Wack A 2011. Vaccine adjuvants alum and MF59 induce rapid recruitment of neutrophils and monocytes that participate in antigen transport to draining lymph nodes. *Vaccine* 29:1812-1823.
13. Iversen TZ, Engell-Noerregaard L, Ellebaek E, Andersen R, Larsen SK, Bjoern J, Zeyher C, Gouttefangeas C, Thomsen BM, Holm B, Thor SP, Mellemegaard A, Andersen MH, Svane IM 2014. Long-lasting disease stabilization in the absence of toxicity in metastatic lung cancer patients vaccinated with an epitope derived from indoleamine 2,3 dioxygenase. *Clin Cancer Res* 20:221-232.
14. Hailemichael Y, Dai Z, Jaffarzar N, Ye Y, Medina MA, Huang XF, Dorta-Estremera SM, Greeley NR, Nitti G, Peng W, Liu C, Lou Y, Wang Z, Ma W, Rabinovich B, Schluns KS, Davis RE, Hwu P, Overwijk WW 2013. Persistent antigen at vaccination sites induces tumor-specific CD8(+) T cell sequestration, dysfunction and deletion. *Nat Med* 19:465-472.
15. Bijker MS, van den Eeden SJ, Franken KL, Melief CJ, van der Burg SH, Offringa R 2008. Superior induction of anti-tumor CTL immunity by extended peptide vaccines involves prolonged, DC-focused antigen presentation. *Eur J Immunol* 38:1033-1042.
16. Zwaveling S, Ferreira Mota SC, Nouta J, Johnson M, Lipford GB, Offringa R, van der Burg SH, Melief CJ 2002. Established human papillomavirus type 16-expressing tumors are effectively eradicated following vaccination with long peptides. *J Immunol* 169:350-358.
17. de Vos van Steenwijk PJ, Ramwadhoebe TH, Lowik MJ, van der Minne CE, Berends-van der Meer DM, Fathers LM, Valentijn AR, Oostendorp J, Fleuren GJ, Hellebrekers BW, Welters MJ, van Poelgeest MI, Melief CJ, Kenter GG, van der Burg SH 2012. A placebo-controlled randomized HPV16 synthetic long-peptide vaccination study in women with high-grade cervical squamous intraepithelial lesions. *Cancer Immunol Immunother* 61:1485-1492.
18. Kenter GG, Welters MJ, Valentijn AR, Lowik MJ, Berends-van der Meer DM, Vloon AP, Drijfhout JW, Wafelman AR, Oostendorp J, Fleuren GJ, Offringa R, van der Burg SH, Melief CJ 2008. Phase I immunotherapeutic trial with long peptides spanning the E6 and E7 sequences of high-risk human papillomavirus 16 in end-stage cervical cancer patients shows low toxicity and robust immunogenicity. *Clin Cancer Res* 14:169-177.
19. Melief CJ 2012. Treatment of established lesions caused by high-risk human papilloma virus using a synthetic vaccine. *J Immunother* 35:215-216.
20. van der Burg SH, Melief CJ 2011. Therapeutic vaccination against human papilloma virus induced malignancies. *Curr Opin Immunol* 23:252-257.
21. Speetjens FM, Kuppen PJ, Welters MJ, Essahsah F, Voet van den Brink AM, Lantrua MG, Valentijn AR, Oostendorp J, Fathers LM, Nijman HW, Drijfhout JW, van de Velde CJ, Melief CJ, van der Burg SH 2009. Induction of p53-specific immunity by a p53 synthetic long peptide vaccine in patients treated for metastatic colorectal cancer. *Clin Cancer Res* 15:1086-1095.

22. Zeestraten EC, Speetjens FM, Welters MJ, Saadatmand S, Stynenbosch LF, Jongen R, Kapiteijn E, Gelderblom H, Nijman HW, Valentijn AR, Oostendorp J, Fathers LM, Drijfhout JW, van de Velde CJ, Kuppen PJ, van der Burg SH, Melief CJ 2013. Addition of interferon-alpha to the p53-SLP(R) vaccine results in increased production of interferon-gamma in vaccinated colorectal cancer patients: a phase I/II clinical trial. *Int J Cancer* 132:1581-1591.
23. Tomita Y, Nishimura Y 2013. Long peptide-based cancer immunotherapy targeting tumor antigen-specific CD4 and CD8 T cells. *Oncoimmunology* 2:e25801.
24. van Poelgeest MI, Welters MJ, van Esch EM, Stynenbosch LF, Kerpershoek G, van Persijn van Meerten EL, van den Hende M, Lowik MJ, Berends-van der Meer DM, Fathers LM, Valentijn AR, Oostendorp J, Fleuren GJ, Melief CJ, Kenter GG, van der Burg SH 2013. HPV16 synthetic long peptide (HPV16-SLP) vaccination therapy of patients with advanced or recurrent HPV16-induced gynecological carcinoma, a phase II trial. *J Transl Med* 11:88.
25. Koopman G, Beenhakker N, Nieuwenhuis I, Doxiadis G, Mooij P, Drijfhout JW, Koestler J, Hanke T, Fagrouch Z, Verschoor EJ, Bontrop RE, Wagner R, Bogers WM, Melief CJ 2013. DNA/long peptide vaccination against conserved regions of SIV induces partial protection against SIVmac251 challenge. *AIDS*.
26. Quakkelaar ED, Melief CJ 2012. Experience with synthetic vaccines for cancer and persistent virus infections in nonhuman primates and patients. *Adv Immunol* 114:77-106.
27. Zhang H, Hong H, Li D, Ma S, Di Y, Stoten A, Haig N, Di GK, Yu Z, Xu XN, McMichael A, Jiang S 2009. Comparing pooled peptides with intact protein for accessing cross-presentation pathways for protective CD8+ and CD4+ T cells. *J Biol Chem* 284:9184-9191.
28. Giodini A, Rahner C, Cresswell P 2009. Receptor-mediated phagocytosis elicits cross-presentation in nonprofessional antigen-presenting cells. *Proc Natl Acad Sci U S A* 106:3324-3329.
29. Menager J, Ebstein F, Oger R, Hulin P, Nedellec S, Duverger E, Lehmann A, Kloetzel PM, Jotereau F, Guilloux Y 2014. Cross-presentation of synthetic long peptides by human dendritic cells: a process dependent on ERAD component p97/VCP but Not sec61 and/or Derlin-1. *PLoS One* 9:e89897.
30. Eikawa S, Kakimi K, Isobe M, Kuzushima K, Luescher I, Ohue Y, Ikeuchi K, Uenaka A, Nishikawa H, Uono H, Oka M, Nakayama E 2013. Induction of CD8 T-cell responses restricted to multiple HLA class I alleles in a cancer patient by immunization with a 20-mer NY-ESO-1f (NY-ESO-1 91-110) peptide. *Int J Cancer* 132:345-354.
31. Rodriguez A, Regnault A, Kleijmeer M, Ricciardi-Castagnoli P, Amigorena S 1999. Selective transport of internalized antigens to the cytosol for MHC class I presentation in dendritic cells. *Nat Cell Biol* 1:362-368.
32. Sijts EJ, Kloetzel PM 2011. The role of the proteasome in the generation of MHC class I ligands and immune responses. *Cell Mol Life Sci* 68:1491-1502.
33. Luciani F, Kesmir C, Mishto M, Or-Guil M, de Boer RJ 2005. A mathematical model of protein degradation by the proteasome. *Biophys J* 88:2422-2432.

34. van MN, Camps MG, Khan S, Filippov DV, Weterings JJ, Griffith JM, Geuze HJ, van HT, Verbeek JS, Melief CJ, Ossendorp F 2009. Antigen storage compartments in mature dendritic cells facilitate prolonged cytotoxic T lymphocyte cross-priming capacity. *Proc Natl Acad Sci U S A* 106:6730-6735.
35. Rudd BD, Brien JD, Davenport MP, Nikolich-Zugich J 2008. Cutting edge: TLR ligands increase TCR triggering by slowing peptide-MHC class I decay rates. *J Immunol* 181:5199-5203.
36. Bonifaz L, Bonnyay D, Mahnke K, Rivera M, Nussenzweig MC, Steinman RM 2002. Efficient targeting of protein antigen to the dendritic cell receptor DEC-205 in the steady state leads to antigen presentation on major histocompatibility complex class I products and peripheral CD8+ T cell tolerance. *J Exp Med* 196:1627-1638.
37. Idoyaga J, Fiorese C, Zbytnuik L, Lubkin A, Miller J, Malissen B, Mucida D, Merad M, Steinman RM 2013. Specialized role of migratory dendritic cells in peripheral tolerance induction. *J Clin Invest* 123:844-854.
38. Cruz LJ, Tacken PJ, Fokkink R, Joosten B, Stuart MC, Albericio F, Torensma R, Figdor CG 2010. Targeted PLGA nano- but not microparticles specifically deliver antigen to human dendritic cells via DC-SIGN in vitro. *J Control Release* 144:118-126.
39. Mohanan D, Slutter B, Henriksen-Lacey M, Jiskoot W, Bouwstra JA, Perrie Y, Kundig TM, Gander B, Johansen P 2010. Administration routes affect the quality of immune responses: A cross-sectional evaluation of particulate antigen-delivery systems. *J Control Release* 147:342-349.
40. Wieber A, Selzer T, Kreuter J 2011. Characterisation and stability studies of a hydrophilic decapeptide in different adjuvant drug delivery systems: a comparative study of PLGA nanoparticles versus chitosan-dextran sulphate microparticles versus DOTAP-liposomes. *Int J Pharm* 421:151-159.
41. Keijzer C, Slutter B, van der Zee R, Jiskoot W, van EW, Broere F 2011. PLGA, PLGA-TMC and TMC-TPP nanoparticles differentially modulate the outcome of nasal vaccination by inducing tolerance or enhancing humoral immunity. *PLoS One* 6:e26684.
42. Slutter B, Plapied L, Fievez V, Sande MA, des RA, Schneider YJ, Van RE, Jiskoot W, Preat V 2009. Mechanistic study of the adjuvant effect of biodegradable nanoparticles in mucosal vaccination. *J Control Release* 138:113-121.
43. Johansen P, Storni T, Rettig L, Qiu Z, Der-Sarkissian A, Smith KA, Manolova V, Lang KS, Senti G, Mullhaupt B, Gerlach T, Speck RF, Bot A, Kundig TM 2008. Antigen kinetics determines immune reactivity. *Proc Natl Acad Sci U S A* 105:5189-5194.
44. Overwijk WW, Restifo NP 2001. B16 as a mouse model for human melanoma. *Curr Protoc Immunol* Chapter 20:Unit.
45. North S, Butts C 2005. Vaccination with BLP25 liposome vaccine to treat non-small cell lung and prostate cancers. *Expert Rev Vaccines* 4:249-257.
46. Cohen S, Alonso MJ, Langer R 1994. Novel approaches to controlled-release antigen delivery. *Int J Technol Assess Health Care* 10:121-130.

47. Demento SL, Cui W, Criscione JM, Stern E, Tulipan J, Kaech SM, Fahmy TM 2012. Role of sustained antigen release from nanoparticle vaccines in shaping the T cell memory phenotype. *Biomaterials* 33:4957-4964.
48. Fifis T, Gamvrellis A, Crimeen-Irwin B, Pietersz GA, Li J, Mottram PL, McKenzie IF, Plebanski M 2004. Size-dependent immunogenicity: therapeutic and protective properties of nano-vaccines against tumors. *J Immunol* 173:3148-3154.
49. Gutierrez I, Hernandez RM, Igartua M, Gascon AR, Pedraz JL 2002. Size dependent immune response after subcutaneous, oral and intranasal administration of BSA loaded nanospheres. *Vaccine* 21:67-77.
50. Zhang Z, Tongchusak S, Mizukami Y, Kang YJ, Ioji T, Touma M, Reinhold B, Keskin DB, Reinherz EL, Sasada T 2011. Induction of anti-tumor cytotoxic T cell responses through PLGA-nanoparticle mediated antigen delivery. *Biomaterials* 32:3666-3678.
51. Mueller M, Schlosser E, Gander B, Groettrup M 2011. Tumor eradication by immunotherapy with biodegradable PLGA microspheres--an alternative to incomplete Freund's adjuvant. *Int J Cancer* 129:407-416.
52. Tenbusch M, Nchinda G, Storcksdieck genannt BM, Temchura V, Uberla K 2013. Targeting the antigen encoded by adenoviral vectors to the DEC205 receptor modulates the cellular and humoral immune response. *Int Immunol* 25:247-258.
53. Sartorius R, Bettua C, D'Apice L, Caivano A, Trovato M, Russo D, Zanoni I, Granucci F, Mascolo D, Barba P, Del PG, De BP 2011. Vaccination with filamentous bacteriophages targeting DEC-205 induces DC maturation and potent anti-tumor T-cell responses in the absence of adjuvants. *Eur J Immunol* 41:2573-2584.
54. Moriya K, Wakabayashi A, Shimizu M, Tamura H, Dan K, Takahashi H 2010. Induction of tumor-specific acquired immunity against already established tumors by selective stimulation of innate DEC-205(+) dendritic cells. *Cancer Immunol Immunother* 59:1083-1095.
55. Yamazaki S, Maruyama A, Okada K, Matsumoto M, Morita A, Seya T 2012. Dendritic cells from oral cavity induce Foxp3(+) regulatory T cells upon antigen stimulation. *PLoS One* 7:e51665.
56. Williams M, Crozat K, Henri S, Tamoutounour S, Grenot P, Devilard E, de BB, Alexopoulou L, Dalod M, Malissen B 2010. Skin-draining lymph nodes contain dermis-derived CD103(-) dendritic cells that constitutively produce retinoic acid and induce Foxp3(+) regulatory T cells. *Blood* 115:1958-1968.
57. Coombes JL, Siddiqui KR, Arancibia-Carcamo CV, Hall J, Sun CM, Belkaid Y, Powrie F 2007. A functionally specialized population of mucosal CD103+ DCs induces Foxp3+ regulatory T cells via a TGF-beta and retinoic acid-dependent mechanism. *J Exp Med* 204:1757-1764.
58. Faham A, Altin JG 2011. Ag-bearing liposomes engrafted with peptides that interact with CD11c/CD18 induce potent Ag-specific and antitumor immunity. *Int J Cancer* 129:1391-1403.
59. Wei H, Wang S, Zhang D, Hou S, Qian W, Li B, Guo H, Kou G, He J, Wang H, Guo Y 2009. Targeted delivery of tumor antigens to activated dendritic cells via CD11c molecules induces potent antitumor immunity in mice. *Clin Cancer Res* 15:4612-4621.

60. Ejaz A, Ammann CG, Werner R, Huber G, Oberhauser V, Horl S, Schimmer S, Dittmer U, von LD, Stoiber H, Banki Z 2012. Targeting viral antigens to CD11c on dendritic cells induces retrovirus-specific T cell responses. *PLoS One* 7:e45102.
61. Chatterjee B, Smed-Sorensen A, Cohn L, Chalouni C, Vandlen R, Lee BC, Widger J, Keler T, Delamarre L, Mellman I 2012. Internalization and endosomal degradation of receptor-bound antigens regulate the efficiency of cross presentation by human dendritic cells. *Blood* 120:2011-2020.
62. Cohn L, Chatterjee B, Esselborn F, Smed-Sorensen A, Nakamura N, Chalouni C, Lee BC, Vandlen R, Keler T, Lauer P, Brockstedt D, Mellman I, Delamarre L 2013. Antigen delivery to early endosomes eliminates the superiority of human blood BDCA3+ dendritic cells at cross presentation. *J Exp Med* 210:1049-1063.
63. Panyam J, Zhou WZ, Prabha S, Sahoo SK, Labhasetwar V 2002. Rapid endo-lysosomal escape of poly(DL-lactide-co-glycolide) nanoparticles: implications for drug and gene delivery. *FASEB J* 16:1217-1226.
64. Kreutz M, Tacke PJ, Figdor CG 2013. Targeting dendritic cells--why bother? *Blood* 121:2836-2844.



Chapter 10

English summary
Nederlandse samenvatting



English summary

Cancer is the collective name given to several neoplastic diseases, which are characterized by uncontrolled growth of malignant cells, their subsequent metastasis and invasion of healthy tissues impairing their normal functioning.

Cancer is an aggressive and unfortunately often fatal disease and very few patients with metastasis survive beyond two years after diagnosis. This is for a large part caused by the fact that conventional cancer therapies, such as surgery, chemotherapy and radiotherapy, have so far failed to lead to the desired clinical benefits in most cancer patients with an advanced disease. Novel and more efficacious treatments are therefore highly necessary.

Cancer immunotherapy, a treatment modality based on the activation of the immune system against tumors have resulted in promising clinical observations and reports of durable or even complete responses in end-stage cancer patients. Immunotherapy boosts the tumor-specific responses and thereby facilitates the eradication of malignant cells.

At the Leiden University Medical Center (LUMC), therapeutic vaccinations using synthetic long peptides (SLP) encoding tumor associated antigens (TAA) have been researched for over 10 years. Several (pre-)clinical studies have conclusively shown that SLP efficiently strengthens the immune system against tumors.

SLP are administered via sub cutaneous injections into the skin of cancer patients. Treatment success and the efficacy of therapeutic vaccines for cancer is critically dependent on the efficient delivery of the SLP, or any other cancer vaccine, to Dendritic cells (DC). DC play a prominent role in the immune system, they are considered the primary and most efficient antigen presenting cell (APC) with strong capacity to initiate and orchestrate immune responses. DC can effectively prime and activate tumor specific cytotoxic CD8⁺ T cells (CTL) which are capable of directing recognizing and killing tumor cells.

Montanide-based water-in-oil (w/o) emulsions have been applied to formulate SLP in the majority of clinical trials assessing the therapeutic capacity of SLP-vaccines. The use of Montanide-based formulations, however, is associated with local but prolonged side effects because of the non-biodegradable nature of the (w/o) emulsions. In addition, poorly defined adjuvant properties, sub-optimal delivery of the vaccine to DC, poorly controlled Ag release rates and lack of long-term stability hamper the use of Montanide as a clinically attractive vaccine delivery system. Biodegradable delivery systems based on poly(lactic-co-glycolic acid) (PLGA) offer a promising alternative approach for SLP-vaccines cancer

vaccines. PLGA is suitable for the preparation of micro- and nanoparticles (NP), which can protect the vaccine-antigen (Ag) from proteolytic enzymatic degradation and rapid clearance, allow co-encapsulation and simultaneous delivery of both Ag and adjuvants, and facilitate Ag delivery to DC. The use of PLGA is Food and Drug Administration (FDA) approved, owing to its biodegradability and biocompatibility, with several slow-release formulations currently on the market.

This thesis describes the results of several studies performed aimed at optimizing the efficacy SLP-vaccines via the encapsulation in PLGA-NP. By encapsulating SLP, or a model protein Ag, in PLGA-NP we attempted to improve the delivery of the SLP to DC, achieve better control of the pharmacokinetics and biodistribution of the vaccine and finally, reduce the therapy related side effects associated with the current (pre-)clinical procedure of administering SLP-vaccines emulsified in Montanide.

The efficiency of Ag-processing by DC is vital for the strength of the ensuing T-cell responses. **Chapter 2** described our studies exploring the Ag-processing and presentation mechanisms underlying the observed *in vivo* therapeutic efficacy of SLP-vaccines. Understanding the mechanisms of SLP-Ag in its free, soluble and chemically unmodified form as it was successfully tested in human trials, allows better understanding of SLP-vaccines and allow further fine-tuning to improve the therapeutic efficacy and improve the treatment of cancer patients. We reported an *in vitro* MHC class I and class II Ag processing and presentation analysis of SLP, in comparison to whole proteins, by murine and human DC. We showed that SLPs were much faster and efficiently processed by DC, resulting in an increased presentation to CD4⁺ and CD8⁺ T cells. The mechanism of access to MHC class I loading appeared to differ between SLP and proteins. Whole soluble protein Ag ended remained in endo-lysosomes whereas SLP were detected very rapidly outside the endo-lysosomes upon internalization by DC resulting in a proteasome- and TAP-dependent MHC class I presentation much like the Ag processing and presentation pathways of endogenous proteins and peptides generated within all cells of the body. Our results suggest that the efficient internalization of SLP, accomplished specifically by DC and characterized by an alternative and faster intracellular routing, leads to enhanced CD8⁺ T-cell activation observed *in vivo*.

SLP-vaccines showed potent therapeutic efficacy against pre-malignant lesions but failed to achieve durable clinical responses in patients with cancer. Therefore, SLP-vaccines require optimization to enhance its therapeutic efficacy in cancer patients. To this end we studied

in **chapter 3** the feasibility to encapsulate SLP in PLGA-NP as a method to improve the immunogenicity of SLP-vaccines, and decrease the onset of adverse effects associated with the use of Montanide in the clinic. The research was aimed at defining physical and formulation parameters necessary to successfully encapsulate SLP in PLGA-NP (PLGA-SLP). Using the standard “double emulsion and solvent evaporation” formulation, well described for the encapsulation of proteins, we observed very low (< 30%) encapsulation efficiency of SLP in PLGA-NP, or extremely high burst release rates (> 70%) upon resuspension of NP in physiological buffers. Therefore, we adjusted the formulation and process parameters and uncovered that the pH of the first emulsion was critical to achieve efficient encapsulation and controlled release of SLP. In particular, we showed that an alkaline inner aqueous phase, instead of the acidic aqueous phase as required to encapsulate proteins, resulted in circa 330 nm sized NP with approximately 40% encapsulation efficiency and low (< 10%) burst release. We next studied the efficacy of MHC class I cross-presentation of these “low-burst release” and CD8⁺ T cell activation by DC loaded with PLGA-SLP in comparison to soluble SLP and observed that PLGA-SLP were superior in facilitating MHC class I presentation and CD8⁺ T cell activation.

A follow up study was subsequently performed in an attempt to characterize the intracellular mechanisms used by DC to process PLGA-SLP and study the immunological effects on SLP-vaccines when combined with an adjuvant. In **chapter 4** we describe that toll like receptor (TLR) 2 stimulation, using the adjuvant Pam3CSK4, enhances MHC class I presentation of PLGA-SLP by DC. However, this effect was not dependent on the co-encapsulation of Pam3CSK4 together with SLP in PLGA-NP (PLGA-SLP/TLR2L). DC loaded with PLGA-SLP or PLGA-SLP/TLR2L route internalized NP into endo-lysosomal compartments and not the cytosol as occurs with sSLP. We detected PLGA-NP encapsulated SLP for prolonged periods inside these endo-lysosomal compartments which led to sustained MHC class I presentation of PLGA-NP encapsulated SLP for up to 96 hr. Vaccinations with PLGA-SLP and especially PLGA-SLP/TLR2L induced sustained CD8⁺ T cell proliferation.

In **chapter 5** we showed that PLGA-NP, encapsulating protein Ag, is a superior vehicle to deliver Ag to DC which could be applied to stimulate Ag-specific CD8⁺ T cells. The DC/PLGA-NP *ex vivo* stimulated CTL used in an adoptive T cell immunotherapy setting showed superior capacity to lyse target cells and were more efficient at tumor control resulting in prolonged survival of tumor bearing animals. In contrast, soluble protein Ag failed to elicit the same effects and thus confirmed that encapsulation of protein Ag or SLP-Ag in PLGA-NP leads to strong improvement of MHC class I presentation and CTL activation.

Chapter 6 discusses a comparative study between NP versus microparticles (MP) in their efficacy to deliver Ag to DC, facilitate MHC class I Ag presentation and stimulate T and B cell responses *in vivo*. We showed that the efficient uptake of Ag is crucial to induce an immune response. Whereas NP were efficiently internalized by DC upon *in vitro* incubation, MP were poorly detectable inside DC, as a result MHC class I presentation was mainly observed when DC were cultured with NP. Upon s.c. vaccinations with NP and MP, we could detect significantly higher numbers of Ag-specific CD8⁺ T cells in mice vaccinated with NP compared to MP or OVA emulsified in incomplete Freund's adjuvant (IFA). Moreover, NP led to better antibody responses compared to MP. We concluded that efficient immune responses are better achieved with NP but not MP.

Chapter 7 and **chapter 8** describes active-targeting strategies to enhance the delivery of vaccine to DC *in vivo*. In general, upon s.c. injection, only a small fraction of the vaccine is delivered to DC whereas the majority is cleared by the body or engulfed by other immune cells. To study how to overcome these negative effects preventing optimal vaccine efficacy we formulated multi-compound particulate vaccines based on PLGA-NP encapsulating TLR and protein-Ag which were subsequently targeted to CD40 (a TNF-receptor family molecule), DEC-205 (a C-type lectin receptor) and CD11c (an integrin receptor). The efficiency of these different targeting strategies to activate DC and elicit a potent CD8⁺ T cell response was studied. We observed that targeted PLGA-(Ag/TLR3+7L) NP were more efficiently bound and internalized by DC *in vitro* compared to the control non-targeted NP and reported a small but significantly improved Ag-delivery using CD40-targeted NP compared to DEC-205 or CD11c targeted NP. In comparison to non-targeted NP, all targeted NP stimulated IL-12 production and induced the expression of co-stimulatory molecules by DC to a similar extent. In line with these effects, targeted NP but not non-targeted NP led to strong proliferation and IFN- γ production by T cells *in vitro*. Vaccinations with CD40, DEC-205 and CD11c targeted NP showed consistently higher efficacy than non-targeted NP to stimulate CD8⁺ T cell responses. There was a trend towards better CD8⁺ T cell priming with CD40-targeted NP. Based on these observations we performed a study with the goal to control tumor outgrowth using CD40-targeting of PLGA-(Ag/TLR2+3L) NP-vaccines. Targeting NP to CD40 very efficiently and selectively delivered the vaccine to DC *in vivo* upon s.c. injection and significantly improved priming of CD8⁺ T cells against two independent tumor associated Ag. Finally, therapeutic application of CD40-targeted NP led to enhanced tumor control and prolonged survival of tumor-bearing mice whereas non-targeted NP-vaccines failed to do so.

In conclusion, the results described here present sufficient evidence to use PLGA-NP as a vaccine delivery system for SLP-vaccines. Especially the use of targeted PLGA-NP will significantly enhance the delivery of SLP-vaccines to DC and be considered as an alternative for Montanide as clinical vaccine carrier.

Nederlandse samenvatting

Kanker is de verzamelnaam voor verschillende ziektes waarin ongecontroleerde groei van maligne cellen plaatsvindt. Kanker wordt soms gekenmerkt door het verspreiden en binnendringen van maligne cellen in gezonde weefsels en organen, ook wel uitzaaiingen genoemd. Door deze uitzaaiingen kan het gezonde weefsel niet meer goed functioneren.

Kanker is een agressieve en helaas vaak dodelijke ziekte waarbij weinig patiënten met uitzaaiingen langer dan twee jaar na de diagnose nog leven. De oorzaak is voor een groot deel te verklaren doordat de conventionele kankertherapieën, zoals chirurgie, chemotherapie en radiotherapie, niet goed genoeg werken in kankerpatiënten met een gevorderde ziekte. Nieuwe en meer effectieve behandelingen zijn dan ook zeer noodzakelijk.

Kanker immunotherapie, een behandelmethode gebaseerd op de activatie van het immuunsysteem tegen tumoren, is een veelbelovende therapie en er zijn zelfs gevallen van volledige genezing van terminale kankerpatiënten. Immunotherapie stimuleert de natuurlijke en tumor-specifieke afweer en versterkt het immuunsysteem waardoor de tumorcellen beter herkend en gedood worden.

In het Leids Universitair Medisch Centrum (LUMC) heeft men veel ervaring met therapeutische vaccinaties tegen tumoren gebaseerd op synthetische lange peptiden (SLP) die coderen voor de tumor-geassocieerde antigenen. Verschillende klinische studies hebben aangetoond dat SLP zeer efficiënt is in het activeren van het immuunsysteem tegen tumoren.

SLP vaccins worden toegediend via injecties in de huid van de patiënten. Het succes van de behandeling en de efficiëntie van therapeutische vaccins tegen tumoren is sterk afhankelijk van de beschikbaarheid van de SLP (of het vaccine) voor de dendritische cellen (DC's). DC's spelen een belangrijke rol in het immuunsysteem en worden beschouwd als de beste en voornaamste antigeen presenterende cel (APC) met de unieke capaciteit om het immuunsysteem te activeren. DC kunnen tumor-specifieke cytotoxische CD8⁺T-cellen (CTL) programmeren, zodat die tumorcellen kunnen herkennen en doden.

Tot nu toe werden in klinische trials met SLP-vaccins de SLP gemengd in Montanide, een water-in-olie (w/o) emulsie. Het gebruik van Montanide-formuleringen leidt echter tot lokale maar langdurige bijwerkingen omdat de w/o emulsie niet biologisch afbreekbaar is. Bovendien heeft Montanide zwakke immuun-stimulerende eigenschappen en wordt het suboptimaal opgenomen door DC's na injectie in de huid, en is het vrijlaten van de

SLP slecht te reguleren. Bovendien hebben Montanide-formuleringen een beperkte houdbaarheid. Al deze eigenschappen van Montanide belemmeren een succesvol en lange-termijngebruik in de kliniek.

Biologisch afbreekbare afgiftesystemen op basis van poly(lactic-co-glycolic acid) (PLGA), een co-polymeer dat bestaat uit melkzuur en glycolzuur, bieden een veelbelovend alternatief voor het toedienen van SLP-vaccins tegen tumoren. PLGA is geschikt voor het formuleren van nano-partikelen (NP) en micro-partikelen (MP) waarin het SLP-vaccin wordt ingekapseld. Deze partikelen beschermen het SLP tegen proteolytische afbraak en verminderen dat het vaccine snel uitgescheiden wordt uit het lichaam.

Het gebruik van PLGA in mensen is goedgekeurd door de Amerikaanse *Food and Drug Administration* (FDA).

Dit proefschrift beschrijft de resultaten van verschillende studies die gericht waren op het optimaliseren van SLP-vaccins door deze in te kapselen in PLGA-NP. Door SLP, of een model eiwit Ag, in te kapselen in PLGA-NP hebben we geprobeerd een betere toediening van SLP aan DC's te bewerkstelligen. Ook wilden we een betere beheersing van de farmacokinetiek en biodistributie van het vaccin bereiken en de bijwerkingen verminderen gerelateerd aan het in Montanide geformuleerde SLP-vaccin.

De efficiëntie van Ag-processing door DC's is essentieel voor de sterkte van de daaropvolgende T-cel immuunresponsen. **Hoofdstuk 2** beschrijft een *in vitro* analyse van de MHC klasse I en klasse II Ag-processing en presentatie van SLP, in vergelijking met het eiwit Ag, door muis en humane DC's. We hebben aangetoond dat SLP veel sneller en efficiënter verwerkt wordt door DC's, wat leidt tot betere stimulering van CD4⁺ en CD8⁺ T-cellen. Het mechanisme van toegang tot MHC klasse I processing was verschillend tussen SLP en eiwitten. Na opname door DC's was het eiwit Ag voornamelijk aantoonbaar in intracellulaire compartimenten, de endo-lysosomen. SLP was in tegenstelling tot eiwitten nauwelijks in de endo-lysosomen detecteerbaar, maar juist zeer snel in het cytosol van de cel aanwezig. Vervolgens werden SLP verwerkt, vergelijkbaar met endogene antigenen geproduceerd in cellen van het lichaam. Onze resultaten suggereren dat een efficiënte internalisatie door DC's van SLP, gekenmerkt door een alternatieve en snellere intracellulaire routing, leidt tot een verhoogde CD8⁺ T-cel-activatie.

SLP-vaccins hebben geleid tot veelbelovende resultaten in patiënten met pre-maligne vormen van kanker. Maar SLP-vaccins zijn minder succesvol in patiënten met vergevorderde kanker. Daarom is het noodzakelijk dat SLP-vaccins verbeterd worden. In **hoofdstuk 3** heb-

ben we bewezen dat het inkapselen van SLP in PLGA-NP (PLGA-SLP) een goede methode is om de immunogeniciteit van SLP-vaccins te verbeteren. In het bijzonder hebben we aangetoond dat MHC klasse I presentatie en CD8⁺ T-cel-activatie door DC's sterk verbeterd worden in vergelijking met niet ingekapseld, oftewel vrij, SLP.

Op basis van deze resultaten werd een vervolgonderzoek uitgevoerd om de intracellulaire mechanismen te beschrijven die door DC worden gebruikt om PLGA-SLP te verwerken. Ook werd onderzocht of de toevoeging van een adjuvant de immunogeniciteit van PLGA-SLP verhoogt. De resultaten hiervan worden beschreven in **hoofdstuk 4**, waarin we beschrijven dat het adjuvant Pam3CSK4 sterk de MHC klasse I presentatie van PLGA-SLP door DC's verbetert zonder dat het samen met de SLP ingekapseld moet zijn in de NP. DC's beladen met PLGA-SLP kunnen langdurig SLP Ag beschermen en kunnen ook voor een langere periode CD8⁺ T-cellen activeren, bepaald tot 96 uur.

In **hoofdstuk 5** laten we zien dat PLGA-NP ook gebruikt kan worden om tumor-specieke CD8⁺ T-cellen te stimuleren *ex vivo*. Transplantatie met de DC/PLGA-NP *ex vivo* gestimuleerde CTL leidde tot een zeer sterk therapeutisch effect tegen tumoren.

Hoofdstuk 6 beschrijft de verschillen tussen NP en MP om DC te beladen met een Ag en vervolgens MHC klasse I Ag presentatie te induceren. In muizen hebben we bestudeerd of NP beter zijn dan MP om T- en B-cel-responsen te activeren. We concludeerden dat een efficiënte opname van Ag door DC's essentieel is om een immuunrespons te induceren. Opname van Ag was het sterkst met het gebruik van NP. Bij s.c. vaccinaties met NP en MP detecteerden wij significant hogere Ag-specifieke CD8⁺ T-cellen na vaccinaties met NP ten opzichte van MP. Bovendien leidde NP tot betere antilichaamresponsen. We concludeerden dat een efficiënte immuunrespons beter wordt bereikt met NP maar niet met MP.

In **hoofdstuk 7** en **hoofdstuk 8** bestuderen we strategieën om PLGA-NP-vaccins specifiek te sturen naar DC's, *DC-targeting*. In het algemeen komt slechts een kleine fractie van een geïnjecteerd vaccin bij de DC's terecht, terwijl de meerderheid wordt uitgescheiden door het lichaam of door andere immuuncellen opgenomen wordt. Om deze negatieve effecten te voorkomen en de werking van een vaccin te verbeteren hebben wij PLGA-NP-vaccins geformuleerd die zowel Ag en adjuvantia bevatten, die vervolgens werden getarget naar moleculen welke tot expressie komen op de oppervlakte van DC's. We hebben vaccins geformuleerd gericht tegen CD40 (een molecuul van de TNF-receptorfamilie), DEC-205 (een C-type lectinereceptor) en CD11c (integrinereceptor). De efficiëntie van deze verschillende targetingstrategieën om DC's te activeren en een krachtige CD8⁺ T-cel-respons op te

wekken werd onderzocht. We ontdekten dat getargette PLGA-(Ag/TLR3+7L) NP efficiënter werden gebonden en geïnternaliseerd door DC's *in vitro* in vergelijking met de controle niet-getargette NP. In vergelijking met niet getargette NP, kon alle getargette NP IL-12 de productie door DC's stimuleren. Getargette NP, maar niet de ongetargette NP, leidde tot een sterke T-cel-respons en IFN- γ -productie door T-cellen. Vaccinaties met CD40, DEC-205 en CD11c getargette NP vertoonden constant een hogere mate van CD8⁺ T-cel-stimulatie van ongetargete NP. CD40 getargette NP was iets beter in het stimuleren van CD8⁺ T-cel-responsen. Op basis van deze observaties hebben we een onderzoek uitgevoerd met als doel de tumoruitgroei te blokkeren door middel van toediening van CD40-getargette PLGA-(Ag/TLR2+3L) NP-vaccins. Targeting van NP-vaccins naar CD40 werkte zeer efficiënt en leverde selectief het vaccin af bij DC na injectie in de huid. Dit leidde tot significant betere activatie van CD8⁺ T-cellen. Tenslotte toonden we aan dat CD40-getargette NP-vaccins een therapeutisch effect hebben en de levensduur van muizen met een tumor verlengde.

Gebaseerd op de resultaten beschreven in dit proefschrift concluderen wij dat PLGA-NP een efficiënt middel is om de effectiviteit van SLP-vaccins te verhogen. Vooral het gebruik van getargette PLGA-NP zullen tot een aanzienlijke verbetering leiden en moeten naar onze mening beschouwd worden als een alternatief voor Montanide voor klinische toepassingen.



Chapter 11

**Dankwoord, Acknowledgements &
Palabranan di Danki**



17 september 2008 begon ik met mijn promotieonderzoek, een periode waar ik met veel plezier op terugkijk en waarin ik me ontzettend veel heb ontwikkeld, niet alleen als wetenschapper maar ook als persoon. Nu dat ik bijna het einde van deze periode heb bereikt en deze, hopelijk, succesvol kan afsluiten op 2 oktober 2014, wil ik graag iedereen bedanken die een bijdrage heeft geleverd aan dit proefschrift en het onderzoek dat erin beschreven wordt.

I would like to thank everybody who helped me in any way with performing the research described in this thesis.

Mi lo ke jama tur hende danki ku a judami i apoyami ku mi investigashon scientifico ku mi a deskribi den e thesis aki.

Mijn co-promotor

Jaap, ik ben jou voor altijd dankbaar voor jouw vertrouwen in mij. Bedankt voor je dagelijkse begeleiding en met het helpen om de basis te leggen voor een succesvolle promotieonderzoek. Dank je wel chef.

Mijn promotors

Ferry, van jou heb ik de immunologie geleerd op een hele gave manier. Jouw denkwijze, je kritische blik, je interpretatie van de de resultaten hebben veel bijgedragen aan mijn ontwikkeling als immunoloog. Je was vanaf de eerste dag betrokken bij mijn onderzoek. We konden vaak over alles en nog wat brainstormen en je ondersteunde me toen het tegenzat. Dank je wel voor alles.

Henk Jan, u was degene die ons team managte en ervoor zorgde dat alles netjes liep. Zonder uw vertrouwen had ik het nooit gered. Dank u wel.

The other captains

Sjoerd, Ik kon altijd bij jou terecht met mijn acute vragen en hypothesen en voor unannounced werkbesprekingen. Je deur stond altijd open. We spraken graag over de immunologie en konden altijd grapjes maken met elkaar. Thanks for all.

Wim, indirect en direct was jij betrokken bij mijn promotieonderzoek. Ook van jou heb ik veel geleerd. You kept Ana and me scherp and guided us in the absence of Ferry, Jaap or Sjoerd. Dank je wel voor je begeleiding en toewijding aan het project.

My PhD counterpart

Ana, we were at times ready to turn our back at each other and then again able to have great conversations like two longtime friends. Thanks for all, I wish you all the best with finishing your thesis and let's go get some new joint publications.

My lab members

Als eerste Marcel, degene die altijd en ook echt altijd bereidbaar was om mij te helpen met experimenten. Marcel wist veel, en wat hij niet direct wist, daar kwam hij later op terug. Kerel, thanks for teaching me how to tackle experiments. Thanks for all, thanks for your friendship.

Luis, gracias por todo amigo!! We sure show them that we, los Caribeños, can deliver and perform at high levels while staying relaxed and smiling. You joined half way during my project and with your skills boosted the scientific output. Together we did some nice work. I am looking forward to collaborating with you in the future.

The TI-group: Marieke, Suzanne, Anke, Selina, Afshin, Dirk, Esther, Eleni, Nadine, Marjolein, Suzanne, Tetje, Gijs, Jan Willem, Natasja, Eleni, Jan Wouter en de rest van de peptide facility, Kees, Peter en Ramon. You guys are all great, thanks for the collaborations and the fun time together.

Kees (Prof) dank u wel voor alles. U had een belangrijke bijdrage aan mijn ontwikkeling als immunoloog en heb veel geleerd van onze joint paper.

Thorbold, bij jou kon ik ook altijd terecht. Met jou kon ik chillen en tegelijkertijd data bespreken. Dank je wel voor je vele tips en insights over mijn experimenten.

The KFT-group: thanks everybody for the workdiscussions and a special thanks to Marion and Mieke for your assistance.

IGFL-group: Lorraine, Rob, Loes, John, Pauline en Maarten. You guys made me feel welcome from day 1. You were kind, always helpful and always open for nice conversations. A special thanks to Lorraine, for the person that you are, for your care for mother earth, and for being such a good colleague and friend.

My former supervisors

Michiel, u was mijn eerste stagebegeleider. U stond aan de basis van mijn wetenschappelijke carrière. Uw adviezen hebben me heel veel geholpen. Dank u wel.

Dear Milan, thank you for accepting me in your research group and lab. My life and work in Prague was great and this period will always have a special place in my thoughts.

Rieneke, jij was een grote motivator, ik leerde van jou wat nodig was om een succesvolle OIO en wetenschapper te worden. Thanks for all.

Tanja, lieve Tanja... Jij was eerst mijn hoogleraar en daarna mij stagebegeleider en daarna ook mijn Prof. en als ik het zo mag noemen, een vriendin. Met jou praten over immunologie is altijd motiverend en jouw carriëretips hebben me veel geholpen en ik waardeer het dat ik altijd terecht kan voor whatever topic. Thanks for all...

Visiting scientists and the students I had the pleasure to supervise

Ivan, we were colleagues in Prague and since then friends. It has always been a pleasure to work with you. I want to thank you again for collaborating with me on my PhD research in Leiden.

Ahmed, as-salamu alaykum, your dedication to my research project and your personality made it a great pleasure to work with you. Thanks for all.

Angelino, cousin, gym buddy and internee... Thanks for having my back, your pipetting skills are flawless.

The paranymphs

Wendy ik kan met jou over alles praten en jij werd heel snel een goede vriendin voor mij. Chillen met jou is gaaf. Dank je wel voor jouw hulp, advies en tips tijdens mijn promotieonderzoek, op het lab en ook daarbuiten.

Bryan, nos a bira bro sinta te patras den klas tijdens e vak clinical oncology na VUmc. Nos tabata gym na VU i nos a sigi gym na Leiden. Bo werkethiek i dedikashon na trabouw ta un ehemplo grandi pami mati! Danki pabo vriendschap, e nood slaapplek ora nos a traha te laat pero vooral danki pabo personalidad.

My family

Mama i Tata, danki pa motivami foi dia mi tabata chiki. Danki pa sinjami tur e kosnan ku mi sa, danki pa bosnan edukashon... sin bosnan, nunca mi no lo a logra.

Julien, mi ruman stima. Bo ta un guy ku kurason di oro, abo a sinjami kon pa ta sosial i alegre. Thanks for keeping your brother crisp, je weet "it's a celebration...".

My loving grandmothers, óma (Mamai) i omá (Chefa), the pillars of my family. Your love, disciplining and care made me who I am today. Bendishon.

Kiki, mi Empress... fala mnogu for believing in me. Fala for your love and your care. Fala for your hugs and support and your calming words. With you, my life is joyful, happy and full of great adventures.



Chapter 12

Curriculum vitae



Curriculum vitae

Rodney Alexander Rosalia werd geboren op 14 november 1981 in Willemstad, Curaçao. In 1999 behaalde hij zijn HAVO-diploma op het Radulphus College op het eiland.

In augustus van hetzelfde jaar verhuisde hij naar Twente, Nederland en begon hij met zijn bacheloropleiding Medische Biochemie aan de Saxion Hogeschool Enschede. Tijdens deze studie voltooide hij een stage bij de Animal Sciences Group te Lelystad, onder begeleiding van Dr. Michiel Harmsen, waar hij werkte aan het selecteren van neutraliserende Llama-antilichamen tegen het Mond-en-klauwzeervirus.

Na zijn BSc-opleiding begon hij met zijn studie MSc in Oncology bij de Vrije Universiteit (VU) in Amsterdam. Aan de hand van zijn keuzevakken, literatuurstudie, stages en scriptie richtte hij zich op het veld van tumorimmunologie en kankerimmunotherapie. Voor het behalen van zijn doctoraal voltooide hij eerst een onderzoekstage aan de Academy of Sciences in Praag, Tsjechië. Doel van het onderzoek was het blokkeren van suppressieve CD4⁺ T-cellen. Zijn stagebegeleiders waren Dr. Milan Reinis en Prof. Jan Bubenik uit Praag en Prof. Dr. Arjan van de Loosdrecht van het VU medical center.

Vervolgens liep hij stage op het Cancer Center Amsterdam van het VU medical center bij Prof. Dr. Tanja de Gruijl, Dr. Rieneke van de Ven en Prof. Dr. Rik Scheper, waar hij werkte aan dendritische celvaccinaties door middel van adenovirus-vectoren.

In 2007 behaalde hij het doctoralexamen, waarna hij terugkeerde naar de tumorimmunologie in de onderzoeksgroep van Dr. Reinis in Praag, waar hij voor 1 jaar werkte aan de samenwerking tussen NK-T cellen en suppressieve CD4⁺ T-cellen in het dempen van tumorimmunoresponsen. Dat onderzoek werd uitgevoerd in samenwerking met Dr. Hetty Bontkes van het VU medical center.

In 2008 keerde hij terug naar Nederland en begon hij aan zijn promotieonderzoek bij de sectie Tumorimmunologie van de afdeling Immunohematologie en Bloodtransfusie in samenwerking met de afdelingen Experimentele Oncologie en Klinische Farmacie en Toxicologie van het Leids Universitair Medisch Centrum en de Drug Delivery Division van de Leiden Universiteit. Dit onderzoek werd begeleid door Prof. Dr. Ferry Ossendorp, Prof. Dr. Sjoerd van der Burg, Prof. Dr. Henk-Jan Guchelaar, Dr. Jaap Oostendorp en Prof. Dr. Wim Jiskoot.

Sinds september 2013 werkt hij in Zürich, Zwitserland, aan de UniversitätsSpital Zürich, afdeling Klinische Immunologie. Zijn onderzoek is gericht op cytokine immunotherapie tegen kanker, onder begeleiding van Prof. Onur Boyman.

Curriculum vitae (English version)

Rodney Alexander Rosalia was born on November 14, 1981 in Willemstad, Curaçao. In 1999 he obtained his high school degree at the Radulphus College on his native island.

In August of the same year he moved to Twente, the Netherlands, where he began his undergraduate training in Medical Biochemistry at the Saxion Hogeschool Enschede. During this study he completed an internship at the Animal Sciences Group, Lelystad, under the guidance of Dr. Michael Harmsen, where he worked on selecting neutralizing Llama antibodies against the foot-and-mouth disease virus.

After completing his BSc program he enrolled for the MSc program in Oncology at the Vrije Universiteit (public university) in Amsterdam. He majored in the field of tumor immunology and cancer immunotherapy.

To graduate he completed two internships, his first research-internship at the Academy of Sciences in Prague, Czech Republic focused on the selective blockade and/or depletion of regulatory CD4⁺ T cells, under the supervision of Dr. Milan Reinis and Prof. Jan Bubenik and Prof. Dr. Arjan van de Loosdrecht from the VU medical center.

Next he performed a six-month internship at the Cancer Center Amsterdam, VU medical center, under the guidance of Prof. Dr. Tanja de Gruijl, Dr. Rieneke van de Ven and Prof. Dr. Rik Scheper, where he focused on dendritic cell vaccination using adenoviral vectors.

In 2007 he received his MSc degree and returned to the tumor immunology research group of Dr. Reinis in Prague, where he worked for an additional year studying the relationship between NK-T cells and regulatory CD4⁺ T cells in modulating tumor immune responses. This research was co-supervised by Dr. Hetty Bontkes of the VU medical center.

In 2008 he started his interdisciplinary PhD research at the section of Tumor Immunology of the department of Immunohematology and Blood Transfusion in collaboration with the Experimental Oncology and Clinical Pharmacy and Toxicology departments of the Leiden University Medical Center and the Drug Delivery Division of the University of Leiden. This research was supervised by Prof. Dr. Ferry Ossendorp, Prof. Dr. Sjoerd van der Burg, Prof. Dr. Henk-Jan Guchelaar, Dr. Jaap Oostendorp and Prof. Dr. Wim Jiskoot.

Since September 2013 he has been working in Zurich, Switzerland, at the UniversitätsSpital Zürich, department of Clinical Immunology. His research focuses on cytokine immunotherapy against cancer, under the supervision of Prof. Onur Boyman.



Chapter 13

Publication list



Rosalía RA, Cruz LJ, Kleinovink JW, Rueda F, Löwik CW, Ossendorp F.

Targeting nanoparticles to CD40, DEC-205 or CD11c molecules on dendritic cells for efficient CD8(+) T cell response: A comparative study. *J Control Release.* 2014 Jul 25. pii: S0168-3659(14)00521-5.

Rosalía RA, Quakkelaar ED, Redeker A, Khan S, Camps M, Drijfhout JW, Silva AL, Jiskoot W, van Hall T, van Veelen PA, Janssen G, Franken K, Cruz LJ, Tromp A, Oostendorp J, van der Burg SH, Ossendorp F, Melief CJ.

Dendritic cells process synthetic long peptides better than whole protein, improving antigen presentation and T-cell activation. *Eur J Immunol.* 2013 Oct;43(10):2554-65.

Rosalía RA, Silva AL, Camps M, Allam A, Jiskoot W, van der Burg SH, Ossendorp F, Oostendorp J.

Efficient ex vivo induction of T cells with potent anti-tumor activity by protein antigen encapsulated in nanoparticles. *Cancer Immunol Immunother.* 2013 Jul;62(7):1161-73.

Silva AL, **Rosalía RA**, Sazak A, Carstens MG, Ossendorp F, Oostendorp J, Jiskoot W.

Optimization of encapsulation of a synthetic long peptide in PLGA nanoparticles: low-burst release is crucial for efficient CD8(+) T cell activation. *Eur J Pharm Biopharm.* 2013 Apr;83(3):338-45.

van de Ven R, Lindenberg JJ, Oosterhoff D, van den Tol MP, **Rosalía RA**, Murakami M, Everts M, Scheffer GL, Scheper RJ, de Gruijl TD, Curiel DT.

Selective transduction of mature DC in human skin and lymph nodes by CD80/CD86-targeted fiber-modified adenovirus-5/3. *J Immunother.* 2009 Nov-Dec;32(9):895-906.

Rosalía RA, Štěpánek I, Polláková V, Šímová J, Bieblová J, Indrová M, Moravcová S, Přibyllová H, Bontkes HJ, Bubeník J, Sparwasser T, Reiniš M.

Administration of anti-CD25 mAb leads to impaired α -galactosylceramide-mediated induction of IFN- γ production in a murine model. *Immunobiology.* 2013 Jun;218(6):851-9.

Harmsen MM, van Solt CB, Fijten HP, van Keulen L, **Rosalia RA**, Weerdmeester K, Cornelissen AH, De Bruin MG, Eblé PL, Dekker A.

Passive immunization of guinea pigs with llama single-domain antibody fragments against foot-and-mouth disease. *Vet Microbiol.* 2007 Mar 10;120(3-4):193-206.

Símová J, Bubeník J, Bieblová J, **Rosalia RA**, Fric J, Reinis M.

Depletion of T(reg) cells inhibits minimal residual disease after surgery of HPV16-associated tumours. *Int J Oncol.* 2006 Dec;29(6):1567-71.

